



PHD

19F NMR sensors for the measurement of pH in biological systems

Jones, Brian George

Award date:
1995

Awarding institution:
University of Bath

[Link to publication](#)

Alternative formats

If you require this document in an alternative format, please contact:
openaccess@bath.ac.uk

Copyright of this thesis rests with the author. Access is subject to the above licence, if given. If no licence is specified above, original content in this thesis is licensed under the terms of the Creative Commons Attribution-NonCommercial 4.0 International (CC BY-NC-ND 4.0) Licence (<https://creativecommons.org/licenses/by-nc-nd/4.0/>). Any third-party copyright material present remains the property of its respective owner(s) and is licensed under its existing terms.

Take down policy

If you consider content within Bath's Research Portal to be in breach of UK law, please contact: openaccess@bath.ac.uk with the details. Your claim will be investigated and, where appropriate, the item will be removed from public view as soon as possible.

^{19}F NMR SENSORS FOR THE MEASUREMENT OF pH IN BIOLOGICAL SYSTEMS

Submitted by

Brian George Jones

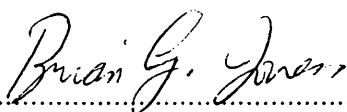
for the degree of PhD
of the University of Bath

1995

The research work carried out in this thesis has been carried out in the School of Pharmacy and Pharmacology, under the supervision of Dr Michael D. Threadgill, Dr Sarah K. Branch and Dr Andrew S. Thompson.

Attention is draw to the fact that copyright of this thesis rests with its author. This copy of the thesis has been supplied on condition that anyone who consults it is understood to recognise that its copyright rests with its author and that no quotation from the thesis and no information derived from it may be published without prior written consent of the author.

The thesis may be made available for consultation within the University Library and may be photocopied or lent to other libraries for the purpose of consultation.


.....

19/12/95
.....

UMI Number: U551900

All rights reserved

INFORMATION TO ALL USERS

The quality of this reproduction is dependent upon the quality of the copy submitted.

In the unlikely event that the author did not send a complete manuscript and there are missing pages, these will be noted. Also, if material had to be removed, a note will indicate the deletion.



UMI U551900

Published by ProQuest LLC 2013. Copyright in the Dissertation held by the Author.
Microform Edition © ProQuest LLC.

All rights reserved. This work is protected against
unauthorized copying under Title 17, United States Code.



ProQuest LLC
789 East Eisenhower Parkway
P.O. Box 1346
Ann Arbor, MI 48106-1346

UNIVERSITY OF BATH
LIBRARY

23

23 AUG 1996

Ph D

5104987

^{19}F NMR SENSORS FOR THE MEASUREMENT OF pH IN BIOLOGICAL SYSTEMS

Submitted by

Brian George Jones

for the degree of PhD

of the University of Bath

1995

The research work carried out in this thesis has been carried out in the School of Pharmacy and Pharmacology, under the supervision of Dr Michael D. Threadgill, Dr Sarah K. Branch and Dr Andrew S. Thompson.

Attention is draw to the fact that copyright of this thesis rests with its author. This copy of the thesis has been supplied on condition that anyone who consults it is understood to recognise that its copyright rests with its author and that no quotation from the thesis and no information derived from it may be published without prior written consent of the author.

The thesis may be made available for consultation within the University Library and may be photocopied or lent to other libraries for the purpose of consultation.

.....
Brian G Jones

.....
19/12/95

^{19}F NMR SENSORS FOR THE MEASUREMENT OF pH IN BIOLOGICAL SYSTEMS

Submitted by

Brian George Jones

for the degree of PhD
of the University of Bath

1995

The research work carried out in this thesis has been carried out in the School of Pharmacy and Pharmacology, under the supervision of Dr Michael D. Threadgill, Dr Sarah K. Branch and Dr Andrew S. Thompson.

Attention is draw to the fact that copyright of this thesis rests with its author. This copy of the thesis has been supplied on condition that anyone who consults it is understood to recognise that its copyright rests with its author and that no quotation from the thesis and no information derived from it may be published without prior written consent of the author.

The thesis may be made available for consultation within the University Library and may be photocopied or lent to other libraries for the purpose of consultation.

Brian G. Jones

19/12/95

^{19}F NMR SENSORS FOR THE MEASUREMENT OF pH IN BIOLOGICAL SYSTEMS

Submitted by

Brian George Jones

for the degree of PhD
of the University of Bath

1995

The research work carried out in this thesis has been carried out in the School of Pharmacy and Pharmacology, under the supervision of Dr Michael D. Threadgill, Dr Sarah K. Branch and Dr Andrew S. Thompson.

Attention is draw to the fact that copyright of this thesis rests with its author. This copy of the thesis has been supplied on condition that anyone who consults it is understood to recognise that its copyright rests with its author and that no quotation from the thesis and no information derived from it may be published without prior written consent of the author.

The thesis may be made available for consultation within the University Library and may be photocopied or lent to other libraries for the purpose of consultation.

Brian G. Jones

19/12/95

ABSTRACT

Intracellular pH (pH_i) is one of the most important factors which influence metabolic processes in cells and affects the sensitivity of tumour cells to drugs. Measurement of pH_i is important in biochemistry and drug design. The potential of acidic and basic trifluoromethylheterocycles to act as pH sensors, through change of ^{19}F chemical shift with state of ionisation, has been studied.

Intracellular pH is currently estimated (i) by microelectrodes, (ii) by pH-sensitive fluorescent compounds, (iii) by ^{31}P NMR of endogenous "inorganic" phosphate. The ^{19}F nucleus has many NMR properties which are particularly suitable for biological NMR studies. It has nuclear spin $I = \frac{1}{2}$ and high sensitivity ($0.833 \times ^1\text{H}$; $12.6 \times ^{31}\text{P}$). Fluorine chemical shifts are very sensitive to changes in its environment and it has a wide chemical shift range (0-960 ppm), allowing fluorinated compounds to be clearly recognised in spite of the line-broadening which is associated with biological studies.

Several series of trifluoromethylheterocycles have been synthesised, including 3,5-bis(trifluoromethyl)pyrazoles, ω -(trifluoromethylpyrazolyl)- and ω -(trifluoromethyl-1,2,4-triazolyl)-alkanols, 2-(trifluoromethyl)benzimidazoles, 2-(trifluoromethyl)imidazopyridines and a 5-(trifluoromethyl)oxazole. Several synthetic routes towards 4-substituted 3,5-bis(trifluoromethyl)pyrazoles were investigated but none were successful. Studies of the condensation reactions of 1,1,1,5,5,5-hexafluoropentane-2,4-dione with aryl- and acylhydrazines have lead to revision of published structures of the products.

Measurements of ^{19}F chemical shift against pH in aqueous solution have been made to establish the pK_a values of the acid-base equilibria for the above compounds and other trifluoromethylheterocycles. Two pyrazoles and two imidazopyridines have pK_a close to physiological pH; ionisation causes a change in ^{19}F chemical shift of up to 2.0 ppm.

ACKNOWLEDGEMENTS

I would like to thank Dr Mike Threadgill, Dr Sarah Branch and Dr Andrew Thompson for their continuous support and encouragement.

Thanks are also due to Mr David Wood and Mr Harry Hartell for provision of NMR spectra and for helpful advice regarding ^{19}F NMR, and to Mr Chris Cryer (Bath) and Dr J. A. Ballantine (Swansea) for the mass spectral data. I would also like to thank Derry Wilman (CRC Centre for Cancer Therapeutics, Sutton) for his assistance with ^{19}F NOE experiments and Professor S. P. Singh (India) for helpful discussion and for supplying 3-(pyridin-4-yl)-5-(trifluoromethyl)pyrazole.

I wish to thank the postgrads and postdocs of labs 3.5 / 3.7 for their friendship and for sharing both chemical knowledge and chemicals.

I also acknowledge the financial support from EPSRC.

Finally, I wish to thank Julie.

CONTENTS

Abstract	i
Acknowledgements	ii
Contents	iii
Lists of Figures, Schemes and Tables	vi
Abbreviations	xiii

Chapter 1 The Study of Intracellular pH 1Chapter 2 The Regulation of Intracellular pH in Cells 112.1 Buffering of pH 11

2.2 The Sodium / Proton Antiporter 12

2.3 Bicarbonate Transport System 16

2.3.1 Introduction 162.3.2 The Sodium-Dependent Bicarbonate / Chloride Ion 17

Antiporter

2.2.3 The Sodium-Independent Bicarbonate / Chloride Ion Antiporter 18

2.2.4 The Bicarbonate / Chloride Ion Symporter 19

2.2.5 Inhibition of Bicarbonate / Chloride Ion exchange 19

2.4 Proton pumps 202.5 Proton Channels 20Chapter 3 Measurement of pH in Biological Systems 22

3.1 Measurement of Homogenates 22

3.2 Radiolabelled Weak Acids / Bases 223.3 Positron Emission Tomography of Weak Acids 243.4 Luminescence 24

3.4.1	Fluorescent Weak Acids / Bases	25
3.4.2	pH-Dependent Fluorescence Absorption / Excitation Spectra	25
3.4.3	Proton-Controlled "on-off" Switching of Fluorescence	28
3.5	Colourimetry, Using pH-Sensitive Dyes	31
3.6	Microelectrodes	32
3.7	Electron Paramagnetic Resonance	33
3.8	Nuclear Magnetic Resonance	34
3.8.1	Introduction	34
3.8.2	³¹ P NMR	34
3.8.3	¹ H NMR	38
3.8.4	¹⁵ N NMR	40
3.8.5	¹⁹ F NMR	40
Chapter 4	Aims of the Study	51
Chapter 5	Pyrazoles	54
5.1	3,5-Bis(trifluoromethyl)pyrazole and Related Compounds	54
5.1.1	3,5-Bis(trifluoromethyl)pyrazole	54
5.1.2	Alkylation of 3,5-Bis(trifluoromethyl)pyrazole	56
5.1.3	Alkylation of 1,1,1,5,5,5-Hexafluoropentane-2,4-dione	59
5.1.4	Alternative Disconnections Towards the Synthesis of 3-Substituted Derivatives of 1,1,1,5,5,5-Hexafluoropentane-2,4-dione	59
5.1.4.1	Trifluoroacetylation of Trifluoromethyl Enol Ethers	60
5.1.4.2	Trifluoroacetylation of Trifluoromethyl Ketones	69
5.1.4.3	Reduction of β -(Trifluoroacetyl)vinyl Ethers	82
5.1.4.4	Synthesis of 3-(Dimethylaminomethylene)-1,1,1,5,5,5-hexafluoro-2,4-dione and Related Compounds	88
5.1.5	The Reaction of 1,1,1,5,5,5-Hexafluoropentane-2,4-	97

	dione with Substituted Hydrazines	
5.2	Trifluoromethylpyrazoles	102
5.2.1	4-Alkyl-3(5)-Trifluoromethylpyrazoles	102
5.2.2	3-Alkyl-5-Trifluoromethylpyrazoles	105
Chapter 6	2-(Trifluoromethyl)benzimidazoles and 2-(Trifluoromethyl)imidazopyridines	107
Chapter 7	Triazoles, Imidazoles and Pyrroles	111
7.1	Triazoles	111
7.2	Imidazoles	115
7.3	Pyrroles	120
7.3.1	Transition Metal-Induced Transformations of 5,6-Dihydro-4 <i>H</i> -1,2-Oxazines and the Synthesis of 2-Trifluoromethylpyrroles	120
7.3.2	Synthesis of 3-Alkyl-2,5-Bis(trifluoromethyl)pyrroles	126
Chapter 8	pH Studies	130
8.1	Introduction	130
8.2	Pyrazoles	130
8.3	Benzimidazoles and Imidazopyridines	136
8.4	Pyridines	139
8.5	Triazoles	141
Conclusion		143
Experimental		145
References		201
Appendix		212

LIST OF FIGURES, SCHEMES AND TABLES

Figures

Figure 1	Equilibrium of bicarbonate and carbonic acid in the blood plasma.	Page 11
Figure 2	Carbonic anhydrase catalysed equilibrium of carbonic acid with carbon dioxide in blood plasma.	Page 11
Figure 3	A schematic representation of the sodium / proton antiporter.	Page 13
Figure 4	Structures of amiloride and ethylisopropyl-amiloride.	Page 14
Figure 5	The pH_i dependence of the activity of the sodium / proton antiporter.	Page 15
Figure 6	A schematic representation of the sodium-dependent bicarbonate / chloride ion antiporter.	Page 18
Figure 7	A schematic representation of the sodium-independent bicarbonate / chloride ion antiporter.	Page 19
Figure 8	Structure of $R(+)$ -[(5,6-dichloro-2,3,9,9 α -tetrahydro-3-oxo-9 α -propyl-1 <i>H</i> -fluoren-7-yl)oxy]acetic acid (B-3(+)).	Page 20
Figure 9	Structures of quin 2 and quene 1.	Page 25
Figure 10	Fluorescence quantum yield vs pH.	Page 28
Figure 11	Structures of aminomethyltetraphenylporphyrin-tin(IV) derivatives.	Page 29
Figure 12	Structures of aminomethylbipyridyl-ruthenium(II) complexes.	Page 30
Figure 13	Structure of <i>p</i> - <i>tert</i> -butylcalix[4]arene-linked ruthenium(II) trisbipyridyl complexes.	Page 31

Figure 14	Structure of Neutral Red.	Page 32
Figure 15	Structures of aldonitrane and related compounds.	Page 34
Figure 16	The phosphate buffer system.	Page 35
Figure 17	N-Substituted derivatives of imidazole and their corresponding pK_a values.	Page 39
Figure 18	Structures of Ro 07-0741 and CCI-103F.	Page 41
Figure 19	Structure of difluoro-derivatives of 1,2-bis(<i>o</i> -aminophenoxy)ethane-N,N,N',N'-tetraacetic acid.	Page 42
Figure 20	Structures of fluorinated derivatives of the chelator <i>o</i> -aminophenol-N,N,O-triacetic acid.	Page 43
Figure 21	Structure of the 4-chlorophenyl ester of 2-amino-4,4-difluoro-3-methylbutanoic acid.	Page 45
Figure 22	Structures of 4-fluoroaniline derivatives.	Page 46
Figure 23	Structure of 6-FPOL.	Page 47
Figure 24	Structure of 3-(N-(4-fluoro-2-trifluoromethylphenyl)-sulphamoyl)propanoic acid.	Page 48
Figure 25	Structure of 1-fluoro-2,6-bis(methylene-imino-diacetate)benzene.	Page 49
Figure 26	^1H NMR spectra of dione (62) at 20.5°C (A), 100°C (B) and 150°C	Page 93
Figure 27	^{19}F NMR spectra of dione (62) at 20.6°C (A), -50.1°C (B) and -90.2°C.	Page 94
Figure 28	^1H - ^1H COSY and NOESY correlations of alkenyloxazole (115).	Page 117
Figure 29	H-F NOE correlations of alkenyloxazole (115).	Page 118
Figure 30	^{19}F chemical shift (ppm) of 3,5-bis(trifluoromethyl)-pyrazole (2) vs pH.	Page 132
Figure 31	^{19}F chemical shift (ppm) of 3-(trifluoromethyl)pyrazole-4-propanol (80) vs pH.	Page 134

Figure 32	¹⁹ F chemical shift (ppm) of 2-(3-trifluoromethylpyrazol-4-yl)ethanol (84) vs pH.	Page 134
Figure 33	¹⁹ F chemical shift (ppm) of 2-(5-trifluoromethylpyrazol-3-yl)ethanol (92) vs pH.	Page 135
Figure 34	¹⁹ F chemical shift (ppm) of pyrazoles (80 , 84 , 92) vs pH.	Page 135
Figure 35	¹⁹ F chemical shift (ppm) of 3-(pyridin-4-yl)-5-(trifluoromethyl)pyrazole vs pH.	Page 136
Figure 36	¹⁹ F chemical shift (ppm) of 2-(trifluoromethyl)-imidazo-[4,5- <i>b</i>]pyridine (96) vs pH.	Page 138
Figure 37	¹⁹ F chemical shift (ppm) of 2-(trifluoromethyl)-imidazo-[4,5- <i>c</i>]pyridine (97) vs pH.	Page 139
Figure 38	¹⁹ F chemical shift (ppm) of 3-(trifluoromethyl)-pyridine vs pH.	Page 140
Figure 39	¹⁹ F chemical shift (ppm) of 3,5-bis(trifluoromethyl)-4-(3-hydroxypropyl)-4 <i>H</i> -1,2,4-triazole (108) vs pH.	Page 141

Schemes

Scheme 1	Page 54
Scheme 2	Page 55
Scheme 3	Page 57
Scheme 4	Page 57
Scheme 5	Page 58
Scheme 6	Page 58
Scheme 7	Page 59
Scheme 8	Page 60
Scheme 9	Page 60
Scheme 10	Page 61

Scheme 11	Page 61
Scheme 12	Page 62
Scheme 13	Page 63
Scheme 14	Page 64
Scheme 15	Page 65
Scheme 16	Page 66
Scheme 17	Page 67
Scheme 18	Page 67
Scheme 19	Page 68
Scheme 20	Page 68
Scheme 21	Page 69
Scheme 22	Page 69
Scheme 23	Page 70
Scheme 24	Page 71
Scheme 25	Page 71
Scheme 26	Page 72
Scheme 27	Page 73
Scheme 28	Page 74
Scheme 29	Page 75
Scheme 30	Page 75
Scheme 31	Page 76
Scheme 32	Page 77
Scheme 33	Page 78
Scheme 34	Page 79
Scheme 35	Page 80
Scheme 36	Page 80
Scheme 37	Page 81
Scheme 38	Page 81
Scheme 39	Page 82
Scheme 40	Page 83
Scheme 41	Page 84

Scheme 42	Page 84
Scheme 43	Page 86
Scheme 44	Page 87
Scheme 45	Page 88
Scheme 46	Page 88
Scheme 47	Page 89
Scheme 48	Page 90
Scheme 49	Page 91
Scheme 50	Page 95
Scheme 51	Page 96
Scheme 52	Page 98
Scheme 53	Page 100
Scheme 54	Page 101
Scheme 55	Page 101
Scheme 56	Page 102
Scheme 57	Page 102
Scheme 58	Page 103
Scheme 59	Page 104
Scheme 60	Page 106
Scheme 61	Page 107
Scheme 62	Page 108
Scheme 63	Page 108
Scheme 64	Page 109
Scheme 65	Page 109
Scheme 66	Page 111
Scheme 67	Page 112
Scheme 68	Page 113
Scheme 69	Page 114
Scheme 70	Page 115
Scheme 71	Page 116
Scheme 72	Page 119

Scheme 73	Page	121
Scheme 74	Page	121
Scheme 75	Page	122
Scheme 76	Page	123
Scheme 77	Page	124
Scheme 78	Page	125
Scheme 79	Page	126
Scheme 80	Page	126
Scheme 81	Page	127
Scheme 82	Page	127
Scheme 83	Page	128

Tables

Table 1		Page	45
Table 2		Page	85
Table 3		Page	95
Table 4	pK _a values of pyrazoles (entries (a-d) are from a report by Elguero <i>et al.</i> ¹¹⁰ and entries (e-l) are from a report by Habracken <i>et al.</i> ¹⁸⁵).	Page	131
Table 5	pK _a values of benzimidazoles (entries (a-c) are from a report by Weast ¹⁸⁶ and entry (d) is from a report by Elguero <i>et al.</i> ¹⁵⁸).	Page	137
Table 6	Reported ¹⁸⁶ pK _a values of pyridines.	Page	140
Table 7	Summary of pK _a values.	Page	142
Table 8	Data for 3,5-bis(trifluoromethyl)pyrazole (2).	Page	212
Table 9	Data for 3-(trifluoromethyl)pyrazole-4-propanol (80).	Page	213
Table 10	Data for 2-(3-trifluoromethylpyrazol-4-yl)ethanol (83).	Page	213

Table 11	Data for 2-(5-trifluoromethylpyrazol-3-yl)ethanol (91).	Page 214
Table 12	Data for 3-(pyridin-4-yl)-5-(trifluoromethyl)-pyrazole.	Page 215
Table 13	Data for 2-(trifluoromethyl)imidazo[4,5- <i>b</i>]pyridine (95).	Page 216
Table 14	Data for 2-(trifluoromethyl)imidazo[4,5- <i>c</i>]pyridine (96).	Page 217
Table 15	Data for 3-(trifluoromethyl)pyridine.	Page 218
Table 16	Data for 3,5-bis(trifluoromethyl)-4-(3-hydroxypropyl)-4 <i>H</i> -1,2,4-triazole (107).	Page 218

ABBREVIATIONS

9-AA	9-aminoacridine
APTRA	<i>o</i> -aminophenol- <i>N,N,O</i> -triacetic acid
ATP	adenosine triphosphate
BCECF	2,7-bis(carboxyethyl)-5(6)-carboxyfluorescein
BCECF-AM	acetoxymethyl ester of 2,7-bis(carboxyethyl)-5(6)-carboxyfluorescein
CI	chemical-ionisation
COSY	correlation spectroscopy
DCM	dichloromethane
DMF	<i>N,N</i> -dimethylformamide
DMO	5,5-dimethyloxazolidine-2,4-dione
DMSO	dimethylsulphoxide
DNA	deoxyribonucleic acid
EI	electron-impact
EIPA	ethylisopropylamiloride
EPR	electroparamagnetic resonance
ether	diethyl ether
ETOB	ethyl 4,4,4-trifluoro-3-oxobutanoate
FAB	fast atom bombardment
<i>n</i> -FBAPTA	1,2-bis(<i>o</i> -aminophenoxy)ethane- <i>N,N,N',N'</i> -tetraacetic acid
6-FPOL	6-fluoropyridoxol
FRIM	fluorescence ratio imaging microscopy
3-FSA	3-fluorosalicylaldehyde
HMDS	hexamethyldisilazane
HMPA	hexamethylphosphoramide
LDA	lithium diisopropylamide
LiHMDS	lithium hexamethyldisilazide
MDR	multidrug resistance
MEM	2-methoxyethoxymethyl

MEMCl	2-methoxyethoxymethyl chloride
MS	mass spectrum
NMR	nuclear magnetic resonance
NOE	nuclear Overhauser enhancement
NOESY	nuclear Overhauser enhancement spectroscopy
PCr	phosphocreatine
PDE	phosphodiester
pH _e	extracellular pH
pH _i	intracellular pH
P _i	inorganic phosphate
PIET	photoinduced electron transfer
PME	phosphomonoester
PPA	phenylphosphonic acid
ppm	parts per million
PTSA	<i>p</i> -toluene sulphonic acid
quene 1	8-[bis(ethoxycarbonylmethyl)amino]-6-methoxy-2-[<i>trans</i> -2-[bis(ethoxycarbonylmethyl)amino]styryl]quinoline
RT	room temperature
SNARF-1	carboxy seminaphthorhodafluor-1
SNR	signal to noise ratio
TBDPS	<i>tert</i> -butyldiphenylsilyl
TFA	trifluoroacetic acid
TFAA	trifluoroacetic anhydride
THF	tetrahydrofuran
tlc	thin layer chromatography
TMS	trimethylsilyl
TMSCl	trimethylsilyl chloride
TMSO	trimethylsiloxy

CHAPTER ONE

Almost exactly 110 years ago T. H. Huxley, in his anniversary address as President of the Royal Society, said "What an enormous revolution would be made in biology, if physics or chemistry could supply the physiologist with a means of making out the molecular structure of living tissues comparable to that which the spectroscope affords to the inquirer into the nature of the heavenly bodies¹". By the discovery of nuclear magnetic resonance (NMR), physics has provided the basic method and chemistry has provided the extensive background for exploration in biological systems.

The opening chapter of this report describes research areas where the measurement of intracellular pH (pH_i) has become important. Chapter Two is concerned with the mechanisms of pH_i regulation thought to be used by a cell. Chapter Three discusses the methods currently available for the determination of pH_i . Chapter Four describes the design requirements of a ^{19}F NMR sensor of pH_i and discusses the aims of the project. Chapters Five, Six and Seven discuss the design and synthesis of some fluorine containing compounds. Chapter Eight describes the method of evaluating the potential of the fluorine containing heterocycles to act as sensors of pH and reports the results of these tests.

1. The Study of Intracellular pH.

In clinical practice today, there is much information about suspected lesions available which is gained from imaging methods. However, for differential diagnosis it is important to have functional or physiological information. The pH_i and extracellular pH (pH_e) of the tissue are two interesting parameters in this regard.

Myocardial ischaemia commonly arises from a partial restriction of coronary blood flow. This results in both a decrease in the supply of oxygen to the tissues and a reduction in the removal of metabolites, such as lactic acid. Depending on the severity of the restriction of coronary blood flow, the pH_i has been reported^{2,3} to drop from the normal value of around 7.2⁴ to values as low as 6.0 to 6.2 or even 5.7, while pH_e was somewhat higher. Similar reductions in pH_i have been reported^{5,6} in cases of cerebral ischaemia.

NMR information about ischaemic tissues regarding the levels of biogenetic metabolites shows a decrease in phosphocreatine and nucleoside triphosphate and a corresponding increase in inorganic phosphate⁷. These changes often resemble those observed during the untreated growth of experimental tumours. Over 60 years ago, studies of glucose consumption in tumour slices incubated aerobically showed a high rate of lactic acid production⁸. Some normal tissues, for example exercising muscle, also produce large amounts of lactic acid which is rapidly removed. However, in the case of tumours with poorly organised vasculature, there is inadequate elimination of protons from the interstitial space^{9,10}. This copious production of lactic acid was for many years thought to result in a decrease in the pH_i ¹¹. It has been confirmed^{12,13,14,15,16} that the pH_i ($\text{pH} = 7.2 - 7.7$) of several rodent tumours is higher than that of the pH_e ($\text{pH} = 5.9 - 7.4$). This is in contrast to normal tissues in which the pH_i ($\text{pH} = 7.0 - 7.4$) is lower than the pH_e ($\text{pH} = 7.3 - 7.8$). That is, the proton gradient is reversed and is invariably¹² a major difference between tumour and normal tissue.

It appears that tumour cells are able to regulate their pH_i under the acidic conditions encountered interstitially within solid tumours. There are three major mechanisms which allow cells to regulate their pH_i under acidic conditions (these mechanisms are discussed in more detail later): (i) The buffering capacity of the cytosolic and organellar contents; (ii) the sodium / proton exchanger; (iii) the sodium-dependent chloride ion / bicarbonate

exchanger. In cells surrounded by an acidic environment in which the concentration of bicarbonate is reduced, the role of the sodium / proton exchanger may be particularly important in controlling pH_i ¹⁰. Agents that inhibit the operation of this exchanger show considerable potential for causing pH_e -dependent cytotoxicity, selectively killing cells in the acidic regions of solid tumours. Rational development of these agents requires greater understanding of tumour pH and its regulation.

Tissue oxygenation is also a major factor in the sensitivity of many non-surgical treatments of malignancies. Hypoxic cells are relatively resistant to radiotherapy and certain types of chemotherapy. In the mechanism of radiotherapy, oxygen is thought to play an important role in the production of cytotoxic DNA species¹⁷. Tissue oxygenation depends principally on the oxygen availability and the respiration rate of cells. When the percentage oxygen saturation of the blood is plotted against the partial pressure of blood, the curve obtained is called the oxygen dissociation curve. Release of oxygen into the tissues is mostly dependent on the shape of this curve, which can be shifted through changes in pH. Other forms of chemotherapy have been able to exploit hypoxia in tumours, for example the bioreductively activated 2-nitroimidazole drugs^{18,19}. There can, therefore, be an advantage in selectively increasing the level of hypoxia in tumours²⁰. There are various measures which can be taken to increase the level of hypoxia in tumours. These include the administration of a vasodilator such as hydralazine, a drug which binds to oxyhaemoglobin and shifts the dissociation curve to the left.

Data on parameters such as pH in tumours have mostly been derived from rodent tumours. This may not adequately represent the multitude of neoplastic tumours encountered in humans¹³. Also the data available on human tumours are sparse and often contain significant errors associated with the techniques currently used for measurement¹³.

In many NMR studies on small rodents, a factor affecting experimental results is stress. It has been demonstrated quantitatively²¹ that the stress of alignment of the rodent within a vertical magnet is superimposed on the stress of hypoxia. This parameter was rarely addressed in early studies and one should, therefore, be cautious about interpretations of NMR data obtained from such experiments because of potential complications.

Problems encountered in the literature are often a consequence of the difficulties in the accurate measurement of pH. It is possible that tumour pH may be a characteristic property of tumour lines rather than individual lesions. Larger tumours may achieve more acid pH values than smaller, better vasculated tumours. Some may maintain a higher glycolytic rate than others under hypoxic conditions, thus leading to the production of more lactic acid^{17,22}.

Spontaneous cell death has been observed within regions of solid tumours²³. The deficiency of nutrients and acidic conditions may contribute to this cell death and necrosis²⁴. However, as already discussed, many cells are known to survive these conditions and are an important cause for the failure of conventional therapies. Acidity may be a factor that could be exploited therapeutically to destroy such cells.

It is now an established fact that an acidic environment greatly increases the thermosensitivity of tissue, inhibits the recovery of tissue from thermal damage and perhaps inhibits the development of thermotolerance^{24,25,26,27}. Response to hyperthermia appears to be a function of pH_i rather than pH_e ²⁸. Thus an increase in the thermosensitivity of tumour cells may be achieved by lowering pH_i . The inhibition of the sodium / proton antiporter has already been mentioned briefly and hyperthermia represents a further exploitation.

Potent and specific inhibitors of sodium / proton exchange have been developed²⁸. Using such compounds, it has been demonstrated that blocking

extrusion of protons from cells produces a lowering of the pH_i and an increase in thermosensitisation²⁸. Importantly, this increase in thermosensitisation was found to be greater in an acidic environment than in a neutral environment. This suggests that the acidic pH_e of tumours may be exploited to increase preferentially the thermal damage in tumours relative to normal tissue.

The use of agents which cause acute acidification of cells in the presence of a low pH_e reduces the development of thermotolerance. Without these agents, heat treatment would be expected to be selectively toxic only to cells which have become acutely acidic within solid tumours. The mechanisms by which heat treatment kills cells is not fully understood, although increased fluidity in cell membranes and protein denaturation are believed to play a primary role²⁴. Further, heat treatment leads to rapid fall in pH_e in many solid tumours. This effect appears to be due to vasoconstriction and coagulation necrosis which results in a marked decrease in blood flow and thus further reduces the accumulation of metabolites.

Any improvements to be made on the selectivity of anti-cancer drugs must be based on differences distinguishing tumours cells from normal tissue. Many of these differences can be detected by the studying the interaction of a drug with its active site. Measurements of the pH_i of tumours have allowed greater understanding of the activity or lack of activity of many drugs. For example, the mechanism underlying the cytotoxicity of 5-fluorouracil is controversial^{29,30}. 5-Fluorouracil and its derivatives are known to be incorporated into DNA. However their adopted geometry when bound to guanine is pH-dependent and is the basis of much of this controversy. Determination of the physiological pH was vital for the binding studies which highlighted a discrepancy in results^{29,30}.

Anti-cancer drugs must be transported into the cells either by active transport or by passive diffusion and frequently undergo intracellular metabolism. Since

all these processes are dependent on the pH_i , the cytotoxicity of the drugs will also be dependent on the pH_i and pH_e . If a drug contains either acidic or basic functionalities and its uptake mechanism is passive diffusion, then transport will be enhanced by values of pH_e that favour the non-ionised form of that compound.

During chemotherapy, tumour cells often lose their sensitivity to drugs. This is often due to an acquired multidrug resistance (MDR) and can occur over a broad range of drug classes and targets. MDR is often, but not always, associated with increased expression of the MDR protein or P-glycoprotein^{31,32,33}. The most widely accepted hypothesis for the mode of action of MDR suggests that the protein actively expels drugs out of the cell. Also supported³³ is the idea that the MDR protein can change the pH_i , thus altering the transmembrane partitioning or intracellular sequestration of drugs. Further studies to address this hypothesis will be helped by the accurate determination of the pH_i of cells experiencing MDR relative to both non-MDR tumour cells and normal cells.

The measurement of pH_i may provide valuable information on the metabolic state of a tissue and could assist in elucidating the chronology and extent of the effects observed following treatment of malignancies³⁴. The absolute determination of pH_i may be a significant marker of response to therapy³⁵. Furthermore, pH_i may give indirect information about the metabolic state of a tissue. An alkaline shift in pH_i following treatment is coincident with increased blood flow and an increased cell proliferation rate³⁶. It is likely that this improved blood flow to the tumour results in an increased lactic acid clearance¹⁷. An alkaline shift in tumour pH could also be the result of a decreased lactic acid production, indicating an improved oxygenation of the tissue.

It has also been observed that the pH_i is positively correlated with the ratio of phosphocreatine to inorganic phosphate. That is, changes in pH_i may be indicative of changes in metabolism of phosphate. However, in contrast to the detection of phosphate metabolites, changes in pH_i have been detected at lower drug doses³⁶. Using non-invasive methods, it should be possible to monitor tumour response to therapy following a low, relatively non-toxic "test-dose" of chemotherapy¹⁷. This would allow patients to avoid the systemic toxicities associated with a full course of therapy and would aid the clinician in selecting treatment protocols for the cancer patient^{37,38}. However, it is important to consider the possibility of drug resistance being acquired by the cells.

The intracellular acidosis which has been reported^{2,3} during ischaemia of the heart muscle has already been mentioned. The effect of pH on contractile elements is of interest for studies of the other muscles in the human body. Measurement of pH_i during and following periods of muscle exercise provides information about the health of the muscle^{5,39}. Muscle contraction can occur under aerobic and / or anaerobic conditions. Even among healthy individuals, there will be large variations in the way they respond metabolically to the same work. Although there is diversity in normal individuals, there are still criteria available by which to identify disease conditions. A decrease in pH_i is observed during dynamic exercise. This occurrence does not depend on the individual muscle or the type of exercise performed. The metabolic switch from aerobic to anaerobic energy supply is invariant and can be used to define normal response³⁹. Additionally, the rate of recovery from this temporary acidosis following exercise provides characteristic indices for healthy muscle. Studies of pH_i provide biochemical information about known muscle diseases and help to elucidate and characterise new diseases. Extensive studies on animals have aided this research and have allowed the design of models for human disease³⁹.

pH_i is an important factor in cellular homeostasis. Many cellular processes, such as enzyme activity, ion channel conductivities, membrane permeability and cell growth and development are sensitive to changes in pH_i^{10,14,40,41}.

The activities of a large number of enzymes, including those used in cellular metabolism, are pH_i-sensitive. A popular example is phosphofructokinase, the rate-limiting enzyme of glycolysis^{40,42}. It is commonly known that insulin is responsible for the stimulation of this enzyme. It does so by interacting with the sodium / proton antiporter in the plasma membrane, resulting in a rise in pH_i which activates the enzyme⁴⁰. The production of urea by hepatocytes is also pH_i-dependent, although somewhat less so than the synthesis of glucose. Both of these processes are inhibited by intracellular acidification which would have important physiological consequences to the body⁴³. It should be noted that, although insulin resulted in an increase in pH_i under these conditions, this response is not general for all cell types. In fact, the observed response to the administration of insulin into skeletal muscle was a slight decrease in pH_i⁴⁴.

In addition to the effects of pH_i on the permeability of a drug through a cell membrane discussed earlier, the conductivities of many ion-channels are also pH_i-dependent. Interesting examples are the potassium channels in many excitable cells. A reduction of pH_i in these cells blocks the potassium ion conductance and depolarises the membrane producing an action potential. pH_i-sensitive potassium channels have been found in crayfish slow muscle fibres and in the squid giant axon⁴⁰.

Changes in pH_i have been shown to be important in cell growth and development^{10,14,41}. Quiescent or dormant cells can be stimulated to reinitiate DNA synthesis and cell division by the addition of certain growth factors^{45,46,47,48}. The effect of insulin on the sodium / proton antiporter in the stimulation of glycolysis in certain cell types has already been discussed. Insulin is known to act synergistically with many growth factors. It is not surprising,

therefore, to find that the stimulation of cells by growth factors is accompanied by a rise in pH_i which is blocked by amiloride, an inhibitor of the sodium / proton antiporter⁴⁶.

The suggestion that the activation of the sodium / proton antiporter and the resulting elevation of pH_i may play a role in the stimulation of cell proliferation originated from the pioneering work of Johnson *et al.*⁴⁹ on sea urchin eggs. It was discovered that fertilisation by sperm causes a rapid increase in the concentration of free cytoplasmic Ca^{2+} , followed by a sustained increase in pH_i ⁴⁷. Interestingly, the stimulation of respiration and motility in the sperm of the sea urchin also appears to be associated with a rise in pH_i ⁵⁰. Conversely, at decreased pH_i , sperm respiration and motility are inhibited. In fact, intracellular alkalinisation has been associated with the activation of the cell cycle in a wide range of organisms. This spans from the initiation of cell differentiation in slime mould⁵¹ to the mitogenic-stimulation of mouse quiescent fibroblasts⁴⁷. There is increasing reason to believe that research into the role of pH_i in the lower organisms may have an important significance to studies of cell proliferation in higher animals. A greater understanding of the involvement of the sodium / proton antiporter and pH_i in the initiation of cell growth and proliferation may be important in the study of tumour growth. Human tumour cells lacking the sodium / proton antiporter have lost or severely reduced their ability to grow tumours¹⁰. The importance of these mechanisms in the design of anti-cancer agents once again becomes apparent.

Estimations of pH_i generally represent the pH of the cytoplasm. Also of interest is the estimation of the pH in subcellular compartments, which has been shown to be feasible⁵². This may be carried out using ^{15}N NMR of amino acids but experiments with ^{31}P NMR have also identified two intracellular components with pH's of 7.1 - 7.3 and ≥ 6.0 which probably represent cytoplasm and vacuole, respectively. Both of these experiments have provided evidence for the intracellular localisation of various amino acids in acidic

organelles. In addition, the acidity of the vacuole relative to the cytoplasm is consistent with its lysosomal nature and the acidic pH optima of many enzymes associated with these organelles⁵².

There have been indications that exposure to sunlight may lead to an improvement of acne⁵³. To investigate the possible reasons for the beneficial effect of sunlight, photobiological studies have been carried out on the bacterium held responsible for this skin disease⁵³. Results indicate that exposure to near-uv light causes membrane damage, notably to the proton gradient generating system. Further investigations of the possible uv-induced effects on pH_i would be of interest and are currently in progress⁵³.

Described above, is a brief account of the research areas where pH_i has become an important consideration. There is clearly a need for an accurate, non-invasive technique for the measurement of pH_i in biological systems.

CHAPTER TWO

2. The Regulation of Intracellular pH in Cells.

2.1 Buffering of pH.

It was once believed that the pH_i of mammalian cells depended only on the pH_e and the membrane potential⁵⁴. In this belief, it was assumed that protons, hydroxy ions and bicarbonate ions were passively distributed across the cell membrane. We now know this to be wrong. In reality, the level of pH_i in mammalian cells is regulated within a narrow range that is compatible with cellular functions.

Normal plasma of the blood has a pH of 7.4 and is maintained under limits ± 0.04 -0.05 pH units⁵⁵. In fact, the concentration of protons is regulated within narrower limits than that of any other electrolyte in the blood. The pH is regulated by the bicarbonate-carbon dioxide buffer system and is defended by the ratio of the dominant acid-base pair in the blood, bicarbonate : carbonic acid, as shown in Figure 1.



Figure 1. Equilibrium of bicarbonate and carbonic acid in the blood plasma.

Carbonic acid is, in turn, in equilibrium with carbon dioxide, in a process catalysed by the enzyme carbonic anhydrase, as shown in Figure 2.

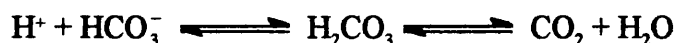


Figure 2. Carbonic anhydrase catalysed equilibrium of carbonic acid with carbon dioxide in blood plasma.

This relationship can be summarised by the Henderson equation (Equation 1).

$$[H^+] = \frac{K(\alpha \cdot P_{CO_2})}{[HCO_3^-]} \quad \text{where,} \quad \begin{array}{l} \alpha = \text{solubility coefficient of } CO_2 \\ K = \text{carbonic acid dissociation constant} \end{array}$$

Equation 1

More familiar is the negative logarithmic transformation of this equation to the Henderson-Hasselbalch equation (Equation 2) with the appropriate numeric equivalents of K and α .

$$pH = 6.1 + \log \frac{[HCO_3^-]}{0.03P_{CO_2}}$$

Equation 2

In practical terms, the kidneys regulate the concentration of bicarbonate, while the lungs sensitively control the carbon dioxide tension (P_{CO_2}).

The values of pH_i commonly observed fall between the range 7.0-7.4, which is higher than would be expected if protons were passively distributed across the cell membrane. For a typical membrane potential of -59 mV, pH_i should be 6.4. This value for pH_i is far too low for normal cellular function, clearly showing that protons are actively extruded from the cell.

An elaborate array of buffers are known to exist in the cell, principally haemoglobin, other proteins and dibasic phosphate (HPO_4^{2-}). The combined buffering capacity of cells has been determined to be between 10 and 50 mM per pH unit, depending on the cell type⁴⁰. However, buffering alone cannot account for the well maintained pH_i observed. There have been four membrane-bound ion-transport mechanisms reported⁵⁶ to play a role in the regulation of pH_i .

2.2 The Sodium / Proton Antiporter.

The sodium / proton antiporter is ubiquitous in mammalian cells and is the

most widely studied⁵⁶ membrane mechanism that is involved in the regulation of pH_i . The importance of this antiporter has already been stressed in the preceding chapter and it is clearly worthy of explanation in some detail. It is responsible for the reversible and electroneutral exchange of sodium ions (or lithium) for protons. Under physiological conditions, where protons are formed continuously intracellularly during metabolism, the antiporter operates to export protons from the cell, as illustrated in Figure 3.

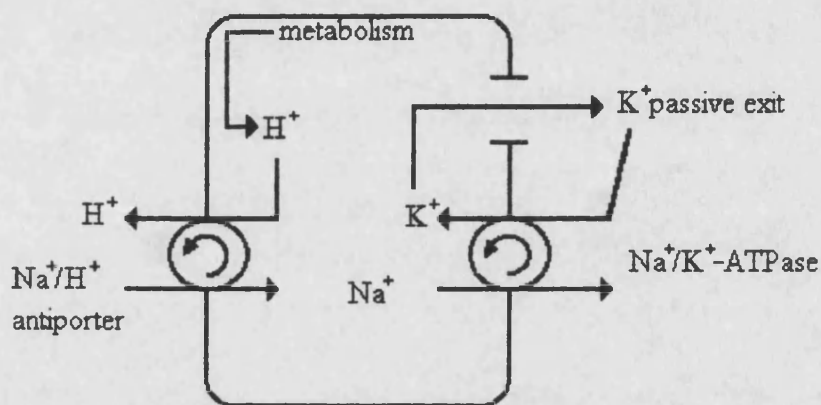
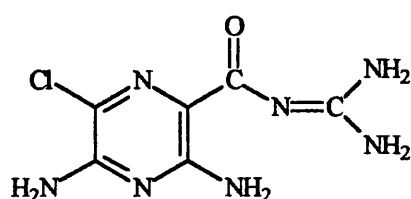
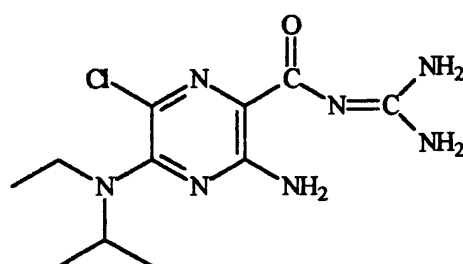


Figure 3. A schematic representation of the sodium / proton antiporter.

The driving force for the extrusion of protons from the cell is produced by a large sodium ion gradient⁴⁰. This gradient is maintained by the extrusion of sodium ions back out of the cell by the sodium / potassium-ATPase. This can be demonstrated by the inhibition of the ATPase with ouabain, which eventually leads to a shut down of the antiporter. Much of the work carried out on the sodium / proton antiporter has been helped by highly potent inhibitors, such as ethylisopropylamiloride, which are derived from the diuretic drug, amiloride, as shown in Figure 4.



Amiloride



Ethylisopropylamiloride (EIPA)

Figure 4. Structures of amiloride and ethylisopropylamiloride.

Amiloride and EIPA inhibit by competitively binding to the extracellular site which accommodates sodium ions.

The activity of the antiporter is known to be dependent on the external concentrations of both sodium ions and protons. If the external concentration of sodium ions or protons is increased, the rate of sodium / proton exchange increases. There have been various binding sites proposed for these cations, including a shared site in the kidney brush border membranes⁵⁷ and distinct binding sites in many non-renal cells¹⁰⁸.

The influence of pH_i on the activity of the antiporter has been extensively studied. However, the interactions of internal sodium ions with the antiporter have received less attention. The activity of the antiporter may be measured as sodium ion influx or proton efflux, and ranges from maximum activity at acid pH_i values to no activity at pH_i values >7.5 . This activity profile is characteristic of the sodium / proton antiporter and, therefore, its main function is to prevent intracellular acidification.

The shape of this pH_i -dependent activity profile varies between cell types. Figure 5 shows two extreme cases between which most other cell types lie⁵⁶. From the shape of the curve it is possible to predict that in the heart, a small variation in pH_i would result in a large change in sodium / proton antiporter

activity. This suggests that the cardiac cells are very sensitive to pH_i , relative to renal cells.

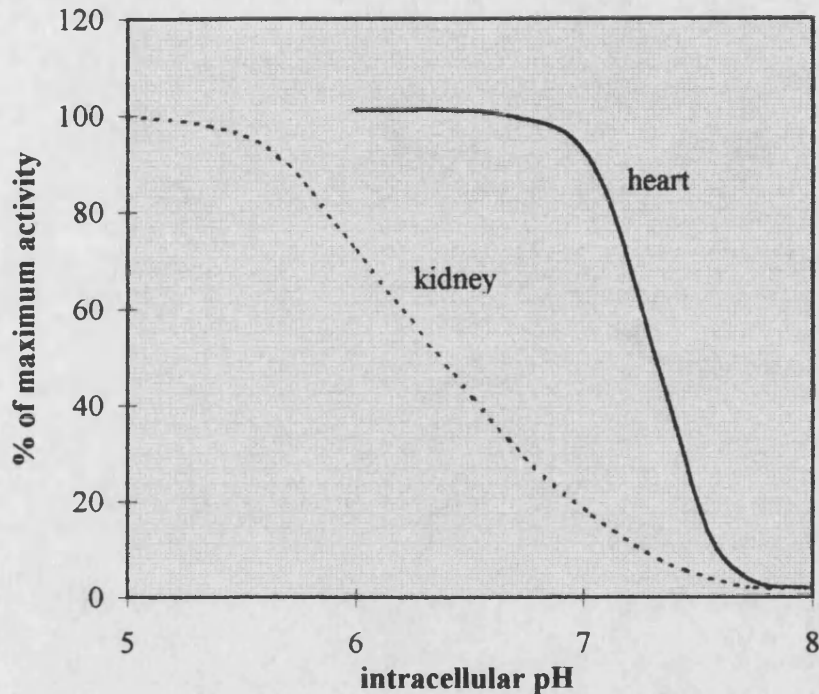


Figure 5. The pH_i dependence of the activity of the sodium / proton antiporter (redrawn from a report by Frelin *et al.*⁵⁶).

Many suggestions have been made for the way in which the sodium / proton antiporter is regulated. The effects of some hormones and growth factors have already been mentioned. However, it should be noted that all of these observations were carried out in the absence of bicarbonate / chloride ion exchange. In mutant cells which lack sodium / proton antiporters this alkalinisation does not occur and cells do not proliferate without artificial elevation of pH_i ⁵⁹. In the presence of bicarbonate / chloride ion exchange growth factors fail to raise pH_i in many cell types. The mode of action of these growth factors in the regulation of pH_i is therefore complex and probably involves the stimulation of three acid-base transporters⁵⁹. The list of effectors of sodium / proton exchange is very long and varied. There have also been

proposed various mechanisms to achieve the activation of the antiporter, which can act simultaneously in the same cell⁶⁰. Of the many activation pathways proposed, the three most widely accepted are:

(i) The C kinase pathway.

This is thought to account for the effect of many mitogens. The binding of the effector to specific membrane receptors activates phospholipase C via a pertussis-toxin-sensitive G protein. Inositol phospholipids are hydrolysed to release diacylglycerol which activates protein kinase C. This then may phosphorylate the antiporter protein⁵⁶. The result is a shift of the pH_i -activity profile to the right, leading to an increased activity of the sodium / proton antiporter in the alkaline range and thus a reduction in pH_i .

(ii) The calcium-dependent pathway.

It has been observed in some cells, that an increase in intracellular concentration of calcium activates the sodium / proton antiporter. It has been suggested that a calcium-calmodulin protein kinase could mediate the calcium ion effect, although many other mechanisms involving calcium ions have been proposed⁵⁶.

(iii) cAMP-dependent regulation.

Increased levels of cAMP lead to a decrease in the activity of the sodium / proton antiporter. The inhibitory effect is produced by a shift in the pH_i -activity profile to the left. That is, an inverse of the mechanism of C kinase activation⁵⁶.

2.3 Bicarbonate Transport Systems

2.3.1 Introduction

Anion exchange is also essential for the regulation of pH_i and, at levels of pH_i close to neutrality, may be more active than the sodium / proton antiporter in

some cell lines⁶¹. The understanding of the role of bicarbonate transport systems in the regulation of pH_i is less advanced than that of the sodium / proton antiporter. This is because (i) there are several transport systems involved, (ii) until recently, there were no selective potent inhibitors of these systems available, and (iii) bicarbonate equilibrates with carbon dioxide which is volatile and is also able to modify pH_i . Three major bicarbonate-dependent mechanisms of regulating pH_i have been suggested. Not all of these systems are present in all cell types and the significance of each combination is not fully understood. They all appear to be under hormonal control, similar to mechanisms described for the sodium / proton antiporter^{62,63,64}.

2.3.2 The Sodium-Dependent Bicarbonate / Chloride Ion Antiporter

The purpose of the sodium-dependent bicarbonate / chloride ion antiporter is to increase the pH_i of the cell following an acid load. Its activity is dependent on intracellular chloride ions and extracellular bicarbonate and sodium ions (not lithium). It is electroneutral, meaning that one sodium ion and two bicarbonate ions are exchanged for chloride ions, or that one sodium ion and one bicarbonate ion are exchanged for a proton and a chloride ion. That is, the bicarbonate influx associated with the functioning of the system is accompanied by an influx of sodium ions. A schematic representation of this mechanism is given in Figure 6.

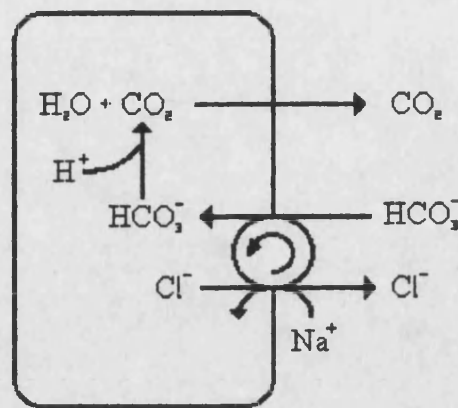


Figure 6. A schematic representation of the sodium-dependent bicarbonate / chloride ion antiporter.

2.3.3 The Sodium-Independent Bicarbonate / Chloride Ion Antiporter

The inward gradient for chloride ions usually exceeds that for bicarbonate and it is often necessary for a system to catalyse the efflux of bicarbonate. One such system is the sodium-independent bicarbonate / chloride ion antiporter which under these conditions acts as a cell acidifying mechanism following an alkaline load. However, if the extracellular concentration of chloride ions is decreased the system then reverses and acts to increase the pH of the cell. The system is electroneutral and a schematic representation of this mechanism is given in Figure 7.

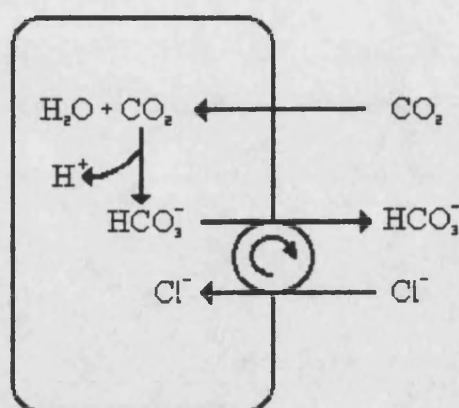


Figure 7. A schematic representation of the sodium-independent bicarbonate / chloride ion antiporter.

2.3.4 The Bicarbonate / Chloride Ion Symporter

This bicarbonate transport system is sodium-selective, independent of chloride ions and electrogenic⁶⁵. It was reported⁶⁶ to act as a bicarbonate influx mechanism in bovine corneal endothelium leading to an increase in pH_i . Conversely, it has been claimed to mediate reabsorption of bicarbonate and sodium ions into the blood in the basolateral membrane of the renal proximal convoluted tubule⁶⁶.

2.3.5 Inhibition of Bicarbonate / Chloride Ion exchange.

Inhibition of the sodium / proton antiporter has been shown to increase the thermosensitivity of tumour cells, as discussed earlier. This thermosensitisation has been reported to be further enhanced by the inhibition of bicarbonate / chloride ion exchange²⁸. One of the most potent and specific inhibitors of bicarbonate / chloride ion exchange available is *R*(+)-[(5,6-dichloro-2,3,9,9a-tetrahydro-3-oxo-9a-propyl-1*H*-fluoren-7-yl)oxy]acetic acid (B-3(+)), illustrated in Figure 8.

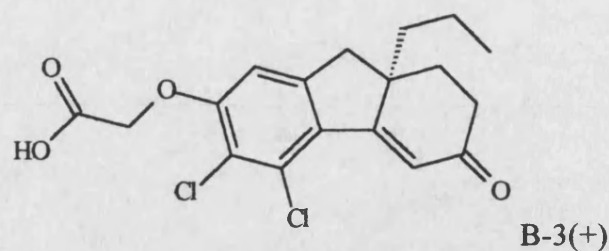


Figure 8. Structure of *R*(+)-[(5,6-dichloro-2,3,9,9a-tetrahydro-3-oxo-9a-propyl-1*H*-fluoren-7-yl)oxy]acetic acid (B-3(+)).

When B-3(+) is used alone there is little change in the thermosensitivity of the tumour, suggesting that the role of bicarbonate / chloride ion exchange in the regulation of pH_i is relatively small. The use of bicarbonate / chloride ion exchange inhibitors in therapy should be considered with caution as they may even reduce the therapeutic index due their toxicity effects.

2.4 Proton Pumps

There have been various proton pumps described which may play a role in the regulation of pH_i . Electrogenic proton-translocating ATPase pumps have been found in the mammalian distal nephron⁶⁷ and in the turtle urinary bladder⁶⁸. Also, electroneutral potassium / proton exchange ATPase pumps are thought to be involved in gastric acid secretion⁵⁶. The energy for these proton pumps is provided by the hydrolysis of ATP. The examples given are all located in the cell membrane and are all efficient in the expulsion of protons from the cytosol. However, their role in the regulation of pH_i is not yet clear.

2.5 Proton Channels

Proton conductive pathways have been observed, for example in renal brush border membrane vesicles⁶⁹ and in neurons⁷⁰. These channels will have a limited role in the regulation of pH_i under physiological conditions and under the extreme circumstances relative to the major systems of regulation.

Therefore, studies of these channels have received less attention.

The above account has described a large array of mechanisms at a cells disposal for the strict regulation of pH_i . Much of this knowledge has required the measurement of pH_i . Furthermore, the very existence of these mechanism illustrates the importance of pH_i to a cell. Therefore, the measurement of pH_i may provide important information about the metabolic state of a tissue and may also highlight areas for possible therapeutic exploitation of pH_i .

CHAPTER THREE

3. Measurement of pH in Biological Systems.

3.1 Measurement of Homogenates.

One of the oldest methods for estimating pH_i , the measurement of the pH of cell lysate or homogenate, was first employed in 1912 by Michaelis and Davidoff⁷¹. The potentially serious problems of this technique were recognised early on. For example, production of lactic acid and carbon dioxide continue after cellular destruction and lead to a fall in pH. In addition, the mixing of intra- and extracellular fluids can lead to changes in pH because the solutions are of different pH and because the intra- and extracellular buffers become diluted. Finally, disruption of intracellular organelles makes it impossible to calculate the pH of the bulk intracellular fluid⁴.

3.2 Radiolabelled Weak Acids / Bases.

Twenty years ago the most popular method of estimating the pH_i was to measure the distribution of a weak acid or base across the cell membrane. This relies on the observation that for some weak acids or bases, the permeability of a biological membrane to the non-ionised form is very much greater than the ionised form⁴². Weak acids will occur in higher concentrations in more alkaline compartments; for weak bases the opposite is true. There are several assumptions made for this method, including:

- (i) It is based on a two compartment system representing intra- and extracellular spaces.
- (ii) The dissociation constant is the same in both compartments.
- (iii) No binding, active transport or metabolism of the indicator occurs.

Problems often associated with this method include:

- (i) The preparation must be biopsied, causing damage to cells and a limit of one measurement per preparation.
- (ii) To measure the intracellular concentration of the non-ionised form of the indicator, a correlation must be applied for contamination with extracellular fluid. For this purpose, markers of extracellular space must be used, for example [^{14}C] inulin, [^{14}C] sorbitol, $^{36}\text{Cl}^-$ and total tissue water (^3HHO). This can be carried out on parallel samples to those being used for pH determination but it is sometimes preferred to determine the extracellular space in the same samples⁴⁹.
- (iii) Binding to intracellular proteins means that measured intracellular concentrations are often higher than free concentrations. An underestimate of pH_i occurs if a weak base binds and an overestimate if a weak acid binds⁴².
- (iv) Only slow changes in pH_i can be monitored due to the time it often takes the indicator to equilibrate between the intra- and extracellular compartments⁷².
- (v) The method is sensitive to changes in cellular volume⁴.
- (vi) Intracellular compartmentation may occur. For example, a weak acid will be excluded from acidic compartments (e.g. lysosomes) and will accumulate in relatively alkaline compartments (e.g. mitochondria). The proportion of the intracellular volume that these compartments occupy in different cell types could have important implications on the value of pH_i measured.
- (vii) Measurements usually have to be carried out in suspension. If the cells are attached to a solid surface, which is a condition often required⁴⁵, then the remaining volume of extracellular fluid can be 20-30 times greater than the intracellular volume. This in itself poses a problem, but in addition, washing of the extracellular fluid results in leakage of the indicator.

These limitations mean that absolute values of pH_i cannot be determined with certainty using this method. The major advantage of this method is cheapness and, despite the many uncertainties, it has found much use in the estimation of

$\text{pH}_i^{45,49}$. The most popular commercially available indicator is the radioactive weak acid, 5,5-dimethyloxazolidine-2,4-dione (DMO)⁴⁹. Here, an increase in pH_i results in an increased accumulation of DMO anion intracellularly.

3.3 Positron Emission Tomography of Weak Acids.

The principle of this method is the same as for radiolabelled weak acids. DMO is once again the compound of choice, but the [¹¹C] DMO isotope is used and detection is by positron emission tomography. The major application of this technique has been in the measurement of brain tissue pH , that is a composite value of pH_i and pH_e ¹³. These measurements do not use extracellular markers as required for the calculation of pH_i . The main limitation associated with this technique is the short half life of the isotope (20.3 minutes).

3.4 Luminescence.

When a molecule undergoes electronic excitation, it can also be taken to a higher vibrational state. In this excited state, the molecule is subjected to collisions with surrounding molecules and gives up energy as it steps down the vibrational levels. If the molecule is able to retain the large energy difference between the excited electronic state and ground electronic state, then it may undergo spontaneous emission of fluorescent radiation. The characteristic fluorescent spectrum produced by many compounds has been exploited in the measurement of pH . There are three types of fluorescent pH probes; those which work on the same principle as radioactive weak acids/bases but use fluorescence as the method of detection, those which exhibit pH -dependent fluorescence absorption and/or excitation spectra, and those which have a proton-controlled fluorescence.

3.4.1 Fluorescent Weak Acids/Bases.

The weak base, 9-aminoacridine (9-AA) is the most popular fluorescent compound which partitions across the cell membrane according to the transmembrane pH gradient⁷³. It was reported⁵⁰ that uptake of 9-AA by sea urchin sperm cells results in a quenching of its fluorescence. This appears to be related to intracellular binding. In this example, the fluorescence served as a measure of the extracellular 9-AA and therefore simplified calculations of pH_i .

3.4.2 pH-Dependent Fluorescence Absorption/Excitation Spectra.

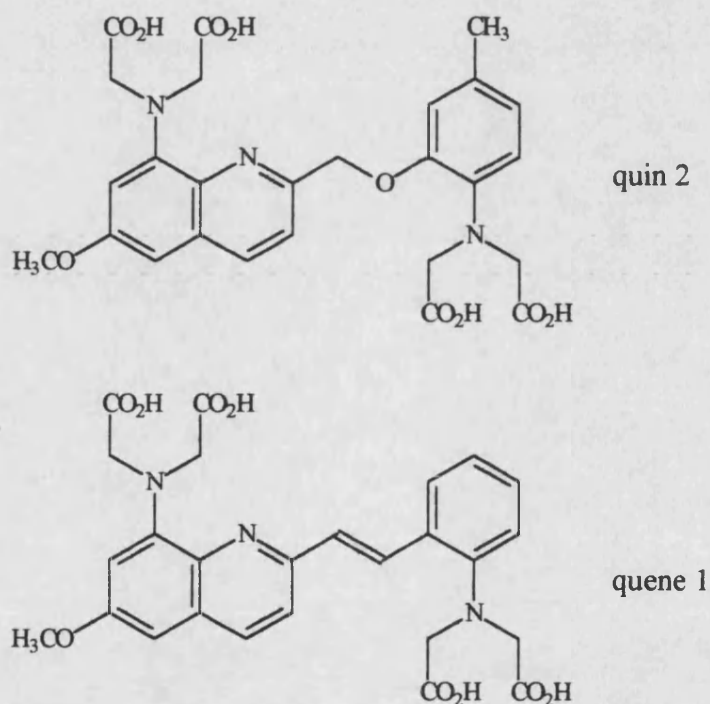


Figure 9. Structures of quin 2 and quene 1.

One of the first fluorescent compounds to be used as a pH_i probe was fluorescein. This exhibits a pH-dependent absorption spectrum between pH 3.0 and 8.0 with maxima at 435 and 495 nm, respectively⁴². Fluorescein found much use in the measurement of pH_i until new improved fluorescent probes

were introduced⁴². The design of the first alternative to fluorescein was based on the fluorescent indicator of calcium ion concentration, quin 2⁴⁷.

The new probe⁴⁷, 8-[bis(ethoxycarbonylmethyl)amino]-6-methoxy-2-[*trans*-2-[bis(ethoxycarbonylmethyl)amino]styryl]quinoline, was named quene 1 and is illustrated in Figure 9. Quene 1 has excitation and emission maxima at 390 and 530 nm respectively, and shows a 30-fold increase in fluorescence between pH 5 and 9 with a pK_a of 7.3. It is claimed that the fluorescence is insensitive to concentrations of calcium and magnesium ions up to 10^{-4} M and to concentrations of sodium and potassium ions up to 100-200 nM⁷⁴. The indicator is loaded into the cells as its tetra(acetoxymethyl) ester derivative which is hydrolysed in the cells to give the tetracarboxylate anion. The main limitation of this compound is its affinity for cations and a correction factor is often required for the pH_i value. Also, some leakage of the probe has been reported⁷⁴.

A fluorescent probe which has found considerable use in recent years is 2,7-bis(carboxyethyl)-5(6)-carboxyfluorescein (BCECF). Excitation and emission wavelengths are 495 and 525 nm, respectively, and the pK_a is 6.98^{10,53}. The compound is loaded into cells as its membrane-permeable acetoxymethyl ester, BCECF-AM. As with the previous esters of probes, hydrolysis by intracellular esterases releases the BCECF, which will be charged and therefore trapped. Unfortunately, this method of administration is not applicable to bacteria due to a very slow rate of absorption⁵³. Once in the cell, the probe can give a good estimation of pH_i . Calibration of pH_i is required and is usually carried out with the potassium/proton ionophore, nigericin⁷⁵. Nigericin sets pH_i equal to pH_e and fluorescence is measured at varying pH_e .

Recently, carboxy seminaphthorhodafluor-1 (SNARF-1) has emerged as a new pH-sensitive fluorescent probe. This has so far found use in pH_i determination of multidrug resistant cells^{31,32,33}. The potential of this probe requires further

investigation, but the initial reports appear promising.

The advantages of pH-sensitive fluorescent probes include:

- (i) They can be used to detect rapid, transient changes in pH_i .
- (ii) Variations in pH_i can be detected in cell populations using spectrofluorimetry, but also in single cells using fluorescence microscopy¹⁵, or using flow cytometry²³.
- (iii) BCECF appears to have a relatively low toxicity towards most cell types⁵³.

Problems often encountered with this method include:

- (i) Leakage is a major limitation^{32,53}. This will particularly affect the results of long term monitoring experiments. To avoid significant errors, appropriate countermeasures need to be taken. Due to the leakage into the supernatant, each sample needs to be resuspended immediately prior to investigation, however a 5% error in the pH_i value can be obtained after only 10 minutes⁵³. Also, these measures reduce the time resolution of observations and can be inconvenient when studying rapid changes. Leakage of these probes could occur by passive diffusion or active transport. In the case of BCECF, the presence of 4/5 negative charges at physiological pH means that passive diffusion is unlikely. Evidence of an ATP-driven transport system involved in BCECF efflux has been suggested for many bacteria⁵³.
- (ii) Fluorescence can respond to changes other than in pH_i , such as altered partitioning between soluble and membrane phases, and changes in cell volume and organelles.
- (iii) Fluorescence can be quenched by intracellular binding⁵⁰.
- (iv) It has been reported⁷⁶ that a lipophilic fluorescent probe can catalyse photo-oxidation reactions.

The free acid form of BCECF has been used for the measurement of pH_e by fluorescent ratio imaging microscopy (FRIM)¹⁵. Under these conditions the maximum of the emission spectrum was found to be pH-sensitive while the

excitation spectrum was pH-insensitive below 440 nm. Thus, pH_e was determined from the ratio of the two values. The *in vivo* application of this technique shows particular promise, for example in showing the difference between normal and tumour pH_e .

3.4.3 Proton-Controlled "on-off" Switching of Fluorescence.

(i) Aminomethyltetraphenylporphyrin-Tin(IV) Derivatives⁷⁷.

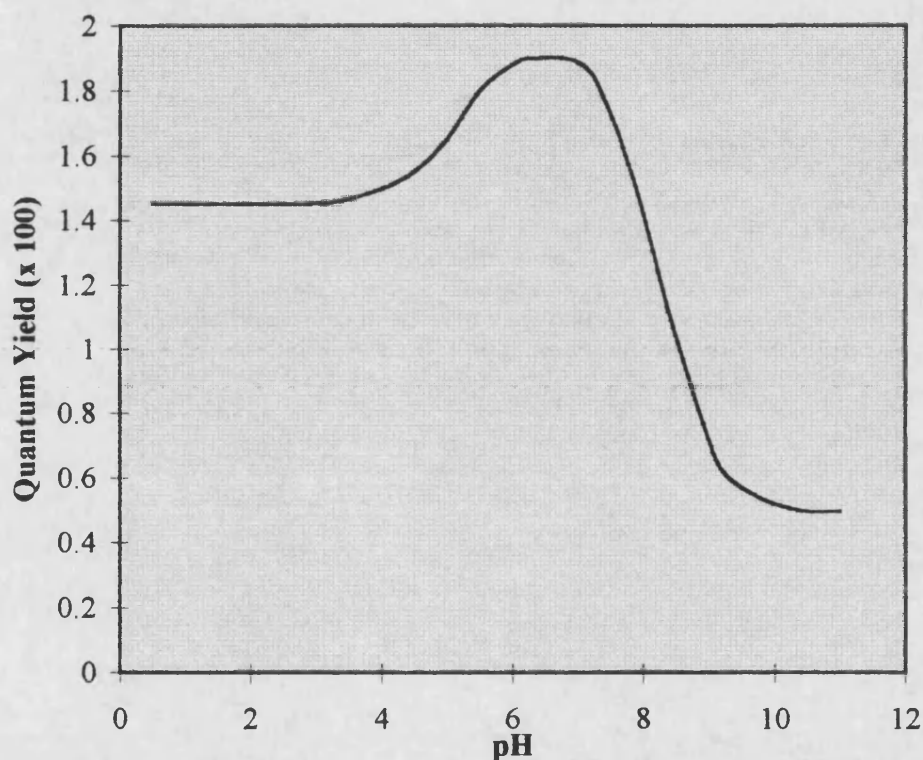


Figure 10. Fluorescence quantum yield vs pH (redrawn from a report by Grigg *et al.*⁷⁷)

For certain complexes, its degree of protonation can determine how important fluorescence will be as a pathway by which to lose excess energy following an electronic transition to an excited state. This can be considered as a proton-controlled "on-off" switching of fluorescence. Grigg and Norbert^{77,78,79} have

synthesised a series of complexes which show luminescent pH sensor activity.

These have fluorescence quantum yield-pH profiles which are composed of two sigmoidal curves of opposite gradients. A typical curve shape is illustrated in Figure 10. Each of the gradients represents a different process of fluorescence quenching. The negative gradient is assignable to a photoinduced electron transfer (PIET) process which takes place between the amino group and the porphyrin moiety when the amino group is not protonated. Examples of these porphyrin-tin(IV) derivatives (I) are shown in Figure 11. The positive gradient is attributed to an axial ligand exchange process across the tin(IV) centre.

For these particular complexes, the proton-controlled changes in the quantum yield (ϕ) occur without alteration of fluorescence band position or vibrational fine structure of fluorescence.

As would be expected for the corresponding parent compound (II) where the amino group is absent, the ϕ -pH profile does not contain the negative gradient of the PIET process.

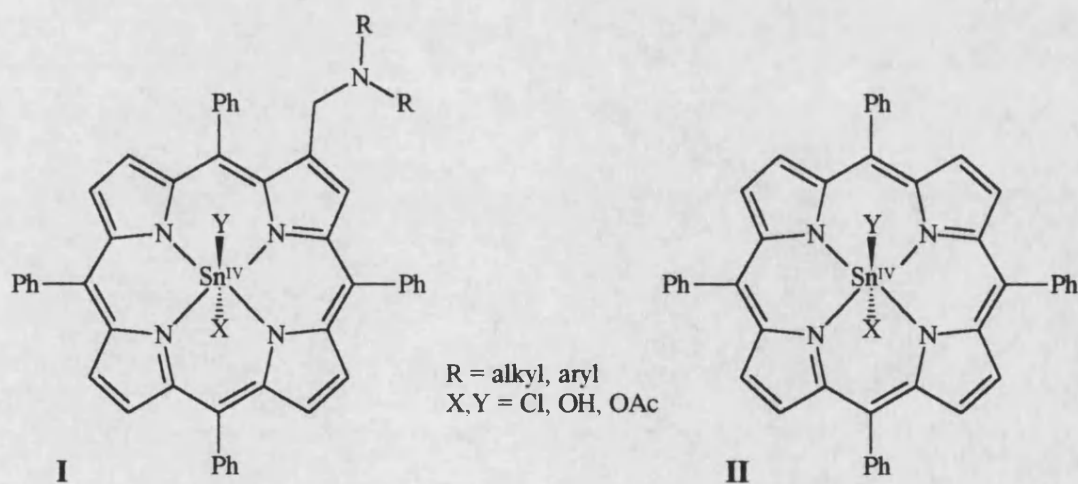


Figure 11. Structures of aminomethyltetraphenylporphyrin-tin(IV) derivatives.

(ii) Aminomethylbipyridyl-Ruthenium(II) Complexes⁷⁸

The complexes illustrated in Figure 12 show proton-controlled quenching of fluorescence by one of two possible mechanisms depending on the attached substituents.

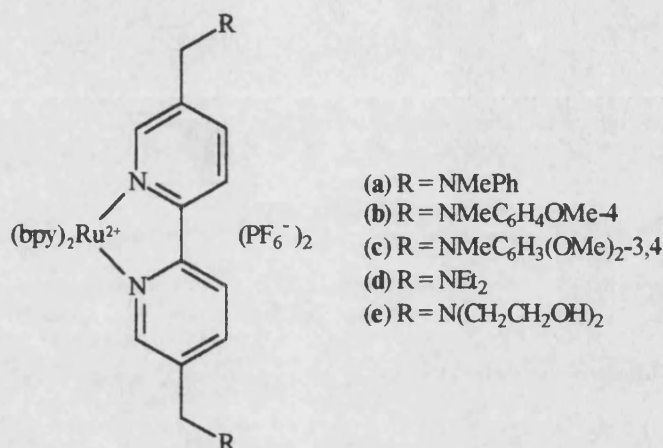


Figure 12. Structures of aminomethylbipyridyl-ruthenium(II) complexes.

For complex (a), the unprotonated form experiences quenching of luminescence by PIET. Conversely, the protonated forms of complexes (b) and (c) have a quenched luminescence by PIET. The protonated and unprotonated forms of complexes (d) and (e) show a negligible quenching of luminescence by PIET, but a substantial quenching arises on protonation due to the generation of a positive charge close to the $[\text{Ru}^{\text{II}}(\text{bpy})_3]^{2+}$ luminophore. As before, a ϕ -pH profile can be constructed for each of these complexes. However, unlike the tin(IV) complexes, the emission maxima of the ruthenium (II) complexes also show pH-dependence. Therefore, two pK_a values can be calculated for each compound corresponding to two different pH profiles.

(iii) *p*-tert-Butylcalix[4]arene-Linked Ruthenium(II) Trisbipyridyl Complexes⁷⁹

These complexes are composed of a trisbipyridylruthenium(II) moiety acting as

the luminophore and free phenolic units of a calix[4]arene as the acid-base site and are illustrated in Figure 13.

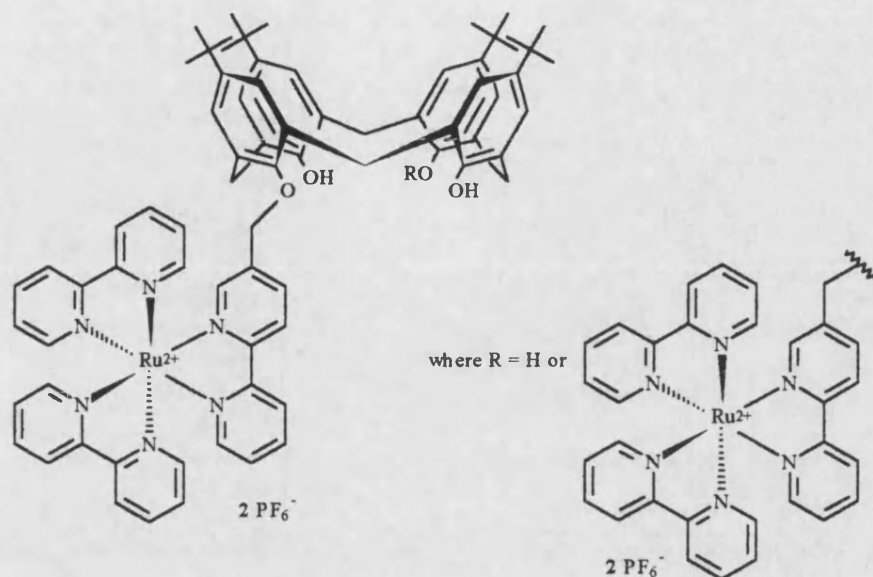


Figure 13. Structure of *p*-tert-butylcalix[4]arene-linked ruthenium(II) trisbipyridyl complexes.

Formation of the phenolate anion(s) causes PIET between the ion(s) and the ruthenium (II) moiety with a quenching of luminescence. A single step ϕ -pH profile can be constructed for each of these complexes and there is no pH-dependent shift in the wavelengths of the maxima in the spectra.

The potential for these complexes to act as pH probes has been demonstrated by Grigg and Norbert^{77,78,79}. However, their application to biological studies has not been evaluated.

3.5 Colourimetry, Using pH-Sensitive Dyes.

It is well established that many compounds undergo a colour change in response to changes in pH. The most widely used colourimetric pH indicator is Neutral Red, as illustrated in Figure 14. This is a relatively non-toxic dye and

has a useful pH range of pH 6.0 (red) to pH 8.0 (yellow). It has the advantages that continuous recording can be made, and rapid changes in pH may be followed as the response of the dye to pH is almost instantaneous, and biopsy of the tissue is not normally required. However, a potential source of error, which affects quantitation of pH_i , is dye-protein binding, since this can affect the activity coefficient of the dye. Additionally, although Neutral Red is reported by most to be non-toxic, effects on glucose metabolism, oxygen consumption, aggregation by the formation of ATP-dye complexes, and systemic cardiovascular changes when the dye has been administered iv. at high concentrations have been reported⁸⁰. Further, the dye has shown a light-activated mutagenic effect through DNA binding, which has become the basis for using the dye in the treatment of recurrent herpes infection⁸⁰. This avid binding of many dyes means that the accurate measurement of pH_i is not feasible⁴².

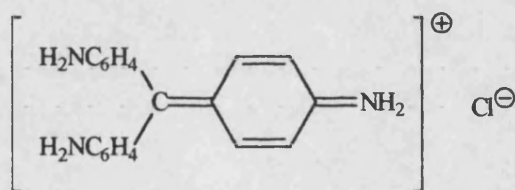


Figure 14. Structure of Neutral Red.

3.6 Microelectrodes.

The principle of microelectrodes is identical to that governing "macro" pH-sensitive glass electrodes. The Hinke-type electrode was the initial breakthrough in microelectrode technology and was first described in 1967⁵⁴. Unfortunately the exposed length of pH-sensitive glass (several hundred micrometres) was too long for most types of cells⁷². Thomas⁸¹ described in 1974 the 1 μm recessed-tip type, but this responds rather slowly and is tedious to make.

In Zurich in 1981, a third type was developed, which depends on a pH-sensitive cocktail⁵⁶. This cocktail is an organic solution sensitive to pH which is held into the tip of a micropipette made hydrophobic by treatment with silanes. However, when the tip of the microelectrode is inserted into a cell, it is separated from the exterior by the cell membrane and hence the potential of the electrode will be determined not only by the pH_i but also by the membrane potential. Therefore, a second electrode is needed to measure membrane potential alone and a "double-barrelled" version was developed⁷² in 1983. This electrode is very similar to the single-barrelled recessed tip electrode, except that the simultaneous measurement of the membrane potential and the pH_i gives a better indication of the intracellular location of the electrode tip.

This method is obviously rather destructive in nature and an inherent problem is that the measurements of pH_i provide a composite value of pH with contributions from the interstitial and intravascular pH which are expected to be at least 50% of the measured value^{13,27}. Although microelectrodes can sometimes give an estimate of pH_i (provided that damage to the cell by the probe is minimised), they tend to have a short and rather unreliable life⁵⁴.

3.7 Electron Paramagnetic Resonance.

It has been observed that the electroparamagnetic resonance (EPR) spectra of many radicals are sensitive to the pH of the medium⁸². pH-sensitive nitroxyl radicals have been put forward as the most promising for pH studies in biological systems. The EPR spectra of dihydro-imidazole and imidazolidine radicals appears to be particularly sensitive to pH, due to protonation of the N-3 atom of the radical heterocycle.

Berezina *et al.*⁸² investigated the potential of dihydroimidazoles for use as pH-sensitive probes. It was revealed that compounds such as the paramagnetic aldonitrane (I), shown in Figure 15, are limited to the pH range 2 to 5.

However, attachment of amine substituents into the 4-position allowed successful manipulation of the pK_a to allow measurement in the pH range 3.3 to 7.8. Examples of the modified compounds (**II**, **III**) are shown in Figure 15.

Little biological work has been carried out on these compounds, therefore their suitability as pH_i indicators has yet to be determined.

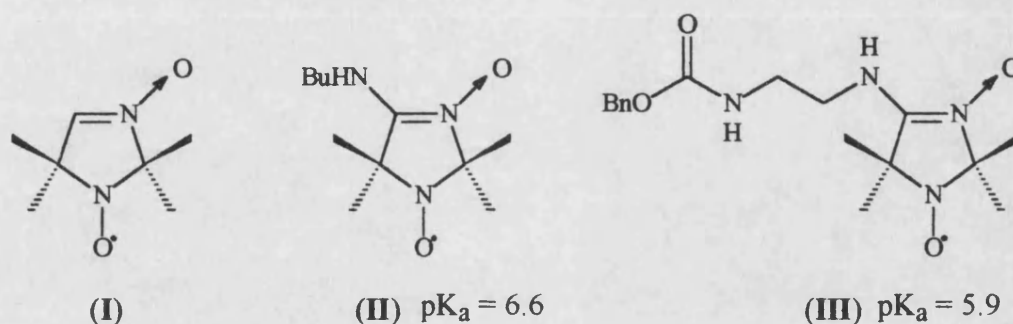


Figure 15. Structures of aldonitrane and related compounds.

3.8 Nuclear Magnetic Resonance.

3.8.1 Introduction.

NMR spectroscopy is non-destructive, non-invasive, relatively non-perturbing and a fairly painless technique for patients. It has the advantage that a particular tissue can be monitored over a period of time. This can be useful for studying changes of pH in disease states before, during and after therapy. Its major limitation is expense. A variety of nuclei have been reported in the literature^{83,84,85,86} to show pH-dependent chemical shifts in the physiological range. These include, ^{31}P , ^1H , ^{15}N and ^{19}F .

3.8.2 ^{31}P NMR.

The naturally abundant ^{31}P nucleus has a fairly wide chemical shift range and

although it is only 0.066 fold as sensitive as ^1H , it has proved to be particularly useful for biological NMR studies. Many phosphorus containing compounds occupy a central role in the bioenergetics of living cell³⁹. In 1975, Moon and Richards⁸³ were the first to demonstrate that the pH-sensitive ^{31}P chemical shift of "inorganic phosphate" (P_i) could serve as a useful probe of pH_i in biological systems.

Measurement of pH_i is generally carried out by determining the difference in chemical shift between the endogenous P_i resonance, which is regulated by the phosphate buffer system, and the resonance of endogenous phosphocreatine (PCr), which is insensitive to pH over the biological range⁵².

Initially, Moon and Richards used 2,3-diphosphoglycerate as the internal standard, but discovered that its chemical shift is influenced by other factors and that most systems do not contain significant concentrations. They suggested the use of PCr and ATP, although since then, ATP has also been proved unsuitable because of its dependence on the Mg^{2+} concentration and the presence of other resonances which result in peak broadening.

In the phosphate buffer system, illustrated in Figure 16, the H_2PO_4^- conjugate acid and the HPO_4^{2-} conjugate base are in rapid exchange⁴ in the range pH 6.1 to pH 7.7. Hence, the corresponding ^{31}P NMR signal appears as a single line at a chemical shift determined by the weighted mean of the relative concentrations of the two species, thus, by the pH of the solution.

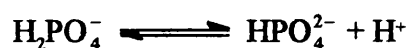


Figure 16. The phosphate buffer system.

An *in vitro* calibration curve is constructed by simple titration and, assuming that such an *in vitro* standardisation curve is applicable to intracellular fluid, pH_i can be obtained from the chemical shift of P_i .

Limitations of this method include:

(i) For the accurate assignment of the P_i chemical shift, a reference signal is required. External standards should be avoided for biological studies because they may lie in a different field due to B_0 (strength of the applied magnetic field) inhomogeneity and local susceptibility effects³⁵. PCr is the usual choice, but the concentrations of PCr are generally so low as to make the ^{31}P signal undetectable in most tumours^{26,34} and in the kidney⁸⁷. It has been suggested that PCr resonances recorded in many tumour spectra are caused by adjacent muscle tissue, overlying skin or infiltrating lymphocytes and endothelial cells rather than the tumour itself²². If this is the case, then the position of the PCr peak is not "tumour specific" and may be experiencing a different B_0 field due to local susceptibility effects³⁵. Therefore, the H_2O peak from the proton spectrum used for shimming is often the reference of choice. This is generally satisfactory provided that the reference signal is derived from the same region of tissue as the P_i signal. Unfortunately, this technique of referencing is not well understood by many research groups²². Alternative methods for reference include the glycerophosphorylcholine resonance but this requires the proton decoupling to resolve the peak. Decoupling requires energy which can be damaging to tissue.

(ii) The P_i peak is often not clearly visible. Low levels of P_i have been reported for many cell types^{88,89} and often in well perfused tissues⁹⁰. The P_i may also be masked by phosphodiester (PDE) signals⁹⁰. The peak is often broad and not resolved into intra- and extracellular compartments. This means that most measurements of pH_i by ^{31}P NMR give a composite pH value with contributions from pH_i expected to be at least 85% of the total¹³, resulting in a large standard error^{16,91}. When multiple P_i peaks do occur, assignment is usually unsuccessful²⁶.

(iii) The P_i resonance can be influenced by factors other than the pH. The concentration of Mg^{2+} in some cell types is high enough to affect the chemical shift. The ionic strength, protein solvation and temperature can also have an influence⁹⁰. Uncertainty about the effects of substances on the chemical shift of P_i introduce errors between 0.1 and 0.5 pH units^{85,92,93}.

(iv) The cellular pH may extend beyond the pH range of P_i . For example, under severe hypoxia⁹⁰.

(v) Poor signal to noise ratio (SNR). This can be due to low concentrations of phosphorus and, to some extent, the relatively low sensitivity of ^{31}P . It introduces two major problems³⁵. Firstly, recognition of peaks becomes difficult and statistical methods are usually applied. Secondly, there is an uncertainty in the position of identified peaks. Poor line shapes and SNR's often mean that mathematical fitting of the data is necessary to measure the peak position³⁵. The broad base line introduced by the presence of the peaks from the phosphomonoesters (PME), PDE and phospholipids may result in an apparent shift in the P_i resonance. Additionally, the magnitude of this shift is expected to vary in different patients, in different tissues and also during tumour therapy where the contribution from PME and PDE will change with regression of the tumour³⁵.

pH_e can also be measured using ^{31}P NMR if an extracellular marker is used. This marker must have a distinct spectral peak position, be non-cytotoxic, have an appropriate pK_a and be largely excluded from the cell. Phosphonic acids, such as phenylphosphonic acid (PPA), have been proposed as extracellular markers in the study of perfused skeletal muscle⁹⁴. However, proof of their confinement in the extracellular fluid over prolonged perfusion periods has not been provided. Further, effects of PPA concentrations and exposure time on muscle contractability, for example, have not been assessed. In order to distinguish the pH of intra- and extracellular compartments using ^{31}P NMR, a

difference of at least 0.3 - 0.4 pH units is normally required. Another method used to distinguish pH_i and pH_e is by comparing spin-lattice relaxation times (T_1) for P_i .

3.8.3 ^1H NMR.

Although ^1H NMR has the advantage of high sensitivity, it is technically more difficult than less abundant nuclei because of the need to suppress the water and fat signals, and also because of the multiple overlapping of metabolite resonances^{5,90}. Surprisingly, despite its obvious drawbacks, ^1H NMR has been used for pH_i determination.

^1H NMR studies of human erythrocytes have been carried out, where pH_i was estimated from the chemical shift of histidine resonances in haemoglobin⁹⁵. However, this method was not straightforward because of the acid dependence of the histidine chemical shifts on the oxy-deoxy status of the haemoglobin⁹⁶.

The first ^1H NMR "probe" to be used for pH_i determination was based on the pH-dependent chemical shifts of imidazole protons⁸⁴. In the initial study⁸⁴, imidazole was introduced into erythrocytes by incubation. Calibration was carried out by ^1H NMR measurements on cell lysates at pH values varied by the addition of aqueous hydrochloric acid or sodium hydroxide solutions and measured directly with a glass electrode. To select the peaks required, ^1H NMR spectra were measured by either a spin-echo method or by a transfer of saturation technique. A single pulse technique is not suitable due to a large number of haemoglobin imidazole resonances which are also visible by this method. The resonances for imidazole 2-H and 4,5-H protons are all pH-dependent with the pK_a values determined to be 7.10 and 7.06 at 37°C respectively. The difference between these two values shows an error in the technique. This early study with erythrocytes highlighted a number of limitations associated with this method. Interactions with cellular substituents

were encountered which affected the imidazole 2-H and 4,5-H proton resonances differently. Also, initially there were two signals for the 2-H proton representing intra- and extracellular compartments. However, these signals coalesced with time into a single resonance peak, indicating that the membrane was sufficiently permeable to both ionised and non-ionised forms of the imidazole to eventually lead to an equilibrium between compartments.

The only other ^1H NMR probe for pH_i , so far, is that developed by Ballesteros *et al.*⁹⁷. This was based on imidazole, with modifications to decrease the membrane permeability of the ionised form and improve its performance as an extrinsic pH_i probe. Acetate, malonate or succinate esters were introduced at the 1-position of imidazole, followed by cleavage to the corresponding acids to increase further the charge of the ionised compound at physiological pH. Examples of these imidazole derivatives are illustrated in Figure 17.

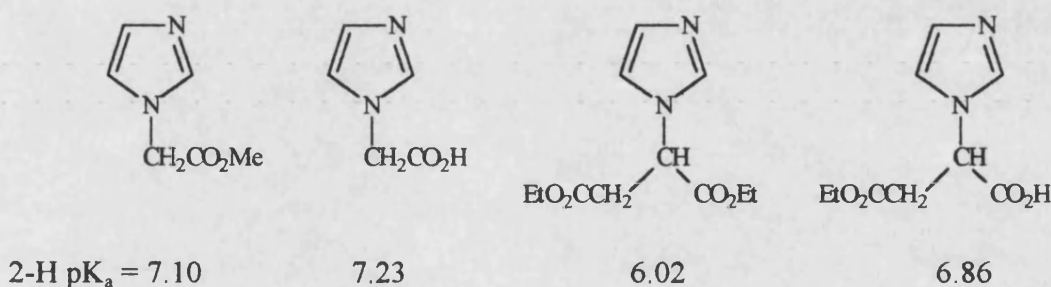


Figure 17. N-Substituted derivatives of imidazole and their corresponding pK_a values.

It can be seen that some of these compounds still contain ester groups. These will generally be cleaved to the corresponding acids once inside the cell, however, not all cells are able to cleave methyl esters. Once again, the chemical shift of the imidazole 2-H proton showed pH-dependence with the pK_a values shown in Figure 17.

It has been demonstrated⁹⁷ that ^1H NMR can be used for the measurement of pH_i . However, the technical expertise required and the large errors introduced

by using such an abundant nucleus, mean that accurate determination of pH_i in biological systems is not feasible by this technique.

3.8.4 ^{15}N NMR.

^{15}N labelled compounds have been used for the measurement of pH using ^{15}N NMR spectroscopy. ^{15}N has the advantage that it shows very substantial chemical shift changes in response to pH^{85} . For example, in the measurement of cytoplasmic and vascular pH in *Neurospora*⁸⁵, using the N3- and N1-nitrogen chemical shifts of histidine, which are very sensitive to pH in the range pH 5 to pH 7.

Another NMR parameter that has been used for pH_i estimation is the line width of proton-coupled ^{15}N resonances of α -amino acids and the guanidine group of arginine. In aqueous solution, the protons attached to these nitrogens undergo base-catalysed exchange with water protons and the rates of exchange increase with pH.

Unfortunately, the N1-nitrogen chemical shift is also dependent on ionic strength, and large quantities of polyphosphates may associate with basic amino acids, introducing an uncertainty of the order of 0.4 pH units⁸⁵. ^{15}N labelled compounds are also very expensive.

3.8.5 ^{19}F NMR.

The naturally occurring ^{19}F nucleus has many NMR properties which make it particularly suitable for biological NMR studies. It has a spin $\frac{1}{2}$ and relatively high sensitivity ($0.833 \times ^1\text{H}$; $12.6 \times ^{31}\text{P}$). Its chemical shifts and relaxation times are very sensitive to changes in its environment and has a wide chemical shift range (0-960 ppm), allowing various fluorinated compounds to be clearly recognised in spite of the line broadening which is often associated with

biological studies. Fluorine is virtually absent from endogenous components of tissue, cells and biological media.

The suitability of ^{19}F NMR for biological work has been shown by its considerable use in metabolism and disposition studies of fluorinated xenobiotics both *in vitro* and *in vivo*^{94,98,99,100}.

The ease of detecting fluorine in biological systems may be illustrated with an example. The tumour selective retention of fluorinated 2-nitroimidazole probes was demonstrated by ^{19}F NMR *in vivo*^{18,37}. Consider the two compounds shown in Figure 18.

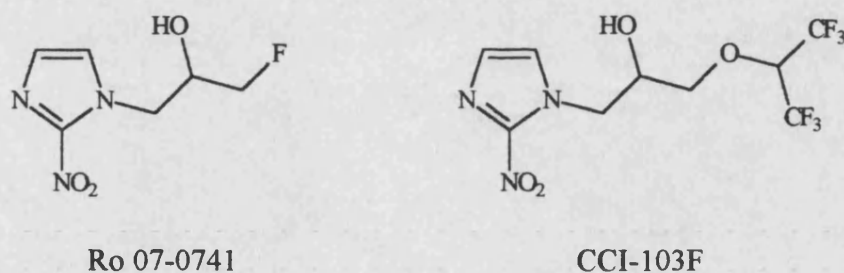


Figure 18. Structures of Ro 07-0741 and CCI-103F.

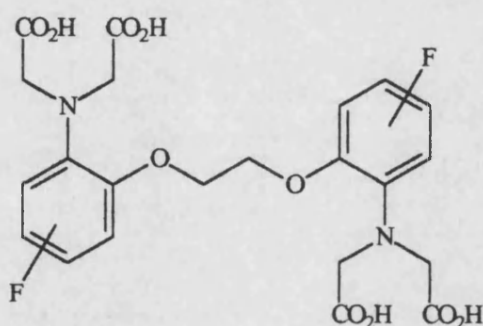
Both the peak for the six fluorine atoms of CCI-103F and the peak for the single fluorine atom of Ro 07-0741 could be clearly identified in the *in vivo* ^{19}F NMR spectra. The estimated practical limits for ^{19}F detection in these studies was in the order of 10^7 atoms of ^{19}F per gram of tissue or 2×10^{-4} molar equivalents of ^{19}F . Moreover, the magnetic field used in the experiments was similar to those routinely used for whole body imaging instruments.

^{19}F NMR chemical shifts are highly sensitive to changes in environment. These include pH, temperature, solvent and ionic strength¹⁰⁰ in addition to the chemical and magnetic environment within the molecule itself.

In Chapter One the sensitivity of the ^{19}F NMR spectrum of 5-fluorouracil to its

adopted geometry once incorporated into DNA was discussed^{29,30}. ^{19}F NMR has become an important probe of base pairing within DNA¹⁰¹ and for the labelling of mRNA¹⁰² and tRNA¹⁰³.

Another exploitation of the sensitivity of ^{19}F chemical shifts has been for the probing of various ions in biological systems. Difluoro-derivatives of 1,2-bis(*o*-aminophenoxy)ethane- N,N,N',N' -tetraacetic acid (*n*FBAPTA), shown in Figure 19, have chemical shifts which are highly sensitive to chelation by divalent cations (M^{2+})⁸⁶.



*n*FBAPTA (The position of the fluorine atom on each ring is denoted by *n*)

Figure 19. Structure of difluoro-derivatives of 1,2-bis(*o*-aminophenoxy)ethane- N,N,N',N' -tetraacetic acid.

An increased understanding of the sensitivity of ^{19}F chemical shifts has allowed the design of more specific ion probes. Indicators for intracellular Mg^{2+} have been developed, based on the chelator *o*-aminophenol- N,N,O -triacetic acid (APTRA)¹⁰⁴. Examples of these fluorinated derivatives are illustrated in Figure 20. These probes have been designed in such a way that chelation of magnesium leads to observation of separate resonances corresponding to complexed and free chelator. However, in most cases chelation of calcium only leads to a broadening and a slight shift of the resonance¹⁰⁴.

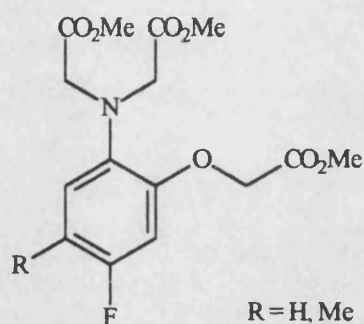


Figure 20. Structures of fluorinated derivatives of the chelator *o*-aminophenol-*N,N,O*-triacetic acid.

These chelators have the advantage of providing a direct identification of the bound ions. Other methods for the measurement of divalent cations in biological systems include indirect calculations based on equilibrium systems, ion-sensitive microelectrodes and null point measurements using metallochromic dyes that are micro-injected into cells or placed into the extracellular space, with frequent lysis of cells. Virtually all of these methods are invasive in nature and require sample destruction prior to analysis. In contrast, NMR has considerable advantage as a non-invasive tool. Furthermore, the ability to carry out studies on opaque cell suspensions and tissues, inaccessible to fluorescent measurements, was highlighted by these cation probes.

The suitability of fluorinated compounds for use as biological probes can, therefore, be easily supported.

The ^{19}F chemical shift can also be sensitive to pH, particularly if the fluorine atom is located near an acidic or basic functional group in a molecule⁸⁶. This phenomenon was first successfully exploited by Deutsch and Taylor in 1981, who have since developed a number of pH probes¹⁰⁵.

They initially used the ^{19}F resonance of trifluoroethylamine for the

measurement of transmembrane pH gradients¹⁰⁵. At 25°C a single broad peak was observed due to rapid exchange of $\text{CF}_3\text{CH}_2\text{NH}_2$ across the membrane. It was necessary for the temperature to be lowered to 4°C before two separate signals could be observed. At this temperature, the pK_a was 6.0, which was far from optimal. However, this early experiment showed that the development of fluorinated probes with pH-dependent chemical shifts is a worthwhile goal.

The next series of experiments investigated the ^{19}F NMR resonances of fluorinated α -methylamino acids¹⁴. In studies on human peripheral blood lymphocytes, (\pm)-2-amino-3,3-difluoro-2-methylpropanoic acid was used for the estimation of pH_i . The methyl ester of this compound was taken up readily by the cells and cleaved to release the free acid inside the cell. The amino acid was present at concentrations as high as 4-5 mM and pH_i determination was possible following relatively short measurement times (1-5 minutes). Unfortunately, leakage of the probe and interactions with intracellular potassium ions lead to complications. However, the results reported were comparable to those obtained using the distribution of radiolabelled DMO in parallel experiments¹⁴.

In later work, a series of such probes were evaluated^{43,52,76}. The reported⁷⁶ pK_a values of these compounds are given in Table 1. As can be seen, these probes cover a large range of pK_a values. In addition, they were specifically designed to be non-metabolisable and non-toxic. The measurements of pH_i with an accuracy of ± 0.06 pH units required the simultaneous use of two of these probes.

Fluorinated Probe	pK _a	change in δ_F /0.1 pH unit
α -trifluoromethylalanine methyl ester	<4	
α -trifluoromethylalanine	5.9	0.12
hexafluorovaline	6.3	0.06
α -difluoromethylalanine methyl ester	5.1	0.14
α -difluoromethylalanine	7.3	0.09
α -monofluoromethylalanine methyl ester	6.4	0.08
α -monofluoromethylalanine	8.5	0.11

Table 1

The major limitation of these probes is the use of methyl esters. As mentioned earlier, not all cells are able to hydrolyse methyl esters^{76,106}. Deutsch and Taylor realised this problem and examined the 4-chlorophenyl esters of fluorinated α -methylamino acids¹⁰⁶. An example is illustrated in Figure 21, which was cleaved rapidly in cells which lack methyl esterases to generate high intracellular levels of the probe. No stereochemical information was provided in these reports^{76,106}. Different diastereoisomers will have different sensitivities of the ^{19}F chemical shift to pH.

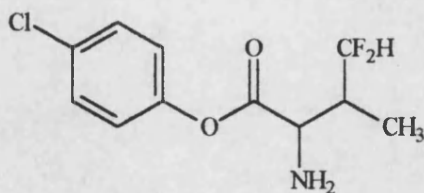


Figure 21. Structure of the 4-chlorophenyl ester of 2-amino-4,4-difluoro-3-methylbutanoic acid.

The next development by Deutsch and Taylor was the use of fluoroanilines as ^{19}F NMR pH indicators¹⁰⁷. Probes were designed such that the fluorine atoms were directly attached to the aromatic ring. This class of compounds has pK_a

values ranging from pH 1 to 6 and total shifts of the ^{19}F resonance from 5 to 15 ppm between the conjugate acid and base. Therefore, a series of probes was investigated with various functional groups attached for the modulation of the pK_a . Figure 22 illustrates the two main strategies used to shift the pK_a of compound (I).

As shown in compound (II), the addition of an electron donating group into the aromatic ring had little appreciable effect on the pK_a and was in the wrong direction. An electron withdrawing group such as a trifluoromethyl group would have been more appropriate. However, N-alkylation, as with compound (III) produced a pK_a slightly closer to physiological pH. The fluoroanilines are very sensitive to pH, with changes in chemical shift of up to 5 ppm per pH unit near the pK_a . This clearly demonstrates the great sensitivity of ^{19}F chemical shift to pH. These examples of fluoroanilines are purely model compounds and have not yet been evaluated *in situ*.

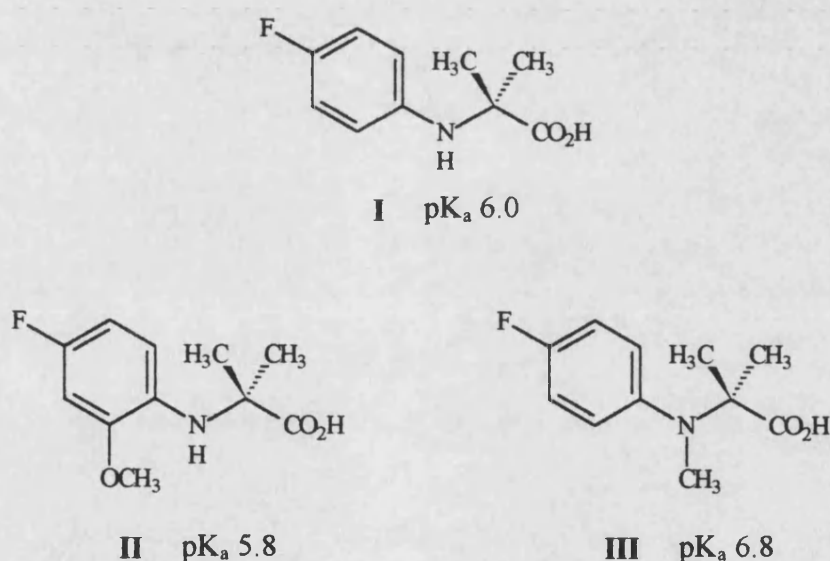


Figure 22. Structures of 4-fluoroaniline derivatives.

Deutsch and Taylor virtually dominated all published research into ^{19}F NMR pH probes in the 1980s but, lately, new probes have begun to appear from other research groups.

Recently demonstrated was the attachment of fluorinated pH indicators to carrier polymers as a means to targetting a probe⁹⁰. This has the advantage that the biological toxicity associated with the pH marker may be masked or altered upon coupling to non-toxic carrier polymers.

Macromolecules such as albumins, globulins, dextrans, and synthetic polymers (for example, polylysine) accumulate in tumour tissue because these tissues have a vascular network characterised by both enhanced permeability of the neovasculature and a lack of lymphatic recovery system. For example, Mehta *et al.*⁹⁰ attached ¹⁹F NMR indicators, such as 3-fluorosalicylaldehyde (3-FSA), to various macromolecules, mainly dextrans. The polymer 3-FSA conjugates had chemical shift sensitivities of 1.36 to 1.41 ppm over a pH range of pH 5.5 to pH 8.5 and a physiological pK_a (*ca.* pH 7.0 to pH 7.2). Unfortunately, this response was not as good as that for the parent probe, 3-FSA which had a chemical shift sensitivity of 2.05 ppm over the pH range.

The same research group have recently reported¹⁰⁸ another possible pH_i indicator based on the vitamin B6 analogue, 6-fluoropyridoxol (6-FPOL), shown in Figure 23.

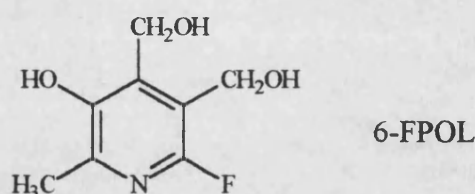


Figure 23. Structure of 6-FPOL

The ¹⁹F resonance of 6-FPOL was shown to be highly sensitive to pH, with a shift of 9.76 ppm between conjugate acid and base, and a pK_a of approximately 8.2 at 37°C. This shift appears to be independent of metal ion concentrations. It was demonstrated that 6-FPOL is permeable across the cell membrane of red

blood cells, with an exchange rate sufficiently slow to provide separate resonances for intra- and extracellular compartments. A sharp signal is observed for each compartment. These measurements on red blood cells compared favourably with those obtained from ^{31}P NMR (pH_i) and pH electrodes (pH_e). Studies *in vivo* are currently in progress, however it would be expected that the sensitivity of detection may be hindered due to there only being one fluorine atom per molecule.

Frenzel *et al.*⁹ have recently suggested that 3-(N-(4-fluoro-2-trifluoromethylphenyl)sulphamoyl)propanoic acid could be a useful ^{19}F NMR pH probe in biological systems. This compound, shown in Figure 24, contains a fluorine atom directly attached to the aromatic ring, which is very sensitive to changes in pH; 5.3 ppm per pH unit close to the pK_a . Also attached to the ring is a trifluoromethyl group which was reported to be "almost" unaffected by changes in pH, and was used as an internal standard. The pK_a was found to be 7.16 (this is worth comparing with the attempt by Deutsch and Taylor¹⁰⁷ to modulate the pK_a of fluoroanilines, in Figure 22).

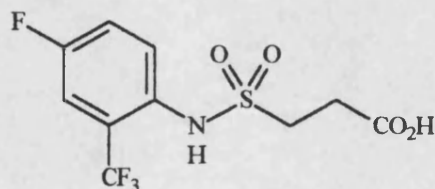


Figure 24. Structure of 3-(N-(4-fluoro-2-trifluoromethylphenyl)-sulphamoyl)propanoic acid.

As may be appreciated from Figure 24, this compound will be ionised at physiological pH. Consequently, the probe was reported to be distributed mainly in the extracellular space and thus provides a measurement of pH_e . The probe was tested by a study of tumour pH_e . Both the fluorine signals were clearly visible *in vivo* and provided values which were in good agreement to those provided by microelectrodes.

Finally, Plenio *et al.*¹⁰⁹ reported that the ^{19}F resonance of 1-fluoro-2,6-bis(methylene-iminodiacetate)benzene, shown in Figure 25, is highly sensitive to changes in pH. They suggested that this compound could be used as a pH probe. Unfortunately, this compound was originally designed as an indicator for metal ions with direct fluorine-metal interactions and is clearly not suitable for accurate pH determination in biological systems. However, this does highlight an important design consideration for ^{19}F NMR pH probes. That is, the pH sensitive fluorine atoms must not be in close proximity to metal chelating functionalities. Further, the acid-base functional group must have limited interactions with cations other than protons.

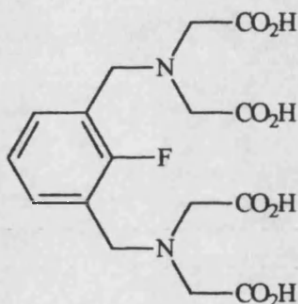


Figure 25. Structure of 1-fluoro-2,6-bis(methylene-iminodiacetate)benzene.

Most of the studies discussed above have been limited to compounds possessing only one pH-sensitive atom. This can lead to relatively poor sensitivity of detection of the signal. Also, many of the examples contained fluorine atoms with neighbouring protons. H-F coupling constants are generally very large and can be observed as far as five bonds away. Coupling will result in splitting of peaks in the ^{19}F NMR spectra and hence, poor SNR¹⁰². Also the use of an internal ^{19}F chemical shift standard directly attached to the probe has only recently been investigated⁹. However, the chemical shifts of fluorine atoms in different chemical and magnetic environments will not be affected by pH by the same magnitude. Therefore, it is advisable to incorporate the reference fluorine atom(s) away from the acid-base centre to ensure pH-

insensitivity.

There is definitely a need for an accurate and non-invasive method for the determination of pH_i . The potential of fluorinated compounds to act as pH sensors in biological systems has been demonstrated. However, there is clearly a lack of understanding of the requirements necessary for the development of a pH probe suitable for biological studies. These requirements will be addressed in the next chapter.

CHAPTER FOUR

4. Aims of the Study

The purpose of this study was to design and synthesise fluorine containing compounds and to evaluate their potential as ^{19}F NMR pH_i sensors for biological systems. In order to design a probe of this type, a number of requirements must be considered. The following section examines these requirements and assesses how they can be met.

(i) Easily detectable in biological systems.

This requires a strong signal in the ^{19}F NMR spectrum with a good signal to noise ratio (SNR). The compound must, therefore, have a large number of chemically and magnetically equivalent pH-sensitive fluorine atoms. The SNR is also improved when the signal is a singlet. To avoid H-F coupling the fluorine atoms must be at least 4-5 bonds away from any protons. A slight line broadening may also appear if the fluorine atoms are very close to an element which has more than one naturally abundant isotope, for example chlorine. The isotope effect on ^{19}F resonances can be illustrated with CFCl_3 , a widely accepted ^{19}F NMR chemical shift standard. Careful examination of the apparent singlet reveals four peaks in the characteristic pattern also observed in mass spectrometry.

(ii) Large sensitivity to changes in pH.

The sensitivity of a ^{19}F resonance to pH is usually related to how close the fluorine is to the acid/base functional group. Many of the probes discussed earlier used a single fluorine atom directly attached to an aromatic ring. The acid/base group was either a heteroatom in the ring or another substituent. This produced a highly pH-sensitive ^{19}F resonance. Unfortunately, using only one fluorine atom leads to poor SNR. If trifluoromethyl groups are used there will be a loss in pH-sensitivity. However, this may be worthwhile in order to

increase the SNR and the ease of detection, and thus improve the accuracy of measuring a shift. Greater shifts in ^{19}F resonances may also be obtained if protonation of the probe results in a large conformational change, for example going from an sp^3 centre to sp^2 .

(iii) The influence of factors other than pH on the ^{19}F resonance must be limited.

^{19}F NMR probes specifically designed to chelate with metal ions have been discussed. Examination of these compounds reveals that carboxylic acid groups should be avoided.

(iv) pK_a values should be close to physiological pH.

Evaluation of a large number of compounds provides information about how different functional groups can influence the pK_a . This knowledge allows strategic selection of suitable synthetic targets and the careful modulation of their pK_a .

(v) An internal reference for ^{19}F NMR chemical shift determination.

The incorporation of pH-insensitive fluorine atoms into the probe provides a suitable reference peak. That is, fluorine atoms not positioned next to acids/base functional groups. It would be preferable if the signal was at a distinctly different chemical shift value to that of the pH-sensitive peak. A different number of equivalent fluorine atoms would also aid a positive peak assignment.

(vi) Good water solubility.

The presence of polar functional groups generally increases water solubility. However, groups which may interfere the ^{19}F sensitivity must be placed with care. The influence that the functional groups may have on the pK_a of the probe must also be considered. One possibility is to incorporate a polyether chain.

(vii) An ability to cross a cell membrane and accumulate inside the cell.

To increase cell membrane permeability a careful balance must be made in the choice of functional groups with respect to water solubility. If the probe is highly ionised it may not be able to penetrate the membrane. It may be useful to attach a targetting moiety to the probe. For example, a 2-nitroimidazole group would lead to an accumulation of the probe in hypoxic cells.

(viii) Low toxicity.

If the probe has many equivalent pH-sensitive fluorine atoms rather than just one, lower concentrations of the probe will be required to reach an adequate molar concentration of ^{19}F for detection.

Using these criteria, a series of model probes was designed as synthetic targets. Chemical synthesis has been towards azaheterocycles bearing one or more trifluoromethyl groups. An important synthetic consideration has been the incorporation of a "handle". This could be a point of attachment for linking to targetting moieties and pH-insensitive fluorine containing groups. The pK_a values of many of these compounds has been characterised by ^{19}F NMR.

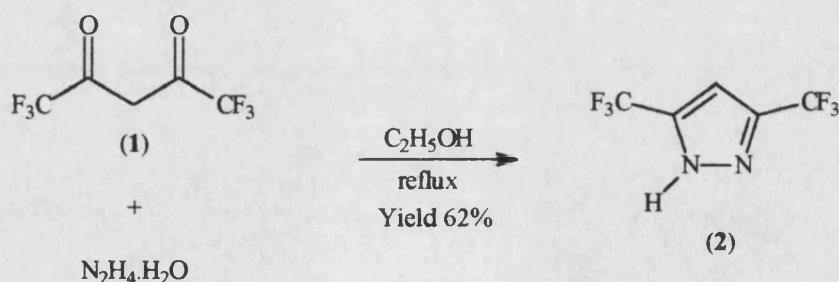
CHAPTER FIVE

5. Pyrazoles.

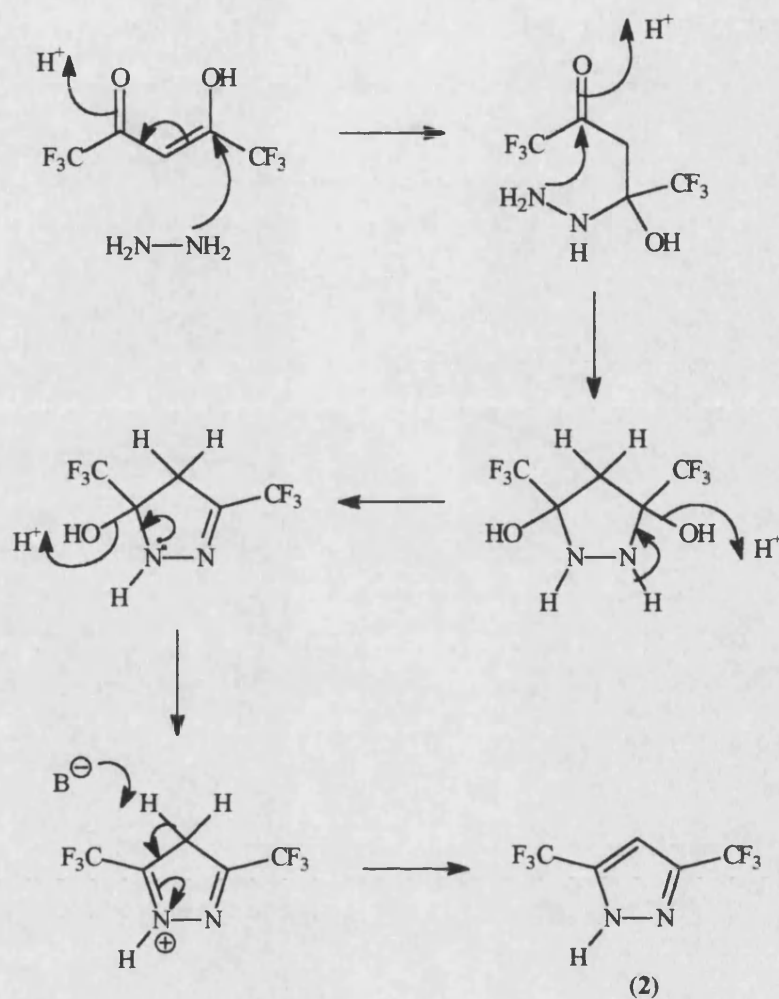
5.1 3,5-Bis(trifluoromethyl)pyrazole and Related Compounds.

5.1.1 3,5-Bis(trifluoromethyl)pyrazole.

Elguero *et al.*¹¹⁰ have investigated the effects of a trifluoromethyl group on the acid-base properties of pyrazoles. It was reported that 3,5-bis(trifluoromethyl)pyrazole (**2**) has an acidic pK_a value of 7.51 at 25°C, determined spectrophotometrically according to a method described by Ernst and Menashi¹¹¹. This compound has six equivalent fluorine atoms and a pK_a value close to physiological pH. Therefore, it is an ideal candidate for the probing nucleus of a ^{19}F NMR pH-sensor. The preparation of 3,5-bis(trifluoromethyl)pyrazole (**2**) has been reported to have been carried out by treatment of 1,1,1,5,5,5-hexafluoropentane-2,4-dione (**1**) with hydrazine hydrate under various conditions^{112,113} and by dipolar cycloaddition of 2-diazo-1,1,1-trifluoroethane with 3,3,3-trifluoropropyne¹¹⁴. The pyrazole (**2**) was synthesised by the treatment of dione (**1**) with an equimolar amount of hydrazine hydrate in boiling ethanol, as shown in Scheme 1.



Scheme 1



Scheme 2

The volatile white solid was obtained in 62% yield. The yield of this reaction strongly depends on the distillation procedure, as observed recently by Venanzi *et al.*¹¹³. It has been suggested¹¹⁵ that the high volatility of pyrazole (2), compared to pyrazoles such as 3,5-dimethylpyrazole, is partly due to the weakening of N-H...H hydrogen bonds between two molecules. This is supported by experimental and theoretical calculations of their solid and gas phase geometries which show interactions between the fluorine atoms and the N1-H (attractive) and the N2 lone pair (repulsive). A possible mechanism for the synthetic reaction is illustrated in Scheme 2. The dione (1) is shown here in its enol form. β -Diketones exist in tautomeric equilibrium between the enol and

keto forms. It is known¹¹⁶ that electron withdrawing groups increase the content of the enol form, while solvents of high polarity will shift the equilibrium back slightly towards the keto form. The presence of two trifluoromethyl groups in dione (1) will have the greatest influence on the equilibrium; thus, the enol is the predominant form under these conditions.

The mechanism proceeds through 3,5-dihydroxypyrazolidine and 5-hydroxy-4,5-dihydropyrazole intermediates which have been characterised by Elguero *et al.*¹¹⁷ using special stop-flow NMR techniques. The participation of the N1 lone pair in the elimination of the second water molecule is supported by the isolation of 5-hydroxy-4,5-dihydropyrazoles when the N1 atom is substituted by an electron-withdrawing group. The isolation of 5-hydroxy-4,5-dihydropyrazoles is a topic of discussion later in this chapter.

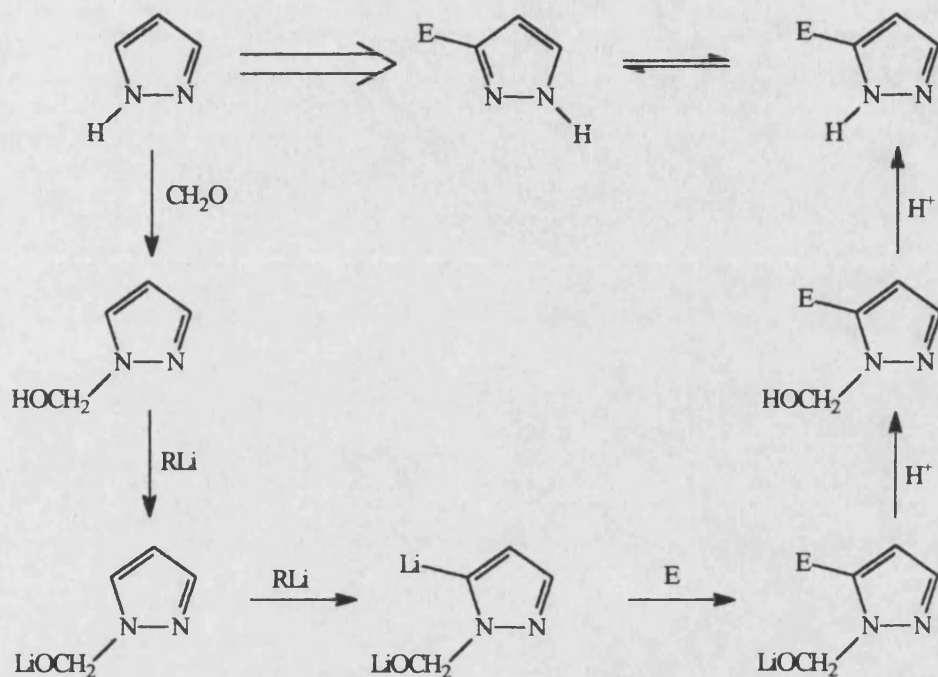
The pK_a was determined by ^{19}F NMR to be 7.55 at 25°C (see Chapter 8). 4-Substituted derivatives of bis(trifluoromethyl)pyrazole (2) would allow the attachment of the other necessary ingredients for a pH-probe such as, a targetting moiety, groups to increase water solubility in aqueous media and pH-insensitive fluorine atoms.

5.1.2 Alkylation of 3,5-Bis(trifluoromethyl)pyrazole.

It was proposed that the 4-position of pyrazole (2) may be activated by lithiation, followed by alkylation with a suitable electrophile.

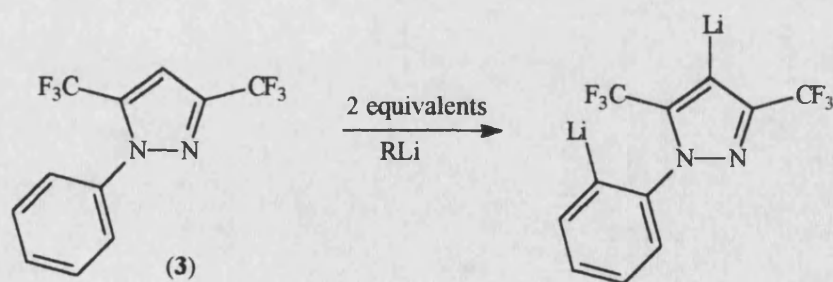
Lithiation of heterocyclic compounds containing an N-H group usually only yields the N-lithio derivative¹¹⁸, but when the nitrogen is substituted, C-lithiation can often occur. If the N-substituent can later be removed, it serves as a protecting group for the N-H, thus maintaining the pK_a of the new pyrazole close to that of the parent pyrazole. Katritzky *et al.*¹¹⁸ have reported a method for a "one-pot" protection, lithiation and alkylation reaction of

pyrazole. Formaldehyde was used as a protecting group for the N-H of pyrazole in the synthesis of 3(5)-substituted pyrazoles, as shown in Scheme 3.



Scheme 3

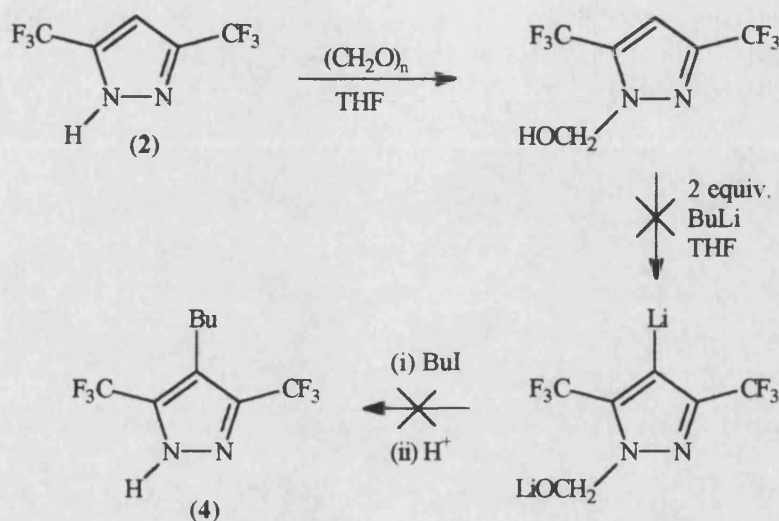
In addition to this, it has been demonstrated by Tanaka *et al.*¹¹⁹ that lithiation of 1-phenyl-3,5-bis(trifluoromethyl)pyrazole (**3**) occurs in the 4-position of the pyrazole ring as well as in the *ortho*-position of the phenyl substituent, as shown in Scheme 4.



Scheme 4

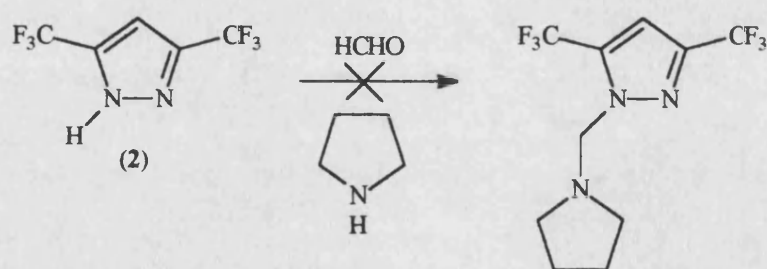
Combining the methods of Katritzky *et al.*¹¹⁸ and Tanaka *et al.*¹¹⁹, the synthetic

route illustrated in Scheme 5 was devised. Unfortunately, this reaction sequence failed to yield any of the 4-substituted pyrazole (4). It is likely that the excess amount of paraformaldehyde and its unsuitability as a protecting group for the pyrazole (2) are to blame.



Scheme 5

Therefore, a "multi-step" synthesis was devised, involving an initial step of N-H protection by lithiation and alkylation by the method of Katritzky *et al.*¹²⁰, as shown in Scheme 6.



Scheme 6

Surprisingly, even this simple N-(dialkylamino)methyl protection of the electron-deficient pyrazole (2) did not work. Therefore, methods of incorporating a 4-substituent into the pyrazole (2) prior to ring closure were

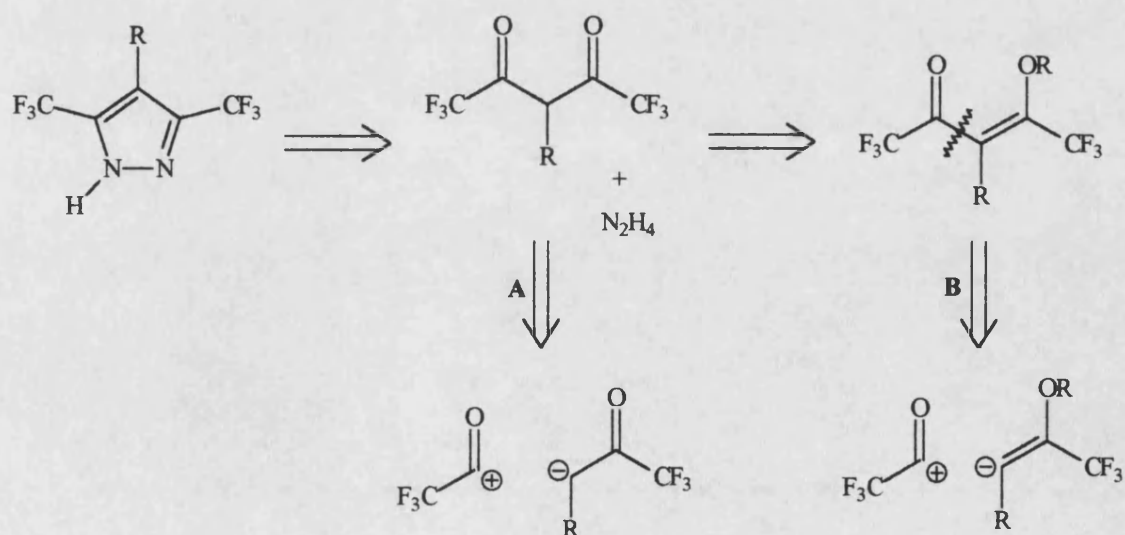
examined.

5.1.3 Alkylation of 1,1,1,5,5,5-Hexafluoropentane-2,4-dione.

If a 4-substituted derivative of the bis(trifluoromethyl)pyrazole (**2**) is to be constructed by a condensation reaction similar to that shown in Scheme 1, then modification of the dione would be the next obvious solution.

A report by Wright and Coville¹²¹, suggested that 1,1,1,5,5,5-hexafluoropentane-2,4-dione (**1**) may be alkylated with an alkyl halide. Heer¹²², a co-worker, briefly investigated this option. The electron-withdrawing effect of the two trifluoromethyl groups of the dione (**1**) allowed a proton from the 3-position to be removed with ease using potassium carbonate. However, the resulting anion was so deactivated by the trifluoromethyl groups that it would not react with benzyl bromide.

5.1.4 Alternative Disconnections Towards the Synthesis of 3-Substituted Derivatives of 1,1,1,5,5,5-Hexafluoropentane-2,4-dione.

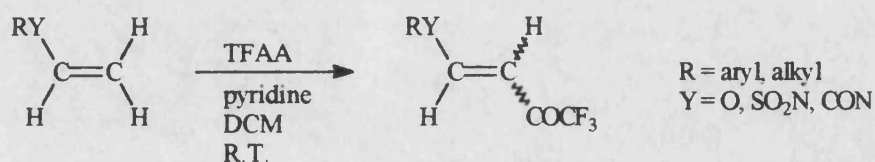


Scheme 7

An alternative point of disconnection is demonstrated by the retrosynthetic analysis shown in Scheme 7. Two possible nucleophiles are suggested in the second disconnection steps; a trifluoromethyl ketone anion (route A) and a trifluoromethyl enol ether nucleophile (route B).

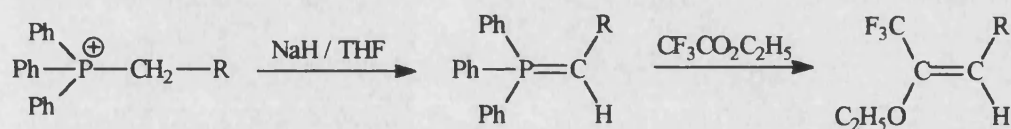
5.1.4.1 Trifluoroacetylation of Trifluoromethyl Enol Ethers.

The trifluoroacetylation of enol ethers has been reported by Hojo *et al.*¹²³ using trifluoroacetic anhydride (TFAA) and pyridine in DCM at room temperature (R.T.), as shown in Scheme 8.



Scheme 8

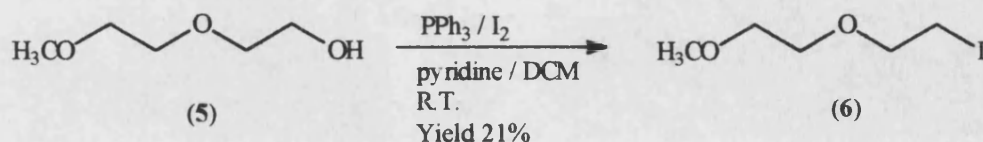
The extension of this reaction to trifluoromethyl enol ethers had not been demonstrated. Therefore, this reaction was investigated as a potential route to 3-substituted derivatives of the dione (1).



Scheme 9

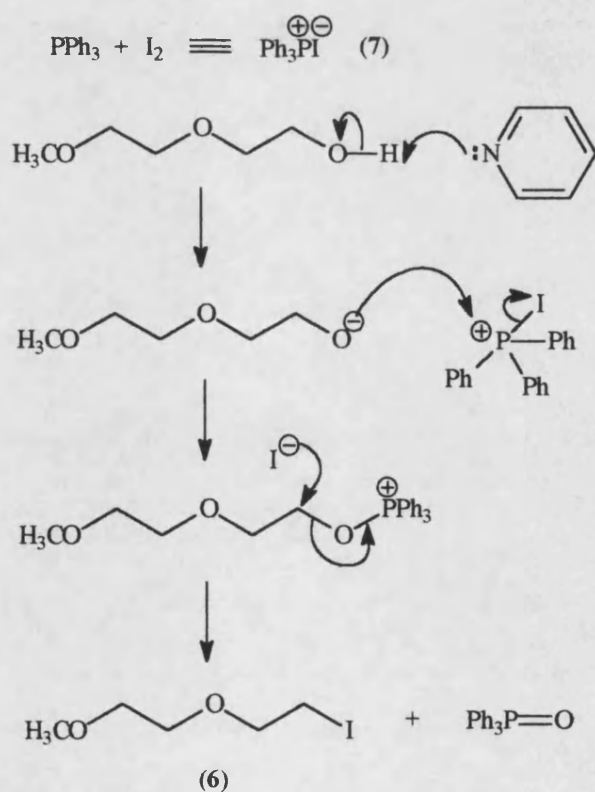
The most conventional method of making an enol ether would be from the corresponding ketone. However, in 1992, Bégué *et al.*¹²⁴ reported a more direct route to the synthesis of trifluoromethyl enol ethers. The preparation involves Wittig reaction of a phosphonium ylide with perfluoroalkyl acid derivatives, which in this case meant ethyl trifluoroacetate, as illustrated in Scheme 9. The phosphonium ylides can be prepared by treatment of the phosphonium salt with a suitably strong, non-nucleophilic base, such as sodium

hydride in THF. A phosphonium salt can be made from its corresponding hydroxy compound *via* its halogenated derivative. The iodide salt was chosen in preference to the bromide salt because it is reputed to be more likely to crystallise.



Scheme 10

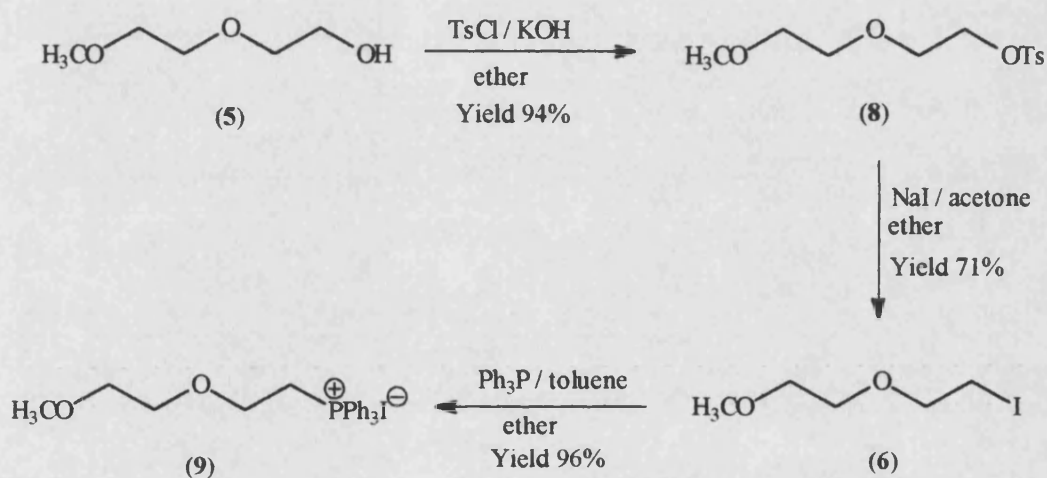
Investigations into this reaction sequence began with a model compound. The hydroxy compound chosen for the trial run was 2-(2-methoxyethoxy)ethanol (5). Its conversion to the iodo derivative (6) was initially carried out by the addition of triphenylphosphine and iodine in the presence of pyridine, as shown in Scheme 10.



Scheme 11

It is currently thought¹²⁵ that such reactions involve the *in situ* formation of triphenylphosphorus-diiodine (7), which then acts as the halogenating agent, Scheme 11.

However, the poor yield (21%) of this reaction was not satisfactory and another approach was sought. As suggested in the mechanism of Scheme 11, despite the fact that iodide is a relatively efficient nucleophile, it is not able to substitute the hydroxy group without activation. Another mode of activation is forming the tosylate first, as shown in Scheme 12.



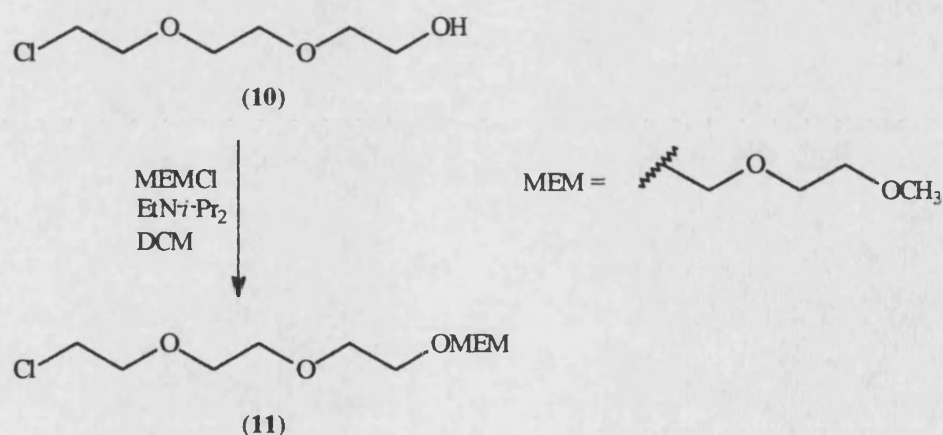
Scheme 12

This was carried out using a method reported by Prugh *et al.*¹²⁶. This method of tosylation is unconventional in that potassium hydroxide is used rather than pyridine. However, the reduced toxicity and the high yield of 94%, suggest it could be a useful alternative. A simple exchange reaction to the iodo-compound (6) was carried out by the Finkelstein reaction, using sodium iodide in acetone, with a good yield of 71%.

The conversion of iodo-compound (6) to the phosphonium salt (9) was accomplished with triphenylphosphine in toluene. As predicted, the phosphonium salt crystallised out and in high yield.

Running parallel with this trial set of experiments, investigations were carried out into suitable protecting groups for a hydroxy function at the non-reacting end of the compound. The 2-methoxyethoxymethyl ether (MEM ether) protecting group appeared to have ideal characteristics for the reaction sequence. It has been reported¹²⁷ to be stable under a wide variety of conditions, including those of reactions attending the use of strong bases, reducing agents, organometallic agents, many oxidising agents, and mild acids.

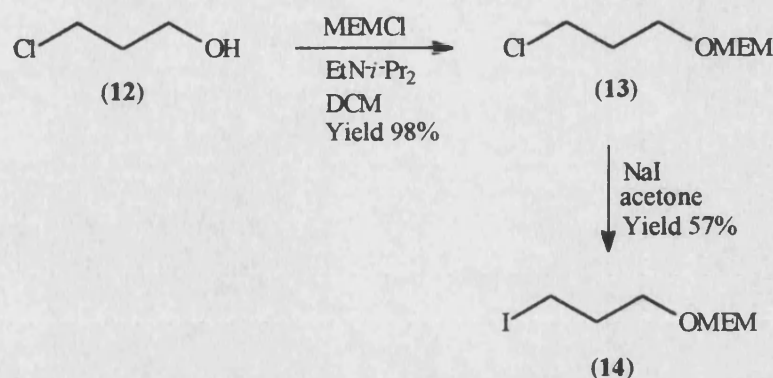
Maintaining the use of compounds containing ether linkages (for enhanced water solubility of the pH-sensor compounds) as with the trial compound, 2-(2-(2-chloroethoxy)ethoxy)ethanol (**10**) was chosen as a starting material. MEM protection of the hydroxy group was performed by the method of Corey *et al.*¹²⁷, Scheme 13.



Scheme 13

The result of this reaction was a very small quantity of product (**11**) and a mixture of dimers, as indicated by the NMR spectra. Due to the expense of the chlorohydrin (**10**), another starting material was used in the modification of reaction conditions and testing of the purity of the MEMCl. The hydroxy function of 3-chloro-1-propanol (**12**) was protected with a MEM group with ease in 98% yield. This was followed by an exchange reaction to the iodo-compound (**14**), again using sodium iodide in acetone in good yield, as shown

in Scheme 14.

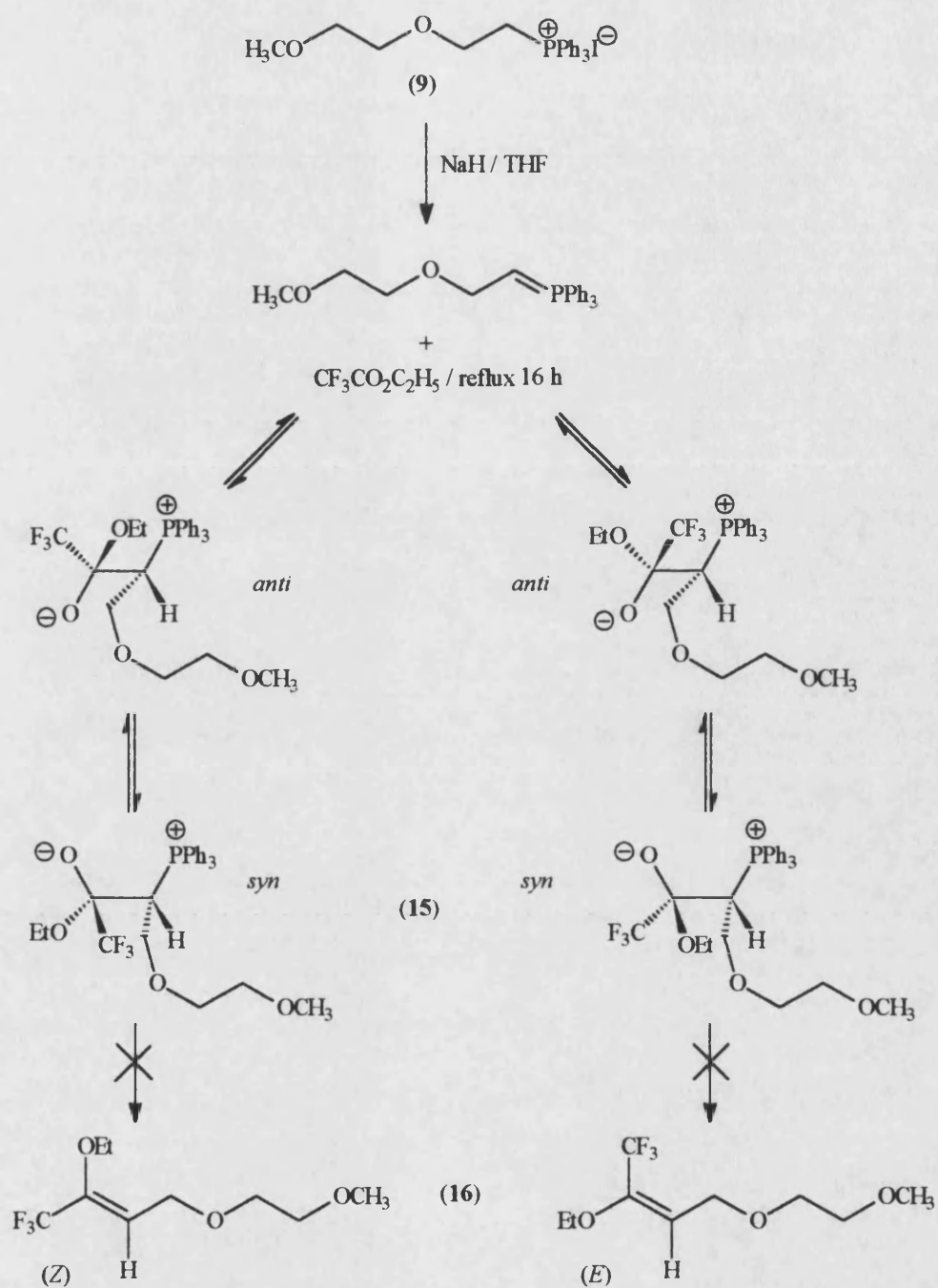


Scheme 14

The moderate yield of the halogen-exchange reaction was explained by the NMR spectra, which indicated that some of the MEM protecting group had been lost, thus making it unsuitable for our reaction sequence. This was unexpected, considering the relatively high stability usually associated with this protecting group¹²⁷.

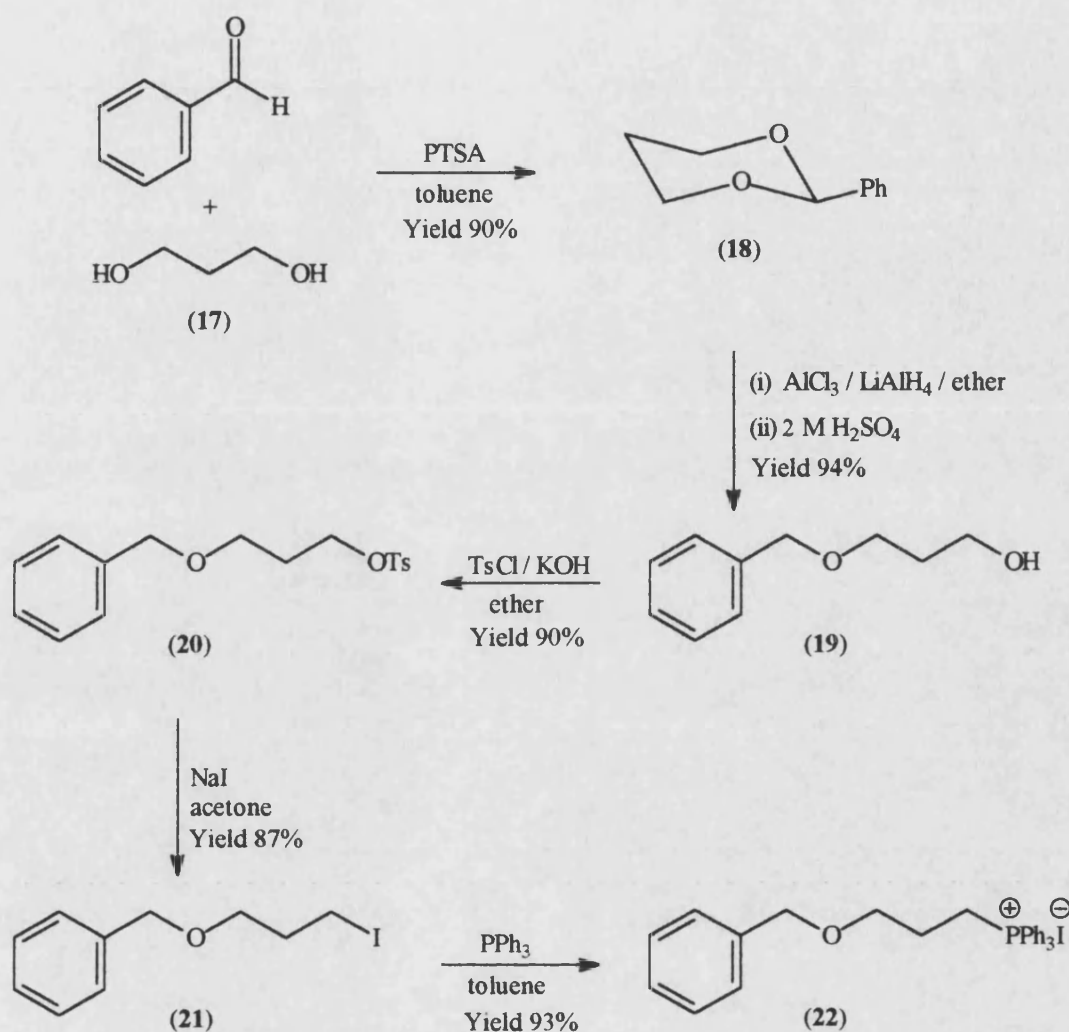
In a parallel series of experiments, the Wittig reaction was attempted with the model phosphonium salt (9), Scheme 15. However, no enol ether (16) was isolated. The spectra of the recovered material corresponded to the betaine intermediate (15), as illustrated in Scheme 15, or another intermediate compound with a very similar structure. The suspected intermediate compound was redissolved in toluene and heated under reflux for 23 h, but no change was observed. Sodium hydride (0.7 equivalents) and hexamethyldisilazane (HMDS) (0.05 molar equivalents) were added and heating was continued for 24 h, after which there was still no change.

The isolation and identification of an intermediate with a structure related to that of the betaine intermediate indicates that the problem does not lie with the reactivity of the alkylidene part of the phosphorane towards the carbonyl group of the ester function. Rather it is the collapse of the betaine to the enol ether



Scheme 15

and triphenylphosphine oxide. The only difference between this starting material and those described by Bégué *et al.*¹²⁴, is the presence of an oxygen atom close to the reacting centre. Assuming that this was in fact the problem, an alternative starting material (22) was synthesised, as illustrated in Scheme 16.

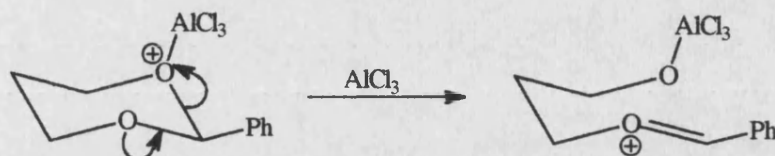


Scheme 16

Once again, a protected hydroxy function was desired, and the more robust benzyl ether group was chosen in preference to MEM ether. 1,3-Propanediol (17) was, therefore, a suitable starting place.

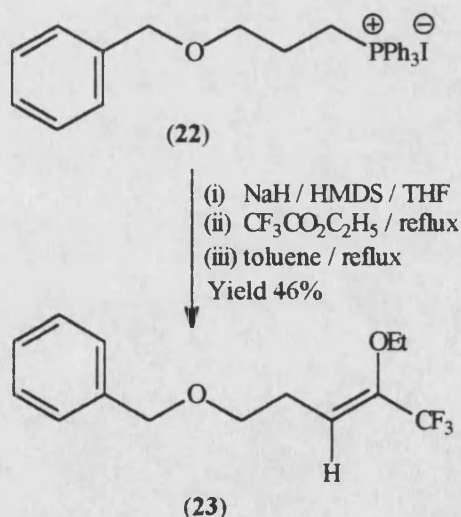
Benzyl ether protection of the hydroxy group is usually carried out by rather drastic conditions (e.g. PhCH_2Cl and KOH at $130\text{--}140^\circ\text{C}$)¹²⁸ although milder conditions are now appearing. In the case of diols, most methods produce a mixture of mono- and disubstituted derivatives and therefore give lower yields and require separation. However, as shown in Scheme 16, the mono-protected diol (19) was synthesised exclusively. This was accomplished by first making

the acetal (**18**), 90% yield, followed by reduction with AlCl_3 / LiAlH_4 in ether¹²⁹, with a 94% yield. In this reaction the AlCl_3 acts as a Lewis acid and opens-up the acetal, as shown in Scheme 17. The resulting intermediate is then reduced by AlH_3 (alane) which is formed *in situ*. The steps to the phosphonium salt (**22**) were carried out as previously described, all with high yields.



Scheme 17

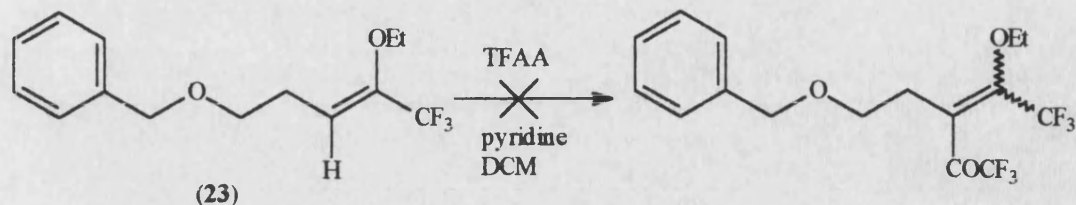
The Wittig reaction with the phosphonium salt (**22**) did eventually work after modification of the reaction conditions. This involved increasing the amount of HMDS to a total of 1.2 equivalents and replacing the THF, after 20 h, with toluene to allow a higher reaction temperature. The moderate yield of 46% was comparable to those reported by Bégué *et al.*¹²⁴ for analogous compounds, Scheme 18.



Scheme 18

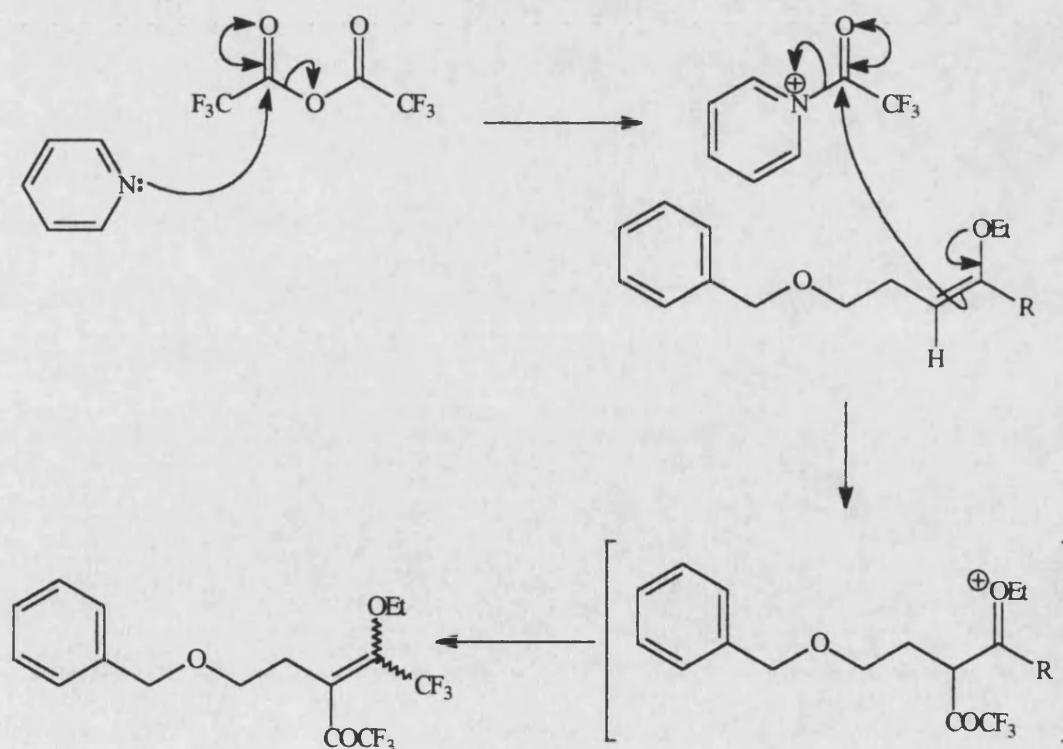
Following our proposed reaction sequence, the next step involved the

trifluoroacetylation of the enol ether (23) by the general method of Hojo *et al.*¹²³, Scheme 19. Unfortunately, even with the addition of 4-dimethylaminopyridine and boiling, the enol ether (23) did not react.



Scheme 19

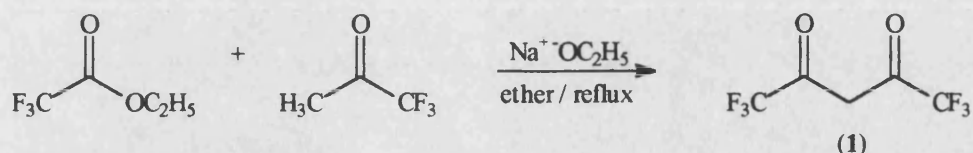
A possible mechanism for this type of reaction could be that illustrated in Scheme 20. When R = H, as with the examples reported by Hojo *et al.*¹²³, the reaction would be expected to work. When R = CF₃, as with our examples, the electron-withdrawing effect of this trifluoromethyl group results in a decrease in the nucleophilicity of the double bond, hence reducing its reactivity towards the electrophilic centre of the acylpyridinium carbonyl group.



Scheme 20

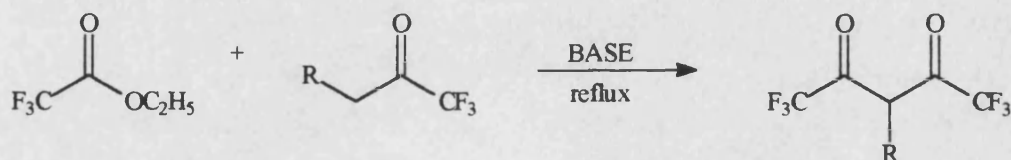
5.1.4.2 Trifluoroacetylation of Trifluoromethyl Ketones.

The classical method for the synthesis of 1,1,1,5,5,5-hexafluoropentane-2,4-dione (**1**) is a Claisen-type reaction described by Henne *et al.*¹³⁰ in 1947. This involved the treatment of ethyl trifluoroacetate with sodium ethoxide in ether followed by the addition of trifluoroacetone, and is shown in Scheme 21.



Scheme 21

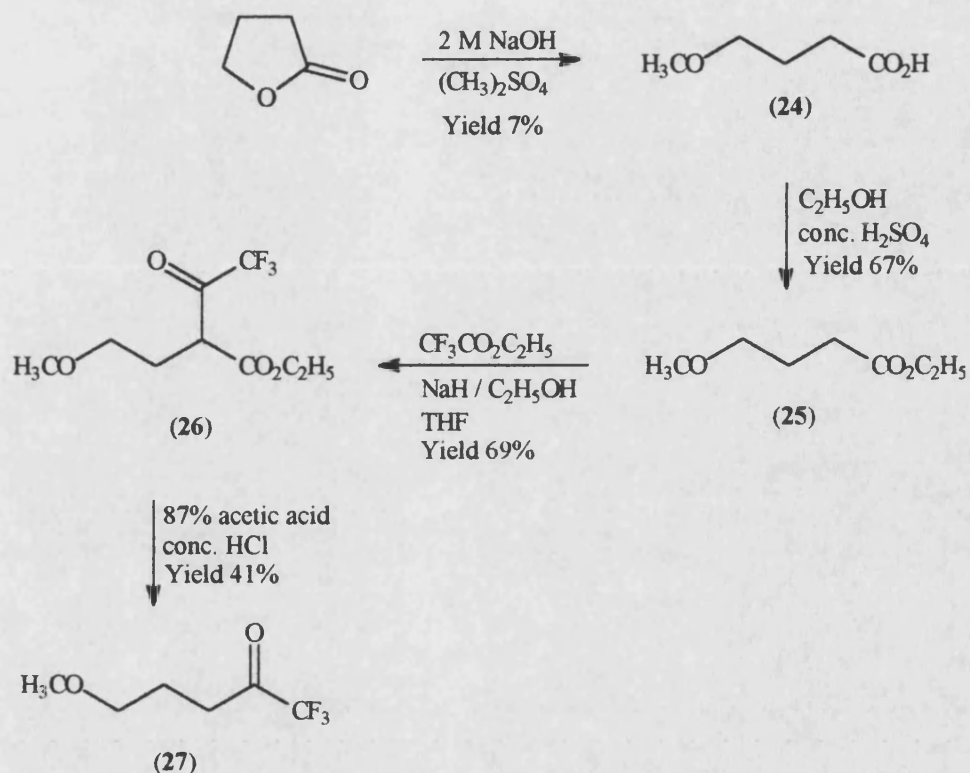
We anticipated that a substituted derivative of the dione (**1**) may be attained by replacing trifluoroacetone with a different trifluoromethyl ketone, as illustrated in Scheme 22. This could then be cyclised to the corresponding pyrazole with hydrazine hydrate in the usual way.



Scheme 22

Using a simple method similar to that described by Archer *et al.*¹³¹, 5-methoxy-1,1,1-trifluoropentan-2-one (**27**) was synthesised, as shown in Scheme 23. This method used relatively harsh reaction conditions and only gave poor yields of the trifluoromethylketone (**27**). Further, the small amount of product (**27**) obtained was eventually lost in additional steps of purification. Consequently, another route was sought. The method of Archer *et al.*¹³¹ was reported in 1979. Since then, a large number of other methods have appeared in the literature and in 1991 a very good and extensive review by Bégué and Bonnet-

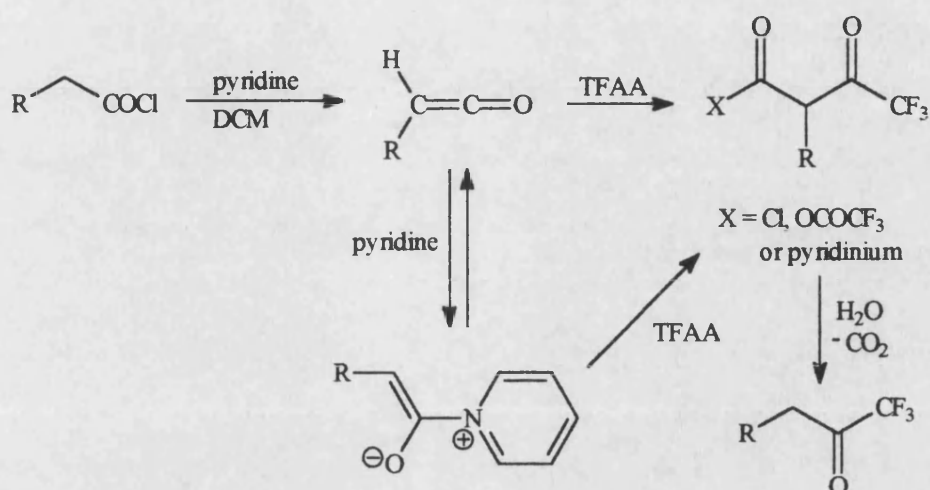
Delpon¹³² was published. Therefore, only the methods actually used in this study will be discussed here.



Scheme 23

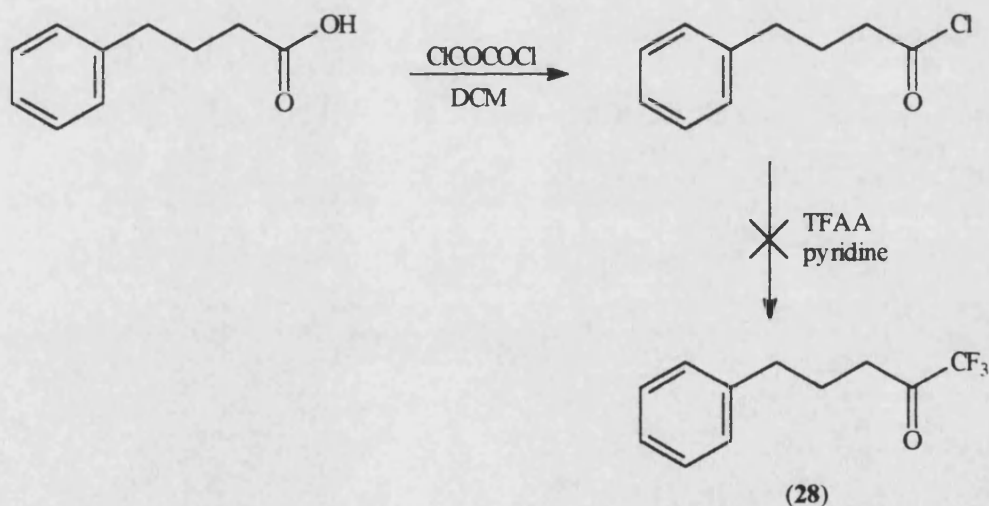
A selection of newer methods available for the synthesis of trifluoromethyl ketones have been investigated. All of these methods had some limitations and problems were encountered with many.

In 1992, Zard *et al.*¹³³ reported a method of synthesising trifluoromethyl ketones from acid chlorides, which has very recently been updated^{134,135}. The reaction involves generation of a ketene from the acid chloride, which is then trapped with TFAA. Hydrolysis and decarboxylation yields the corresponding ketone, as illustrated in Scheme 24. This procedure was applied to 4-phenylbutanoic acid, which was converted *in situ* to its acid chloride using oxalyl chloride in DCM, Scheme 25.



Scheme 24

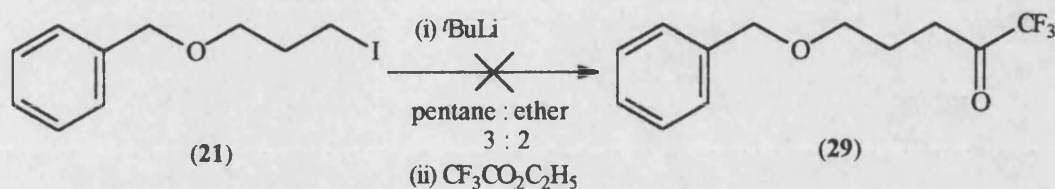
Unfortunately, a black tar-like mixture was produced following the "work-up" from which no trifluoromethyl ketone (**28**) could be isolated. Zard *et al.*¹³³ reported that their procedure was impractical for the acid chloride of 2-phenylethanoic acid. Together with our result, this indicates that this reaction does not tolerate all functionalities.



Scheme 25

Problems were also experienced using a method reported by Villuendas *et al.*¹³⁶ in 1994. This method involves the lithiation of iodo-compounds with 1.1

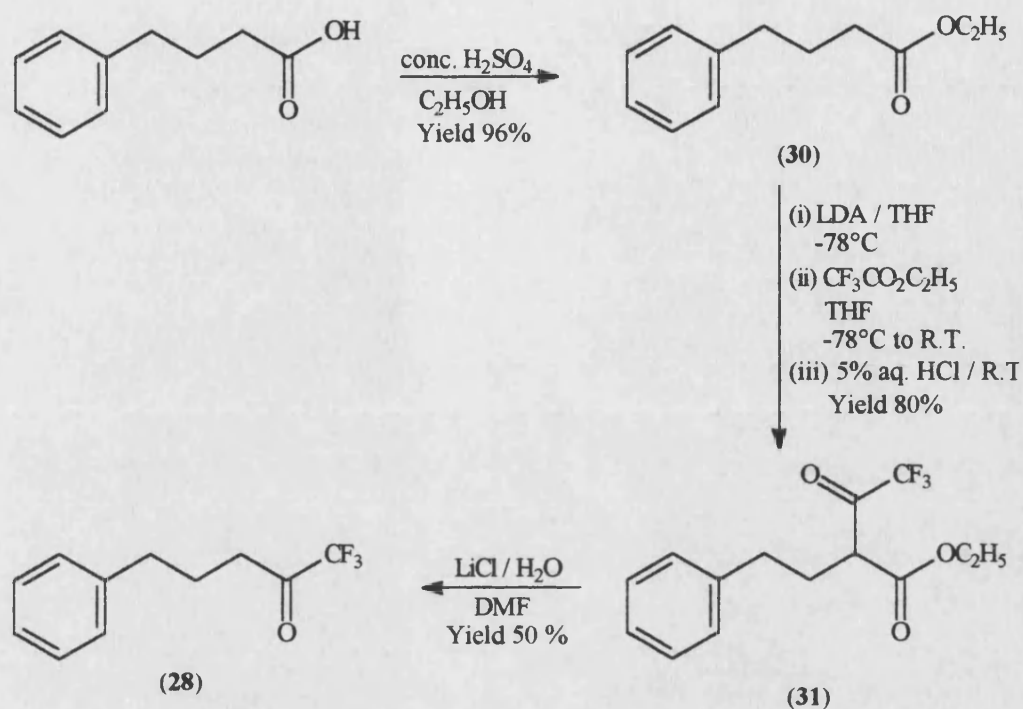
equivalents of *tert*-butyllithium followed by treatment with a trifluoroacetylating agent. This procedure was tested using 1-iodo-3-(phenylmethoxy)propane (**21**), which was synthesised as described earlier. The attempted trifluoroacetylation is illustrated in Scheme 26.



Scheme 26

Once again, no trifluoromethyl ketone (**29**) was isolated. This may be due to the presence of an excess of base in the reaction mixture, resulting in lithiation on and around the benzyl moiety or possibly proton extraction from the solvent (ether). Moreover, the primary organolithium derivative initially formed may give rise to an intramolecular cyclisation reaction with the benzyl moiety. Therefore, this procedure proved to be unsuitable for our requirements.

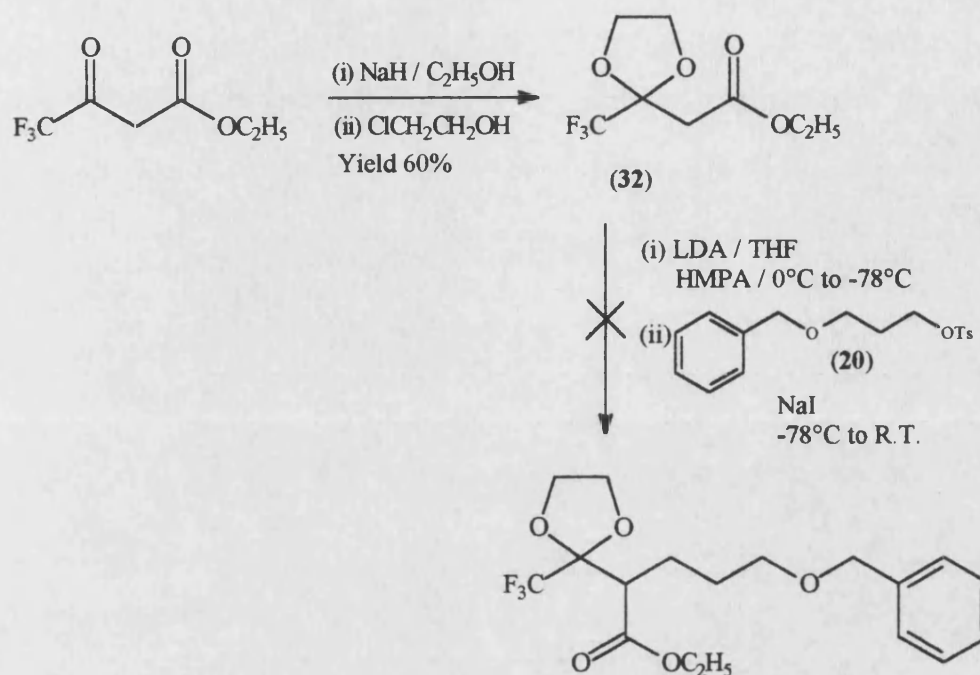
The trifluoroacetylation of an ethyl ether followed by decarboxylation was described earlier in the synthesis of 5-methoxy-1,1,1-trifluoropentan-2-one (**27**) using the method of Archer *et al.*¹³¹. The yields in this reaction sequence were not satisfactory. Therefore, modified reaction conditions were developed based on this sequence. A trifluoromethyl ketone with a relatively low volatility for subsequent trial reactions was required. The ethyl ester (**30**) of 4-phenylbutanoic acid was prepared in the usual way in high yield. The ester (**30**) was trifluoroacetylated using lithium diisopropylamine (LDA) as the base and ethyl trifluoroacetate as the trifluoroacetylating agent with a very good yield. Decarboxylation of the β -keto ester (**31**) was carried out using water / lithium chloride as described by Langlois *et al.*¹³⁷. The corresponding trifluoromethyl-ketone (**28**) was produced in good yield and the reaction sequence is illustrated in Scheme 27.



Scheme 27

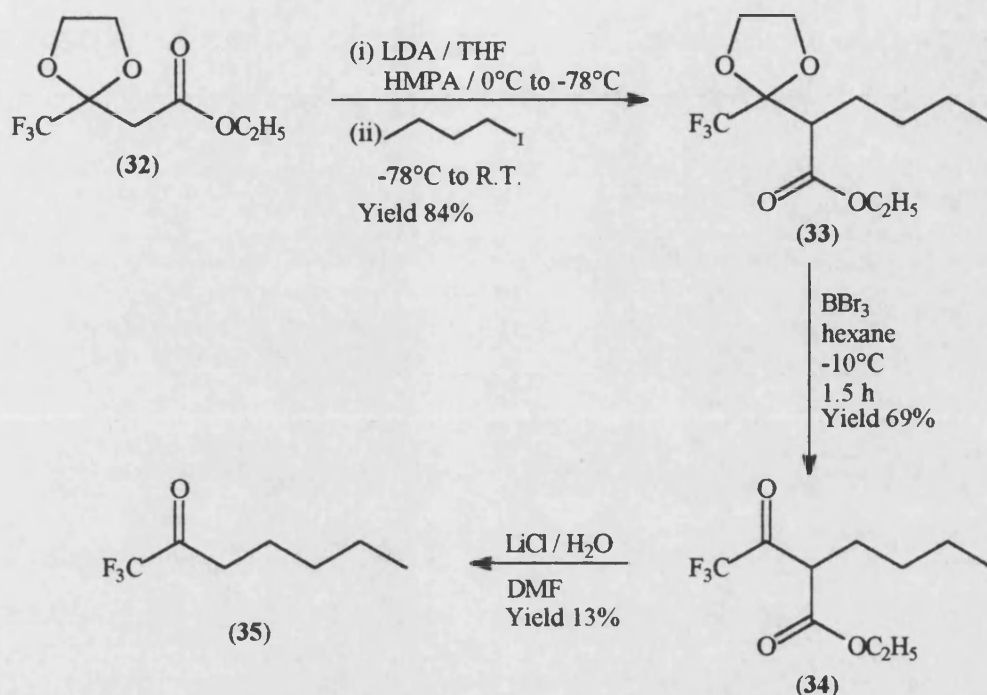
A very versatile method for making trifluoromethyl ketones is described by Langlois *et al.*¹³⁷. This involves the C-alkylation of ethyl 4,4,4-trifluoro-3-oxobutanoate (ETOB) with an alkyl halide, in which the ketone carbonyl of ETOB is masked.

The carbonyl function of ETOB was protected as the dioxole (32) by treatment with sodium ethoxide followed by 2-chloroethanol in 60% yield. The anion was formed using LDA in HMPA / THF and an attempt to alkylate with the tosylate compound (20) failed, even in the presence of sodium iodide, Scheme 28.



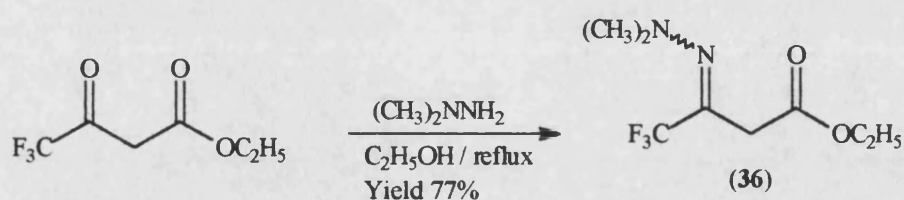
Scheme 28

This illustrated that the tosylate was not an adequate leaving group for the reaction and that an iodo-derivative was necessary. The commercially available 1-iodobutane was used to test the reaction. The desired alkylation product (33) was obtained in 84% yield, as illustrated in Scheme 29. The carbonyl group was deprotected using 1.5 equivalents of boron tribromide in hexane to give the β -keto ester (34) in 69% yield. This yield is an estimate from the ^1H NMR. Enolisation meant that isolation and purification were difficult and, therefore, the crude material was carried forward to the next step. Decarboxylation was carried out with 1 equivalent of water in the presence of lithium chloride in DMF. Isolation and purification were straightforward at this stage and the trifluoromethyl ketone (35) was obtained in 13% yield, as shown in Scheme 29. The low yield was due to the high volatility of the product (bp 80°C).



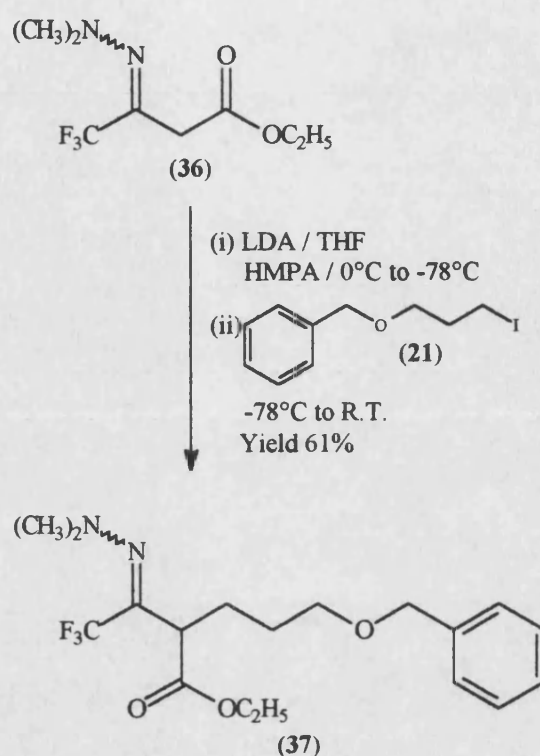
Scheme 29

At this stage it was realised that boron tribromide would be unsuitable for the deprotection of the ketone in the presence of a benzyl protection group. Therefore, a hydrazone protecting group was used for the ketone. The dimethylhydrazone (36) of ETOB was synthesised using the method of Langlois *et al.*¹³⁷ in 77% yield, as illustrated in Scheme 30.



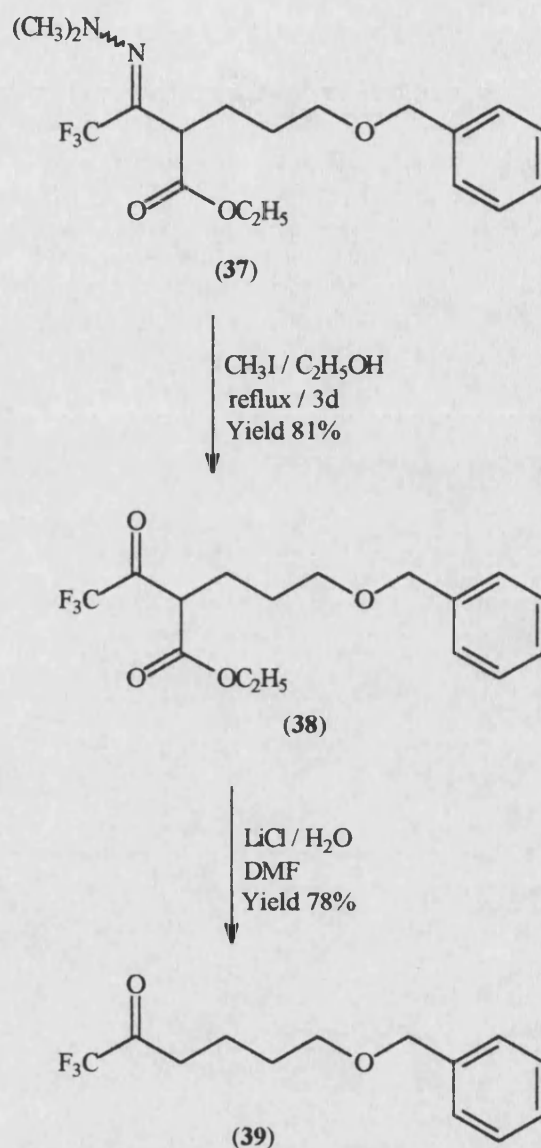
Scheme 30

The 2-position of the hydrazone (36) was deprotonated using LDA in HMPA / THF and alkylated with the iodo-compound (21) with a good yield of 61%, as illustrated in Scheme 31.



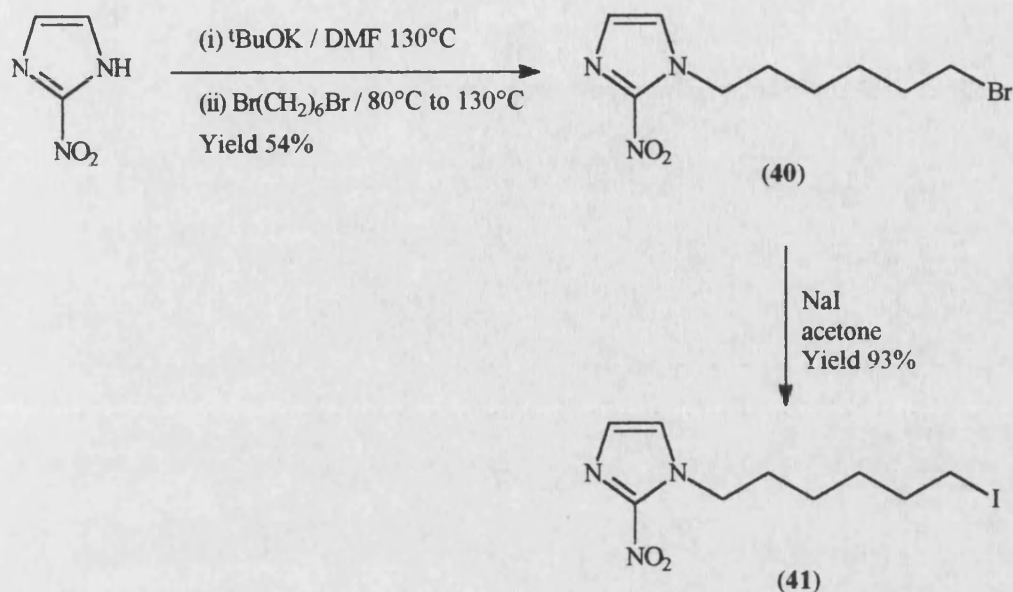
Scheme 31

Deprotection of the ketone was carried out in 81% yield by heating the hydrazone (**36**) with iodomethane in ethanol : water (95 : 5) for 3 days. Isolation and purification of the alkylated hydrazone (**37**) and the β -keto ester (**38**) were difficult, as described earlier for compounds (**33**) and (**34**). Column chromatography at each stage did "clean-up" the samples enough to allow relatively good ^{19}F NMR spectra to be recorded. The peaks obtained were in good agreement with those reported by Langlois *et al.*¹³⁷ for compounds with different alkyl chains. This meant that the reaction sequence was carried through to the trifluoromethyl ketone (**39**) for complete characterisation. The decarboxylation to the trifluoromethyl ketone (**39**) was carried out using water / lithium chloride in DMF with a 78% yield, as shown in Scheme 32.



Scheme 32

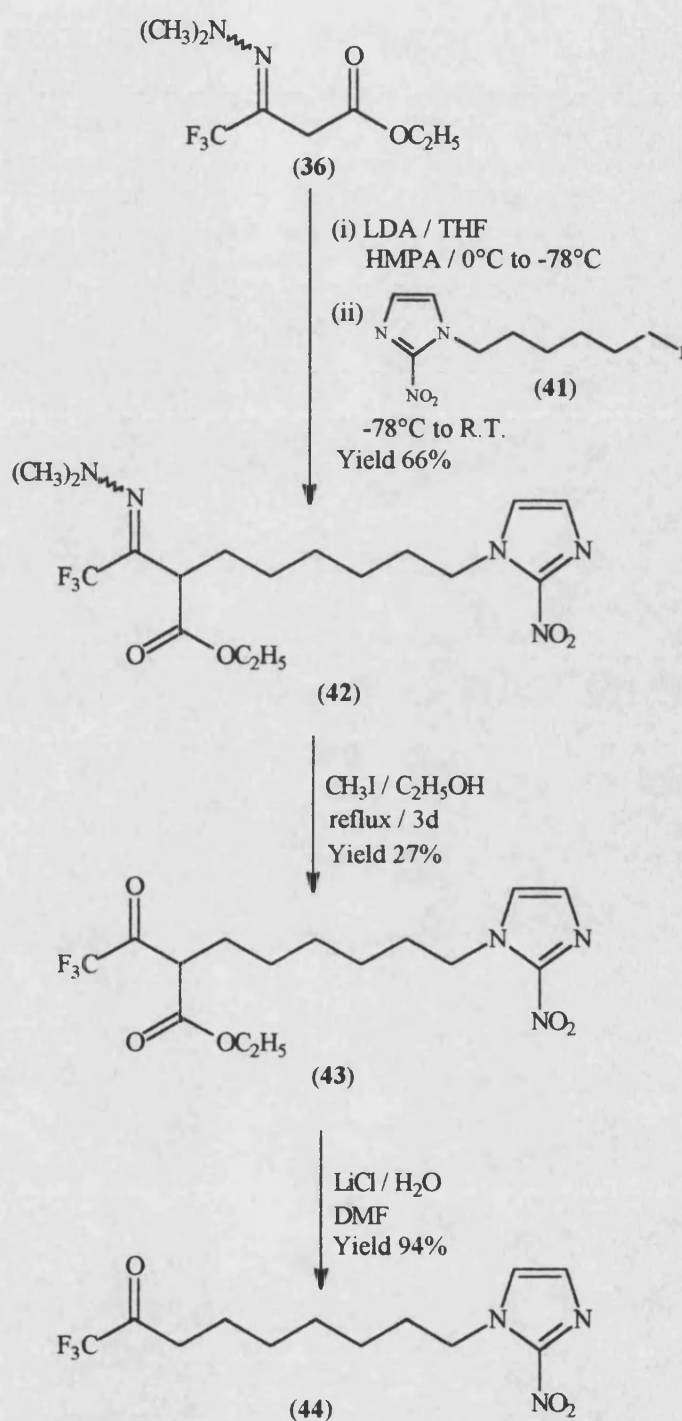
This method of synthesising trifluoromethyl ketones was shown to be very versatile and applicable to compounds containing a variety of functionalities. The tumour-selective retention of fluorinated 2-nitroimidazoles has been demonstrated by Maxwell *et al.*¹⁸. We anticipated that the incorporation of a 2-nitroimidazole group into the pH-probe will allow the accurate determination of pH_i in hypoxic cells. To investigate whether or not this functionality may be introduced into a trifluoromethylketone, the iodo-derivative **(41)** was synthesised as illustrated in Scheme 33.



Scheme 33

The initial step involved the N-alkylation of 2-nitroimidazole with 1,6-dibromohexane. The imidazole was deprotonated using 1 equivalent of potassium *tert*-butoxide in DMF at 130°C . Three equivalents of 1,6-dibromohexane were added at ambient temperature followed by further heating at 130°C . This procedure gave a 54% yield of the mono-addition product (40). The bromo-compound (40) was converted to its iodo-derivative (41) by the Finkelstein reaction using sodium iodide in dry acetone, with a high yield of 93%.

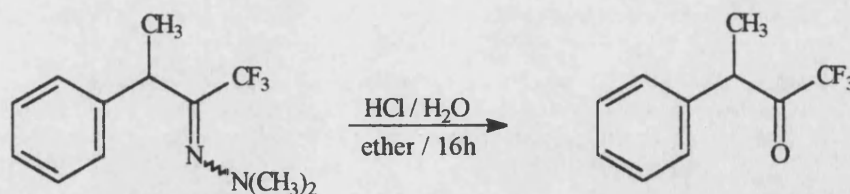
The hydrazone (36) was alkylated with the iodo compound (41), followed by deprotection of the ketone and decarboxylation to the corresponding trifluoromethyl ketone (44), as described earlier. For this example, the alkylated hydrazone (42) and the corresponding β -keto ester (43) were isolated with less difficulty and purified to a higher standard but this led to a low yield of 23% for the β -keto ester (43). This was partially compensated for by a high yield of 94% for the decarboxylation step, as illustrated in Scheme 34.



Scheme 34

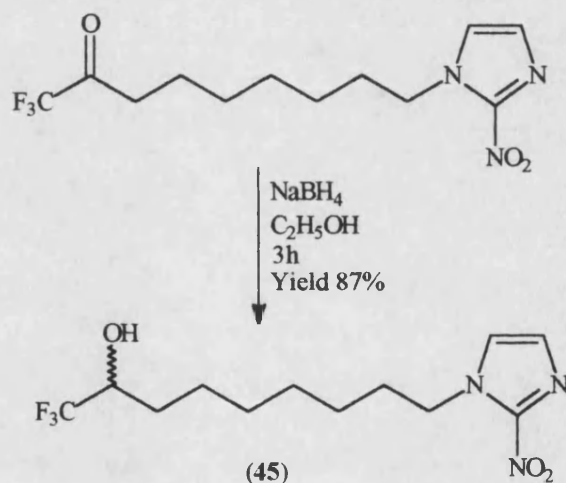
Since this work was carried out, a method of deprotecting hydrazones of trifluoromethylketones has been reported by Felix *et al.*¹³⁸. They used 20% HCl aqueous solution in ether. An example is illustrated in Scheme 35. This

may be a useful alternative to the iodomethane method which was often very long and messy.



Scheme 35

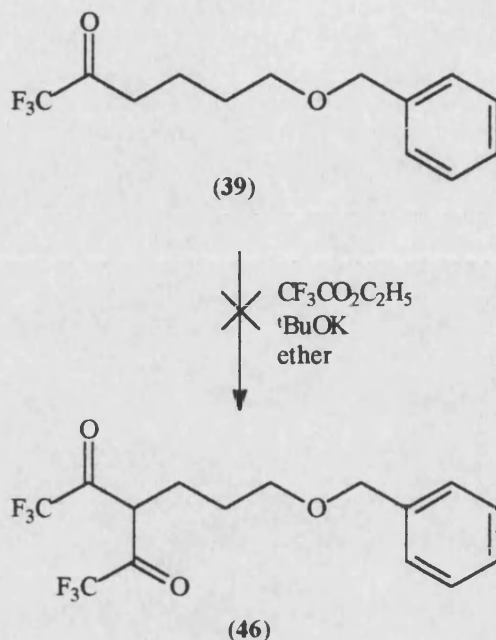
A small quantity of the 2-nitroimidazole trifluoromethylketone (**44**) was selectively reduced to the corresponding alcohol (**45**) using 0.5 molar equivalents of sodium borohydride in ethanol, as shown in Scheme 36.



Scheme 36

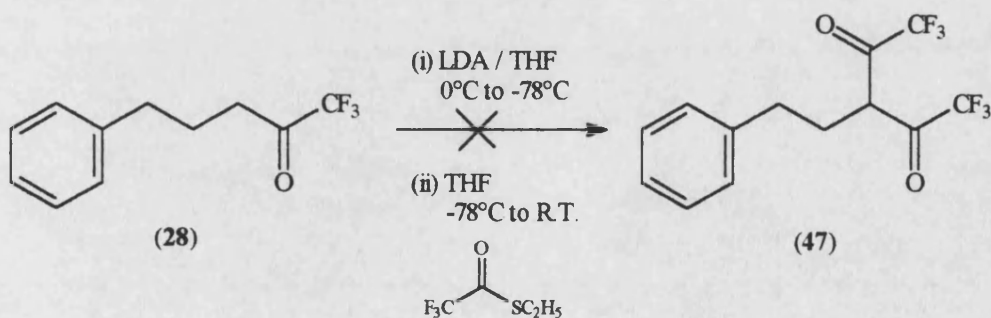
A number of attempts were made to trifluoroacetylate a trifluoromethyl ketone using a variety of reaction conditions. Firstly, a set of conditions were derived from the synthesis of 1,1,1,5,5,5-hexafluoropentane-2,4-dione (**1**) as described by Henne *et al.*¹³⁰ and was discussed earlier. The readily available potassium *tert*-butoxide was used as the base rather than sodium ethoxide formed *in situ* from ethanol and sodium. Ethyl trifluoroacetate was used as the trifluoroacetylating agent, ether was used as the solvent and the trifluoromethyl

ketone (39) was used as the substrate, as illustrated in Scheme 37. These reaction conditions failed to produce any of the desired β -diketone (46).



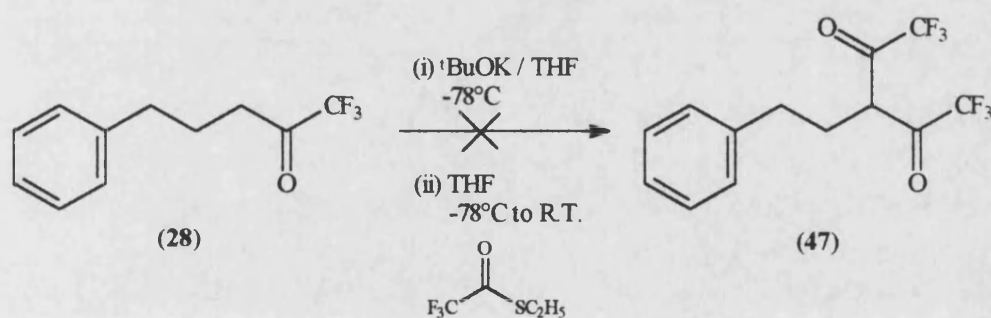
Scheme 37

The next attempt used LDA as the base in THF and ethyl thiotrifluoroacetate as the trifluoroacetylating agent, as illustrated in Scheme 38. The thio-derivative of ethyl trifluoroacetate was used because it contains a more efficient leaving group. These reaction conditions were also unsuccessful in producing a β -diketone (47).



Scheme 38

Finally, the base was changed back to potassium *tert*-butoxide. This was because from trifluoroacetylation reactions using LDA as the base, a colourless crystalline material was recovered which was had signals in the ^1H NMR similar to a diisopropylamide and a signal in the ^{19}F NMR consistent with a trifluoroacetamide. The high resolution chemical-impact (CI) mass spectrum showed a major $(\text{M} + \text{H})^+$ peak at m/z 197.1027, corresponding to the molecular formula $\text{C}_8\text{H}_{14}\text{F}_3\text{NO}$. This suggests that either LDA or non-lithiated diisopropylamine reacts with the trifluoroacetylating reagent to produce N,N-diisopropyl-2,2,2-trifluoroacetamide. Therefore, to avoid any possible interference of the reaction by this side reaction, LDA was avoided. Lower yields for trifluoroacetylation reactions where LDA was used as the base have been reported¹³⁹. Further, potassium *tert*-butoxide is soluble in THF. Again, ethyl thiotrifluoroacetate was used as the trifluoroacetylating agent, as illustrated in Scheme 39. Unfortunately, these reaction conditions failed to trifluoroacetylate the trifluoromethyl ketone (28).

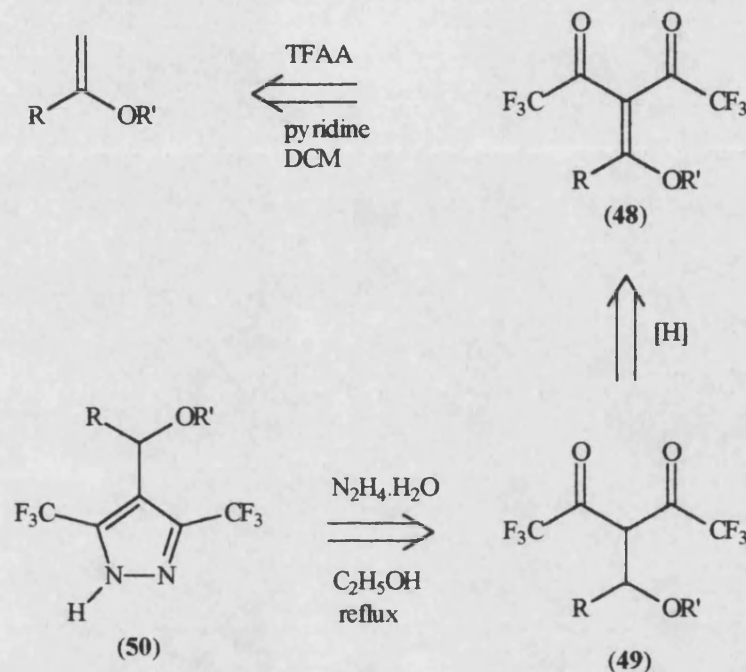


Scheme 39

5.1.4.3 Reduction of β -(Trifluoroacetyl)vinyl Ethers.

Hojo *et al.*¹⁴⁰ described the synthesis of β,β -bis(trifluoroacetyl)vinyl ethers (48), as illustrated in Scheme 40. It was anticipated that selective reduction of the vinylic double bond may be feasible. This would lead to a 3-substituted derivative (49) of 1,1,1,5,5,5-hexafluoropentane-2,4-dione (1) which could

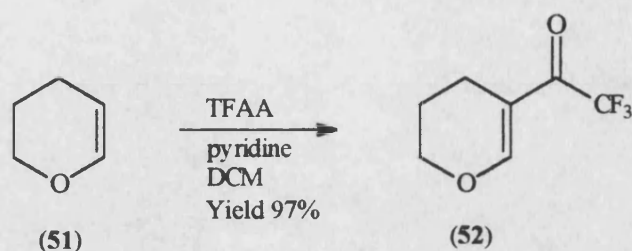
then be cyclised with hydrazine hydrate to the corresponding pyrazole (50). Furthermore, the ether group of pyrazole (50) is benzylic to the pyrazole ring. Therefore, if necessary, this bond may be cleaved by catalytic hydrogenation without affecting the ring.



Scheme 40

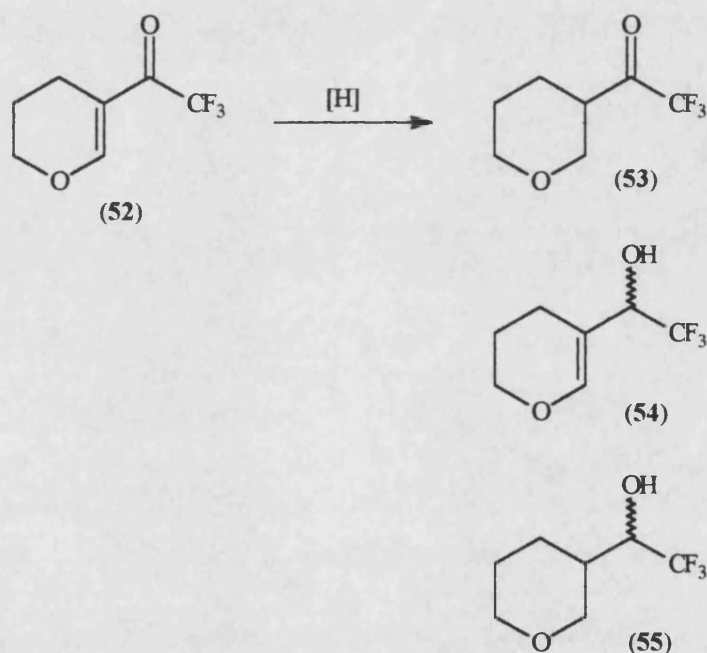
To investigate the potential of this reaction sequence, 3,4-dihydro-2H-pyran (51) was trifluoroacetylated with TFAA and pyridine in DCM, as shown in Scheme 41. The 97% yield of this reaction is notably higher than that reported by Hojo *et al.*¹⁴¹.

The trifluoroacetylpyran (52) was used as a model compound of β,β -bis(trifluoroacetyl)vinyl ethers (47), noting that the reduction potential of the two compound types will differ slightly.



Scheme 41

Three possible outcomes of the reduction of pyran (**52**) are illustrated in Scheme 42; the desired product from mono-reduction of the vinylic bond (**53**), the product from mono-reduction of the ketone (**54**) and the double-reduction product (**55**).



Scheme 42

Hydrogenation of carbonyl groups to the corresponding alcohol is usually carried out under mild conditions over platinum, Raney nickel or ruthenium. Therefore, these catalysts were not investigated. Hydride reducing agents such as LiAlH_4 and NaBH_4 were also avoided. Conversely, palladium is generally not very active for the hydrogenation of ketones. Its selectivity for the vinylic

group of enones has also been reported¹⁴².

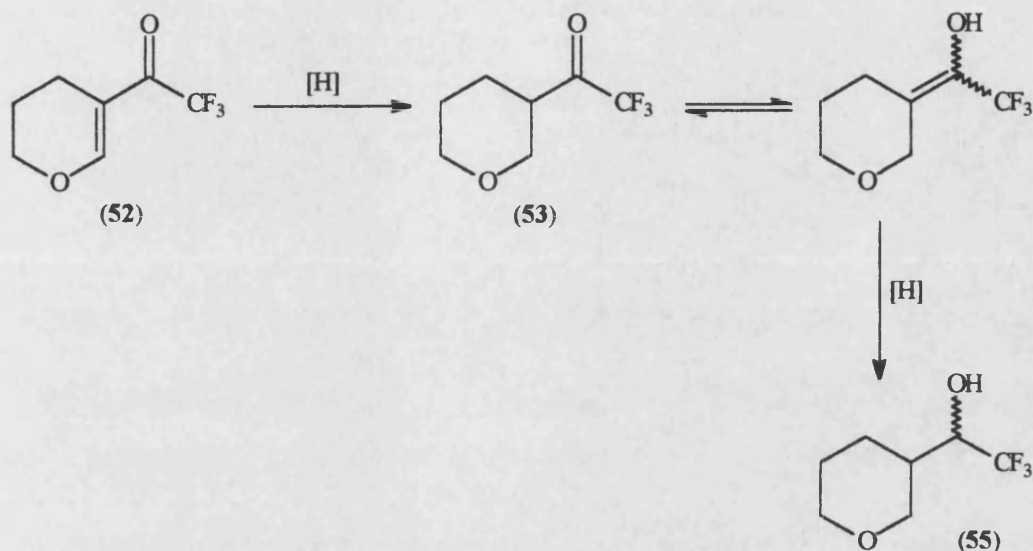
Various conditions under which 10% palladium on activated charcoal was used are listed in Table 2, together with other methods to be discussed later.

	Method	Result
(a)	Pd / C, H ₂ / CH ₃ OH / R.T.	(55) in 98% yield
(b)	Pd / C, H ₂ / hexane / THF / R.T.	(55) in 100% yield
(c)	Pd / C, H ₂ / CH ₃ OH / -78°C to -0°C	(55) in 100% yield
(d)	Pd / C, H ₂ / CH ₃ OH / CH ₃ CO ₂ K / R.T.	(55) in 76% yield
(e)	Bu ₃ SnH / CuI / LiCl / THF / N ₂	starting material (52) recovered
(f)	aqueous TiCl ₃	starting material (52) recovered

Table 2

Firstly, a general reduction in methanol at ambient temperature was carried out, entry (a). After 4 h, none of the starting material (52) was visible by t.l.c.. Under these conditions, both the vinylic double bond and the carbonyl group were reduced to give the alcohol (55) in 98% yield. Under these conditions, the reduction of a ketone would not be expected to occur¹⁴². If the first step of this double reduction involves the reduction of the vinylic double-bond to give ketone (53), then enolisation may occur, followed by further reduction. Thus, a second reduction could effectively remove the ketone functionality to give the alcohol (55). This mechanism is illustrated in Scheme 43. Further, the NMR spectra showed the presence of both diastereoisomers of alcohol (55). Hydrogenation of an unsaturated compound takes place by adsorption of the compound onto the catalyst surface, followed by transfer of hydrogen from the catalyst to the molecule which is adsorbed onto it. When two functionalities are being reduced, there are two possible mechanisms. (i) The compound may be adsorbed onto the catalyst, during which both of the functionalities are reduced. (ii) The compound may be adsorbed onto the catalyst and one of the two functionalities is reduced, followed by desorption and then readsorption to

reduce the second functionality. This information together with the NMR data suggests that the two reduction steps were probably not simultaneous.



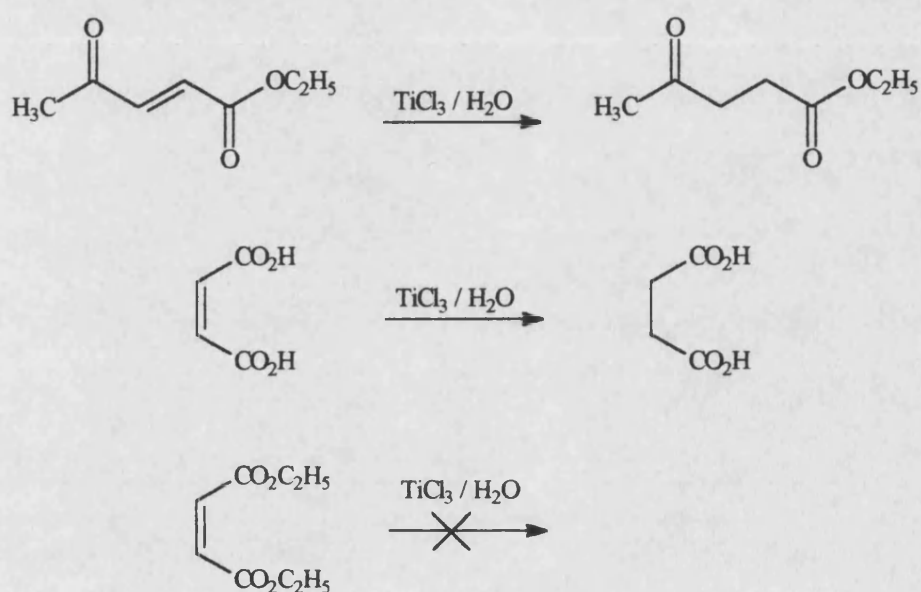
Scheme 43

Attempts were made to reduce the amount of enolisation and to allow the isolation of the desired ketone (**53**). To investigate the effects of solvent polarity on the extent of enolisation, a similar reaction was carried out in hexane, using a small amount (5%) of THF to aid solvation, entry (b). This produced the alcohol (**55**) in quantitative yield and in only 0.5 h.

The effect of temperature on the degree of enolisation was also investigated, entry (c). It was anticipated that lowering the temperature of the reaction mixture would reduce the rate of enolisation of the ketone (**53**) and allow the isolation of the ketone or, at least, allow the intermediate to be viewed by t.l.c.. The reaction was begun at -78°C and maintained at this temperature for 3 h, after which t.l.c. indicated mostly starting material (**52**) together with a material with the same R_f value as the alcohol (**55**). The temperature of the reaction mixture was allowed to rise in 10°C increments over a 3 h period, however, t.l.c. indicated little change until -10°C was reached. No other spots appeared on the t.l.c. plate during this period and after 0.5 h at -10°C , t.l.c.

indicated that there was no starting material (**52**) left. From the reaction mixture was isolated the alcohol (**55**) in quantitative yield.

The effect of the presence of potassium acetate on the selectivity of a reduction with Pd / C was briefly investigated. This approach also proved to be unsuccessful and the alcohol (**55**) was isolated in 76% yield, entry (d).

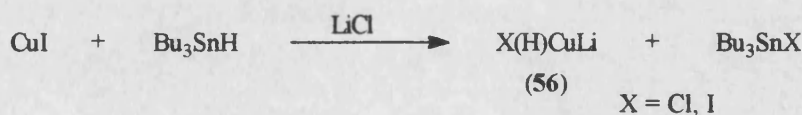


Scheme 44

Another method of selective reduction investigated was with low-valent titanium species. Titanium (III), conveniently available as TiCl₃, is a mild reducing agent in aqueous solution^{143,144}. The reagent has found particular use in the selective reduction of ene-diones, as illustrated in Scheme 44. Reactions such as those illustrated are usually complete within 0.25 h at ambient temperature. However, these conditions do not work for diesters, presumably because of the more negative reduction potential of esters versus ketones¹⁴⁵. In the case of the trifluoroacetylpyran (**52**), the α,β -unsaturated ketone portion of the compound favours this reaction, but the enol ether portion does not. The treatment of the trifluoroacetylpyran (**52**) with aqueous TiCl₃ resulted in the recovery of the starting material, entry (f) in Table 2. This suggests that the

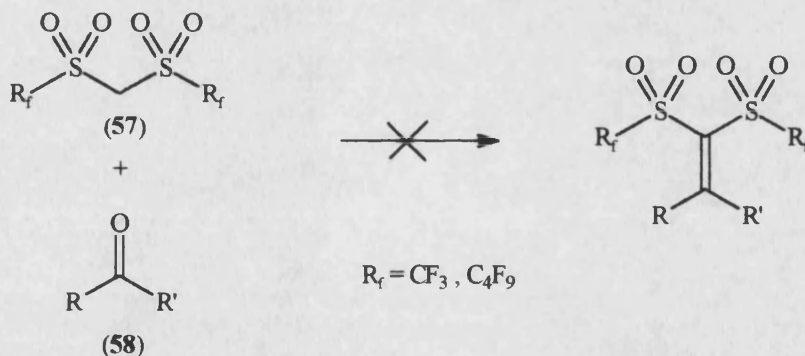
reduction potential of the trifluoroacetylpyran (**52**) is too negative for these conditions.

The selective reduction of α,β -unsaturated ketones has been reported¹⁴⁶ using *in situ* generated hydridocuprates. The trifluoroacetylpyran (**52**) was treated with a mixture of Bu_3SnH , CuI and LiCl in DMF, however, only starting material was recovered, entry (e). The active reagent formed from this combination of reagents is thought to be a hydridohalocuprate species (**56**) arising as shown in Scheme 45¹⁴⁶.



Scheme 45

5.1.4.4 Synthesis of 3-(Dimethylaminomethylene)-1,1,1,5,5,5-hexafluoro-2,4-dione and Related Compounds.

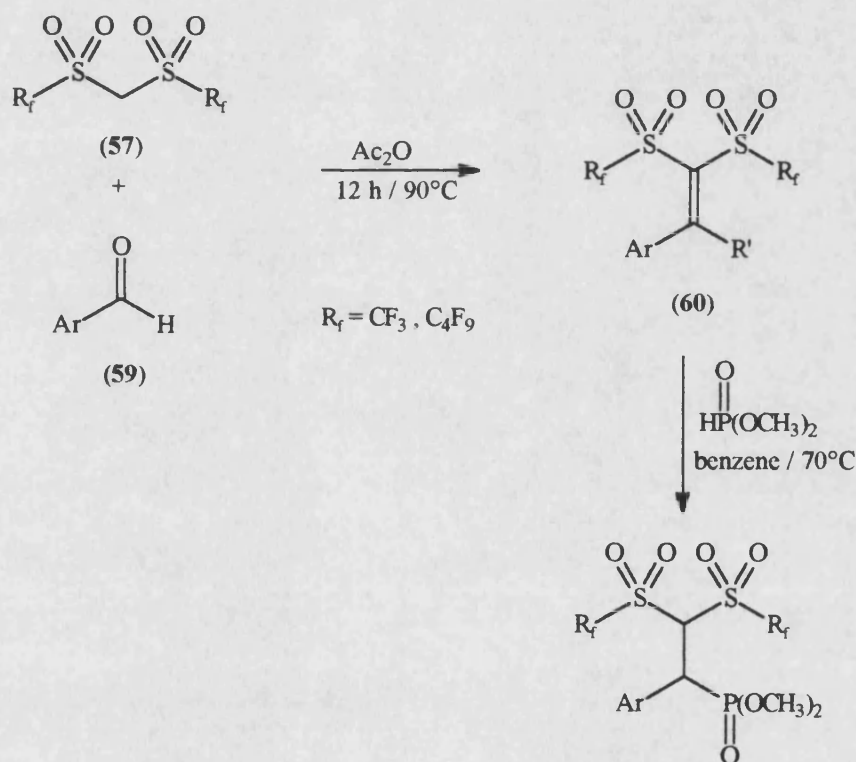


Scheme 46

The reason for the failure of attempted C-alkylations of 1,1,1,5,5,5-hexafluoropentane-2,4-dione (**1**) was attributed to the high stability of the easily formed anion due to the strong inductive effect of the two trifluoromethyl groups. Hannock *et al.*¹⁴⁷ reported a similar problem with the reaction of bis(perfluoroalkanesulphonyl)methanes (**57**) with aldehydes and

ketones (**58**), as illustrated in Scheme 46.

This problem was recently addressed by Zhu¹⁴⁸. It was reported that bis(perfluoroalkanesulphonyl)methanes (**57**) may be condensed with aromatic aldehydes (**59**) in acetic anhydride to give 1-aryl-2,2-bis(perfluorosulphonyl)ethylenes, as shown in Scheme 47. Furthermore, it was demonstrated¹⁴⁸ that the carbon-carbon double bond in the condensation product (**60**) is very polar due to the strong electron-withdrawing groups. This should allow the addition of a nucleophile. So far, this has been demonstrated using dimethylphosphite as the nucleophile in benzene, Scheme 47.

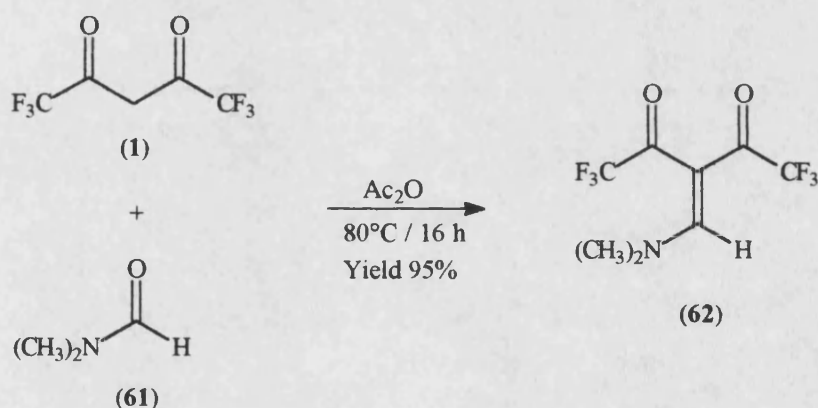


Scheme 47

It was anticipated that 1,1,1,5,5,5-hexafluoropentane-2,4-dione (**1**) would condense with carbonyl compounds in a similar fashion to the bis-sulphonyl compounds (**57**) and subsequently undergo addition reactions with nucleophiles. This should lead to a 3-substituted derivative of dione (**1**) which

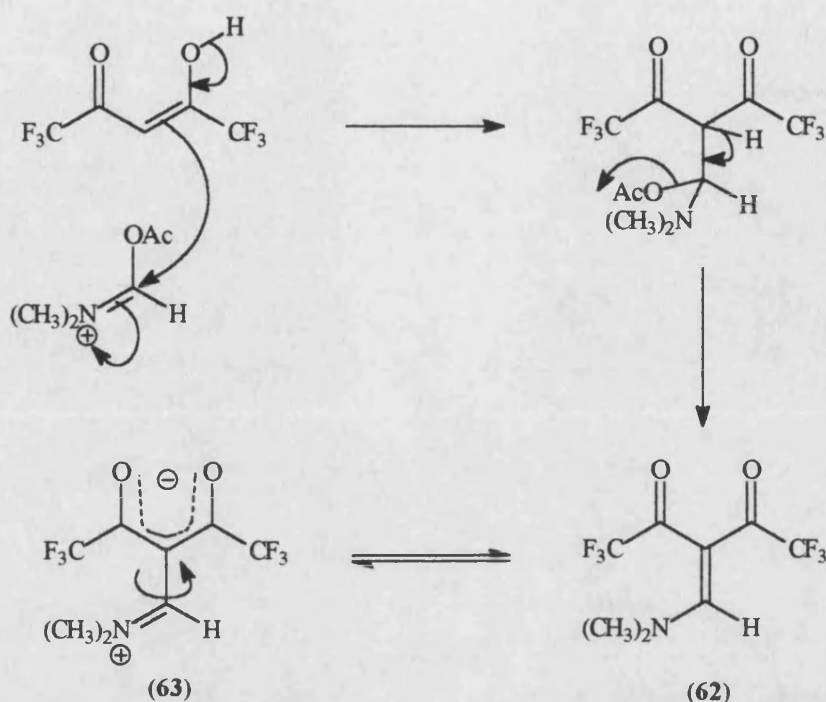
could then be cyclised with hydrazine hydrate to the corresponding pyrazole.

It was noted from the work of Zhu¹⁴⁸ that the presence of an electron-withdrawing substituent in the 4-position of the aromatic ring led to lower yields of the condensation product (60). The carbonyl group of dimethylformamide (61) is relatively electron rich due to the positive mesomeric effect of the dimethylamino group. Therefore, to examine the required electrophilicity of the carbonyl compound, an equimolar mixture of the dione (1) and dimethylformamide (61) were heated in acetic anhydride for 16 h. A low melting yellow solid was isolated from the reaction mixture, which was shown to be 3-(dimethylaminomethylene)-1,1,1,5,5,5-hexafluoropentan-2,4-dione (62). The condensation product (62) was obtained with an excellent yield of 95% and the reaction is illustrated in Scheme 48.



Scheme 48

A possible mechanism for the reaction is illustrated in Scheme 49. An extensive NMR study has been carried out on the dione (62). The NMR data suggest that the structure of the condensation product (62) is closer to that of compound (63), which is also illustrated in Scheme 49.



Scheme 49

The ^1H NMR spectrum at 20°C in $(\text{CD}_3)_2\text{SO}$ showed two sharp singlets at 2.78 and 3.54 ppm, corresponding to the two methyl groups. At 100°C , these signals became very broad and moved together slightly to resonate at 2.84 and 3.51 ppm. When 150°C was reached, the signals coalesced into a broad singlet resonating at 3.05 ppm. These data are illustrated in the ^1H NMR spectra shown in Figure 26. As can be seen, there is an impurity visible in the ^1H NMR spectra. The samples examined at high temperature were also examined at ambient temperature before and after raising the temperature. This was to evaluate the effects of high temperatures on the dione (62) when dissolved in $(\text{CD}_3)_2\text{SO}$. This indicated no significant further decomposition. It appears that the dione (62) may be sensitive to moisture, as reported by Zhu¹⁴⁸ for the sulphonyl analogues (60). It would have been interesting to evaluate the potential of this compound to act as a ^{19}F NMR pH-sensor. Unfortunately, this was not possible due to its moisture-sensitivity.

The ^{19}F NMR spectrum of dione (62) at 21°C in CDCl_3 showed a sharp singlet

at -73.39 ppm. At -50°C, the singlet broadened and resonated at -72.94 ppm. In *d*₈-THF at 20°C, the sharp singlet was observed at -73.16 ppm. *d*₈-THF allowed the NMR to be run at -90°C, where the signal became very broad and resonated at -72.6 ppm. These data are illustrated in the ¹⁹F NMR spectra shown in Figure 27.

These data show that rotation about the newly formed carbon-carbon bond of the dione (**62**) is less restricted than rotation about the C-N(CH₃)₂ bond. A temperature of 150°C was required before the two separate signals for the two methyl groups would coalesce. If this is taken to be the coalescence temperature (*T*_c), then the free energy for the activation for the rotation (ΔG^\ddagger) may be calculated using Equation 3¹⁴⁹. Where, *T*_c is expressed in Kelvin, *R* is the gas constant and $\Delta\nu$ is the frequency separation of the individual sharp lines at ambient temperature.

$$\Delta G^\ddagger = R \cdot T_c [23 + \ln(T_c/\Delta\nu)]$$

Equation 3

Thus, the free energy of activation for the rotation about the C-N(CH₃)₂ bond in dione (**62**) is approximately 81.92 kJmol⁻¹. It may also be assumed that the free energy of rotation for the carbon-carbon bond is less than this value.

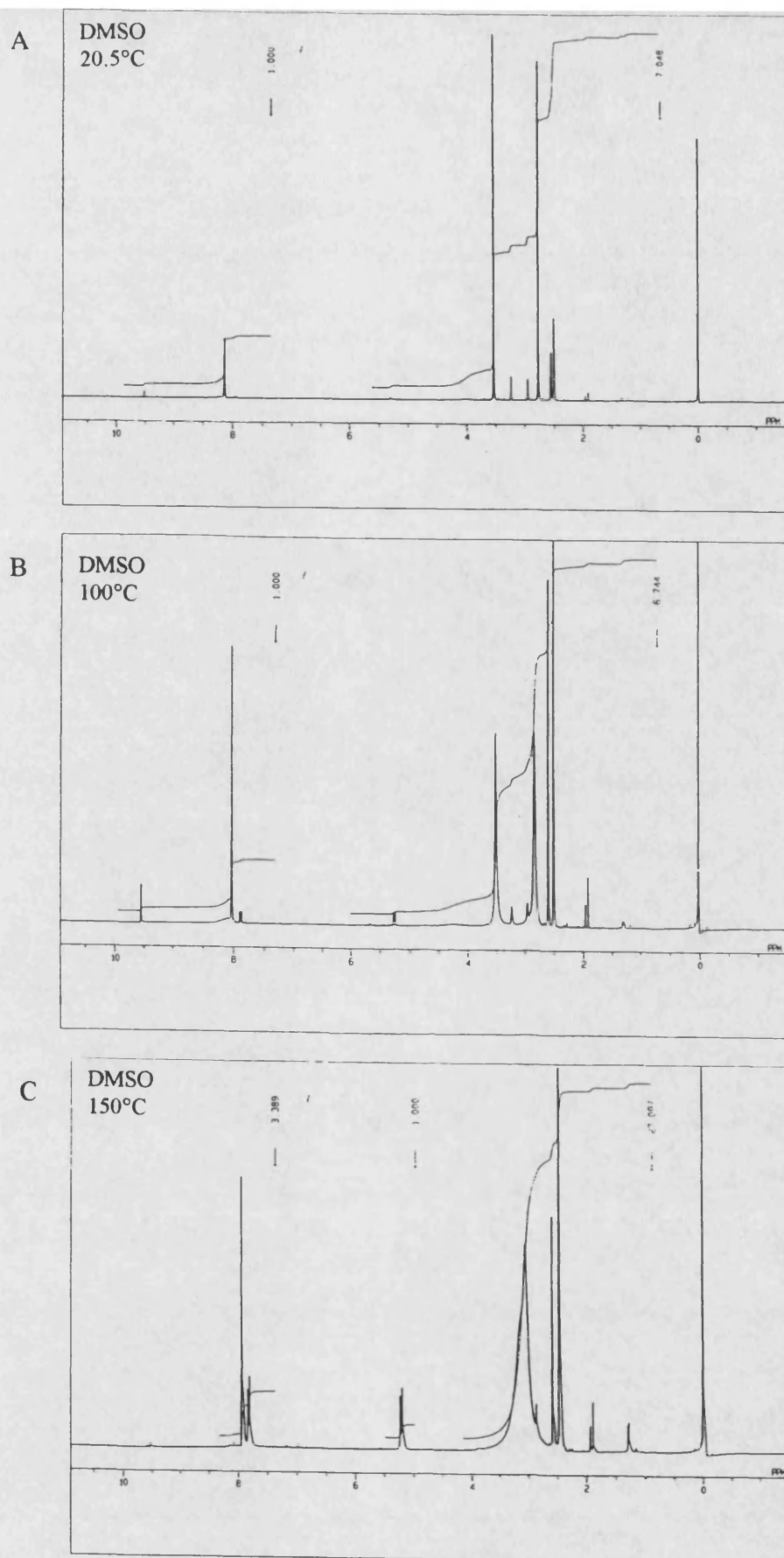


Figure 26. ^1H NMR spectra of dione (**62**) at 20.5°C (A), 100°C (B) and 150°C (C).

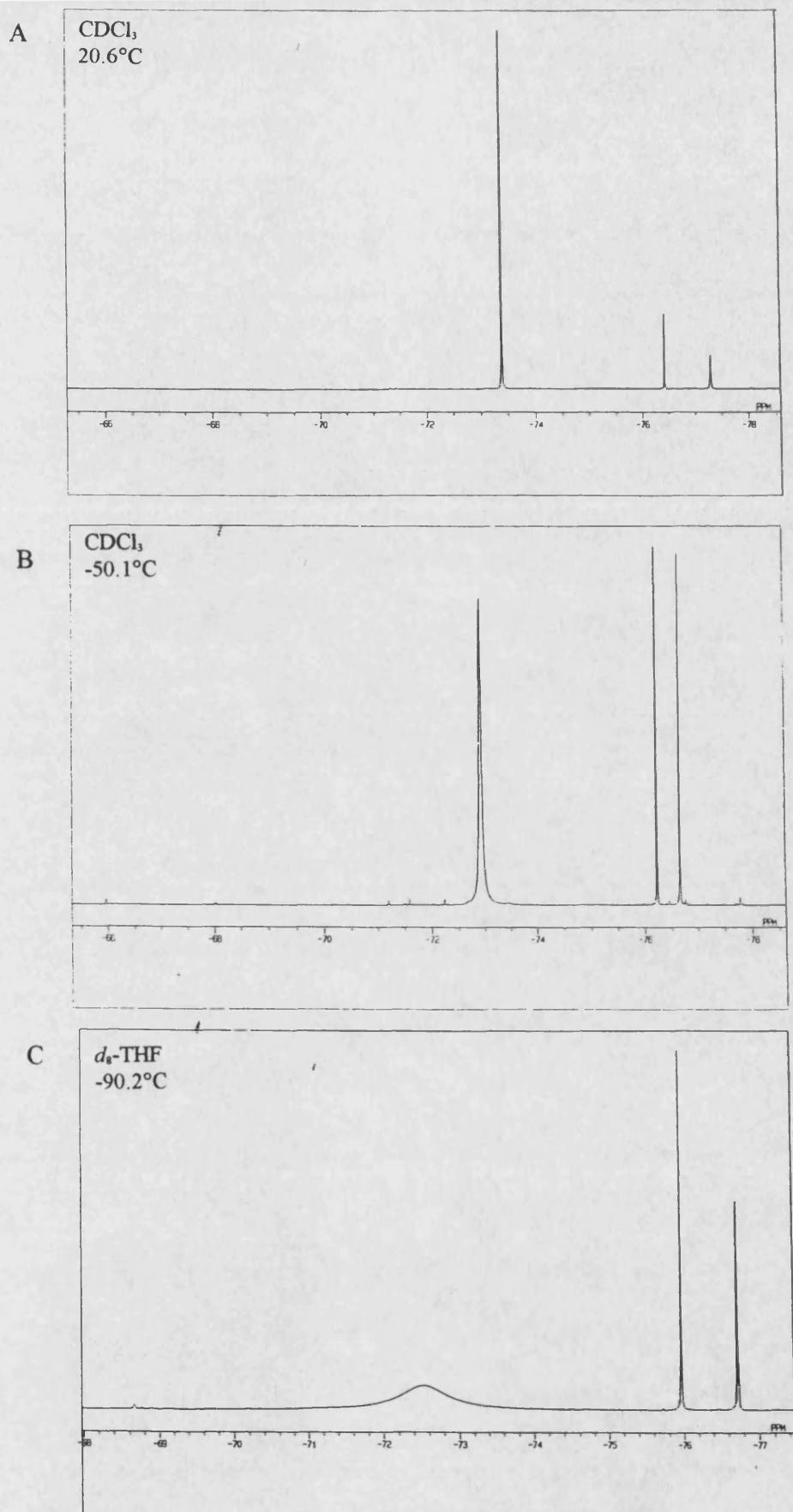
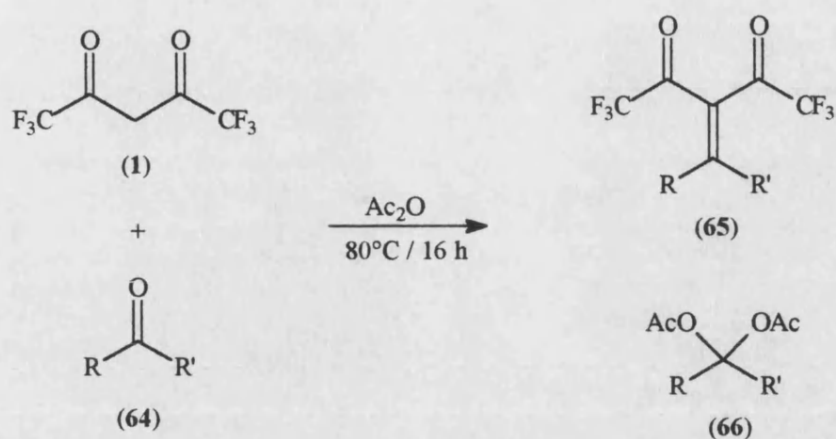


Figure 27. ¹⁹F NMR spectra of dione (62) at 20.6°C (A), -50.1°C (B) and -90.2°C (C).



Scheme 50

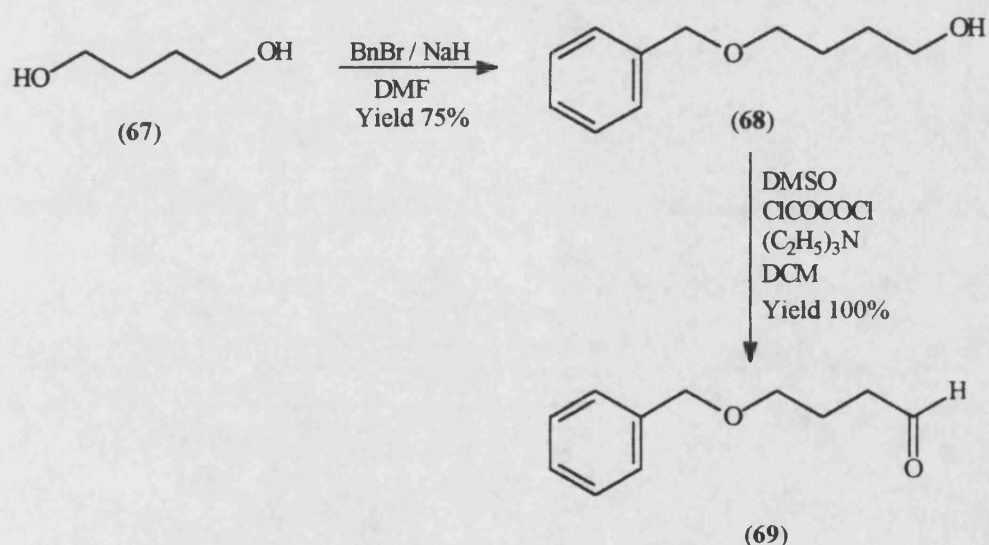
	R	R'	Result
(a)	4-(CF ₃)C ₆ H ₄	H	acetal (66)
(b)	3-(CF ₃)C ₆ H ₄	H	acetal (66)
(c)	CH ₃ (CH ₂) ₈	H	acetal (66)
(d)	C ₆ H ₅ (CH ₂) ₂	H	acetal (66)
(e)	C ₆ H ₅ CH ₂ O(CH ₂) ₃	H	acetal (66)
(f)	4-(C ₆ H ₄ CH ₂ O)C ₆ H ₄	H	mixture
(g)	C ₆ H ₅ S	H	mixture
(h)	C ₆ H ₅	CF ₃	acetal (66)

Table 3

The general reaction illustrated in Scheme 50 was attempted with a variety of carbonyl-containing compounds (64), as listed in Table 3. Two major possible outcomes of the reaction could be the formation of the desired condensation product (65) or the formation of the corresponding acetal (66). Most of the carbonyl compounds (64) were chosen for testing the limitations of the reaction.

If a trifluoromethyl-containing aromatic group could be incorporated into the dione adduct (65), then it would serve as a relatively pH-insensitive reference

peak in the ^{19}F NMR spectrum. From the treatment of 1,1,1,5,5,5-hexafluoropentane-2,4-dione (**1**) with 4-trifluoromethylbenzaldehyde in acetic anhydride was isolated a compound containing only one trifluoromethyl signal in the ^{19}F NMR spectrum and a ^1H NMR spectrum which suggested that the acetal (**66**) had formed, entry (a) in Table 3. The trifluoromethyl group in 3-trifluoromethylbenzaldehyde should have less of an electron-withdrawing effect on the aldehyde. However, this also led to the isolation of its corresponding acetal (**66**) under the same reaction conditions, entry (b).



Scheme 51

Aliphatic aldehydes were also examined, entries (c-e) in Table 3. These compounds also failed to condense onto the dione (**1**), as indicated by their ^{19}F NMR spectra. Once again, the corresponding acetals were shown by the ^1H NMR spectra. The aliphatic aldehyde for entry (e) was synthesised by the mono-benylation of 1,4-butanediol (**67**), followed by a Swern¹⁵⁰ oxidation of the alcohol (**68**) to the aldehyde (**69**), both with very good yields, as illustrated in Scheme 51. Swern oxidations involve the use of an activated DMSO reagent. The most popular activator of DMSO is oxalyl chloride and the suitability of this reagent for the conversion of alcohols to aldehydes was demonstrated by the quantitative yield obtained here.

The more electron-rich carbonyl group of 4-benzyloxybenzaldehyde showed a much higher reactivity towards the dione (1), entry (f). The reaction mixture was carefully distilled and the ^1H NMR spectra of the fractions did not show the presence of the corresponding acetal (66). The ^{19}F NMR confirmed that the aldehyde had reacted with the dione (1), but showed a mixture of adducts. The mixture was examined by t.l.c. using a large number of solvent systems. However, most of the compounds were present as streaks. An attempt was made to separate the mixture by column chromatography, but no individual compound could be isolated. Closer inspection of the ^1H and ^{19}F NMR spectra suggested that a condensation reaction had occurred between the aldehyde and the dione (1), together with intramolecular cyclisation reactions involving the benzyl groups.

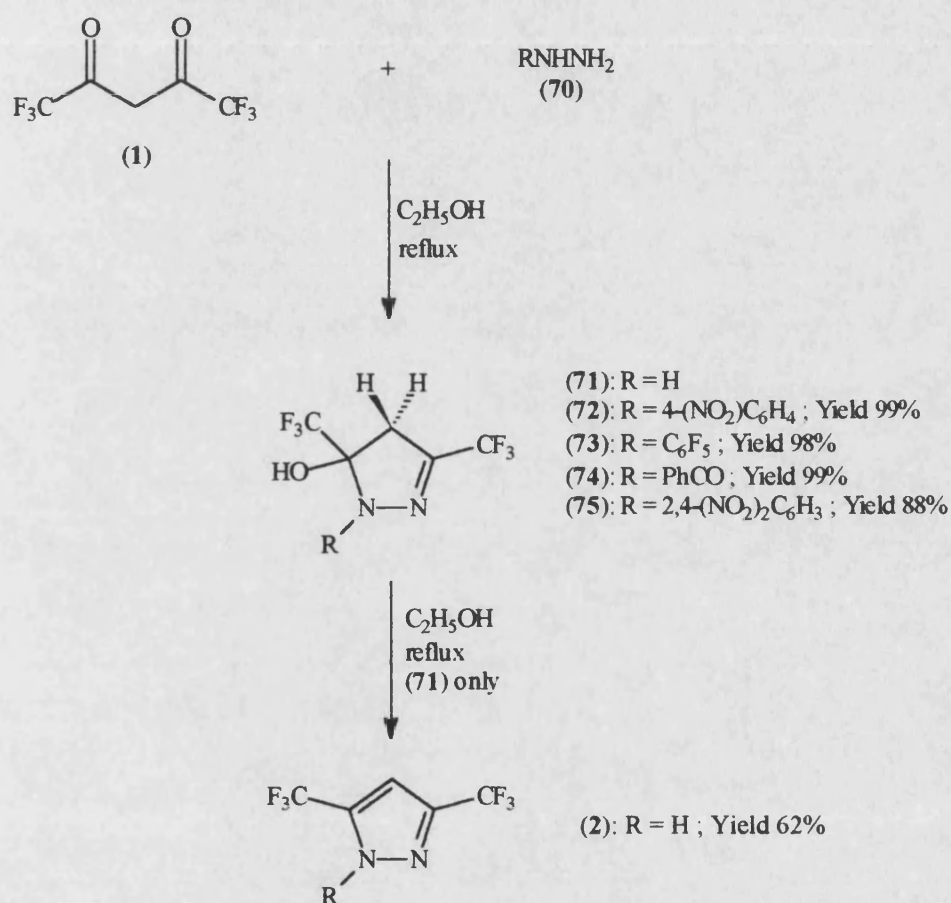
2-Thiophenecarboxaldehyde also reacted with the dione (1), entry (g). The ^1H NMR spectra of the distillation fractions did not indicate the presence of an acetal (66). The ^{19}F NMR spectra confirmed that a reaction had taken place, but showed the presence of a large number of adducts. Unfortunately, the mixture could not be separated by distillation or chromatography.

Finally, the reactivity of trifluoroacetophenone was examined, entry (h). This failed to react with the dione (1), as shown by ^{19}F NMR, and the ^1H NMR spectrum indicated the presence of the corresponding acetal (66).

5.1.5 The Reaction of 1,1,1,5,5,5-Hexafluoropentane-2,4-dione with Substituted Hydrazines.

McCleverty *et al.*¹¹² have reported the synthesis of 3,5-bis(trifluoromethyl)-pyrazole (2). In the same report, the synthesis of 1-aryl and 1-aroyl-3,5-bis(trifluoromethyl)pyrazoles (76-79) was claimed by the reaction of substituted hydrazines (70) with 1,1,1,5,5,5-hexafluoropentane-2,4-dione (1) in

boiling ethanol. Since it is difficult to rationalise the spectroscopic data reported¹¹² with the aromatic pyrazole claimed, and there are reports^{117,151} that 5-hydroxy-4,5-dihydropyrazoles are often isolated when the nitrogen atom is substituted with an electron-withdrawing group, a re-investigation of the reaction of dione (1) with hydrazines (70) was undertaken, as illustrated in Scheme 52.



Scheme 52

The synthesis of 3,5-bis(trifluoromethyl)pyrazole (2) from the treatment of dione (1) with hydrazine hydrate in boiling ethanol was discussed earlier. The ^1H NMR is consistent with an aromatic pyrazole structure. The 4-H atom gives a resonance at 6.95 ppm, which is slightly broadened by coupling to fluorine. Only one ^{19}F NMR signal is evident in pyrazole (2), owing to rapid site

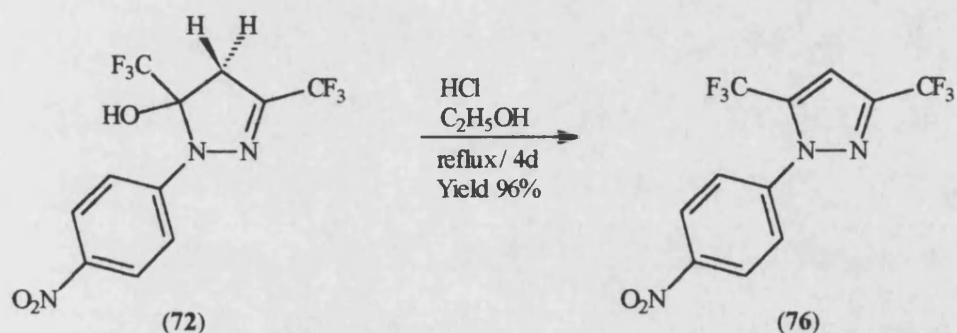
exchange of the NH proton. The electron-impact (EI) mass spectrum of this pyrazole shows an abundant molecular ion at m/z 204, with no evidence of ions at higher mass (e.g. m/z 222 for the hydroxydihydropyrazole structure).

However, the ^1H NMR spectra of the heterocycles formed from dione (1) and the substituted hydrazines (70) showed no signal in the region expected for the 4-H atom of an aromatic pyrazole (5.8-7.2 ppm)^{152,153}. McCleverty *et al.*¹¹² also report no signals in this region but claim that 4-H resonates at approximately 3.6 ppm; no integral or multiplicity data were given. The extensive study by Tensmeyer and Ainsworth¹⁵³ of substituent effects on the chemical shifts of pyrazoles does not support this assignment. In our work, the signals in the region 3-4 ppm comprised two doublets, the integral of each doublet corresponding to one proton. The coupling constants between these doublets were >14 Hz, typical values for geminal coupling. Thus these signals can be assigned to a prochiral CH_2 group in an asymmetric environment. Broad resonances due to OH were also observed. On the bases of these data, the hydroxydihydropyrazole structures (72-75) are proposed rather than the pyrazoles (76-79) claimed¹¹².

The EI mass spectra of the 5-hydroxydihydropyrazoles (72-75) at 70 eV ionisation energy revealed abundant molecular ions. The molecular ion of 1-benzoyl-3,5-bis(trifluoromethyl)-4,5-dihydro-5-hydroxypyrazole (74) was present in the EI spectrum only at 1% abundance but abundant ions were observed at m/z 326 (M) in the CI spectrum and at m/z 327 (M + H) in the positive ion fast atom bombardment (FAB) spectrum. Dehydration was not favoured (giving M - 18) but loss of $\cdot\text{CF}_3$ gave highly abundant peaks at (M - 69) in all cases. The reported interpretation¹¹² of similar data, representing the ions at highest mass as molecular clusters of (pyrazole + H_2O), is unlikely under EI conditions.

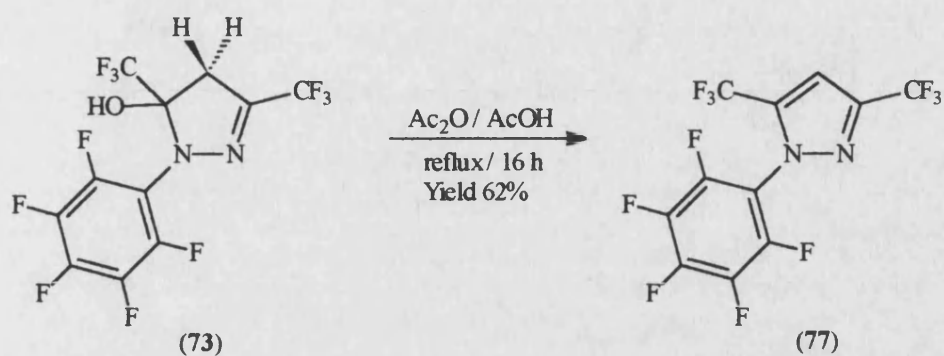
Various conditions for the dehydration of 5-hydroxy-4,5-dihydropyrazoles (72-

75) to the corresponding pyrazoles (**76-79**) were investigated. Dehydration of 3,5-bis(trifluoromethyl)-4,5-dihydro-5-hydroxy-1-(4-nitrophenyl)pyrazole (**72**) was achieved by treatment with a small quantity of acid in boiling ethanol for 4 days. This method proved to be very effective for this example and the corresponding pyrazole (**76**) was obtained in high yield, as illustrated in Scheme 53. The presence of the acid will favour the protonation of the hydroxy group, creating a better leaving group.



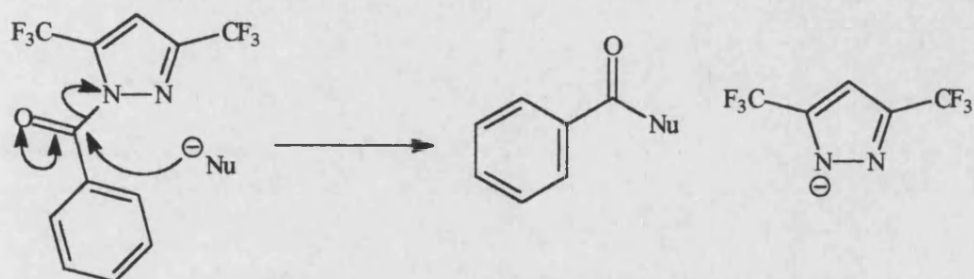
Scheme 53

For 3,5-bis(trifluoromethyl)-4,5-dihydro-5-hydroxy-1-(pentafluorophenyl)pyrazole (**73**), the presence of acid did not lead to dehydration. Therefore, an alternative method was investigated involving a better leaving group. The hydroxypyrazole (**73**) was treated with acetic anhydride and acetic acid under reflux for 16 hours. The corresponding pyrazole (**77**) obtained in good yield, as illustrated in Scheme 54. These reaction conditions led to the conversion of the hydroxy group to an acetoxy group which acts as an efficient leaving group for the dehydration.



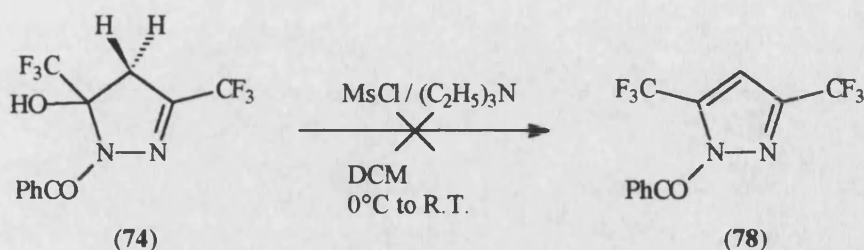
Scheme 54

For the dehydration of 1-benzoyl-3,5-bis(trifluoromethyl)-4,5-dihydro-5-hydroxypyrazole (**74**), relatively non-nucleophilic conditions are required. Consider the mechanism illustrated in Scheme 55.



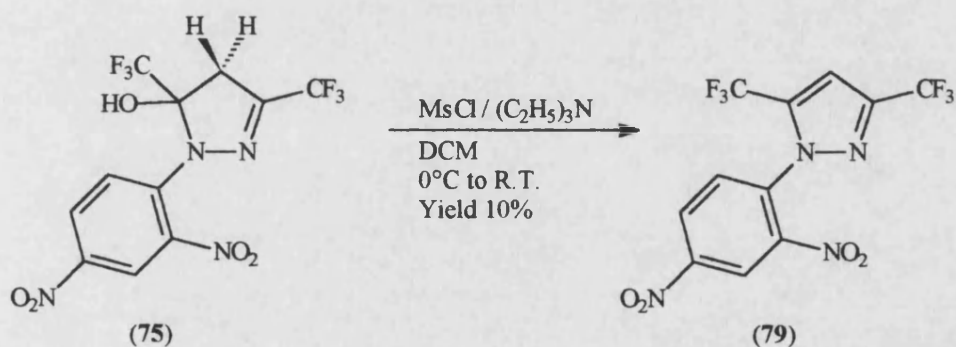
Scheme 55

The ability of a nucleophile to attack the carbonyl group is affected by the pK_a of the resulting anionic leaving group. The pK_a of 3,5-bis(trifluoromethyl)pyrazole (**2**) is 7.55 at 25°C (see Chapter 8). This value may be compared to *p*-nitrophenol, which is known to be a good leaving group and has a pK_a value of 7.15. It was anticipated that formation of the mesylate of hydroxypyrazole (**74**) would allow dehydration to occur, without elimination of the pyrazole. Thus, hydroxypyrazole (**74**) was treated with triethylamine and methane sulphonylchloride in DCM, as illustrated in Scheme 56. A large mixture of products was obtained, but none of the corresponding acylpyrazole (**78**) was isolated. It is likely that the acylpyrazole (**78**) may have been made but was degraded during the "work-up".



Scheme 56

However, similar reaction conditions did lead to the dehydration of 3,5-bis(trifluoromethyl)-4,5-dihydro-1-(2,4-dinitrophenyl)-5-hydroxypyrazole (75) to the corresponding pyrazole (79), as illustrated in Scheme 57.



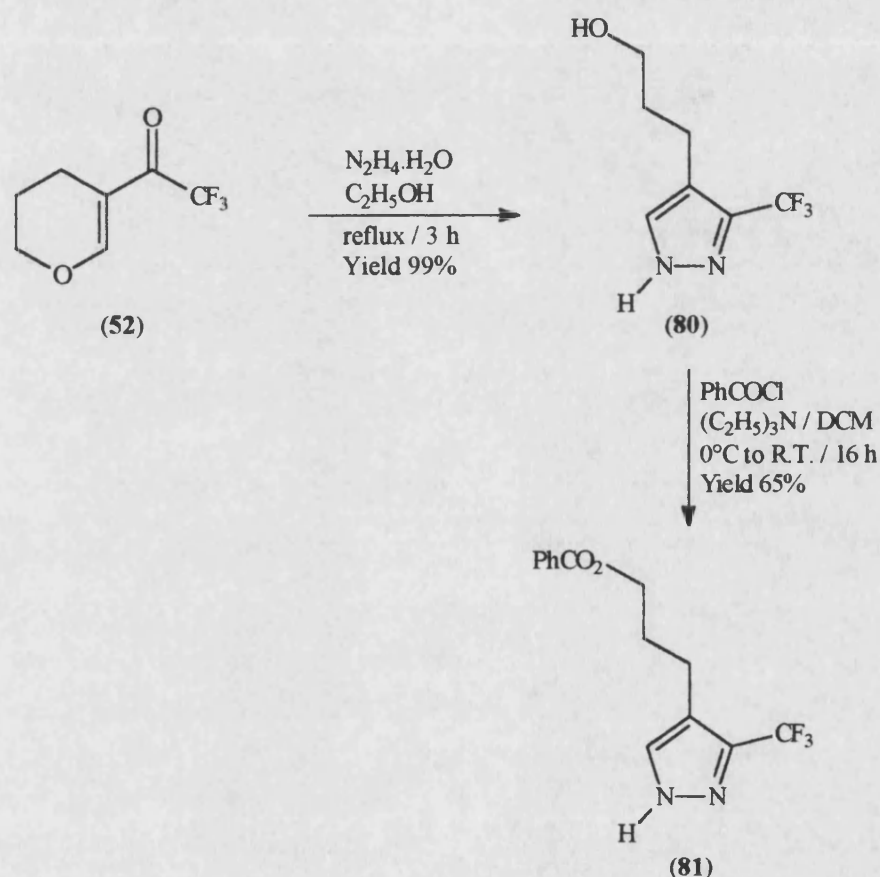
Scheme 57

5.2 Trifluoromethylpyrazoles.

5.2.1 4-Alkyl-3(5)-Trifluoromethylpyrazoles.

In Section 5.1.4.3, the synthesis of 5-trifluoroacetyl-3,4-dihydro-2H-pyran (52) by the trifluoroacetylation of 3,4-dihydro-2H-pyran was described and is illustrated in Scheme 41. It was observed that trifluoroacetylpyran (52) contains a masked 1,3-diketone. Condensation of trifluoroacetylpyran (52) with hydrazine hydrate produced 3-(trifluoromethyl)pyrazole-4-propanol (80) in high yield, as illustrated in Scheme 58. Furthermore, this condensation revealed a ω -hydroxyalkyl function as a leaving group, thus obviating the need

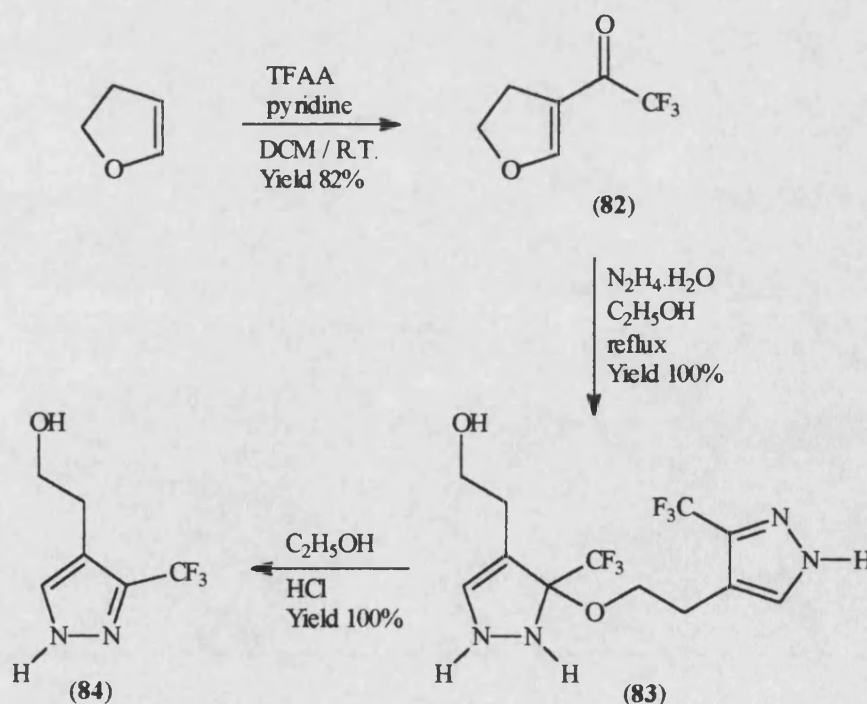
for earlier introduction and possible protection of the hydroxy group. The trifluoromethylpyrazole (**79**) has a single resonance peak in the ^{19}F NMR which is sensitive to pH. The pK_a value was determined by ^{19}F NMR to be 12.07 at 25°C (see Chapter 8). To ensure that the hydroxy group could be derivatised without interference from the pyrazole, the corresponding benzoate ester (**81**) was formed in the usual way, as illustrated in Scheme 58.



Scheme 58

Since this work was carried out, Tang and Hu¹⁵⁴ have reported the synthesis of 3-(trifluoromethyl)pyrazole-4-propanol (**80**) by the addition of the expensive iodopentafluoroethane across the enol ether of 3,4-dihydro-2H-pyran, in the presence of sodium dithionitrite, and treatment of the pentafluoroethyl-tetrahydropyran with hydrazine.

It was anticipated that 3-trifluoroacetyl-4,5-dihydrofuran (**82**) would undergo a condensation reaction with hydrazine hydrate, analogous to that performed by 5-trifluoroacetyl-3,4-dihydro-2*H*-pyran (**52**). The trifluoroacetylfuran (**82**) was synthesised by the treatment of 2,3-dihydrofuran with TFAA and pyridine in DCM. However, treatment of the five-membered ring compound with hydrazine did not give the expected pyrazoleethanol (**84**) directly. Under essentially the same conditions as described for trifluoroacetylpyran (**52**), a quantitative yield of the dimer (**83**) was formed. In this dimer, one molecule of the fully condensed aromatic pyrazole (**84**) has intercepted another molecule where the elimination of water from the intermediate is not complete. It is noteworthy that no material could be isolated where ethanol, rather than the pyrazoleethanol (**84**), has reacted as the incoming nucleophile, despite the much higher concentration of the former. The dimer (**83**) readily formed the target trifluoromethylpyrazole (**84**) upon reflux in the presence of a trace of acid, as illustrated in Scheme 59.



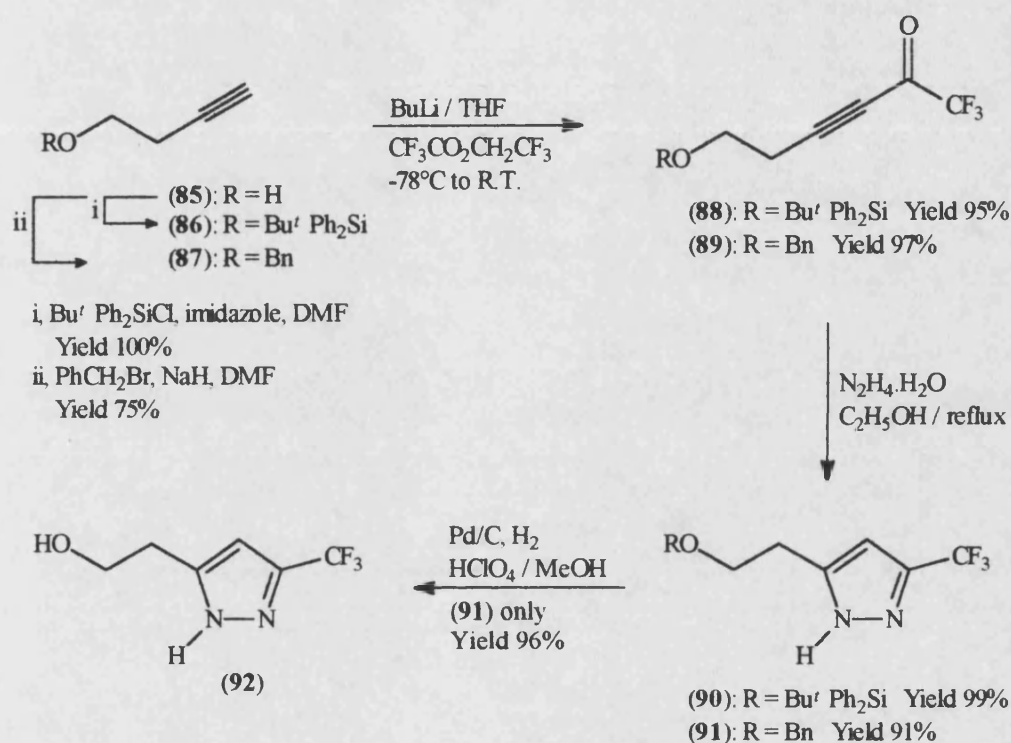
Scheme 59

In a control experiment, it was demonstrated that pyrazole (**84**) was not converted into the dimer (**83**) under the condensation conditions. This indicates that the dimer had not been formed from two molecules of the trifluoromethylpyrazole (**84**). The pK_a value of trifluoromethylpyrazole (**84**) was determined by ^{19}F NMR to be 11.97 at 25°C (see Chapter 8).

5.2.2 3-Alkyl-5-Trifluoromethylpyrazoles.

In an approach to 3-alkyl-5-trifluoromethylpyrazoles, ring formation from hydrazine and an α,β -acetylenic ketone was investigated. In this case, it was not possible to design a process in which the hydroxyalkyl group was revealed during the condensation reaction and it was necessary to assemble an appropriate trifluoromethyl ketone containing the alcohol in a protected form. Butan-3-ynol (**85**) was protected as its TBDPS ether (**86**), essentially by the method of Delome *et al.*¹⁵⁵. This allowed formation of the acetylenic carbanion by treatment with butyl lithium at low temperature. Addition of 2,2,2-trifluoroethyl trifluoroacetate as the electrophile afforded the TBDPS-protected acetylenic trifluoromethylketone (**88**) in high yield. Other electrophilic trifluoroacetylating agents, such as trifluoroacetic anhydride, ethyl trifluoroacetate and ethyl thiotrifluoroacetate were considerably less effective. Condensation of this ketone (**88**) with hydrazine hydrate formed the TBDPS-protected pyrazole-5-ethanol (**90**) in virtually quantitative yield. Unexpectedly, however, it proved impossible to remove the silyl protecting group with fluoride under any conditions under which the product hydroxyethylpyrazole (**92**) could be isolated, as illustrated in Scheme 60. Repetition of the sequence using *O*-benzyl-protection was more successful. The alcohol (**86**) was benzylated, essentially by the method of Johnson *et al.*¹⁵⁶, to give the ether (**87**). As before, formation of the acetylenic anion and trifluoroacetylation, with 2,2,2-trifluoroethyl trifluoroacetate, gave the ketone (**89**) in very high yield. Condensation with hydrazine hydrate in boiling ethanol afforded the protected 3,5-disubstituted pyrazole (**91**). Exposure of the hydroxy group was effected

by hydrogenation under acidic conditions to afford the target trifluoromethylpyrazoleethanol (**92**) with substituents in the desired 3,5-arrangement, as illustrated in Scheme 60. The pK_a value of trifluoromethylpyrazole (**92**) was determined by ^{19}F NMR to be 12.79 at 25°C (see Chapter 8).



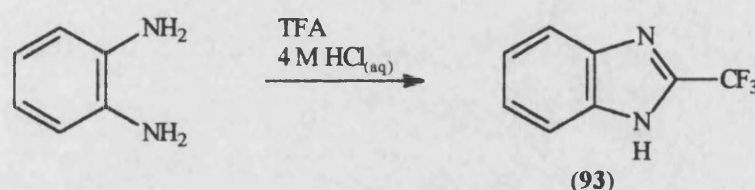
Scheme 60

The reaction sequences towards the synthesis of 4-substituted-3,5-bis(trifluoromethyl)pyrazoles were generally unsuccessful. The deactivating nature of a trifluoromethyl group was a hindrance in many of the reactions. The condensation reactions of carbonyl compounds with 1,1,1,5,5,5-hexafluoropentane-2,4-dione (**1**) were carried out towards the end of this study and are probably the most promising development towards the synthesis of a 3-substituted derivative of dione (**1**). The synthesis of trifluoromethylpyrazoles has been much more successful. Convenient and generally high yielding synthetic routes have been developed to trifluoromethylpyrazoles carrying ω -hydroxyalkyl substituents.

CHAPTER SIX

6. 2-(Trifluoromethyl)benzimidazoles and 2-(Trifluoromethyl)imidazopyridines.

Smith *et al.*¹⁵⁷ have reported the synthesis of 2-(trifluoromethyl)benzimidazole (**93**) from the condensation reaction of the corresponding diamine with trifluoroacetic acid (TFA), as illustrated in Scheme 61.

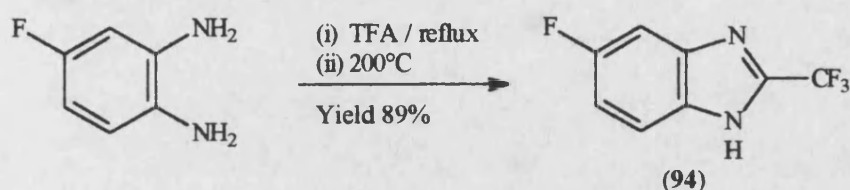


Scheme 61

The acidic pK_a value of 2-(trifluoromethyl)benzimidazole (**93**) was reported¹⁵⁸ to be 8.13. This value is too alkaline to act as a pH sensor in biological systems. It was anticipated that inclusion of a fluorine atom or a trifluoromethyl group into the benzene ring may lower the pK_a value closer to the physiological pH range. Smith *et al.*¹⁵⁷ described the synthesis of 5-fluoro-2-(trifluoromethyl)benzimidazole (**94**) by the condensation reaction of the corresponding diamine with TFA in the presence of aqueous dilute acid. They¹⁵⁷ obtained the benzimidazole (**94**) with a low yield (32%). A much improved set of reaction conditions for the synthesis of the benzimidazole (**94**) and related compounds has been devised.

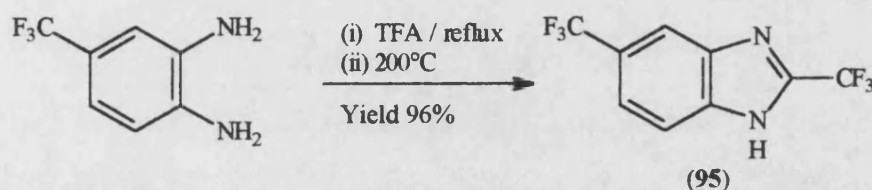
4-Fluorobenzene-1,2-diamine was heated with TFA under reflux for 5 days. The excess TFA was removed by evaporation. ¹H and ¹⁹F NMR indicated the presence of partial condensation products. Therefore, the crude material was sublimed at high temperature to complete the condensation. This straightforward method produced 5-fluoro-2-(trifluoromethyl)benzimidazole

(94) in high yield, as illustrated in Scheme 62.



Scheme 62

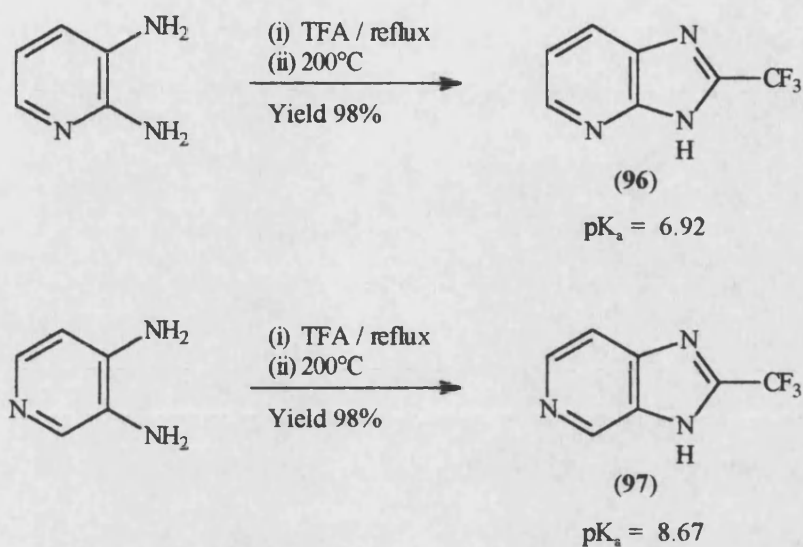
Using similar reaction conditions, 2,5-bis(trifluoromethyl)benzimidazole (95) was synthesised in very high yield, as illustrated in Scheme 63.



Scheme 63

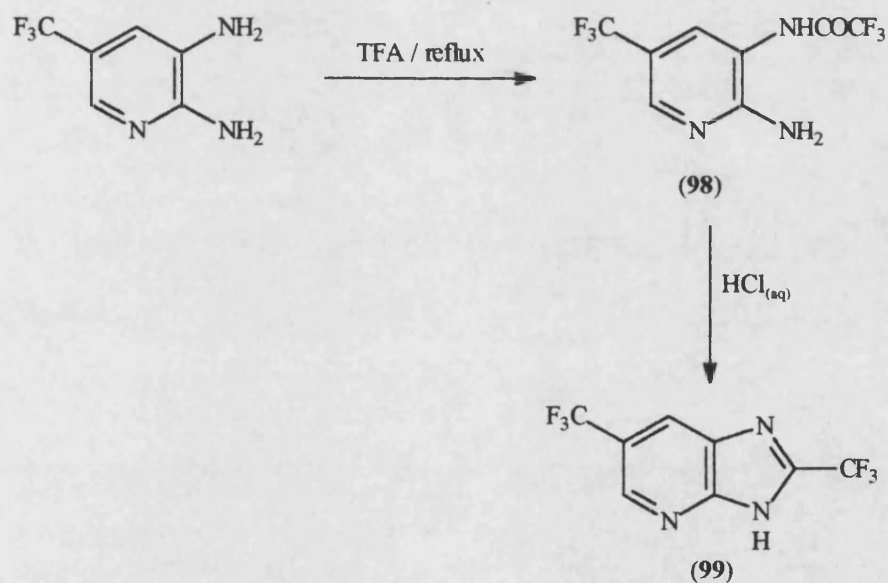
Unfortunately, both of these benzimidazoles (94, 95) were insufficiently soluble in aqueous media to allow determination of the pK_a values by ^{19}F NMR.

It was predicted that 2-(trifluoromethyl)imidazopyridines may have appropriate pK_a values and have better solubilities in water. 2-(Trifluoromethyl)imidazo[4,5-*b*]pyridine (96) and 2-(trifluoromethyl)imidazo[4,5-*c*]pyridine (97) were synthesised by condensation of the corresponding diamine with TFA. Once again, pyrolysis was necessary to complete the elimination and both compounds were obtained in very high yield, as illustrated in Scheme 64. As predicted, both compounds were sufficiently soluble in aqueous media to allow determination of their pK_a values by ^{19}F NMR, as shown in Scheme 64 (see Chapter 8).



Scheme 64

Doherty¹⁵⁹ reported briefly the synthesis of 2,6-bis(trifluoromethyl)imidazo-[4,5-*b*]pyridine (**99**), as illustrated in Scheme 65.



Scheme 65

They¹⁵⁹ implied that the mono-trifluoroacetylated intermediate (**98**) is isolated before pyrolysis in aqueous acid to form the imidazopyridine (**99**).

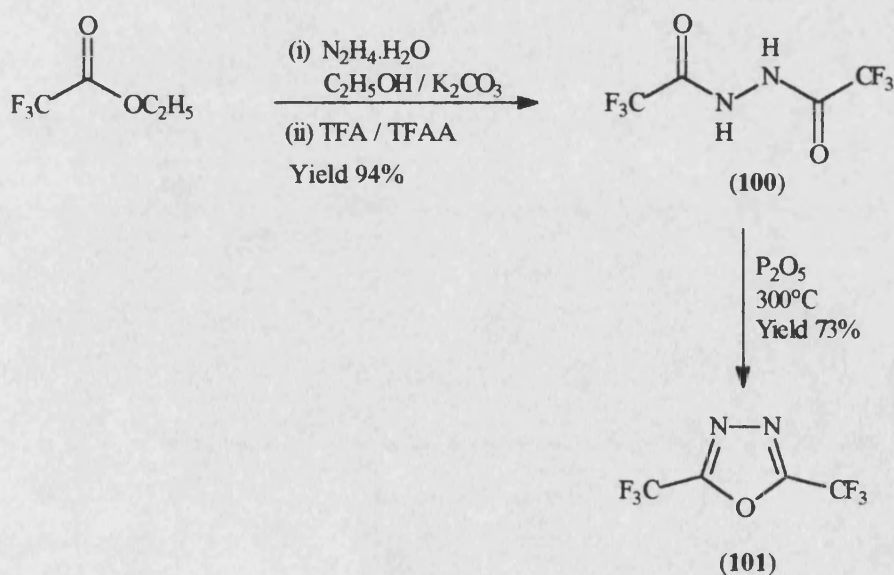
A high yielding set of reaction conditions have been developed for the synthesis of 2-(trifluoromethyl)benzimidazoles and 2-(trifluoromethyl)imidazopyridines. The pK_a values of the imidazopyridines (96, 97) are very promising. Furthermore, both sets of compounds have many positions available for attachment of other substituents, such as groups to modulate the pK_a value and groups to increase the solubility in aqueous media. Therefore, 2-(trifluoromethyl)benzimidazoles and 2-(trifluoromethyl)imidazopyridines are ideal candidates for further development as ^{19}F NMR pH-sensors. It is unfortunate that this work was carried out towards the end of the study.

CHAPTER SEVEN

7. Triazoles, Imidazoles and Pyrroles.

7.1 Triazoles.

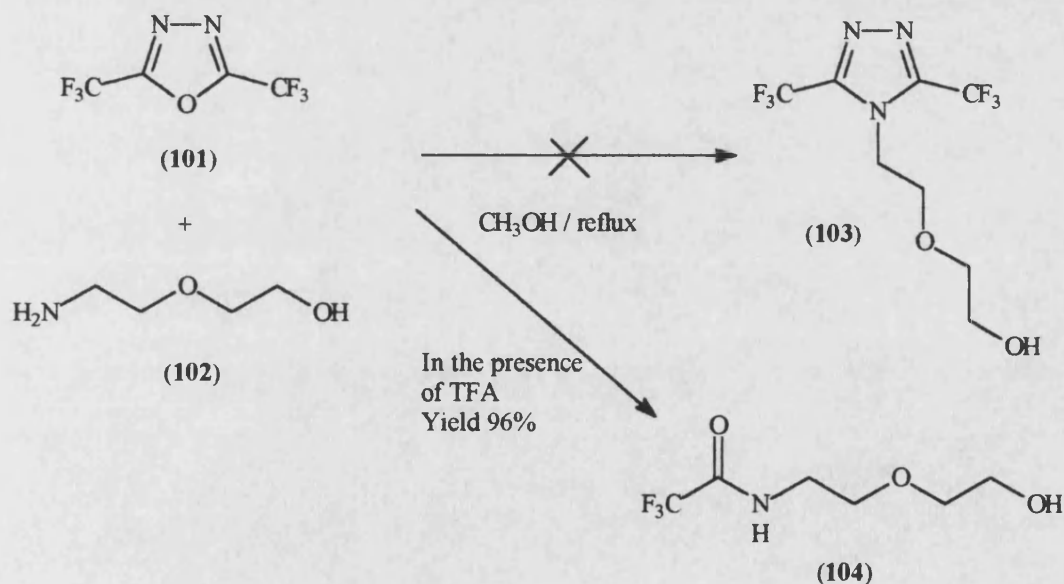
A 1,2,4-triazole bearing trifluoromethyl groups in the 3- and 5-positions would provide a symmetrical compound with 6 fluorine atoms which would be equivalent in the ^{19}F NMR spectrum. A functionalised substituent could occupy the N-4 position without affecting the symmetry. The synthesis of symmetrical 3,5-bis(trifluoromethyl)-4-alkyl-1,2,4-triazoles has been described by Reitz and Finkes¹⁶⁰. The technique involves the synthesis of 2,5-bis(trifluoromethyl)-1,3,4-oxadiazole (**101**) from the corresponding diacylhydrazine (**100**), followed by condensation with a suitable amine. In a modification of the technique used by Reitz and Finkes¹⁶⁰, 1,2-bis(trifluoromethyl)hydrazine (**100**) was cyclised to form the oxadiazole (**101**) in good yield by dehydration with phosphorus pentoxide at high temperature, as illustrated in Scheme 66. The pyrolysis is carried out without the use of solvent. Therefore, it is essential that the reactants are intimately mixed.



Scheme 66

Other methods for the synthesis of oxadiazoles from the corresponding diacyl hydrazines have been reported^{161,162}. The use of SO_3 (in oleum) as the dehydrating agent has been described by Vasilier *et al.*¹⁶¹. Milder conditions have been reported by Sitzman *et al.*¹⁶² for the synthesis of SF_5 containing 1,3,4-oxadiazoles, which should be applicable to trifluoromethyloxadiazoles. These conditions involve dehydration with either phosphorus pentachloride and / or phosphorus oxychloride in refluxing DCM. The techniques described above avoid the use of high temperatures. This may be desirable in the presence of certain functional groups.

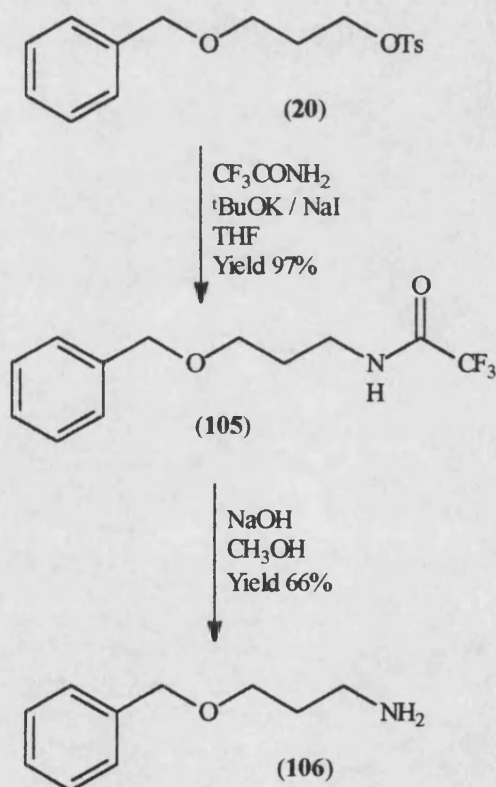
As with all fluorinated heterocycles in this report, it was desirable to introduce a functionalised substituent into the triazole. At first, a condensation reaction between the oxadiazole (101) and unprotected 2-(2-aminoethoxy)ethanol (102) was attempted. This resulted in the isolation of N-(2-(2-hydroxyethoxy)ethyl)-2,2,2-trifluoroacetamide (104) rather than the desired triazole (103), as illustrated in Scheme 67.



Scheme 67

It is likely that acetamide (104) was produced from the reaction of the amine

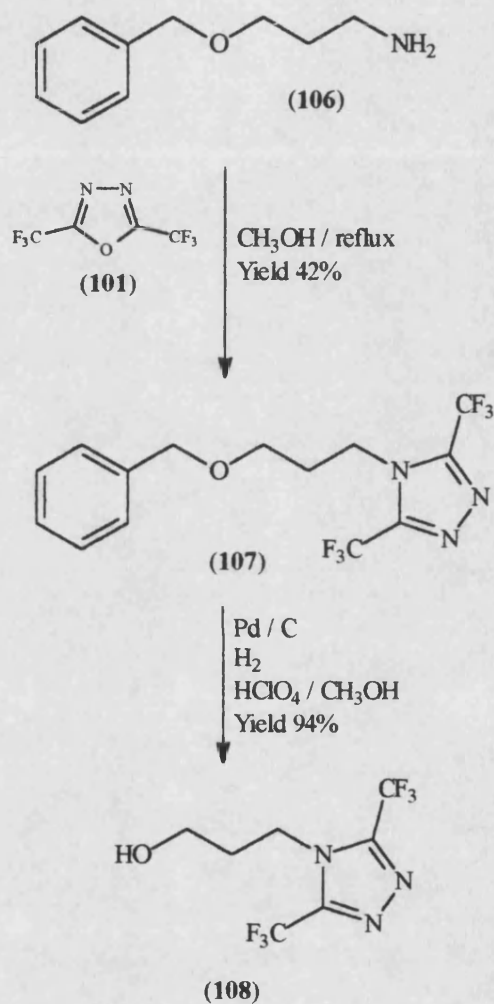
with TFA (either residual or a decomposition product). To avoid possible interference in the reaction from the hydroxy group, an *O*-protected hydroxyalkylamine was synthesised. Once again, the relatively robust benzyl protection group was chosen. 3-Benzyloxypropylamine was synthesised from the mono-*O*-benzyl-protected propane-1,3-diol (**19**). Activation of the alcohol as the tosylate (**20**) was achieved as described earlier and illustrated in Scheme 16. Substitution with the anion derived from trifluoroacetamide served to introduce the nitrogen atom, giving N-(3-(phenylmethoxy)propyl)-2,2,2-trifluoroacetamide (**105**) in very high yield. Selective hydrolytic deprotection under basic conditions afforded the required *O*-benzyl-protected hydroxypropylamine (**106**) in good yield, as illustrated in Scheme 68.



Scheme 68

The amine (**106**) was condensed with the oxadiazole (**101**) with a yield which is comparable to those reported by Reitz and Finkes¹⁶⁰ for other 4-substituted

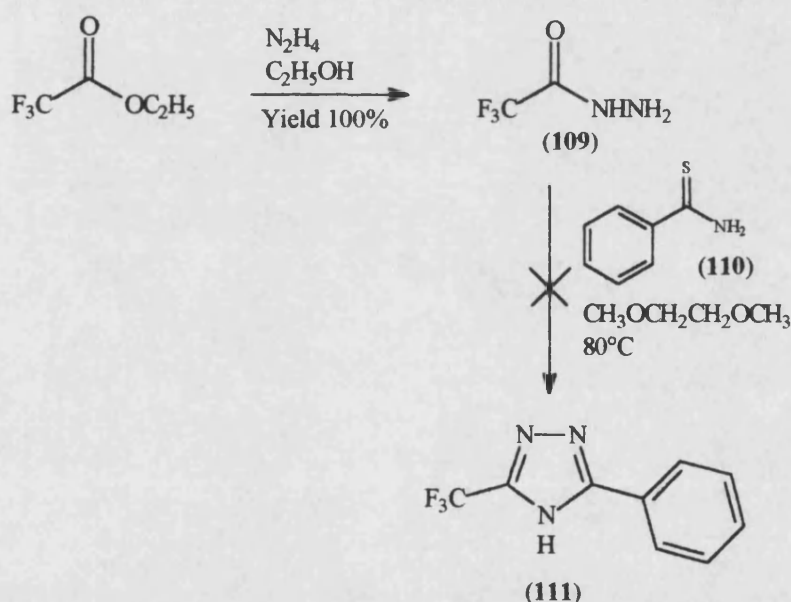
3,5-bis(trifluoromethyl)-1,2,4-triazoles. Exposure of the hydroxy group was effected by hydrogenation under acidic conditions to afford 3,5-bis(trifluoromethyl)-4-(3-hydroxypropyl)-4*H*-1,2,4-triazole (**108**) in high yield, as illustrated in Scheme 69.



Scheme 69

Triazole (**108**) gave a single resonance peak in the ^{19}F NMR spectrum. The position of the peak was sensitive to pH, but only over a very narrow chemical shift range. Furthermore, the pK_a of the conjugate acid was estimated to be approximately 4, which is too acidic for the pH-sensor requirements (see Chapter 8).

A mono-trifluoromethyltriazole could have a more appropriate pK_a value and may show a greater sensitivity in its ^{19}F chemical shift to pH (*c.f.* the greater pH-sensitivity shown by mono-(trifluoromethyl)pyrazoles (**80**, **84**, **92**) compared to bis(trifluoromethyl)pyrazole (**2**)). The synthesis of a trifluoromethyltriazole was briefly investigated towards the end of this study. Unsymmetrical 1,2,4-triazoles are commonly made by thermal condensation of an acylhydrazine with a (thio)amide (the Pellizzari reaction)¹⁶³ or by condensation of a diacylamine with hydrazine (the Einhorn-Brunner reaction)¹⁶⁴. It was anticipated that the synthesis of trifluoromethyltriazole (**111**) could involve the reaction of trifluoroacetylhydrazine (**109**) with thiobenzamide (**110**), as illustrated in Scheme 70. Unfortunately, none of the desired triazole (**111**) was isolated under these conditions.

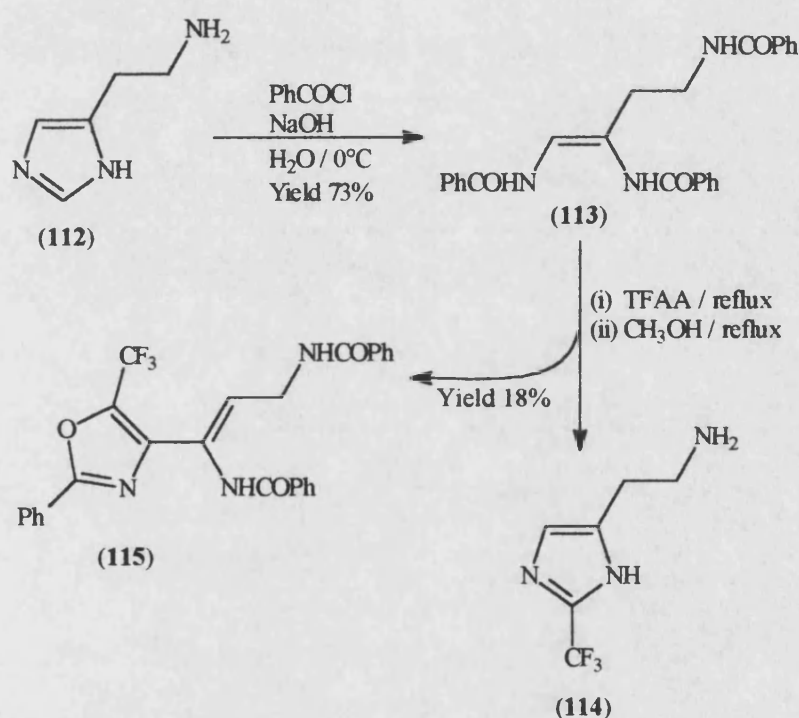


Scheme 70

7.2 Imidazoles.

An imidazole bearing a trifluoromethyl group in the 2-position and a functionalised substituent in the 5-position was required for evaluation as a ^{19}F NMR pH-sensor. The synthesis of 2-trifluoromethylhistamine (**114**) has been

reported by Cohen *et al.*¹⁶⁵ involving Bamberger cleavage of histamine (112), followed by cyclisation with boiling TFAA and acid-catalysed hydrolysis of the side chain benzamide. Cohen *et al.*¹⁶⁵ also noted the formation a major unidentified side-product. An attempt to reproduce this reaction led to the isolation and characterisation of the side product as a trifluoromethyl-4-alkenyloxazole which is formed by an interesting alternative cyclisation, as illustrated in Scheme 71.



Scheme 71

As expected¹⁶⁶, Bamberger fragmentation of histamine (112) gave *S*-1,2,4-tris(benzamido)butene (113). Treatment with boiling TFAA, followed by methanol, gave a poorly soluble solid in moderate yield. The high resolution CI mass spectrum showed a major (M + H)⁺ peak at m/z 492.1535, corresponding to the molecular formula C₂₇H₂₀F₃N₃O₃. ¹⁹F NMR showed only one singlet at δ -58.89; thus one trifluoromethyl group or two equivalent trifluoromethyl groups are present. The ¹H NMR spectrum revealed the presence of only one CH₂ (δ 4.19) and one alkene proton, along with fifteen aromatic protons and

two NH protons. Hence one of the CH₂ of the triamide (113) has become involved in the reaction. A ¹H-¹H COSY spectrum indicated coupling from the CH₂ to the vinylic-H and the upfield NH, as illustrated in Figure 28. No coupling was evident between the alkene-H and either NH. These data show compound (115) to have the alkenyloxazole structure shown. A ¹H-¹H NOESY experiment gave a cross peak between the downfield NH (δ 10.5) and the CH₂ showing Z stereochemistry about the carbon-carbon double bond, as shown in Figure 28.

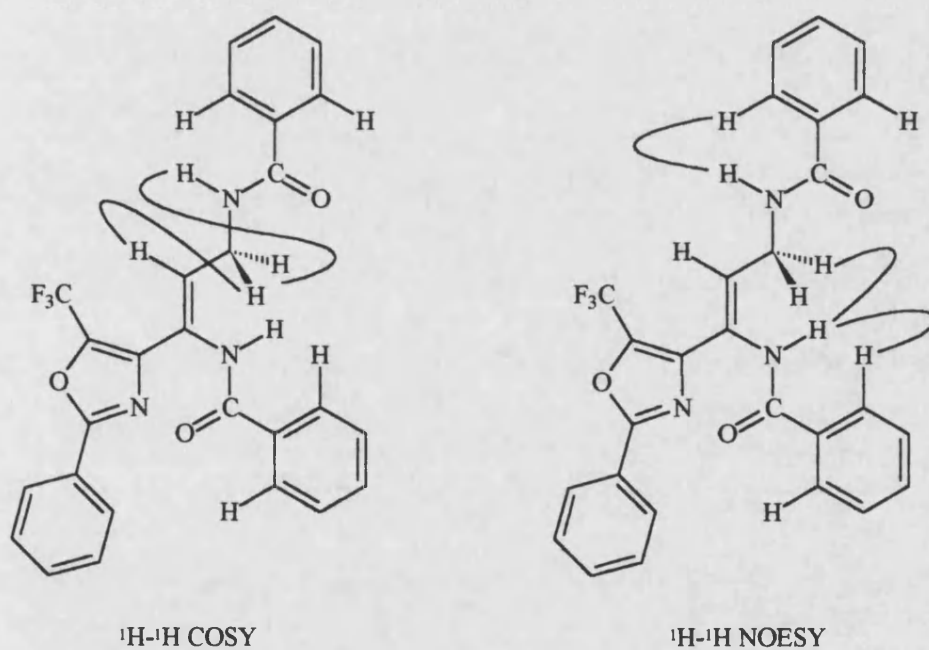


Figure 28. ¹H-¹H COSY and NOESY correlations of alkenyloxazole (115).

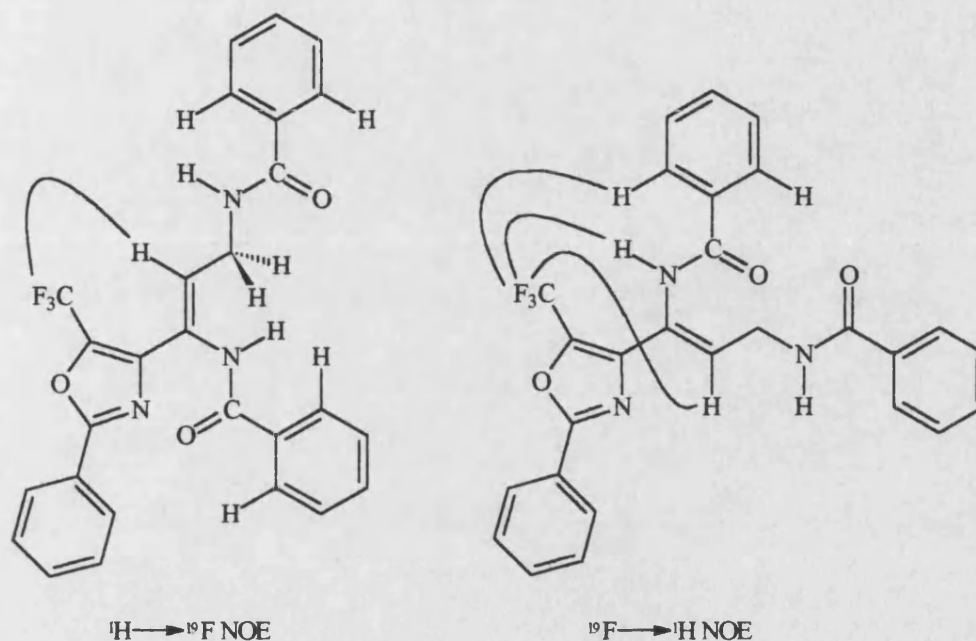
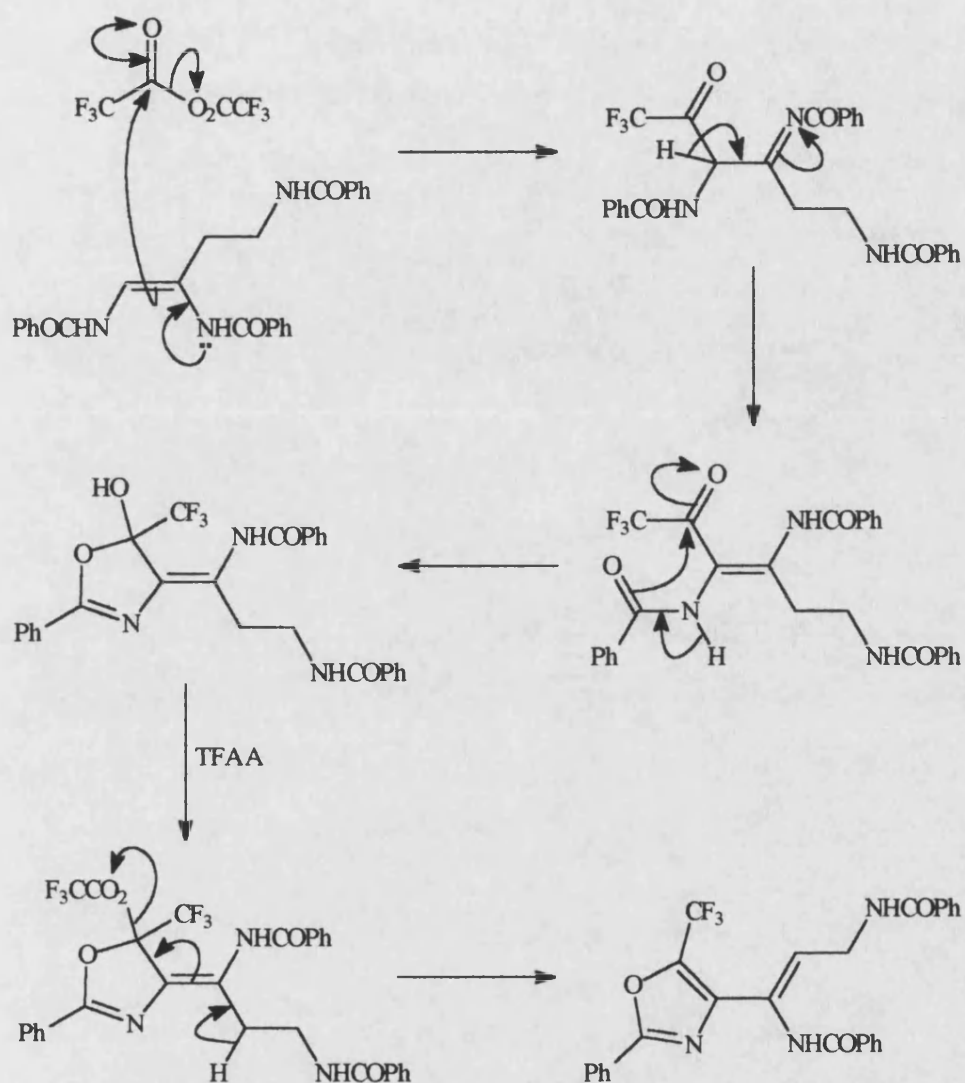


Figure 29. H-F NOE correlations of alkenyloxazole (115).

An NOE enhancement was observed in the ^{19}F signal of the trifluoromethyl group on irradiation at the ^1H frequency of the alkene-H but not on irradiation at the ^1H frequency of the CH_2 , which corroborated this structural assignment, as illustrated in Figure 29. The converse NOE experiment, involving irradiation at the δ_{F} of the trifluoromethyl group, showed enhancement of the ^1H signals of the downfield NH, the vinylic-H and, more weakly, to the 2,6- H_2 of one benzamide, shown in Figure 29.



Scheme 72

To rationalise this unexpected cyclisation, a mechanism such as that shown in Scheme 72 is proposed. Acylation of the triamide (113) at the more sterically accessible enamine position is followed by nucleophilic attack of the amide oxygen on the trifluoromethyl ketone. Trifluoroacetylation of the tetrahedral intermediate at oxygen provides an excellent leaving group for the 1,4-elimination to afford the alkenyloxazole (115).

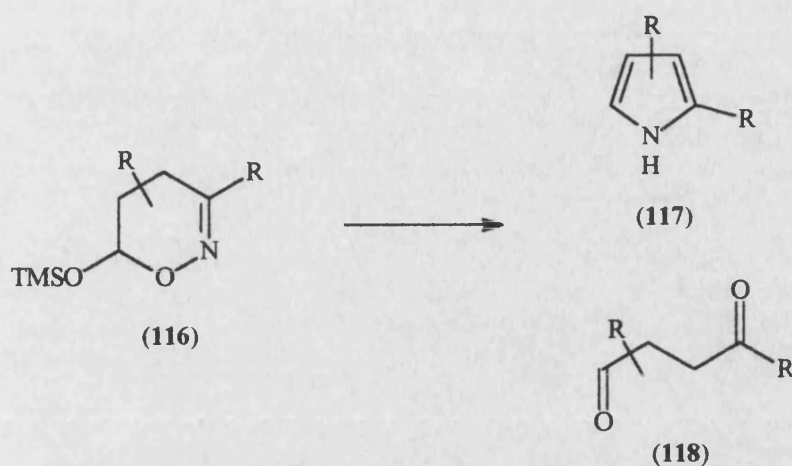
After numerous attempts, these reactions did not produce any of the required 2-trifluoromethylhistamine (114).

7.3 Pyrroles.

A trifluoromethylated pyrrole bearing a functionalised substituent would be an interesting candidate for evaluation as an acidic ^{19}F NMR pH-sensor. Although some pyrroles possessing a perfluoroalkyl group have been prepared by classical methods, such as Knorr condensation¹⁶⁷, more specific approaches have been developed to meet more complicated design requirements. The synthesis of trifluoromethylpyrroles has been carried out by direct trifluoromethylation^{168,169} or by the use of trifluoromethyl-containing synthetic precursors^{170,171,172,173}. Direct trifluoromethylation is usually carried out by electrochemical or photochemical techniques which require special equipment¹⁶⁸. Other direct methods involve highly reactive, often very hazardous reagents, for example bis(perfluoroalkanoyl)peroxides¹⁷⁴. Most methods involving trifluoromethyl-containing synthetic precursors require high temperatures and pressures in thick-walled reaction vessels^{171,172,173,175}.

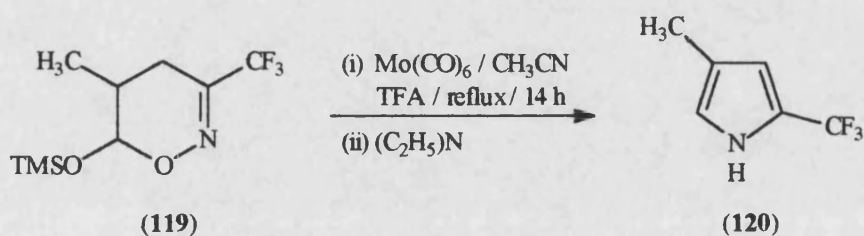
7.3.1 Transition Metal-Induced Transformations of 5,6-Dihydro-4*H*-1,2-Oxazines and the Synthesis of 2-Trifluoromethyl Pyrroles.

Reißig *et al.*¹⁷⁶ have reported the synthesis of 1,2-oxazines (116). They have demonstrated that such compounds contain the required carbon backbone, at the correct oxidation level, for the corresponding pyrroles (117) or dicarbonyl derivatives (118), as illustrated in Scheme 73. The cleavage of N-O bonds with molybdenum hexacarbonyl has been well supported^{177,178,179}. Reißig *et al.*^{176,177} showed that treatment of 1,2-oxazines (116) with molybdenum hexacarbonyl in boiling acetonitrile may lead directly to the formation of the corresponding pyrrole (117), as illustrated in Scheme 73.



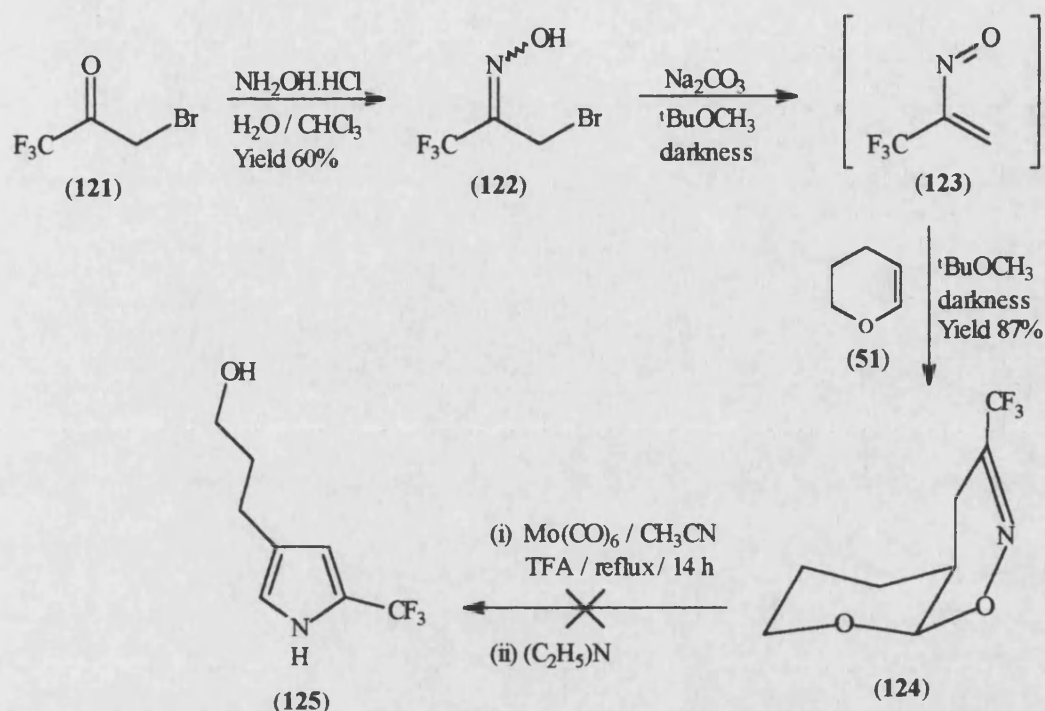
Scheme 73

They¹⁷⁶ suggested that this reaction may be applied to 3-(trifluoromethyl)-1,2-oxazines with one example. This involved the treatment of 5-methyl-5,6-dihydro-3-(trifluoromethyl)-6-(trimethylsiloxy)-4H-1,2-oxazine (119) with molybdenum hexacarbonyl in the presence of trifluoroacetic acid (TFA) in boiling acetonitrile. The result was the isolation of the corresponding 2-(trifluoromethyl)pyrrole (120), as illustrated in Scheme 74.



Scheme 74

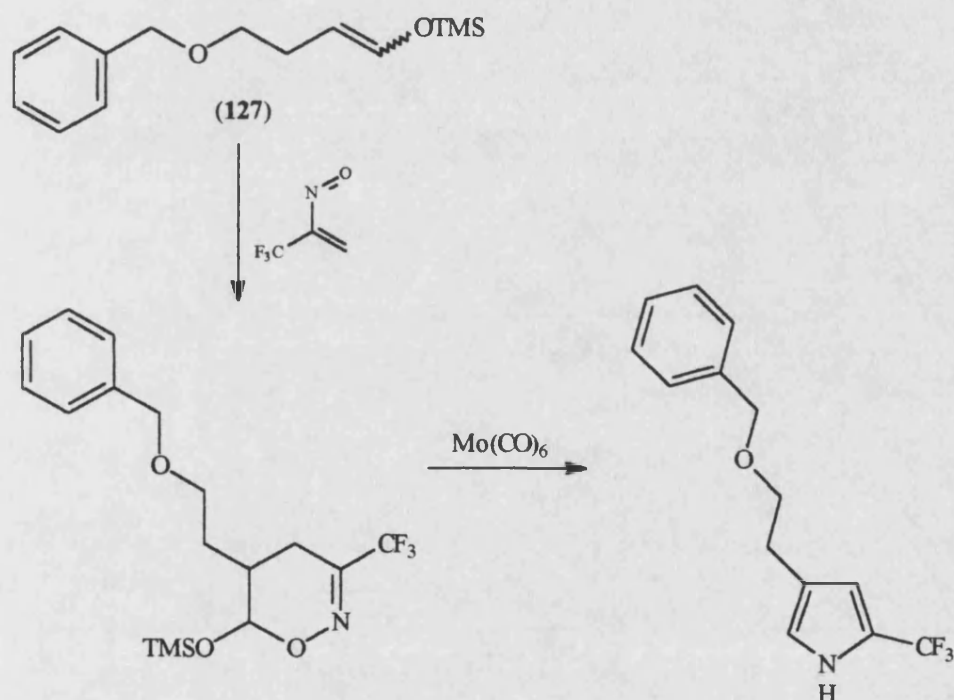
The pyrrole formed in this reaction has a trifluoromethyl group next to a free N-H group and an alkyl substituent in the 4-position. If a compound with a functionalised alkyl substituent could be provided by this reaction, then it would be an ideal candidate for evaluation as a ^{19}F NMR pH-sensor. In the design of a reaction sequence for the synthesis of a 2,4-disubstituted pyrrole, the possibility of revealing a hydroxyalkyl group during ring cleavage with molybdenum hexacarbonyl was investigated.



Scheme 75

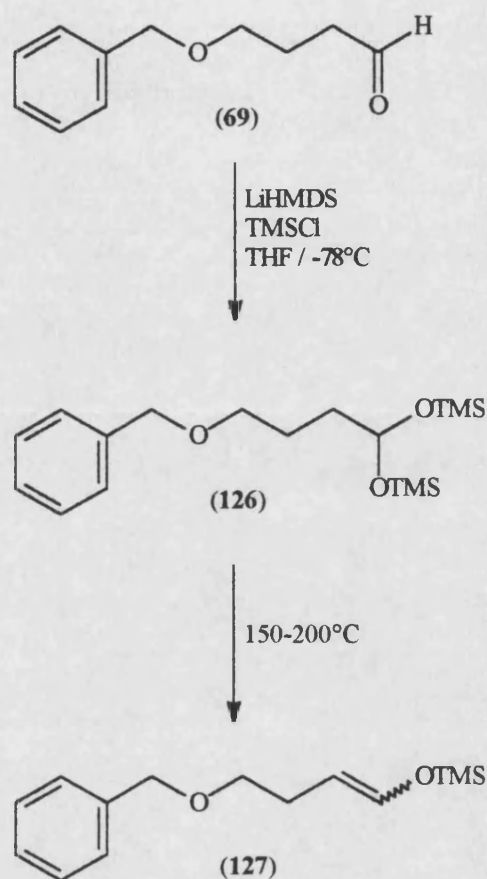
Reiig *et al.*¹⁷⁶ described the synthesis of 4,4a,5,6,7,8a-hexahydro-3-(trifluoromethyl)pyrano[4,5-*e*]-1,2-oxazine (**(124)**) involving the $[4\pi + 2\pi]$ cycloaddition reaction of 1,1,1-trifluoro-2-nitroso-2-propene (**(123)**) with 3,4-dihydro-2H-pyran (**(51)**). Treatment of 1-bromo-3,3,3-trifluoropropan-2-one (**(121)**) with hydroxylamine in a two-phase system ($\text{CHCl}_3 / \text{H}_2\text{O}$) and careful distillation gave the α -bromooxime (**(122)**) which is converted *in situ* to the nitroso alkene (**(123)**) by treatment with base. From the deterioration of an NMR sample, it was observed that the α -bromooxime (**(122)**) is sensitive to light. Reiig *et al.*¹⁷⁶ reported a low yield (31%) for the cycloaddition reaction, which was attributed to the relatively low reactivity of nitrosoalkenes towards *Z* enol ethers. However, considering that reaction usually takes five days for completion, the low yield is more likely to be due to decomposition of the starting material by light. As predicted, the yield of the reaction was increased dramatically using essentially the same reaction conditions described by Reiig *et al.*¹⁷⁶ but keeping the reaction mixture in darkness, as illustrated in Scheme 75. ^1H NMR indicated that only the *cis*-isomer of the pyrano-1,2-

oxazine (124) had formed. The coupling constant between the bridgehead protons is 2.5 Hz. From this information, the protons could be axial-equatorial or equatorial-equatorial. However, an equatorial-equatorial arrangement of the protons would require the ring bonds to be axial-axial which is extremely unlikely for this compound. Furthermore, an axial-equatorial arrangement of the bridgehead protons would be expected from a $[4\pi + 2\pi]$ cycloaddition reaction. Unfortunately, treatment of the oxazine (123) with molybdenum hexacarbonyl in the presence of TFA failed to produce any of the desired pyrrole (125).



Scheme 76

The one example of a 2-(trifluoromethyl)pyrrole described by Reißig *et al.*¹⁷⁶, involved a 6-(trimethylsiloxy)-1,2-oxazine (119). The trimethylsiloxy group (TMSO) may play an important role in this reaction. Therefore, a reaction sequence leading to a 6-(trimethylsiloxy)-1,2-oxazine was devised. The target compounds are illustrated in Scheme 76.

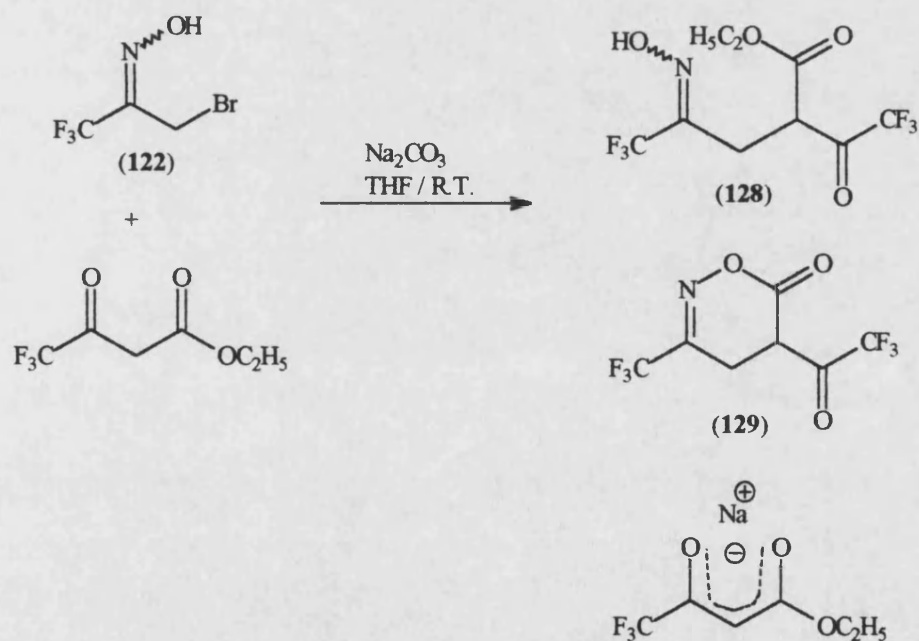


Scheme 77

Trimethylsilyl enol ethers may be prepared from the aldehyde using the method described by Corey *et al.*¹⁸⁰. The aldehyde (69) corresponding to the trimethylsilyl enol ether (127) shown in Scheme 76 was synthesised as described in Chapter Five and in Scheme 51. The enolate of the aldehyde (69) was formed using lithium hexamethyldisilazide (LiHMDS) and was trapped with trimethylchlorosilane (TMSCl). However, the ¹H NMR of the crude material did not contain the characteristic signals of the vinylic protons of a silyl enol ether. Rather, it suggested that the corresponding acetal (126) had formed, as illustrated in Scheme 77. Elimination of one of the TMSO groups was attempted by distillation of the crude material at high temperature. The ¹H NMR of the distillation fractions indicated that elimination of a TMSO group had occurred. However, this was accompanied by decomposition, possibly

involving an intramolecular cyclisation of the enol ether into the benzyl group.

A further investigation into the reactivity of the nitrosoalkene (**123**) was carried out. This involved the generation *in situ* of the nitrosoalkene (**123**), followed by treatment with ethyl 4,4,4-trifluoro-3-oxobutanoate (ETOB) in THF at room temperature. A pale yellow solid was recovered from the reaction mixture. The ^1H and ^{19}F NMR spectra were consistent with that of ETOB. Therefore, the solid recovered from the reaction mixture was probably the sodium salt of ETOB. The CI mass spectrum showed a major $(\text{M} + \text{H})^+$ peak at m/z 185, a moderate sized peak at m/z 310 and a small peak at m/z 264. The major peak represents ETOB. Two products expected from this reaction are the adduct (**128**) and its cyclised derivative (**129**), as illustrated in Scheme 78. It is possible that these compounds are represented in the CI mass spectrum by the two smaller peaks m/z 310 and 264, respectively.



Scheme 78

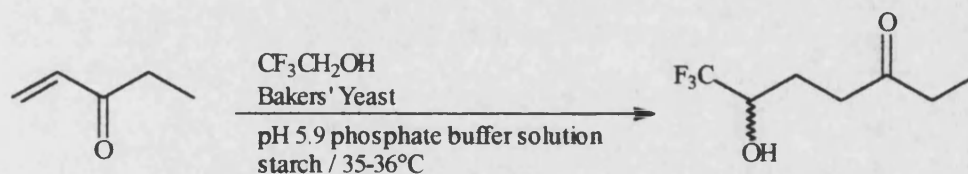
7.3.2 Synthesis of 3-Alkyl-2,5-Bis(trifluoromethyl)pyrroles.

A suitable precursor for the synthesis of a 3-alkyl-2,5-bis(trifluoromethyl)pyrrole (**130**) could be the corresponding 2,5-diketone (**131**), as illustrated by the retrosynthetic analysis of Scheme 79.



Scheme 79

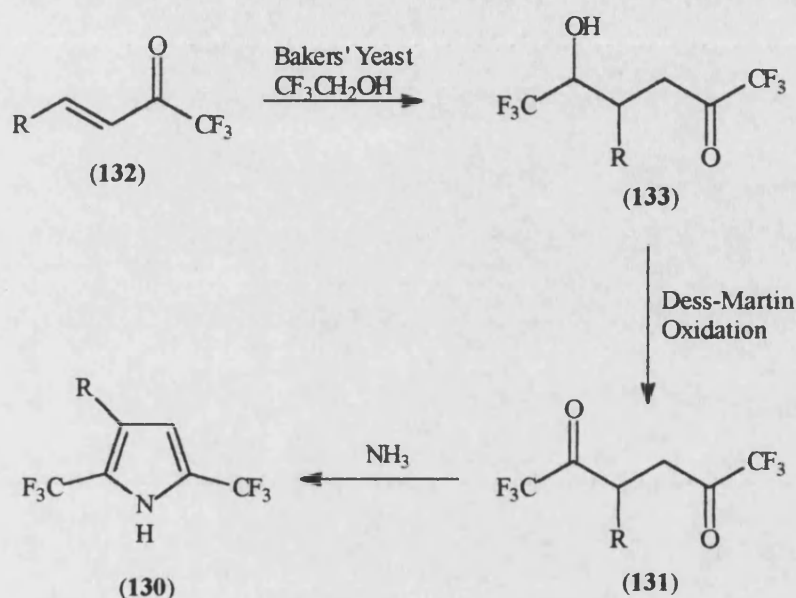
Kitazume *et al.*¹⁸¹ reported a microbial carbon-carbon bond formation between 2,2,2-trifluoroethanol and an α,β -unsaturated ketone, as illustrated in Scheme 80.



Scheme 80

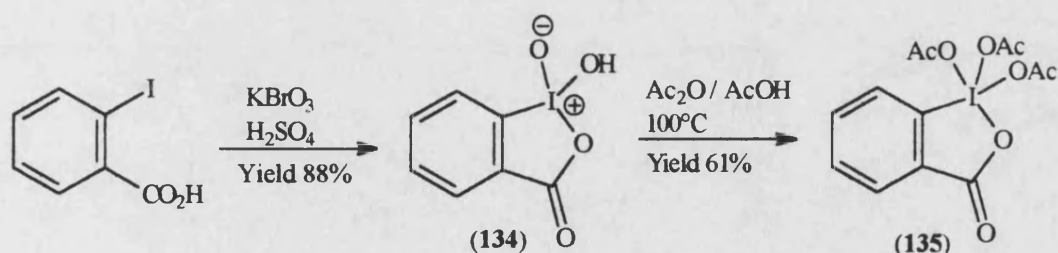
It was anticipated that a similar microbial carbon-carbon bond forming reaction may be induced between 2,2,2-trifluoroethanol and an α,β -unsaturated trifluoromethyl ketone (**132**) to produce a 1,6-bis(trifluoromethyl)carbinol (**133**). The alcohol may be oxidised using the Dess-Martin¹⁸² reagent (**135**). The planned reaction sequence is illustrated in Scheme 81. The synthesis of β -alkyl- α,β -unsaturated trifluoromethyl ketones (**132**) has been reported by Linderman *et al.*^{183,184}. This involves the reduction of the corresponding acetylene followed by oxidation of the alcohol back to the ketone using the Dess-Martin reagent (**135**). The synthesis of two α,β -unsaturated

trifluoromethyl ketones (**88**, **89**) was described in Section 5.2.2 and in Scheme 60. A reduction of 6-((1,1-dimethylethyl)diphenylsilyloxy)-1,1,1-trifluorohex-3-yn-2-one (**88**) was carried out using lithium aluminium hydride. This led to the elimination of the silyl protection group. However, the relatively more robust benzyl-protected acetylene (**89**) was reduced under essentially the same reaction conditions to provide the α,β -unsaturated alcohol (**136**).



Scheme 81

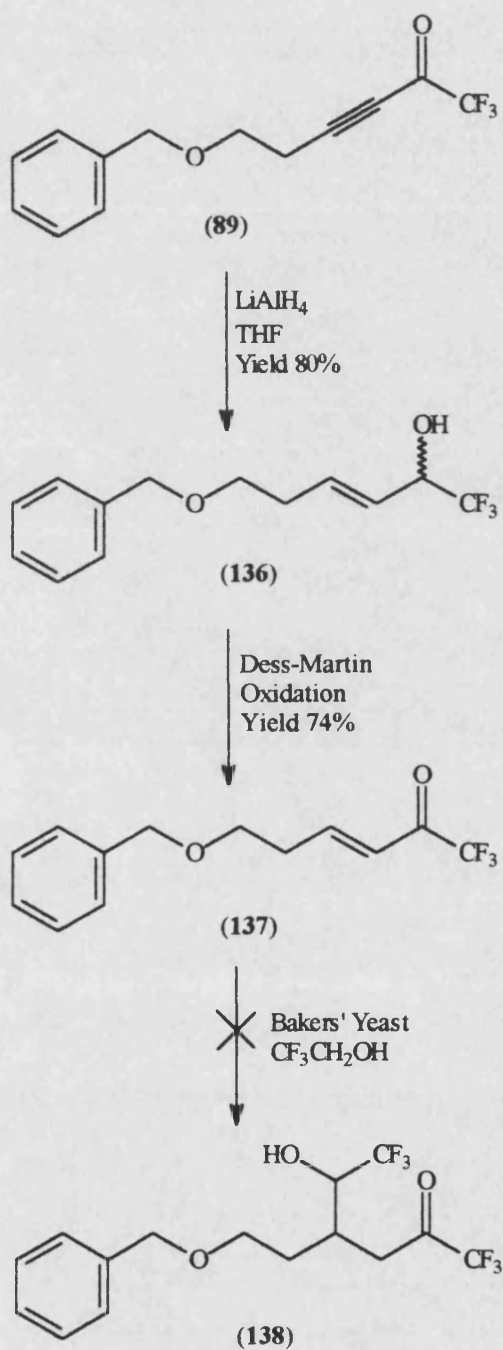
The Dess-Martin reagent (**135**) was prepared in two steps from 2-iodosobenzoic acid, as illustrated in Scheme 82.



Scheme 82

This reagent allowed the successful oxidation of the α,β -unsaturated alcohol

(136) to the corresponding ketone (137) in good yield. Unfortunately, the microbial transformation using bakers' yeast failed to produce the required carbinol (138), as illustrated in Scheme 83.



Scheme 83

A trifluoromethylated pyrrole bearing a functionalised substituent was not

obtained from either of the synthetic routes described. However, it is possible that 3-(trifluoromethyl)-1,2-oxazines may lead to other interesting chemistry. In the case of the microbial transformation described, it is likely that the presence of either the trifluoromethyl group or the benzyl group are not compatible with the reaction.

CHAPTER EIGHT

8. pH Studies.

8.1 Introduction.

Investigations were carried out into the potential of fluorinated pyrazoles, imidazopyridines, benzimidazoles, triazoles and pyridines to act as sensors of pH through variation of ^{19}F chemical shift with state of ionisation and hence pH in aqueous media. This involved making NMR samples of each compound in a range of buffer solutions. Immediately before examining the ^{19}F NMR spectrum, the pH of the solution was measured. Preliminary investigations revealed that the pK_a value was only slightly different when the experiments were carried out at 25°C rather than at 37°C . Therefore, for the initial evaluation of the compounds, the pH measurement of each solution and the NMR accumulations were all carried out at 25°C . It was also found that adjusting the ionic concentrations of the samples to a particular value had an insignificant effect on the pK_a value obtained. Deuterated solvents were not used and, therefore, the NMR samples were run without a deuterium lock. CFCl_3 was used as external chemical shift standard before and after each experiment and no drift was experienced. Each NMR sample was run three times and all the ^{19}F chemical shift values obtained were plotted with the corresponding pH value.

8.2 Pyrazoles.

Unsubstituted pyrazole has an acidic pK_a value of 14.18^{110} . The effect of a trifluoromethyl group on the acid-base properties of pyrazoles has been investigated by Elguero *et al.*¹¹⁰ (entries (a-d) in Table 4). The pK_a values in their report were determined spectrophotometrically according to a method described by Ernst and Menashi¹¹¹. Habracken *et al.*¹⁸⁵ investigated the effects

of a nitro-substituent on the absorption spectra of pyrazoles. The report by Habracken *et al.*¹⁸⁵ also discusses the effects of various substituents on the pK_a value of pyrazoles (entries (e-l) in Table 4). The pK_a values reported¹⁸⁵ were once again obtained spectrophotometrically. The data of these two reports are combined in Table 4.

The ¹⁹F chemical shift of 3,5-bis(trifluoromethyl)pyrazole (2) was found to be pH-dependent between pH 5 and pH 10. The total shift observed in the ¹⁹F NMR spectrum over this pH range was 1.47 ppm. The data are listed in Table 8 in the Appendix and are illustrated in Figure 30. The curve shown in Figure 30, has a sigmoidal shape which is characteristic of one acid-base equilibrium. As the acidity of the medium decreases, there will be an increase in the degree of ionisation of the pyrazole, associated with proton loss. This increases the degree of negativity of the N-1 atom, resulting in an upfield shift in the ¹⁹F NMR spectrum. Hence, the curve has a positive gradient.

	pyrazole	acid pK _a
(a)	unsubstituted	14.18
(b)	3,5-dimethyl-	15.00
(c)	3(5)-(trifluoromethyl)-5(3)-methyl-	12.33
(d)	3,5-bis(trifluoromethyl)-	7.51
(e)	4-nitro-	9.67
(f)	3(5)-nitro	9.81
(g)	4-methyl-3(5)-nitro-	10.10
(h)	4-ethyl-3(5)-nitro-	10.09
(i)	3(5)-nitro-4-phenyl-	9.11
(j)	3(5)-nitro-5(3)-phenyl-	8.75
(k)	3(5)-nitro-5(3)-(4-nitrophenyl)-	7.59
(l)	3,5-dinitro-	3.14

Table 4. pK_a values of pyrazoles (entries (a-d) are from a report by Elguero *et al.*¹¹⁰ and entries (e-l) are from a report by Habracken *et al.*¹⁸⁵).

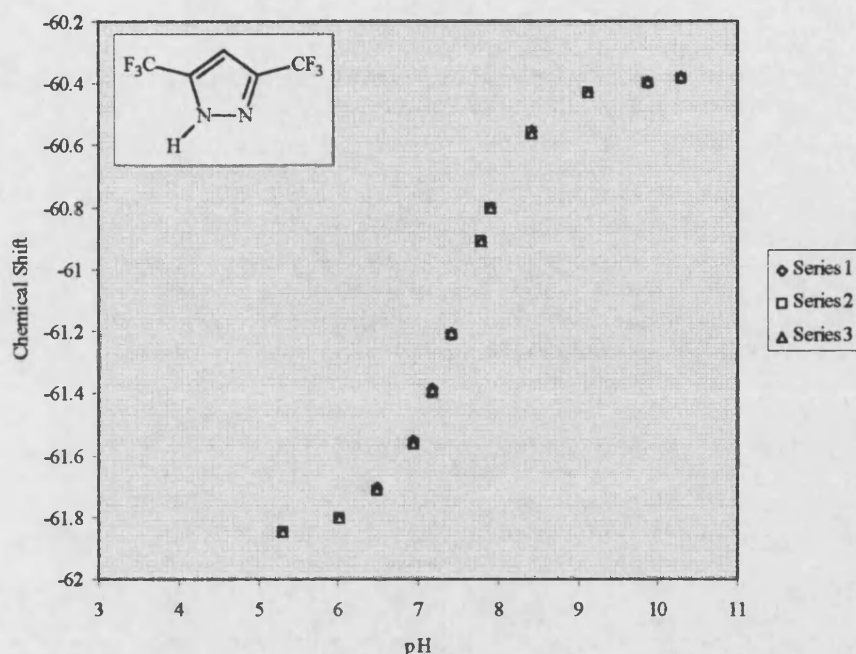


Figure 30. ^{19}F chemical shift (ppm) of 3,5-bis(trifluoromethyl)pyrazole (2) vs pH.

The pK_a value is the pH value where half of the mixture is ionised. On the curve, this is the point of inflection, which is where the curve is changing from being concave upwards to being concave downwards. On a symmetrical sigmoidal curve, such as that shown in Figure 30, this is usually taken to be the point on the curve which falls halfway between the maximum and the minimum. Thus, the pK_a value of bis(trifluoromethyl)pyrazole (2) is 7.55 at 25°C . This value is comparable to the value reported¹¹⁰ by Elguero *et al.* and shown in Table 4.

The pK_a values of 3-(trifluoromethyl)pyrazole-4-propanol (80), 2-(3-trifluoromethylpyrazol-4-yl)ethanol (84) and 2-(5-trifluoromethylpyrazol-3-yl)ethanol (92) were also determined using ^{19}F NMR. The report by Elguero *et al.*¹¹⁰ suggests that the absence of a trifluoromethyl group would lead to a large increase in the pK_a value, as shown for entry (c) in Table 4. In fact, the pK_a values of trifluoromethylpyrazoles (80, 84, 92) were shifted such that the

maxima of the corresponding pH- δ_F curves were beyond the practical limits of this technique. However, extrapolation of the curves allowed good estimates of the pK_a values. The pK_a value of 3-(trifluoromethyl)pyrazole-4-propanol (**80**) was estimated to be 12.07 at 25°C (Table 9 in the Appendix and Figure 31), while the pK_a value of 2-(3-trifluoromethylpyrazol-4-yl)ethanol (**84**) was estimated to be 11.97 at 25°C (Table 10 in the Appendix and Figure 32). The slightly lower pK_a value of pyrazole (**84**) compared to pyrazole (**80**) is probably due to a combination of effects. This may include the increasing degree of hyperconjugation (compare 4-methyl-3(5)-nitro-pyrazole, entry (g) in Table 4, with 4-ethyl-3(5)-nitro-pyrazole, entry (h)) and the increasing importance of the negative inductive effect of the hydroxy group. The pK_a value of 2-(5-trifluoromethylpyrazol-3-yl)ethanol (**92**) was estimated to be 12.79 at 25°C, as illustrated in Table 11 in the Appendix and Figure 33. The different pK_a values encountered when moving the ethanol group from the 4-position to the 3(5)-position is unexpected when compared the pK_a value of 3(5)-(trifluoromethyl)-5(3)-methyl-pyrazole (entry (c) in Table 4). It is interesting that the total shifts with pH observed in the ^{19}F NMR spectra for the trifluoromethylpyrazoles (**80**, **84**, **92**) (2.21 ppm, 2.09 ppm and 2.33 ppm, respectively) are significantly larger than that observed for bis(trifluoromethyl)pyrazole (**2**). The three δ_F -pH plots of trifluoromethylpyrazoles (**80**, **84**, **92**) are combined in Figure 34.

3-(Pyridin-4-yl)-5-(trifluoromethyl)pyrazole was kindly donated by Professor S. P. Singh, Kurukshetra University, Kurukshetra, India. The pK_a value of this compound was determined by ^{19}F NMR to be 9.49, as illustrated in Table 12 in the Appendix and Figure 35. The ^{19}F chemical shift was sensitive to the pH of the medium over the range pH 8 to pH 11 with a total shift in the ^{19}F NMR spectrum of 2.04 ppm. This value suggests that it may be feasible to shift the pK_a of a trifluoromethylpyrazole to a value close to that of physiological pH. This may also allow the greater total shift observed for trifluoromethylpyrazoles compared to bis(trifluoromethyl)pyrazoles to be

maintained.

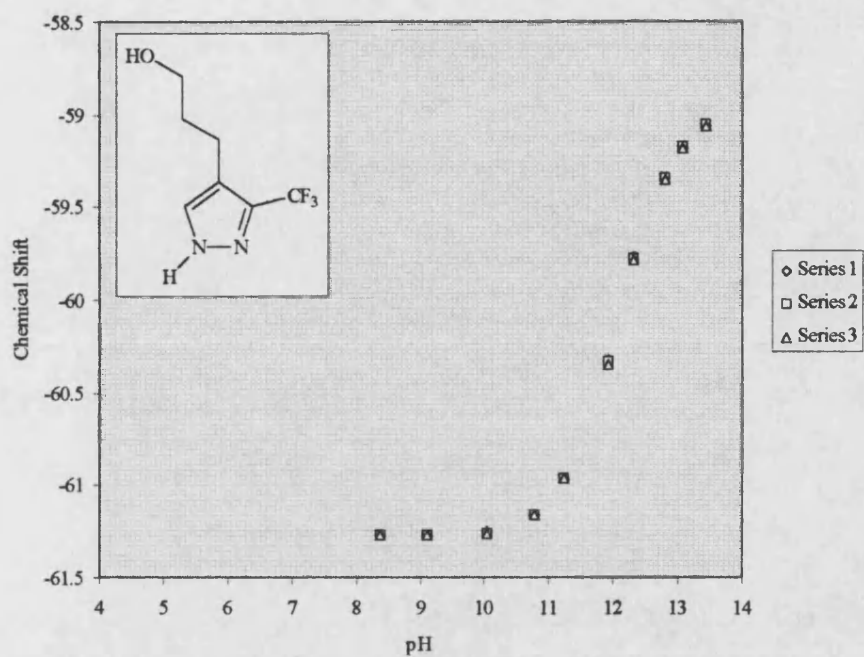


Figure 31. ^{19}F chemical shift (ppm) of 3-(trifluoromethyl)pyrazole-4-propanol (80) vs pH.

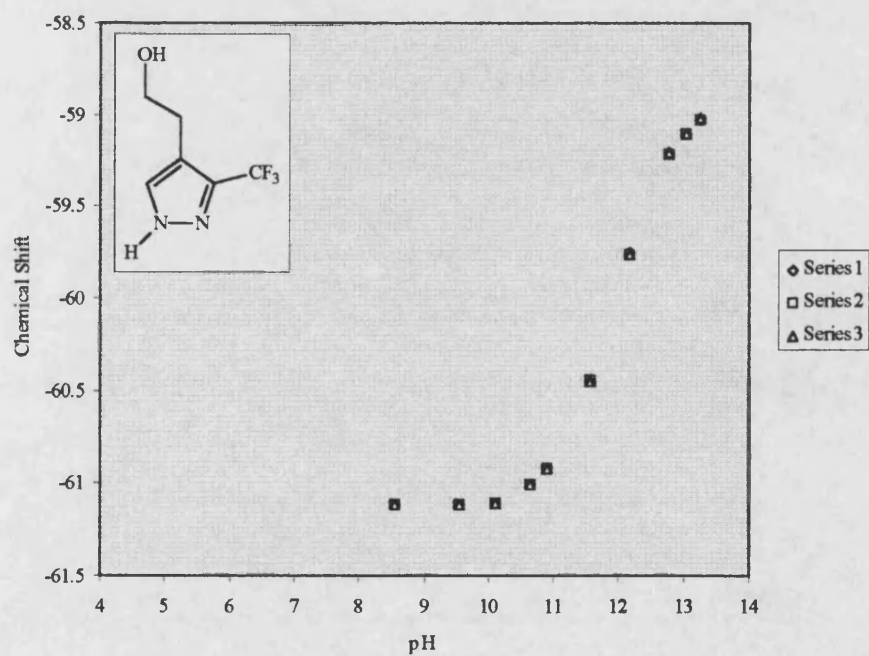


Figure 32. ^{19}F chemical shift (ppm) of 2-(3-trifluoromethylpyrazol-4-yl)ethanol (84) vs pH.

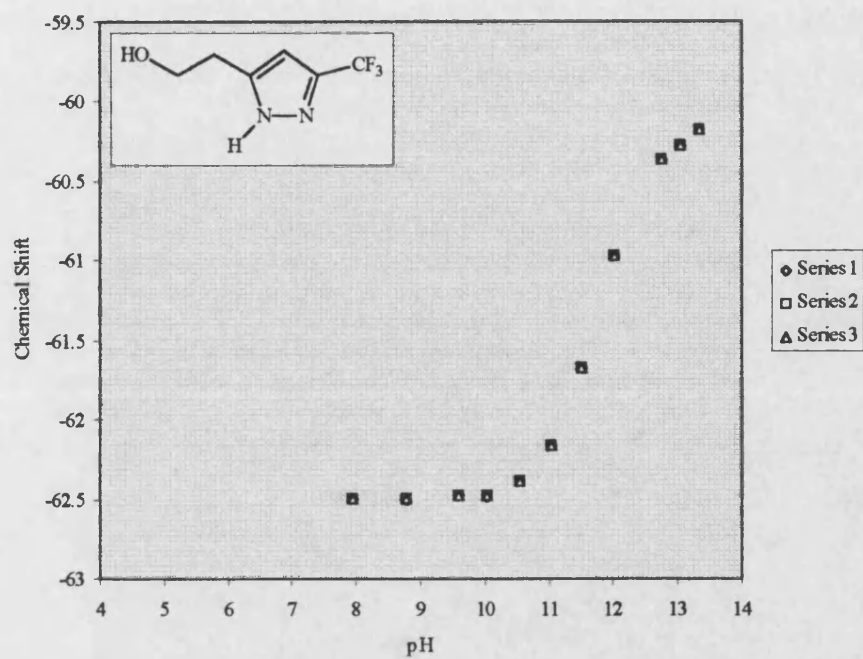


Figure 33. ^{19}F chemical shift (ppm) of 2-(5-trifluoromethylpyrazol-3-yl)ethanol (92) vs pH.

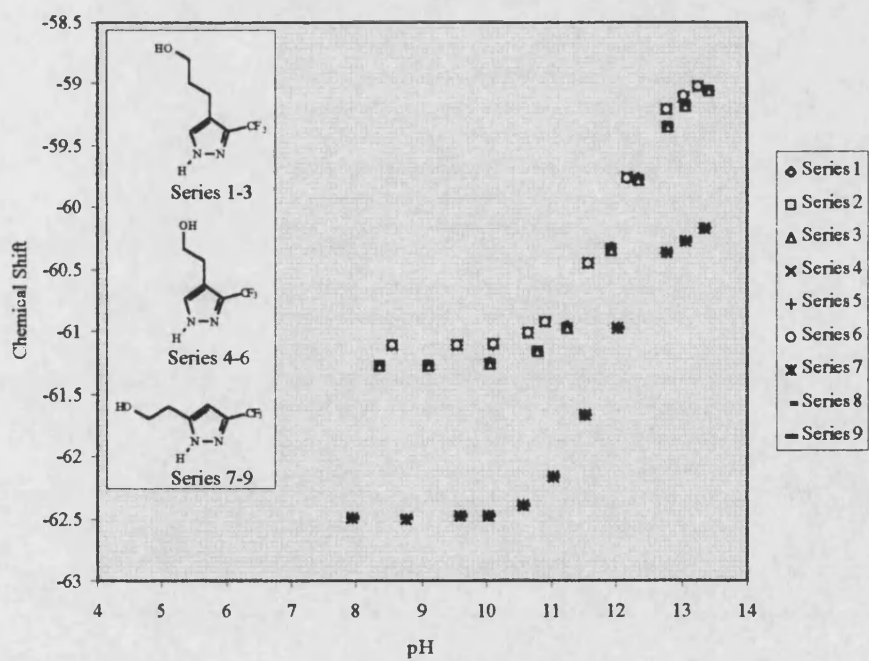


Figure 34. ^{19}F chemical shift (ppm) of pyrazoles (80, 84, 92) vs pH.

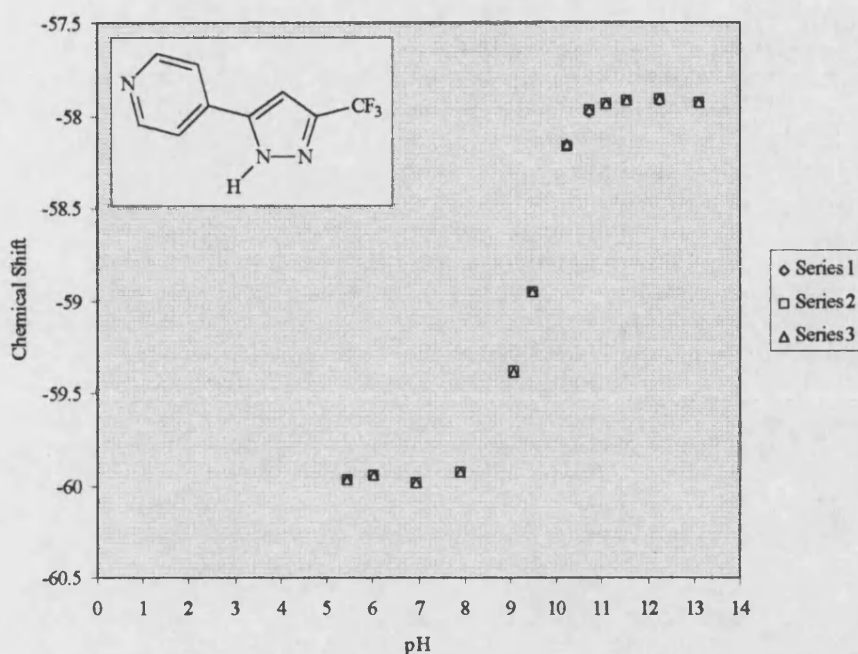


Figure 35. ^{19}F chemical shift (ppm) of 3-(pyridin-4-yl)-5-(trifluoromethyl)pyrazole vs pH.

8.3 Benzimidazoles and Imidazopyridines.

The pK_a values of a number of benzimidazoles are listed in Table 5. The acidic pK_a value of unsubstituted benzimidazole is much lower than physiological pH, entry (a) in Table 5. The introduction of a trifluoromethyl group into the 2-position was reported¹⁵⁸ to raise the pK_a value to 8.13, entry (d). If the reported¹⁵⁸ pK_a value of 2-trifluoromethylbenzimidazole is correct, then the introduction of a trifluoromethyl group or a fluorine atom into the benzene ring would be expected to lower the pK_a , possibly to a value closer to physiological pH. Furthermore, this may serve as an internal reference peak in the ^{19}F NMR.

2,5-Bis(trifluoromethyl)benzimidazole (**95**) and 5-fluoro-2-(trifluoromethyl)-benzimidazole (**94**) were synthesised but are insufficiently soluble in aqueous media to allow determination of their pK_a values by ^{19}F NMR.

	benzimidazole	acidic pK _a
(a)	unsubstituted	5.52
(b)	2-ethyl-	6.18
(c)	2-phenyl-	5.23
(d)	2-trifluoromethyl-	8.13

Table 5. pK_a values of benzimidazoles (entries (a-c) are from a report by Weast¹⁸⁶ and entry (d) is from a report by Elguero *et al.*¹⁵⁸.

Fortunately, 2-(trifluoromethyl)imidazopyridines (**96**, **97**) were sufficiently soluble in aqueous media. The ¹⁹F chemical shift of 2-(trifluoromethyl)imidazo-[4,5-*b*]pyridine (**95**) was found to be pH-dependent between pH 1 and pH 8. The data are listed in Table 13 in the Appendix and are illustrated in Figure 36. As can be seen in Figure 36, the total shift is comprised of two sigmoidal curves, both with positive gradients. The two pK_a values are 6.92 and approximately 2.2 at 25°C. The larger of the two sigmoidal curves, which has a pK_a value of 6.92, represents the N-H of the imidazole. The smaller sigmoidal curve, which has an estimated pK_a value of 2.2, could either correspond to the N-3 position, the N-7 position or to the basic pK_a of the imidazole N-H. Considering reported¹⁸⁶ pK_a values and pK_a values determined in this study for pyridines, this pK_a value probably represents the N-7 position. The total shift observed in the ¹⁹F NMR spectrum for the higher pK_a value is 0.55 ppm, which is the difference between the minimum and maximum of the corresponding sigmoidal curve. The total shift observed in the ¹⁹F NMR spectrum for the lower pK_a value is 0.23 ppm. The combined shift observed between pH 1 and pH 8 is 0.78 ppm. The acidic pK_a value of the imidazole N-H is very close to physiological pH. Furthermore, the introduction of an alkyl substituent on the pyridine ring should result in a minor shift in the pK_a value towards physiological pH.

The ¹⁹F NMR chemical shift of 2-(trifluoromethyl)imidazo[4,5-*c*]pyridine (**97**) was found to be pH-dependent between pH 2 and pH 10.5. The data are listed

in Table 14 in the Appendix and are illustrated in Figure 37. The total shift is comprised of one sigmoidal curve with a positive gradient and a downwards drift at lower pH values, probably associated with a second pK_a . The pK_a value of the sigmoidal curve is 8.78 at 25°C and is the acidic pK_a of the N-H of the imidazole-portion of the compound. The total shift observed in the ^{19}F NMR spectra is 0.87 ppm, which is the difference between the minimum and maximum of the sigmoidal curve.

Both of the imidazopyridines have very promising pK_a values. It would be interesting to measure the pK_a of a 4-, 5- or 7-trifluoromethyl derivative of 2-(trifluoromethyl)imidazo[4,5-*c*]pyridine (97). The presence of an extra trifluoromethyl group may lower the pK_a to a value close to physiological pH.

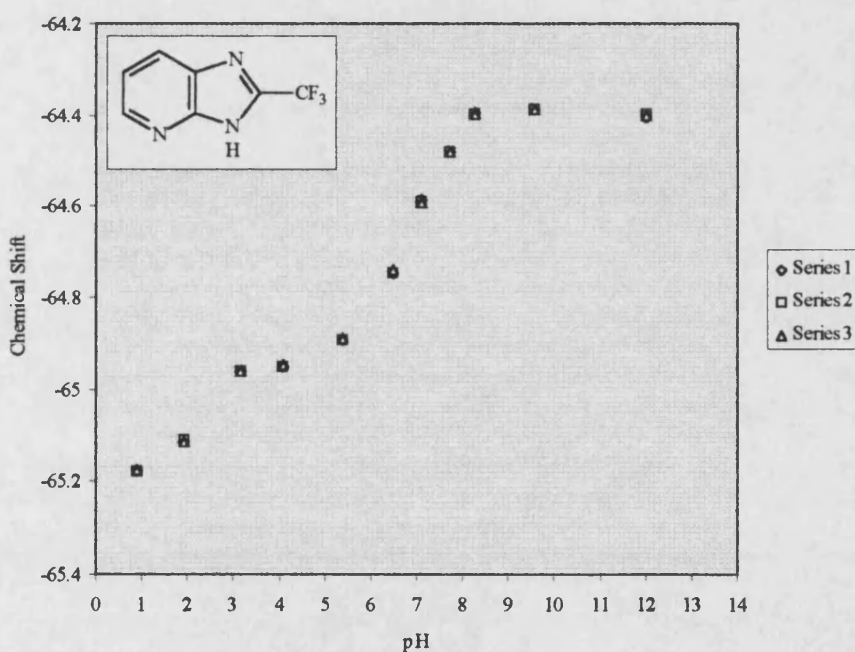


Figure 36. ^{19}F chemical shift (ppm) of 2-(trifluoromethyl)imidazo-[4,5-*b*]pyridine (96) vs pH.

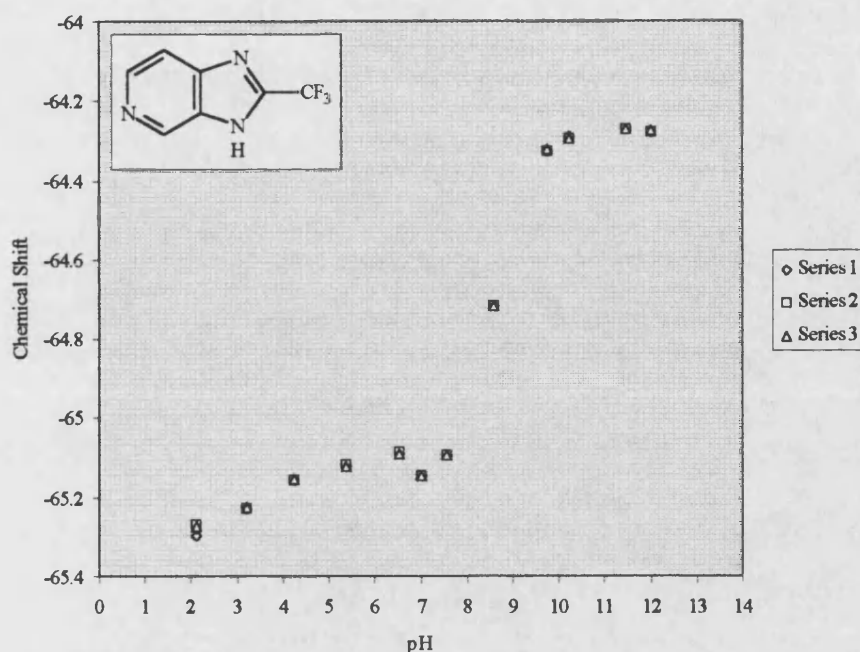


Figure 37. ^{19}F chemical shift (ppm) of 2-(trifluoromethyl)imidazo-[4,5-*c*]pyridine (**97**) vs pH.

8.4 Pyridines.

The reported pK_a values of substituted pyridines are listed in Table 6. The effect of a trifluoromethyl group on the pK_a was investigated. The ^{19}F chemical shift of 4-(trifluoromethyl)pyridine was examined between pH 3 and pH 11. No shift in the position of the peak in the ^{19}F NMR spectra was observed. It is likely that the pK_a value lies below pH 3, which was considered to be too low to warrant further investigation.

The ^{19}F chemical shift of 3-(trifluoromethyl)pyridine was also initially examined between pH 3 and pH 11. A slight upfield shift of the trifluoromethyl peak was observed. Therefore, further examinations of the ^{19}F chemical shift were carried out at lower pH values. The data are listed in Table 15 in the Appendix and are illustrated in Figure 38. The ^{19}F chemical shift of 3-(trifluoromethyl)pyridine was found to be pH-dependent between pH 1 and pH 4. The

sigmoidal curve has a positive gradient and the total shift between the minimum and maximum is 1.00 ppm. The pK_a value is 2.67 at 25°C. As expected, this value is much lower than physiological pH. The presence of electron-donating groups on the pyridine ring would increase the pK_a to a more suitable value.

pyridine	pK_a
unsubstituted	5.25
4-amino-	9.11
2-benzyl-	5.13
2-ethyl-	5.89
3-methyl-	5.68
3-chloro-	2.84

Table 6. Reported 186 pK_a values of pyridines.

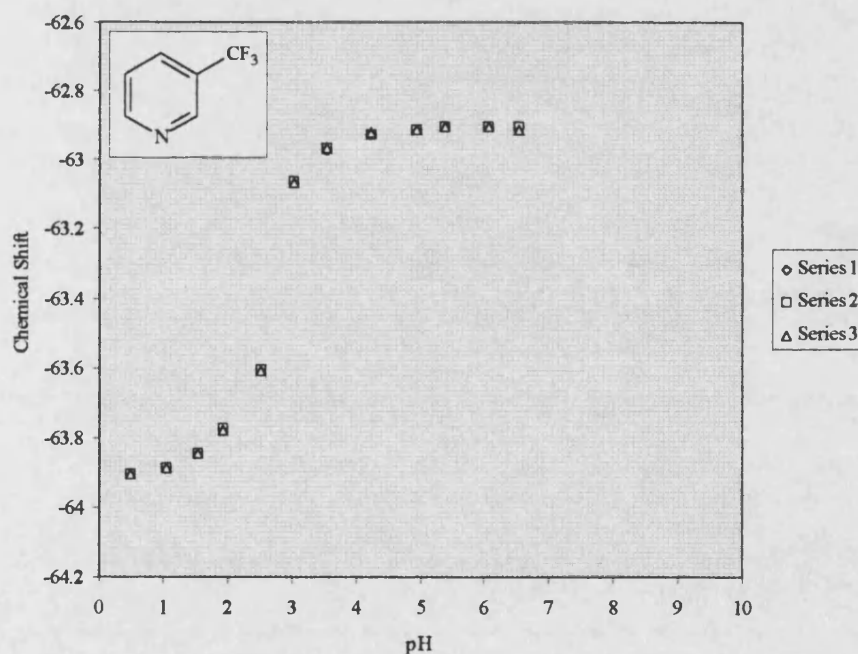


Figure 38. ^{19}F chemical shift (ppm) of 3-(trifluoromethyl)pyridine vs pH.

8.5 Triazoles.

The ^{19}F chemical shift of 3,5-bis(trifluoromethyl)-4-(3-hydroxypropyl)-4*H*-1,2,4-triazole (**108**) was examined between pH 0.02 and pH 10. Below pH 5, a slight downfield shift was observed. The data are listed in Table 16 in the Appendix and are illustrated in Figure 39. The total shift observed in the ^{19}F NMR spectra was only 0.09 ppm. If the curve shown in Figure 39 is assumed to be a sigmoidal curve with a negative gradient, then the pK_a value is approximately 4 at 25°C. Due to the very small shift observed, further examination of the pK_a of this compound was not carried out.

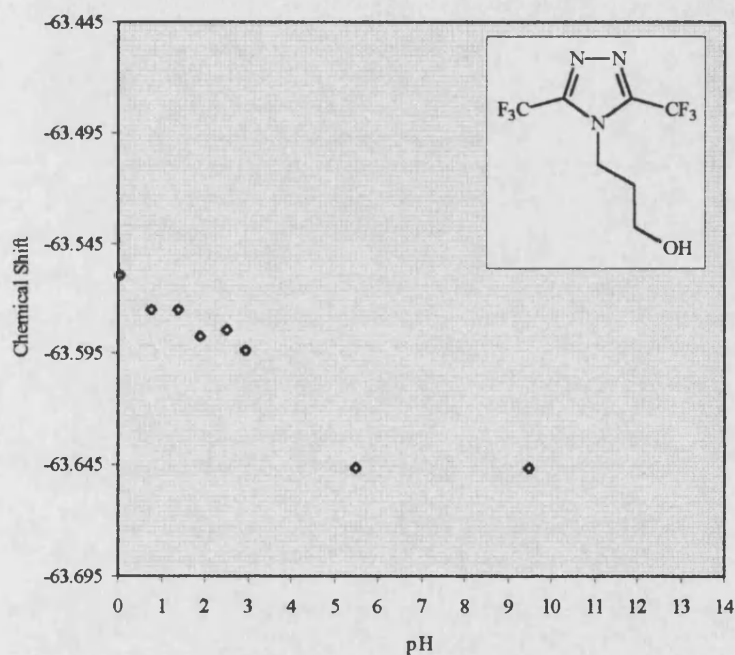


Figure 39. ^{19}F chemical shift (ppm) of 3,5-bis(trifluoromethyl)-4-(3-hydroxypropyl)-4*H*-1,2,4-triazole (**108**) vs pH.

compound	pK _a (25°C)	total shift of ¹⁹ F NMR signal (ppm)
3,5-bis(trifluoromethyl)pyrazole (2)	7.55	1.47
3-(trifluoromethyl)pyrazole-4-propanol (80)	12.07	2.21
2-(3-trifluoromethylpyrazol-4-yl)ethanol (84)	11.97	2.09
2-(5-trifluoromethylpyrazol-3-yl)ethanol (92)	12.79	2.33
3-(pyridin-4-yl)-5-(trifluoromethyl)pyrazole	9.49	2.04
2-(trifluoromethyl)imidazo[4,5- <i>b</i>]pyridine (96)	6.92 (2.2)	0.55 (0.23)
2-(trifluoromethyl)imidazo[4,5- <i>c</i>]pyridine (97)	8.67	0.87
3-(trifluoromethyl)pyridine	2.67	1.00
3,5-bis(trifluoromethyl)-4-(3-hydroxypropyl)- 4 <i>H</i> -1,2,4-triazole (108)	4	0.09

Table 7. Summary of pK_a values.

The pK_a data discussed in this section are combined in Table 7. The trifluoromethylpyrazole showed the largest total shifts in the ¹⁹F NMR spectra. It may be possible to modulate the pK_a of these compounds to a more suitable value. The pK_a of 3-(pyridin-4-yl)-5-(trifluoromethyl)pyrazole suggests that the attachment of two heterocycles to the pyrazole may result in a pK_a value close to physiological pH. If such a compound could be constructed, then it would provide many more points of attachment for other substituents. The pK_a values of 2-(trifluoromethyl)imidazopyridines (**96**, **97**) are also very promising and warrant further investigation.

CONCLUSION

A variety of reaction sequences towards the synthesis of 4-substituted-3,5-bis(trifluoromethyl)pyrazoles have been attempted. The targets have been approached at three different oxidation levels. Many reactions in each approach were hindered by the deactivating nature of the trifluoromethyl group. Progress was made towards the synthesis 3-substituted derivatives of 1,1,1,5,5,5-hexafluoropentane-2,4-dione. This involved the condensation reaction of carbonyl compounds with the dione. Convenient and generally high yielding syntheses of three ω -(trifluoromethylpyrazolyl)alkanols have been developed. ^{19}F NMR pH studies of these compounds and other pyrazoles have provided information about the effects of various substituents on the pK_a of the parent pyrazole.

A reinvestigation into a previous report of the claimed synthesis of 1-aryl and 1-aroyle-3,5-bis(trifluoromethyl)pyrazoles was carried out. It was revealed that the reaction of substituted hydrazines with 1,1,1,5,5,5-hexafluoropentane-2,4-dione produces the corresponding 5-hydroxy-4,5-dihydropyrazoles, contrary to the previous report. A number of methods leading to the dehydration of these compounds to the corresponding aromatic pyrazoles have been developed.

The structure of a major unidentified side-product, from a report regarding the synthesis of 2-trifluoromethylhistamine, was determined using a variety of spectroscopic techniques. The compound was characterised as a 5-trifluoromethyl-4-alkenylloxazole.

Two 2-(trifluoromethyl)benzimidazoles and two 2-(trifluoromethyl)imidazopyridines were synthesised, all with high yields. The pK_a values of the 2-(trifluoromethyl)imidazopyridines were found to be close to physiological pH. Furthermore, both sets of compounds have many positions available for attachment of other substituents, such as groups to modulate the pK_a value,

groups to increase the solubility in aqueous media and targetting groups. Therefore, 2-(trifluoromethyl)benzimidazoles and 2-(trifluoromethyl)imidazopyridines are ideal candidates for further development as ^{19}F NMR pH-sensors.

EXPERIMENTAL

General procedures.

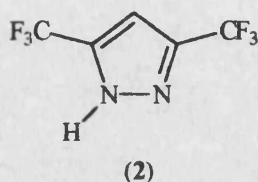
NMR data were recorded on a Jeol FX90Q spectrometer (84.25 MHz ^{19}F), a Jeol GX270 spectrometer (270.05 MHz ^1H ; 67.8 MHz ^{13}C), a Jeol EX400 spectrometer (399.65 MHz ^1H ; 100.4 MHz ^{13}C ; 376.05 MHz ^{19}F) and a Bruker AM 250 ($^1\text{H} \rightarrow ^{19}\text{F}$ and $^{19}\text{F} \rightarrow ^1\text{H}$ heteronuclear NOE experiments). CFCl_3 was used as an internal standard for ^{19}F NMR samples dissolved in $(\text{CD}_3)_2\text{SO}$, d_8 -THF or CDCl_3 and as an external standard for samples dissolved in D_2O . Tetramethylsilane was used as an internal standard for $^1\text{H} / ^{13}\text{C}$ NMR samples dissolved in CDCl_3 or $(\text{CD}_3)_2\text{SO}$, and 3-(trimethylsilyl)propanoic acid-2,2,3,3- d_4 acid was used for samples dissolved in D_2O . Multiplicities are indicated by s (singlet), d (doublet), t (triplet), q (quartet), qu (quintet) and m (multiplet). Non-phase sensitive two dimensional COSY and NOESY spectra (Jeol) were acquired with 16 scans. During data processing a 90° -shifted squared sine bell function was used in both ω_1 (1024) and ω_2 (512) dimensions. The FID in ω_2 was zero-filled to 1K prior to Fourier transformations to give a $1\text{K} \times 1\text{K}$ spectrum. Infrared spectra were recorded on a Perkin-Elmer 782 IR spectrometer, either as liquid film (film), Nujol mull (Nujol) or KBr disc (disc). Peak intensities in the IR spectrum are indicated by s (strong), m (medium) and w (weak). Mass spectra (MS) were obtained by electron-impact (EI), chemical-ionisation (CI) or fast atom bombardment (FAB) using a VG7070 spectrometer and a ZAB-E spectrometer. Data are reported in the form m/z (intensity relative to base = 100) for selected ions.

Where repetitive experimental procedures were employed, only one description is provided. All solutions were aqueous unless stated otherwise. Solvents for reactions, extractions and chromatography were distilled from the indicated drying agents according to standard procedures: tetrahydrofuran, pentane

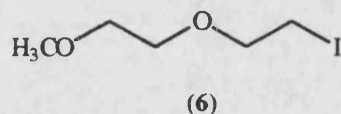
(sodium/benzophenone); dichloromethane, chloroform (phosphorus (v) oxide); diethyl ether, toluene (sodium). Analytical thin layer chromatography was carried out on Merck Kieselgel 60F plates. Visualisation was accomplished by UV light, iodine, phosphomolybdic acid, or iron (iii) chloride. Flash chromatography was performed using Merck Silica Gel 60 (0.040 - 0.063 mm) flash silica. Melting points and boiling points are uncorrected. Kugelrohr distillations were carried out in a Büchi GKR-51 apparatus and the boiling points given correspond to the Kugelrohr oven temperature.

pH Studies.

pH values were obtained using a Corning 240 pH meter and a 3.7 mm pH 0-14 Russell CLSCH11/1m electrode. Buffer solutions were made using the standard procedures of the British Pharmacopoeia 1988¹⁸⁷. ¹⁹F NMR data were recorded on a Jeol EX400 spectrometer at 376.05 MHz. ¹⁹F chemical shifts were recorded in parts per million (ppm) and were referenced relative to the ¹⁹F resonance peak of an external sample of CFCl₃ in CDCl₃ (0.00 ppm, 298 K). The ¹⁹F NMR spectra were collected between -100 ppm and 0 ppm using 131072 data points, providing 0.29 Hz per data point.



3,5-Bis(trifluoromethyl)pyrazole (2). 1,1,1,5,5,5-Hexafluoropentane-2,4-dione (6.45 g, 31.0 mmol) was added to hydrazine hydrate (1.5 ml, 31.0 mmol) in ethanol (60 ml) and acetic acid (0.05 ml). The mixture was boiled under reflux for 5 h and allowed to cool. The solvent was distilled off carefully at atmospheric pressure. The residue, in DCM (30 ml), was dried (MgSO₄) and the solvent was distilled off. Pentane (15 ml) was added and colourless crystals formed with scratching. Due to presence of an oil, the pentane was removed by distillation to yield 3.95 g (62%) of 3,5-bis(trifluoromethyl)pyrazole (2), after distillation (Kugelrohr). Data: colourless crystals; mp 69-70°C; bp 120-130°C (literature¹¹² mp 71-72°C); ¹⁹F NMR (376 MHz, D₂O) -62.02 (s).



1-Iodo-2-(2-methoxyethoxy)ethane (6).

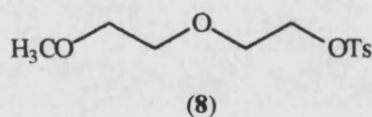
Method A:

To a solution of 2-(2-methoxyethoxy)ethanol (6.89 ml, 6.00 mmol) in anhydrous DCM (100 ml) and anhydrous pyridine (62.3 ml, 769 mmol), under a nitrogen atmosphere, was added triphenylphosphine (22.8 g, 9.00 mmol) followed by the slow addition of iodine (24.3 g, 100 mmol) at ambient temperature. When iodination was complete by t.l.c. (3.3 h), the reaction mixture was washed with saturated aqueous sodium metabisulphite solution (3 × 25 ml), saturated sodium hydrogen carbonate solution (3 × 25 ml) and brine (25 ml). The organic layer was dried (MgSO₄) and the solvent was evaporated. The residue was dissolved in ether (30 ml) and the triphenylphosphine oxide was removed by filtration through silica gel. The solvent of the filtrate was evaporated and the yellow oil was distilled (Kugelrohr) to yield 2.85 g (21%) of 1-iodo-2-(2-methoxyethoxy)ethane (6).

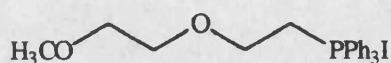
Method B:

To a stirred solution of 2-(2-methoxyethoxy)ethyl-4-methyl-benzenesulphonate (**8**) (12.7 g, 46.1 mmol) in anhydrous acetone (150 ml) was added sodium iodide (25.0 g, 167 mmol). The solution was stirred at ambient temperature in the dark and in a nitrogen atmosphere for 24 h. The reaction mixture was filtered and most of the acetone was evaporated. To the residue was added ether (90 ml) and water (100 ml) and the organic layer was washed with half saturated metabisulphite solution (2 × 25 ml) and brine (25 ml). After drying (MgSO₄), the solvent was evaporated and the crude material was distilled (Kugelrohr) to yield 7.70 g (71%) of 1-iodo-2-(2-methoxyethoxy)ethane (**6**).

Data: colourless oil; bp₂₀ 130-135°C (literature¹²⁶ bp₁₀₋₁₂ 107-109°C); ¹H NMR (270 MHz, CDCl₃) 3.26 (2H, m, CH₂CH₂-I), 3.38 (3H, s, CH₃OCH₂), 3.56 (2H, m, OCH₂CH₂-I), 3.64 (2H, m, CH₃OCH₂CH₂O), 3.75 (2H, m, CH₃OCH₂CH₂O); IR (film) 1120 (s).



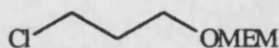
2-(2-Methoxyethoxy)ethyl 4-methylbenzenesulphonate (8). 2-(2-Methoxyethoxy)ethyl-4-methylbenzenesulphonate (**8**) was synthesised essentially by the method described by Prugh's group¹²⁶. To a solution of 2-(2-methoxyethoxy)ethanol (6.54 ml, 50.0 mmol) in anhydrous ether (50 ml) was added powdered potassium hydroxide (2.80 g, 50.0 mmol). To this suspension was added 4-methylbenzenesulphonyl chloride (9.53 g, 50.0 mmol), with caution. Stirring was continued under a nitrogen atmosphere for 3 h. The reaction mixture was filtered and the filtrate was washed with water (2 × 20 ml) and dried (MgSO₄). The solvent was evaporated to yield 12.9 g (94%) of 2-(2-methoxyethoxy)ethyl 4-methylbenzenesulphonate (**8**). Data: colourless oil; IR (disc) 1365 (s), 1180 (s).



(9)

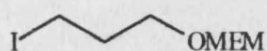
2-(2-Methoxyethoxyethyl)triphenylphosphonium iodide (9).

Triphenylphosphine (16.9 g, 64.0 mmol) was dissolved in anhydrous toluene (100 ml) and 1-iodo-2-(2-methoxyethoxy)ethane (**6**) (7.20 g, 31.0 mmol) in toluene (50 ml) was added. The mixture was boiled under reflux for 14 h under a nitrogen atmosphere. After cooling, a yellow oil separated and ether was added (50 ml). Crystals were produced by agitation of the oil and were filtered and washed with cold ether (10 ml) to yield 14.6 g (96%) of 2-(2-methoxyethoxyethyl)triphenylphosphonium iodide (**9**). Data: white solid; mp 101.5–102.5°C; ^1H NMR (270 MHz, $(\text{CD}_3)_2\text{SO}$) 3.06 (3H, s, CH_3O), 3.15 (2H, m, $\text{CH}_3\text{OCH}_2\text{CH}_2\text{O}$), 3.28 (2H, m, $\text{CH}_3\text{OCH}_2\text{CH}_2$), 3.69 (2H, dt, $J = 20.9$ Hz, $J = 5.5$ Hz, $\text{CH}_2\text{CH}_2\text{P}$), 3.96 (2H, m, $\text{OCH}_2\text{CH}_2\text{P}$), 7.77 (15H, m, Ph_3P).



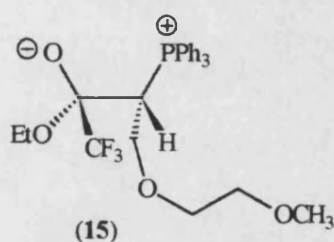
(13)

1-Chloro-3-(2-methoxyethoxymethoxy)propane (13). A mixture of 3-chloro-1-propanol (3.30 g, 35.0 mmol) and MEMCl (5.99 ml, 52.5 mmol) in DCM (60 ml) was cooled to 0°C and N,N -diisopropylethylamine (9.1 ml, 52.5 mmol) was added dropwise. The colourless solution was allowed to warm gradually to ambient temperature and then was stirred for 3 h. The reaction mixture was washed with water (2×15 ml), 5% HCl solution (20 ml) and saturated sodium hydrogen carbonate solution (20 ml). The organic layer was dried (MgSO_4) and the solvent evaporated to yield 6.29 g (98%) of 1-chloro-3-(2-methoxyethoxymethoxy)propane (**13**) following distillation (Kugelrohr). Data: colourless liquid; $\text{bp}_{0.7}$ 40–50°C; ^1H NMR (270 MHz, CDCl_3) 2.04 (2H, qu, $J = 6.0$ Hz, $\text{CH}_2\text{CH}_2\text{CH}_2$), 3.40 (3H, s, CH_3O), 3.6 (8H, m, CH_2O), 3.70 (2H, t, $J = 5.9$ Hz, CH_2Cl), 4.73 (4H, s, OCH_2O); IR (film) 1050 (s).

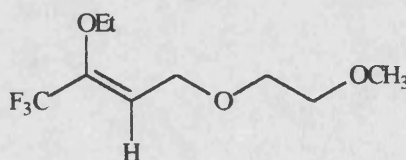


(14)

1-Iodo-3-(2-methoxyethoxymethoxy)propane (14). 1-Chloro-3-(2-methoxyethoxymethoxy)propane (**13**) (6.00 g, 32.8 mmol) was dissolved in anhydrous acetone (100 ml) and sodium iodide (10.0 g, 66.7 mmol) was added slowly producing a slight exotherm. The mixture was stirred at ambient temperature in the dark under a nitrogen atmosphere for 4 h. The reaction mixture was filtered and most of the solvent evaporated. The residue was redissolved in ether (100 ml) and washed with water (2 × 25 ml) and half saturated sodium metabisulphite solution (2 × 25 ml). The organic extracts were dried (MgSO₄) and the solvent was evaporated to yield 5.15 g (57%) of 1-iodo-3-(2-methoxyethoxymethoxy)propane (**14**). Data: yellow oil; ¹H NMR (270 MHz, CDCl₃) 2.06 (2H, m, CH₂CH₂CH₂), 3.40 (3H, s, CH₃O), 3.65 (10H, m, 4 × CH₂O and CH₂I), 4.73 (2H, s, OCH₂O).



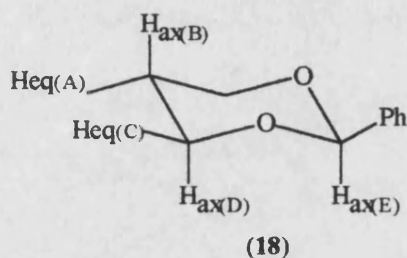
(15)



(16)

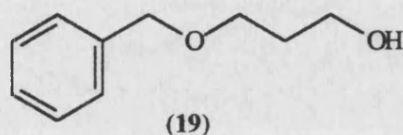
(Z)-1,1,1-Trifluoro-2-ethoxy-4-(2-(2-methoxyethoxy))but-2-ene (16). The attempted synthesis of (Z)-1,1,1-trifluoro-2-ethoxy-4-(2-(2-methoxyethoxy)methyl)but-2-ene (**16**) led to the isolation of an intermediate. (2-(2-Methoxyethoxyethyl)triphenylphosphonium iodide (**9**) (7.39 g, 15.0 mmol) and HMDS (0.3 ml) were added to a suspension of sodium hydride (80% dispersion in oil, 0.43 g, 15.0 mmol) in anhydrous THF (40 ml). The mixture was boiled under reflux in a nitrogen atmosphere for 3 h. The deep red-brown slurry was cooled to ambient temperature and ethyl trifluoroacetate (1.78 ml, 15.0 mmol) in THF (5 ml) was added dropwise. The mixture was boiled under reflux for 16 h. The reaction mixture was cooled to ambient temperature and pentane (40 ml) was added. The suspension was filtered

through silica gel (eluted with pentane : ether ; 97 : 3) and the solvents evaporated to give a mixture of triphenylphosphine oxide and the suspected intermediate (15). After analysis, the mixture was dissolved in anhydrous toluene (20 ml) and boiled under reflux for 23 h. T.l.c. indicated no change and sodium hydride (80% dispersion, 0.3 g) and HMDS (0.01 ml) were added and boiling under reflux was continued for 24 h. After cooling to ambient temperature, the suspension was filtered and the solvent of the filtrate was evaporated. The residue was columned (petroleum ether bp 40-60°C : ethyl acetate ; 2 : 1). Data: red-brown amorphous powder; ^1H NMR (270 MHz, $(\text{CD}_3)_2\text{SO}$) 3.32 (3H, s, CH_3O), 3.50 (2H, t, $J = 4.2$ Hz, CH_2O), 3.74 (2H, t, $J = 3.9$ Hz, CH_2O), 7.5 (15H, m, Ph_3P); ^{19}F NMR (84 MHz, CDCl_3) -157.24 (s).

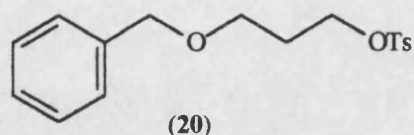


2-Phenyl-1,3-dioxane (18). A mixture of benzaldehyde (10.0 g, 94.2 mmol), propane-1,3-diol (7.89 g, 104 mmol) and 4-methylbenzenesulphonic acid (0.18 g, 0.90 mmol) in toluene (100 ml) was stirred and boiled under reflux in a Dean and Stark apparatus. After 1½ h the reaction mixture was allowed to cool to ambient temperature and then ether (100 ml) was added (1.4 ml of water had been produced of the 1.72 ml expected). This was washed with 0.6 M sodium hydrogen carbonate solution (3×15 ml) and the organic layer dried (MgSO_4). The solvents were evaporated and the crude yellow liquid was distilled (Kugelrohr) to yield 18.8 g (90%) of 2-phenyl-1,3-dioxane (18). Data: white crystals; mp $<25^\circ\text{C}$; bp₂₀ 145-155°C (literature¹²⁹ bp₁₂ 115°C); ^1H NMR (270 MHz, $(\text{CD}_3)_2\text{SO}$) 1.45 (1H, dtt, $J_{\text{gem}} = 13.6$ Hz, $J_{\text{B-D}} = 2.6$ Hz, $J_{\text{B-C}} = 1.3$ Hz, $\text{H}_{\text{ax(B)}}$), 2.23 (1H, m, $J_{\text{gem}} = 13.6$ Hz, $J_{\text{A-D}} = 10.1$ Hz, $J_{\text{A-C}} = 4.9$ Hz, $\text{H}_{\text{eq(A)}}$), 3.99 (2H, m, $J_{\text{gem}} = 12.5$ Hz, $J_{\text{D-A}} = 10.1$ Hz, $J_{\text{D-B}} = 2.6$ Hz, $\text{H}_{\text{ax(D)}}$), 4.26 (2H, m, $J_{\text{gem}} = 12.5$ Hz, $J_{\text{C-A}} = 4.9$ Hz, $J_{\text{C-B}} = 1.3$ Hz, $\text{H}_{\text{eq(C)}}$), 5.50 (1H, s, $\text{H}_{\text{ax(E)}}$),

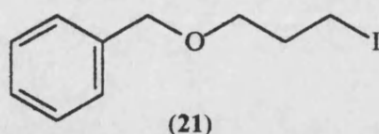
7.35 (3H, m, Ar 2,4,6-H₃), 7.48 (2H, m, Ar 3,5-H₂); ¹³C NMR (68 MHz, (CD₃)₂SO) 25.75 (CH₂CH₂CH₂), 67.35 (CH₂CH₂O), 101.64 (O₂CCHR), 125.96 (Ar 4-C), 128.22 (Ar 3,5-C), 128.75 (Ar 2,6-C); IR (disc) 3020 (m), 1105 (s).



3-(Phenylmethoxy)propan-1-ol (19). 3-(Phenylmethoxy)propan-1-ol (19) was synthesised essentially by the method described by Kozikowski's group¹²⁹. Cold, anhydrous ether (250 ml) was added cautiously to aluminium trichloride (24.4 g, 183 mmol) at 0°C resulting in a moderate exotherm. Following dissolution, lithium aluminium hydride (1.73 g, 48.7 mmol) was added portionwise to the mixture. Stirring was continued at 0°C for 30 min, followed by the dropwise addition of 2-phenyl-1,3-dioxane (18) (8.00 g, 48.7 mmol) in ether (50 ml). The suspension was allowed to warm to ambient temperature. After stirring for a further 2 h, the mixture was cooled to 0°C and quenched by the slow addition of 2 M sulphuric acid solution (250 ml). A heavy precipitate formed which required some agitation before stirring could be continued. After warming to ambient temperature, two layers formed. The layers were separated and the aqueous phase was extracted with ether (2 × 50 ml). The combined organic extracts were dried (MgSO₄) and the solvent evaporated to yield 7.63 g (94%) of 3-(phenylmethoxy)propan-1-ol (19) following distillation (Kugelrohr). Data: colourless liquid; bp_{0.7} 115-120°C; ¹H NMR (270 MHz, CDCl₃) 1.83 (2H, qu, *J* = 5.9 Hz, CH₂CH₂CH₂), 3.66 (2H, t, *J* = 5.9 Hz, CH₂CH₂OH), 3.78 (2H, t, *J* = 5.7 Hz, BnOCH₂CH₂), 4.53 (2H, s, PhCH₂O), 7.33 (5H, m, PhCH₂O); IR (film) 3800 (br), 1100 (s), 745 (s), 705 (s); MS (EI) 166 (M⁺, 7), 107 (100) 91 (96).

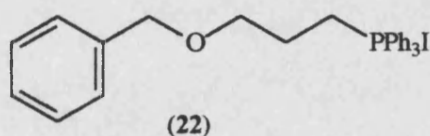


3-(Phenylmethoxy)propyl 4-methylbenzenesulphonate (20). 3-(Phenylmethoxy)propyl 4-methylbenzenesulphonate (20) was synthesised by the procedure described by Prugh's group⁶³. To a solution of 3-phenylmethoxy-1-propanol (19) (7.61 g, 45.8 mmol) in anhydrous ether (50 ml) was added powdered potassium hydroxide (2.60 g, 45.8 mmol). To this suspension was added 4-methylbenzenesulphonyl chloride (8.73 g, 45.8 mmol), with caution. Stirring was continued under a nitrogen atmosphere for 6 h. Another portion of powdered potassium hydroxide (2.00 g, 35.6 mmol) was added and stirring was continued for another 2.5 h. The reaction mixture was filtered and the filtrate was washed with water (2 × 25 ml) and dried (MgSO₄). The solvent was evaporated to yield 13.3 g (91%) of 3-(phenylmethoxy)propyl 4-methylbenzenesulphonate (20). Data: colourless crystals; mp <30°C (literature¹⁸⁸ mp 37°C); ¹H NMR (270 MHz, CDCl₃) 1.88 (2H, qu, *J* = 6.1 Hz, CH₂CH₂CH₂), 2.45 (3H, s, ArCH₃), 3.52 (2H, t, *J* = 6.0 Hz, BnOCH₂CH₂), 4.19 (2H, t, *J* = 6.2 Hz, CH₂CH₂OTs), 4.43 (2H, s, PhCH₂O), 7.30 (7H, m), 7.82 (2H, d, *J* = 8.3 Hz, 2,5-H₂, Ts); IR (Nujol) 1370 (s) 1185 (s); MS (CI, iso-butane) 321 (M⁺ + H, 17), 181 (9), 155 (10), 107 (12), 91 (100).



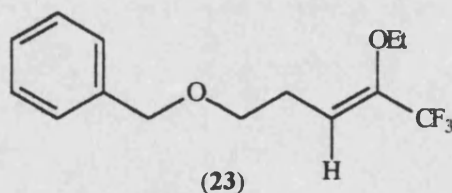
1-Iodo-3-(phenylmethoxy)propane (21). To a stirred solution of 3-(phenylmethoxy)propyl 4-methylbenzenesulphonate (20) (6.00 g, 18.7 mmol) in anhydrous acetone (60 ml) was added sodium iodide (9.60 g, 64.2 mmol). The solution was stirred at ambient temperature in the dark and under a nitrogen atmosphere for 6 h. The reaction mixture was filtered and most of the acetone was evaporated. To the residue was added ether (50 ml) and water (10 ml) and the organic layer was washed with half saturated metabisulphite

solution (2×15 ml) and brine (10 ml). After drying (MgSO_4), the solvent was evaporated and the crude material was distilled (Kugelrohr) to yield 4.87 g (87%) of 1-iodo-3-(phenylmethoxy)propane (**21**). Data: pale yellow liquid; bp_{20} 150-165°C (literature¹⁸⁹ bp_{7-10} 123-130°C); ^1H NMR (270 MHz, CDCl_3) 2.09 (2H, qu, $J = 6.6$ Hz, $\text{CH}_2\text{CH}_2\text{CH}_2$), 3.31 (2H, t, $J = 6.6$ Hz, $\text{CH}_2\text{CH}_2\text{I}$), 3.54 (2H, t, $J = 5.7$ Hz, $\text{BnOCH}_2\text{CH}_2$), 4.53 (2H, s, PhCH_2O), 7.34 (5H, m, PhCH_2O); IR (film) 1110 (s), 740 (s), 705 (s).



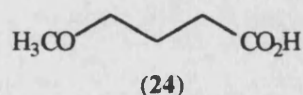
3-(Phenylmethoxy)propyltriphenylphosphonium iodide (**22**).

Triphenylphosphine (9.20 g, 35.0 mmol) was dissolved in anhydrous toluene (60 ml) and 1-iodo-3-(phenylmethoxy)propane (**21**) (4.36 g, 15.8 mmol) in toluene (20 ml) was added. The mixture was boiled under reflux for 16 h under a nitrogen atmosphere. After cooling, a yellow oil separated and ether was added (50 ml). The crystals were produced by agitation of the oil and were filtered and washed to yield 7.94 g (93%) of 3-(phenylmethoxy)propyltriphenylphosphonium iodide (**22**). Data: white crystals; mp 94.5-95.0°C; ^1H NMR (270 MHz, $(\text{CD}_3)_2\text{SO}$) 1.89 (2H, m, $\text{CH}_2\text{CH}_2\text{CH}_2$), 3.82 (2H, m, $\text{BnOCH}_2\text{CH}_2\text{P}$), 4.51 (2H, s, PhCH_2O), 7.31 (5H, m, PhCH_2O), 7.72 (15H, m, Ph_3P).



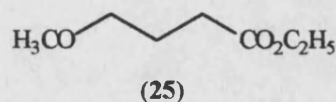
(*Z*)-1,1,1-Trifluoro-2-ethoxy-5-(phenylmethoxy)pent-2-ene (**23**). (*Z*)-1,1,1-Trifluoro-2-ethoxy-5-(phenylmethoxy)pent-2-ene (**23**) was synthesised using a procedure based on that described by Bégue's group¹²⁴. 3-(Phenylmethoxy)propyltriphenylphosphonium iodide (**22**) (3.00 g, 5.57 mmol)

was added to a stirred suspension of sodium hydride (80% dispersion in oil, 0.17 g, 5.57 mmol) in anhydrous THF (20 ml). HMDS (0.2 ml, 1.50 mmol) was added to the mixture and a small exotherm was observed. The reaction mixture was boiled under reflux and under a nitrogen atmosphere. A pale orange colour was observed and, after 3 h, a further portion of HMDS (0.7 ml, 5.25 mmol) was added dropwise. This resulted in the formation of a deep red mixture which was boiled under reflux for 14 h and cooled. Ethyl trifluoroacetate (0.66 ml, 5.57 mmol) in THF (0.5 ml) was added slowly to the mixture at ambient temperature. The mixture was boiled under reflux for 7 d. T.l.c. showed that the reaction was proceeding very slowly, therefore the THF was distilled off under a nitrogen atmosphere and anhydrous toluene (15 ml) was added. The suspension was boiled under reflux for 7 d. After cooling, the reaction mixture was filtered and the solvent of the filtrate was evaporated. Pentane (40 ml) was added to the residue and the suspension was filtered. The solvent was evaporated from the filtrate to yield 0.71 g (46%) of (*Z*)-1,1,1-trifluoro-2-ethoxy-5-(phenylmethoxy)pent-2-ene (**23**) following distillation (Kugelrohr). Data: colourless liquid; bp₂₀ 140-145°C; ¹H NMR (400 MHz, CDCl₃) 1.30 (3H, t, *J* = 7.0 Hz, CH₃CH₂O), 2.50 (2H, m, C=C-CH₂CH₂), 3.52 (2H, t, *J* = 6.4 Hz, BnOCH₂CH₂), 3.91 (2H, q, *J* = 7.0 Hz, CH₃CH₂O), 4.52 (2H, s, PhCH₂O), 5.73 (1H, t, *J* = 7.3 Hz, CHCCH₂), 7.33 (5H, m, PhCH₂O); ¹⁹F NMR (376 MHz, CDCl₃) -70.04 (s); IR (film) 1690 (s), 740 (s), 700 (s); MS (EI) 274.1138 (M⁺, 1) (C₁₄H₁₇F₃O₂ requires 274.1181), 188 (2), 91 (100).



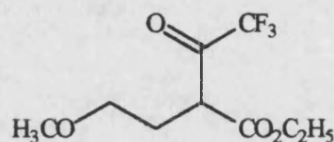
4-Methoxybutanoic acid (24). 4-Methoxybutanoic acid (**24**) was synthesised essentially by the method described by Archer's group¹³¹. A mixture of tetrahydrofuran-2-one (43.0 g, 500 mmol) in 2 M NaOH solution (500 ml) was stirred at ambient temperature for 2 d and was heated under reflux for 3.5 h. After cooling, the alkaline solution was washed with ether (3 × 50 ml) and the was solvent evaporated to give a white slurry. The slurry was dissolved in 10

M NaOH solution (75 ml) and was then treated alternately with dimethyl sulphate (3×25 ml) and 10 M NaOH solution (3×25 ml). The mixture was heated to 90°C resulting in a moderate exotherm and the precipitation of a white solid. The temperature was maintained between 60 – 70°C for 1 h. After cooling, the reaction mixture was extracted with ether (3×100 ml) and the combined extracts were washed with brine (50 ml) and dried (MgSO_4). The solvent was evaporated to give a yellow oil which was distilled (Kugelrohr) to give a colourless oil, later found to still contain some lactone. The oil was dissolved in ether (100 ml) and washed with saturated sodium hydrogen carbonate solution (2×100 ml). The alkaline solution was then acidified and extracted with ether (3×100 ml). The organic extracts were dried (MgSO_4) and the solvent was evaporated to yield 3.93 g (7%) of 4-methoxybutanoic acid (**24**). Data: colourless oil; bp_{20} 125 – 130°C (literature¹³¹ bp_8 103 – 105°C); ^1H NMR (270 MHz, CDCl_3) 1.88 (2H, qu, $J = 7.3$ Hz, $\text{CH}_2\text{CH}_2\text{CH}_2$), 2.43 (2H, t, $J = 7.3$ Hz, $\text{CH}_2\text{CH}_2\text{CO}_2\text{H}$), 3.32 (3H, s, CH_3O), 3.41 (2H, t, $J = 6.2$ Hz, $\text{CH}_3\text{OCH}_2\text{CH}_2$), 10.70 (1H, br, CO_2H); IR (film) 3000 (br), 1715 (s), 1150 (s).



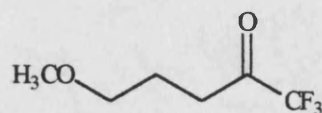
Ethyl 4-methoxybutanoate (25). Ethyl 4-methoxybutanoate (**2**) was synthesised essentially by the method described by Archer's group¹³¹. A solution of 4-methoxybutanoic acid (**24**) (20.8 g, 17.6 mmol) was heated for 16 h in ethanol (70 ml) and concentrated HCl (0.5 ml). Most of the solvent was removed by evaporation and to the remaining residue was added saturated sodium hydrogen carbonate solution (150 ml). The mixture was extracted with ether (5×50 ml) and the combined organic extracts were washed with brine (50 ml), dried (MgSO_4) and the solvent evaporated. The residue was distilled (Kugelrohr) to yield 2.57 g (67%) of ethyl 4-methoxybutanoate (**25**). Data: colourless oil; bp 170 – 175°C (literature¹³¹ bp_{15} 75 – 76°C); ^1H NMR (270 MHz, CDCl_3) 1.26 (3H, t, $J = 7.1$ Hz, $\text{CO}_2\text{CH}_2\text{CH}_3$), 1.82 (2H, qu, $J = 6.4$ Hz,

CH₂CH₂CH₂), 2.31 (2H, t, $J = 7.5$ Hz, CH₂CH₂CO₂), 3.25 (3H, s, CH₃O), 3.34 (2H, t, $J = 6.2$ Hz, CH₃OCH₂CH₂), 4.06 (2H, q, $J = 7.2$ Hz, CO₂CH₂CH₃); IR (film) 1740 (s).



(26)

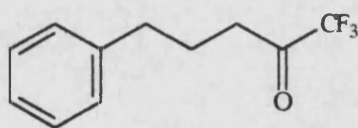
Ethyl 4-methoxy-2-(trifluoroacetyl)butanoate (26). Ethyl 4-methoxy-2-(trifluoroacetyl)butanoate (26) was synthesised essentially by the method described by Archer's group¹³¹. Ethanol (0.01 ml) was added to a stirred slurry of NaH (80% dispersion in oil, 1.00 g, 42.0 mmol) in THF (10 ml) under a nitrogen atmosphere. This was followed by the dropwise addition of ethyl 4-methoxybutanoate (25) (1.60 g, 10.0 mmol) in THF (5 ml) and ethyl trifluoroacetate (1.45 ml, 12.0 mmol) in THF (10 ml). The mixture was heated under reflux for 2 h followed by stirring at ambient temperature for 48 h. After acidification with 2 M HCl, water (100 ml) was added and the aqueous layer was extracted with ether (3 × 100 ml). The combined organic extracts were washed with brine (50 ml) and dried (MgSO₄). The solvent was evaporated and the crude residue was distilled (Kugelrohr) to yield 2.66 g (69%) of ethyl 4-methoxy-2-(trifluoroacetyl)butanoate (26). Data: colourless oil; bp₂₀ 100°C (literature¹³¹ bp₁₃ 85-86°C); ¹⁹F NMR (84 MHz, CDCl₃) -84.28 (s, hydrate?), -78.19 (s, keto), -67.40 (s, enol); IR (film) 2750 (br), 1790 (s), 1750 (s), 1170 (s), 700 (m).



(27)

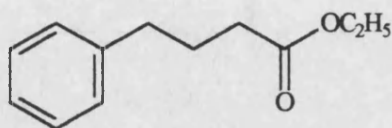
5-Methoxy-1,1,1-trifluoropentan-2-one (27). 5-Methoxy-1,1,1-trifluoropentan-2-one (27) was synthesised essentially using the method described by

Archer's group¹³¹. A solution of ethyl 4-methoxy-2-(trifluoroacetyl)butanoate (**26**) (1.73 g, 7.16 mmol) in acetic acid : water (87 : 13) (2 ml) and concentrated HCl (0.02 ml) was heated under reflux for 16 h. The mixture was allowed to cool and then was carefully neutralised with potassium carbonate. Water (5 ml) was added and the mixture was extracted with ether (4 × 5 ml). The combined organic extracts were washed with 4% aqueous sodium hydrogen carbonate solution (10 ml), they were then dried (MgSO₄) and the solvent was removed by evaporation. The crude material was distilled (Kugelrohr) to yield 0.50 g (41%) of 5-methoxy-1,1,1-trifluoropentan-2-one (**27**). Data: colourless oil; bp 115-125°C at atmospheric pressure (literature¹³¹ bp 120-123°C); ¹H NMR (270 MHz, CDCl₃) 1.99 (2H, qu, *J* = 6.4 Hz, CH₂CH₂CH₂), 2.83 (2H, t, *J* = 7.0 Hz, CH₂CH₂COCF₃), 3.33 (3H, s, CH₃OCH₂), 3.42 (2H, t, *J* = 5.7 Hz, CH₃OCH₂CH₂); ¹⁹F NMR (84 MHz, CDCl₃) -77.40 (s); IR (film) 3250 (br), 1715 (s), 1400 (m), 1110 (m).



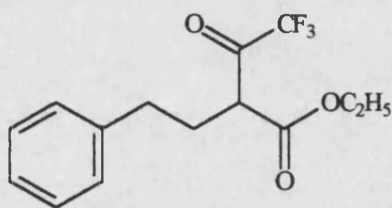
(28)

5-Phenyl-1,1,1-trifluoropentan-2-one (28). A solution of ethyl 4-phenyl-2-(trifluoroacetyl)butanoate (**31**) (3.00 g, 10.4 mmol) in anhydrous DMF (24 ml) was heated under reflux in the presence of lithium chloride (0.88 g, 20.8 mmol) and water (0.19 ml, 10.4 mmol) for 4.5 h. Water (12 ml) and DCM (100 ml) were added and the organic phase was washed with water (5 × 10 ml) and dried (MgSO₄). Chromatography (hexane : ethyl acetate ; 5 : 1) of the evaporation residue gave a yellow liquid which was further purified by distillation (Kugelrohr) to yield 1.13 g (50%) of 5-phenyl-1,1,1-trifluoropentan-2-one (**28**). Data: colourless liquid; bp₂₀ 100°C (literature¹⁹⁰ bp₁₀ 90°C); ¹H NMR (270 MHz, CDCl₃) 2.01 (2H, qu, *J* = 7.3 Hz, CH₂CH₂CH₂), 2.67 (2H, t, *J* = 7.7 Hz, CH₂CH₂COCF₃), 2.71 (2H, t, *J* = 7.2 Hz, PhCH₂CH₂), 7.24 (5H, m, Ph); ¹⁹F NMR (376 MHz, CDCl₃) -79.80 (s).



(30)

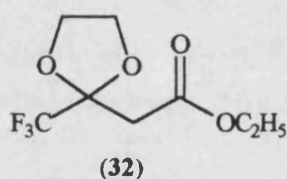
Ethyl 4-phenylbutanoate (30). 4-Phenylbutanoic acid (10.0 g, 60.9 mmol) was dissolved in ethanol (500 ml) and concentrated sulphuric acid (5 ml) was added cautiously. The solution was boiled under reflux for 3 h. The reaction mixture was allowed to cool to ambient temperature and most of the solvent was evaporated. Ether (250 ml) was added followed by the slow addition of saturated sodium hydrogen carbonate solution (50 ml), which resulted in a moderate exotherm. The mixture was stirred for 30 min then separated. The organic phase was washed with saturated sodium hydrogen carbonate solution (50 ml), water (2 × 50 ml) and brine (30 ml). The organic phase was dried (MgSO_4) and the solvent evaporated to yield 11.7 g (96%) of ethyl 4-phenylbutanoate (30). Data: pale yellow oil; ^1H NMR (270 MHz, CDCl_3) 1.21 (3H, t, $J = 7.2$ Hz, $\text{CO}_2\text{CH}_2\text{CH}_3$), 1.91 (2H, qu, $J = 7.5$ Hz, $\text{CH}_2\text{CH}_2\text{CH}_2$), 2.28 (2H, t, $J = 7.7$ Hz, $\text{CH}_2\text{CH}_2\text{CO}_2$), 2.61 (2H, t, $J = 7.3$ Hz, PhCH_2CH_2), 4.08 (2H, q, $J = 7.1$ Hz, $\text{CO}_2\text{CH}_2\text{CH}_3$); IR (film) 1740 (s).



(31)

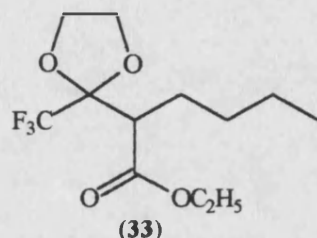
Ethyl 4-phenyl-2-(trifluoroacetyl)butanoate (31). LDA (19.5 mmol) was prepared by the addition of *n*-butyl lithium (2.5 M solution in hexanes, 8.6 ml, 21.5 mmol) to a stirred solution of diisopropylamine (2.74 ml, 19.5 mmol) in THF (30 ml) at 0°C . After 15 min stirring, the temperature was reduced to -78°C and a solution of ethyl 4-phenylbutanoate (30) (2.50 g, 13.0 mmol) in THF (15 ml) was added dropwise. The mixture was stirred at -78°C for 30

min. A solution of ethyl trifluoroacetate (3.1 ml, 26.0 mmol) in THF (10 ml) was added dropwise. The mixture was maintained at -78°C for 20 min before being allowed to warm gradually to ambient temperature. After stirring for a further 24 h the reaction was quenched with 1 M aqueous HCl solution (15 ml). The organic phase was washed with water (10 ml) and brine (10 ml). The aqueous phase of the reaction mixture was extracted with ether (2×25 ml) and the organic extracts washed with brine (10 ml). The combined organic phases were dried (MgSO_4) and the majority of the solvent was evaporated. The remaining solvent and TFA was removed by distillation (Kugelrohr) at atmospheric pressure yielding 3.00 g of ethyl 4-phenyl-2-(trifluoroacetyl)-butanoate (**31**). Data: yellow oil; NMR data includes values for the 10% enolisation of (**31**) observed; ^1H NMR (400 MHz, CDCl_3) 1.26 (2.7H, t, $J = 6.7$ Hz, $\text{CO}_2\text{CH}_2\text{CH}_3$), 1.27 (0.3H, m, $\text{CO}_2\text{CH}_2\text{CH}_3$, enol), 2.30 (2H, m, PhCH_2CH_2), 2.65 (1.8H, m, $\text{CH}_2\text{CH}_2\text{CHCO}_2\text{Et}(\text{COCF}_3)$), 2.70 (0.2H, m, $\text{CH}_2\text{CH}_2\text{CCO}_2\text{Et}(\text{CCF}_3\text{OH})$, enol), 3.81 (0.9H, t, $J = 7.3$ Hz, $\text{CH}_2\text{CHCO}_2\text{Et}(\text{COCF}_3)$), 4.21 (1.8H, q, $J = 5.9$ Hz, $\text{CO}_2\text{CH}_2\text{CH}_3$), 4.24 (0.2H, q, $J = 5.9$ Hz, $\text{CO}_2\text{CH}_2\text{CH}_3$, enol), 7.24 (5H, m, Ph), 12.91 (0.1H, s, OH, enol); ^{19}F NMR (376 MHz, CDCl_3) -84.01 (s, hydrate?), -77.10 (s, keto), -67.37 (s, enol); IR (film) 1750 (s), 1680 (s)



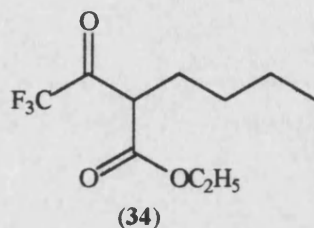
Ethyl 2-trifluoromethyl-4,5-dihydro-1,3-dioxole-2-acetate (32). Ethyl 2-trifluoromethyl-4,5-dihydro-1,3-dioxole-2-acetate (**32**) was synthesised essentially using the method described by Langlois's group¹³⁷. Ethyl 4,4,4-trifluoro-3-oxobutanoate (7.94 ml, 54.3 mmol) was added to sodium hydride (80% dispersion in oil, 1.63 g, 54.3 mmol) in ethanol (40 ml). The mixture was stirred for 40 min and the solvent was evaporated to give an off white solid. Chloroethanol (10 ml) was added to the solid and the solution was boiled

under reflux for 2 d. After cooling to ambient temperature, ice (*ca.* 15 g) was added followed by 5 M HCl solution (0.5 ml). The aqueous layer was extracted with ether (3 × 20 ml) and the combined organic extracts were washed to neutrality with water (3 × 20 ml) followed by a wash with brine (20 ml). The organic phase was dried (MgSO₄) and the was solvent evaporated to yield 7.44 g (60%) of ethyl 2-trifluoromethyl-4,5-dihydro-1,3-dioxol-2-acetate (**32**) following distillation (Kugelrohr). Data: colourless liquid; bp₂₀ 90-95°C (literature¹³⁷ bp₂₀ 96-98°C); ¹H NMR (400 MHz, CDCl₃) 1.28 (3H, t, *J* = 7.3 Hz, CO₂CH₂CH₃), 2.89 (2H, s, RCH₂CO₂), 4.20 (6H, m, CH₂O); ¹⁹F NMR (376 MHz, CDCl₃) -84.16 (s); IR (film) 1750 (s), 1175 (s).

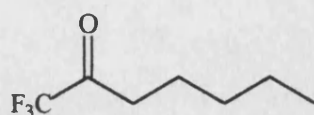


Ethyl 2-trifluoromethyl-4,5-dihydro-1,3-dioxol- α -(1-butyl)acetate (33). LDA (4.90 mmol) was prepared by the addition of *n*-butyl lithium (2.5 M solution in hexanes, 3.19 ml, 5.38 mmol) to diisopropylamine (0.69 ml, 4.90 mmol) at 0°C. After 15 min stirring, the temperature of the gel was reduced to -78°C and ethyl 2-trifluoromethyl-4,5-dihydro-1,3-dioxol-2-acetate (**32**) (1.00 g, 4.40 mmol) in anhydrous THF (8 ml) was added dropwise forming a yellow-brown solution which was stirred in a nitrogen atmosphere at -78°C for 1 h. HMPA (2.04 ml, 11.4 mmol) (caution: carcinogen) was added to the solution followed by 1-iodobutane (0.5 ml, 4.38 mmol) in THF (2 ml) after 15 min. The mixture was stirred at -78°C for 1 h before being allowed to warm to ambient temperature during a 16 h period. The reaction mixture was quenched by the addition of 2 M HCl solution (5ml) and extracted with ethyl acetate (5 × 10 ml). The combined organic extracts were washed with half saturated sodium metabisulphite solution (2 × 15 ml) and washed to neutrality with water (3 × 15 ml). The solvent was evaporated and the residue was dissolved in ether

(100 ml) and further washed with water (5×10 ml) to remove any HMPA. After drying (MgSO_4), the solvent was evaporated to yield 1.04 g (84%) of ethyl 2-(trifluoromethyl-4,5-dihydro-1,3-dioxol- α -(1-propyl)acetate (**33**) following distillation (Kugelrohr). Data: pale yellow oil; $\text{bp}_{0.4}$ 95-105°C; ^1H NMR (400 MHz, CDCl_3) 0.89 (3H, t, $J = 7.0$ Hz, $\text{CH}_2\text{CH}_2\text{CH}_3$), 1.27 (3H, t, $J = 7.0$ Hz, OCH_2CH_3), 1.2-1.8 (6H, m, $\text{CH}_2\text{CH}_2\text{CH}_2\text{CH}_3$), 2.97 (1H, dd, $J = 3.1, 11.9$ Hz, CHCO_2), 4.17 (6H, m, $\text{OCH}_2\text{CH}_2\text{O}$ and $\text{CO}_2\text{CH}_2\text{CH}_3$); ^{19}F NMR (376 MHz, CDCl_3) -81.20 (s); MS (EI) 284.1234 (M^+ , 41) ($\text{C}_{12}\text{H}_{19}\text{F}_3\text{O}_4$ requires 284.1235), 239 (10).

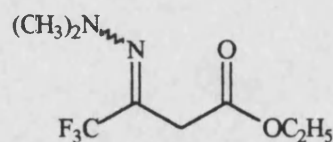


Ethyl 2-(trifluoroacetyl)hexanoate (34). To a stirred solution of ethyl 2-trifluoromethyl-4,5-dihydro-1,3-dioxol- α -(1-butyl)acetate (**33**) (1.00 g, 3.50 mmol) in hexane (20 ml) at -10°C was added boron tribromide (5.25 ml, 5.25 mmol). After 1.5 h, water (10 ml) was added carefully. The mixture was extracted with ether (3×15 ml) and the combined organic extracts were washed to neutrality with water (5×10 ml) and then washed with brine (10 ml). After being dried (MgSO_4), the solvent was evaporated to yield 0.56 g (69%) of ethyl 2-(trifluoroacetyl)hexanoate (**34**). Data: yellow oil; ^1H NMR (400 MHz, CDCl_3) 0.92 (3H, t, $J = 6.8$ Hz, $\text{CH}_2\text{CH}_2\text{CH}_3$), 1.27 (3H, m, OCH_2CH_3), 1.35 (4H, m, $\text{CH}_2\text{CH}_2\text{CH}_2\text{CH}_3$), 3.85 (1H, m, CH, chiral centre), 4.22 (2H, q, $J = 7.1$ Hz, OCH_2CH_3); ^{19}F NMR (376 MHz, CDCl_3) -78.32 (s, enol), -78.55 (s, keto); MS (EI) 241.0998 (M^+ , 28, ^{13}C isotope) ($^{13}\text{CC}_9\text{H}_{15}\text{F}_3\text{O}_3$ requires 241.1007), 240 (M^+ , 100), 239.0896 ($\text{M}^+ - \text{H}$, 46) ($\text{C}_{10}\text{H}_{14}\text{F}_3\text{O}_3$ requires 239.0895).



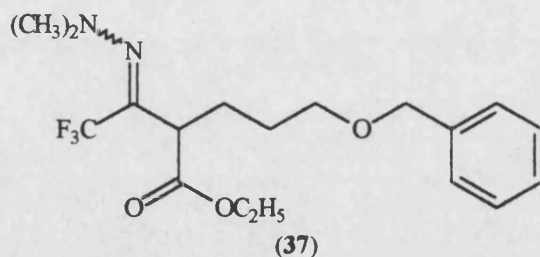
(35)

1,1,1-Trifluoroheptan-2-one (35). A solution of ethyl 2-(trifluoroacetyl)-hexanoate (**34**) (0.55 g, 2.30 mmol) in anhydrous DMF (8 ml) was heated to 100°C in the presence of lithium chloride (0.28 g, 6.66 mmol) and water (0.11 ml, 3.33 mmol) for 2 h 15 min. The solution was allowed to cool to ambient temperature and water (4 ml) was added. The mixture was extracted with petroleum ether bp 40-60°C (4 × 10 ml) and the combined organic extracts were washed with water (5 × 10 ml) and with brine (10 ml). After being dried (MgSO₄), the solvent was evaporated to yield 0.05 g (13%) of 1,1,1-trifluoroheptan-2-one (**35**) following distillation (Kugelrohr). Data: colourless liquid; bp 80-85°C (literature¹⁹¹ bp 100°C); ¹H NMR (400 MHz, CDCl₃) 0.91 (3H, t, *J* = 6.7 Hz, CH₂CH₃), 1.63 (4H, m, CH₂CH₂CH₂CH₃), 2.04 (2H, qu, *J* = 7.3 Hz, CF₃COCH₂CH₂CH₂), 2.70 (2H, t, *J* = 7.3 Hz, CF₃COCH₂); ¹⁹F NMR (84 MHz, CDCl₃) -79.75 (s).

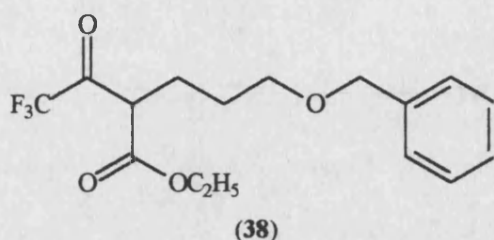


(36)

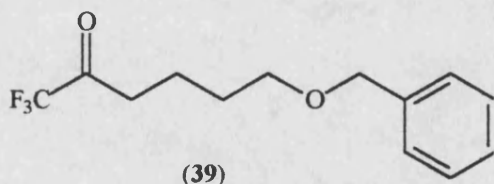
Ethyl 1,1,1-trifluoro-2-(dimethylhydrazono)butanoate (36). Ethyl 1,1,1-trifluoro-2-(dimethylhydrazono)butanoate (**36**) was synthesised essentially using the method described by Langlois's group¹³⁷. A solution of ethyl 4,4,4-trifluoro-3-oxobutanoate (6.90 g, 37.5 mmol) and 1,1-dimethylhydrazine (2.75 g, 45.8 mmol) in ethanol (14 ml) was boiled under reflux for 20 h. After cooling, the solvent was evaporated to yield 6.50 g (77%) of ethyl 1,1,1-trifluoro-2-(dimethylhydrazono)butanoate (**36**) following distillation (Kugelrohr). Data: pale yellow liquid; bp₂₀ 85-90°C (literature¹³⁷ bp₁₇ 85-86°C); ¹⁹F NMR (84 MHz, CH₂CH₂OH) -70.44 (s).



Ethyl 5-(phenylmethoxy)-2-(2,2,2-trifluoro-1-(dimethylhydrazono)ethyl)pentanoate (37). LDA (8.15 mmol) was prepared by the addition of *n*-butyl lithium (2.5 M solution in hexanes, 3.58 ml, 8.95 mmol) to diisopropylamine (1.14 ml, 8.15 mmol) in THF (15 ml) at 0°C. After 15 min stirring, the temperature was reduced to -78°C and ethyl 1,1,1-trifluoro-2-(dimethylhydrazono)butanoate (**36**) (1.68 g, 7.41 mmol) was added to the solution dropwise. After being stirred for 15 min at -78°C, the temperature of the reaction mixture was allowed to warm to 0°C for 30 min. The temperature was lowered to -78°C and 1-iodo-3-(phenylmethoxy)propane (**21**) (2.25 g, 8.15 mmol) in THF (5 ml) was added dropwise, followed immediately by HMPA (caution: carcinogen) (3.98 ml, 22.2 mmol). The temperature was allowed to warm to 0°C for 2 h and then to ambient temperature for 31 h. The reaction mixture was quenched by the addition of 10% aqueous HCl solution (10 ml) and stirring continued for 1 h. The mixture was extracted with ether (5 × 10 ml) and the combined organic extracts were washed with half saturated sodium metabisulphite solution (2 × 15 ml) and with water (3 × 10 ml). The organic phase was dried (MgSO₄) and the solvent was evaporated to yield 1.67g (61%) of ethyl 5-(phenylmethoxy)-2-(2,2,2-trifluoro-1-(dimethylhydrazono)ethyl)pentanoate (**37**) after chromatography (DCM). Data: pale yellow liquid; ¹⁹F NMR (84 MHz, CDCl₃) -66.01.

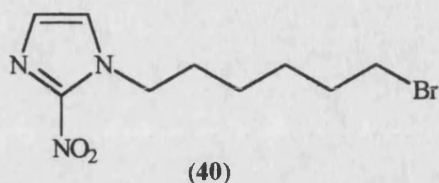


Ethyl 5-(phenylmethoxy)-2-(trifluoroacetyl)pentanoate (38). To a solution of ethyl 5-(phenylmethoxy)-2-(2,2,2-trifluoro-1-(dimethylhydrazono)ethyl)-pentanoate (37) (1.47 g, 3.93 mmol) in ethanol : water (95 : 5) (15 ml) was added iodomethane (3.67 ml, 59.0 mmol) and the mixture was boiled under reflux for 3 d. After cooling, the solvent and reagent were evaporated to give an orange liquid and white solid. DCM (50 ml) was added and the suspension was filtered. The solvent of the filtrate was evaporated to yield 1.06 g (81%) of ethyl 5-(phenylmethoxy)-2-(trifluoroacetyl)pentanoate (38) after chromatography (petroleum ether 40/60 : ethyl acetate ; 3 : 1). Data: dark green liquid; ^{19}F NMR (84 MHz, CDCl_3) -83.84 (s, hydrate?), -77.84 (s, keto), -66.96 (s, enol).

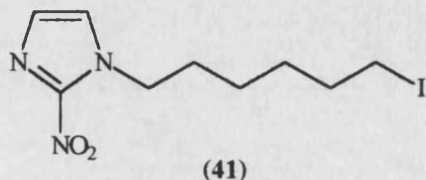


6-(Phenylmethoxy)-1,1,1-trifluorohexan-2-one (39). A solution of ethyl 5-(phenylmethoxy)-2-(trifluoroacetyl)pentanoate (38) (1.02 g, 3.05 mmol) in anhydrous DMF (8 ml) was heated to 100°C in the presence of lithium chloride (0.26 g, 6.10 mmol) and water (0.06 ml, 3.05 mmol) for 3 h. The solution was allowed to cool to ambient temperature and water (4 ml) and DCM (20 ml) were added. The organic layer was washed with water (5 × 5 ml) and the solvent was evaporated to yield 0.62 g (78%) of 6-(phenylmethoxy)-1,1,1-trifluorohexan-2-one (39) after chromatography (petroleum ether 40/60 : ethyl acetate ; 2 : 1). Data: colourless liquid; ^1H NMR (400 MHz, CDCl_3) 1.65 (2H, *ca.* qu, J = 5.8 Hz, $\text{CF}_3\text{COCH}_2\text{CH}_2\text{CH}_2$), 1.79 (2H, qu, J = 7.9 Hz,

CH₂CH₂CH₂OBn), 2.75 (2H, t, $J = 7.3$ Hz, CF₃COCH₂CH₂), 3.49 (2H, t, $J = 5.8$ Hz, CH₂CH₂OBn), 4.49 (2H, s, OCH₂Ph), 7.33 (5H, m, PhCH₂O); ¹⁹F NMR (CDCl₃) -79.82 (s); MS (EI) 260.1010 (M^+ , 5) (C₁₃H₁₅F₃O₂ requires 260.1024), 107 (31), 91 (100).

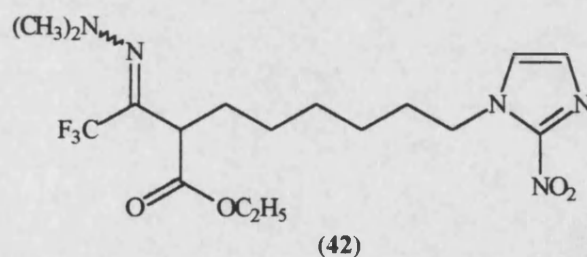


1-(6-Bromohexyl)-2-nitroimidazole (40). A solution of 2-nitroimidazole (3.00 g, 26.5 mmol) in anhydrous DMF (150 ml) was treated with potassium *tert*-butoxide (3.13 g, 26.5 mmol) and the mixture was heated at 130°C for 20 min. The resulting solution was cooled to ambient temperature and treated with 1,6-dibromohexane (20 g, 79.6 mmol). The solution was heated at 130 °C for 1.5 h. After being cooled, most of the solvent was removed by evaporation. Water (50 ml) was added to the residue and the mixture was extracted with DCM (3 × 50 ml). The combined organic extracts were washed with water (5 × 10 ml) and dried (MgSO₄) and the solvent was evaporated. Chromatography (hexane : ethyl acetate ; 4 : 3 to 1 : 1) yielded 3.99 g (54%) of 1-(6-bromohexyl)-2-nitroimidazole (40). Data: yellow oil; ¹H NMR (400 MHz, CDCl₃) 1.39 (2H, m, imidazole-CH₂CH₂CH₂CH₂CH₂CH₂Br), 1.52 (2H, m, imidazole-CH₂CH₂CH₂CH₂CH₂CH₂Br), 1.89 (4H, m, imidazole-CH₂CH₂CH₂CH₂CH₂CH₂Br), 3.41 (2H, t, $J = 6.6$ Hz, CH₂CH₂Br), 4.43 (2H, t, $J = 7.3$ Hz, imidazole-CH₂CH₂), 7.10 (1H, d, $J = 1.1$ Hz, imidazole 4-H), 7.15 (1H, d, $J = 1.1$ Hz, imidazole 5-H); IR (film) 1540 (s).



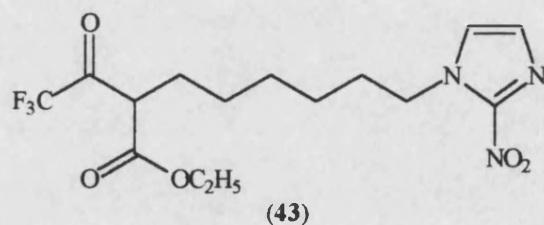
1-(6-Iodoheptyl)-2-nitroimidazole (41). To a stirred solution of 1-(6-

bromohexyl)-2-nitroimidazole (**40**) (3.94 g, 12.3 mmol) in anhydrous acetone (40 ml) was added sodium iodide (7.20 g, 48.0 mmol). The solution was stirred at ambient temperature in the dark and in a nitrogen atmosphere for 16 h. The reaction mixture was filtered and most of the acetone was evaporated. To the residue was added ether (50 ml) and water (10 ml) and the organic layer was washed with half saturated metabisulphite solution (2×15 ml) and brine (10 ml). After being dried (MgSO_4), the solvent was evaporated to yield 3.69 g (93%) of 1-(6-iodohexyl)-2-nitroimidazole (**41**). Data: pale yellow liquid; ^1H NMR (270 MHz, CDCl_3) 1.43 (4H, m, imidazole- $\text{CH}_2\text{CH}_2\text{CH}_2\text{CH}_2\text{CH}_2\text{CH}_2\text{I}$), 1.84 (4H, m, imidazole- $\text{CH}_2\text{CH}_2\text{CH}_2\text{CH}_2\text{CH}_2\text{CH}_2\text{I}$), 3.19 (2H, t, $J = 6.8$ Hz, $\text{CH}_2\text{CH}_2\text{I}$), 4.49 (2H, t, $J = 7.3$ Hz, imidazole- CH_2CH_2), 7.12 (1H, d, $J = 0.9$ Hz, imidazole 4-H), 7.15 (1H, d, $J = 1.1$ Hz, imidazole 5-H).



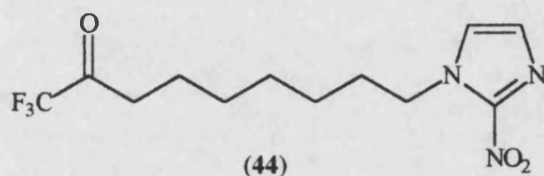
Ethyl 2-(2,2,2-trifluoro-1-(dimethylhydrazono)ethyl)-8-(2-nitroimidazol-1-yl)octanoate (42). LDA (11.1 mmol) was prepared by the addition of *n*-butyl lithium (2.5 M solution in hexanes, 4.9 ml, 12.3 mmol) to diisopropylamine (1.56 ml, 11.1 mmol) in THF (5 ml) at 0°C . After 15 min stirring, the temperature was reduced to -78°C and ethyl 1,1,1-trifluoro-2-(dimethylhydrazono)butanoate (**36**) (2.29 g, 10.1 mmol) in THF (8 ml) was added to the solution dropwise. After stirring for 15 min at -78°C , the formation of a green anion was observed and the temperature was allowed to warm to 0°C for 40 min. The temperature was lowered to -78°C and 1-(6-iodohexyl)-2-nitroimidazole (**41**) (3.60 g, 11.1 mmol) in THF (7 ml) was added dropwise, followed immediately by HMPA (caution: carcinogen) (5.29 ml, 30.4 mmol). The temperature was allowed to warm to 0°C for 2 h and then to

ambient temperature for 19 h. The reaction mixture was quenched with 10% aqueous HCl solution (5 ml) and stirring continued for 30 min. The mixture was extracted with ether (5 × 20 ml) and the combined organic extracts were washed with half saturated sodium metabisulphite solution (2 × 20 ml) and with water (3 × 10 ml) to neutrality. The organic phase was dried (MgSO₄) and the solvent was evaporated to yield 2.80 g (66%) of ethyl 2-(2,2,2-trifluoro-1-(dimethylhydrazono)ethyl)-8-(2-nitroimidazol-1-yl)octanoate (**42**) after chromatography (hexane : ethyl acetate ; 2 : 1). Data: yellow oil; ¹H NMR (400 MHz, CDCl₃) 1.24 (3H, t, *J* = 7.3 Hz, CO₂CH₂CH₃), 1.38 (4H, m, imidazole-CH₂CH₂CH₂CH₂CH₂CH₂), 1.85 (6H, m, imidazole-CH₂CH₂CH₂CH₂CH₂CH₂CH(C(NNMe₂)CF₃)CO₂Et), 2.62 (6H, s, NMe₂), 4.17 (2H, t, *J* = 6.41 Hz, imidazole-CH₂CH₂), 4.28 (1H, t, *J* = 7.02 Hz, CH₂CH(C(NNMe₂)CF₃)CO₂Et), 4.41 (2H, q, *J* = 7.6 Hz, CO₂CH₂CH₃), 7.10 (1H, d, *J* = 0.9 Hz, imidazole 4-H), 7.14 (1H, d, *J* = 0.9 Hz, imidazole 5-H); ¹⁹F NMR (376 MHz, CDCl₃) -66.25 (s); MS (CI) 422.2015 (M⁺ + H, 100) (C₁₇H₂₇F₃N₅O₄ requires 422.2015), 392 (25), 324 (20).

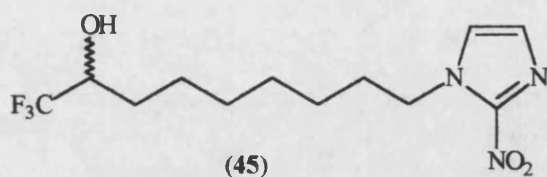


Ethyl 2-(trifluoroacetyl)-8-(2-nitroimidazol-1-yl)octanoate (43). To a solution of ethyl 2-(2,2,2-trifluoro-1-(dimethylhydrazono)ethyl)-8-(2-nitroimidazol-1-yl)octanoate (**42**) (2.60 g, 6.17 mmol) in ethanol : water (95 : 5) (26 ml) was added iodomethane (5.8 ml, 92.5 mmol) and the mixture was boiled under reflux for 5 d. After cooling, the solvent and reagent were evaporated, and DCM (50 ml) was added. The suspension was washed with half saturated sodium metabisulphite solution (2 × 10 ml) and brine (10 ml). The organic phase was dried (MgSO₄) and the solvent was evaporated to yield 0.63 g (27%) of ethyl 2-(trifluoroacetyl)-8-(2-nitroimidazol-1-yl)octanoate

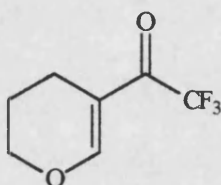
(43) after chromatography (hexane : ethyl acetate ; 4 : 3 to 3 : 4). Data: dark red oil; ^1H NMR (270 MHz, CDCl_3) 1.27 (3H, t, $J = 7.0$ Hz, $\text{CO}_2\text{CH}_2\text{CH}_3$), 1.37 (6H, m, imidazole- $\text{CH}_2\text{CH}_2\text{CH}_2\text{CH}_2\text{CH}_2\text{CH}_2\text{CH}(\text{COCF}_3)\text{CO}_2\text{Et}$), 1.95 (4H, m, imidazole- $\text{CH}_2\text{CH}_2\text{CH}_2\text{CH}_2\text{CH}_2\text{CH}_2$), 4.22 (2H, q, $J = 7.1$ Hz, $\text{CO}_2\text{CH}_2\text{CH}_3$), 4.26 (1H, m, $\text{CH}_2\text{CH}(\text{COCF}_3)\text{CO}_2\text{Et}$), 4.41 (2H, t, $J = 7.5$ Hz, imidazole- CH_2CH_2), 7.09 (1H, d, $J = 0.9$ Hz, imidazole 4-H), 7.15 (1H, d, $J = 1.1$ Hz, imidazole 5-H); ^{19}F NMR (376 MHz, CDCl_3) -84.02 (s, hydrate), -78.22 (s, keto), -67.26 (s, enol); MS (CI) 380 ($\text{M}^+ + \text{H}$, 100), 350 (20), 333 (38).



2-Nitro-1-(8-oxo-9,9-trifluorononyl)imidazole (44). A solution of ethyl 2-(trifluoroacetyl)-8-(2-nitroimidazol-1-yl)octanoate (43) (0.62 g, 1.63 mmol) in anhydrous DMF (4 ml) was heated to 100°C in the presence of lithium chloride (0.14 g, 3.26 mmol) and water (0.03 ml, 1.63 mmol) for 4 h. The solution was allowed to cool to ambient temperature and water (4 ml) and DCM (20 ml) were added. The organic layer was washed with water (5×5 ml) and the solvent evaporated to yield 0.47 g (94%) of 2-nitro-1-(8-oxo-9,9-trifluorononyl)imidazole (44). Data: pale yellow oil; ^1H NMR (400 MHz, CDCl_3) 1.37 (6H, m, imidazole- $\text{CH}_2\text{CH}_2\text{CH}_2\text{CH}_2\text{CH}_2\text{CH}_2\text{CH}_2\text{COCF}_3$), 1.68 (2H, qu, $J = 6.7$ Hz, $\text{CH}_2\text{CH}_2\text{CH}_2\text{COCF}_3$), 1.86 (2H, qu, $J = 7.3$ Hz, imidazole- $\text{CH}_2\text{CH}_2\text{CH}_2$), 2.72 (2H, t, $J = 7.0$ Hz, $\text{CH}_2\text{CH}_2\text{COCF}_3$), 4.41 (2H, t, $J = 7.3$ Hz, imidazole- CH_2CH_2), 7.11 (1H, d, $J = 0.9$ Hz, imidazole 4-H), 7.15 (1H, d, $J = 0.9$ Hz, imidazole 5-H); ^{19}F NMR (376 MHz, CDCl_3) -79.85 (s); MS (CI) 308.1222 ($\text{M}^+ + \text{H}$, 100) ($\text{C}_{12}\text{H}_{17}\text{F}_3\text{N}_3\text{O}_3$ requires 308.1222), 278 (15), 261 (30).

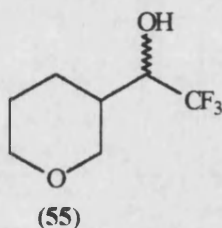


(±)-1,1,1-Trifluoro-9-(2-imidazol-1-yl)nonan-2-ol (45). 2-Nitro-1-(8-oxo-9,9,9-trifluorononyl)imidazole (**44**) (0.10 g, 0.33 mmol) was dissolved in ethanol : water (95 : 5) (1 ml) and sodium borohydride (0.006 g, 0.16 mmol) was added. The mixture was stirred at ambient temperature for 3 h, then quenched with 2 M aqueous HCl solution (3 ml). Extraction of the reaction mixture with ether (3 × 10 ml) followed by washing of the extracts with brine (5 ml), drying (MgSO₄) and evaporation of the solvent yielded 0.09 g (87%) of (±)-1,1,1-trifluoro-9-(2-imidazol-1-yl)nonan-2-ol (**45**). Data: colourless oil; ¹H NMR (400 MHz, CDCl₃) 1.29 (8H, m, imidazole-CH₂CH₂CH₂CH₂-CH₂CH₂CH₂CH(OH)CF₃), 1.54 (2H, m, CH₂CH₂CH(OH)CF₃), 1.78 (2H, m, imidazole-CH₂CH₂CH₂), 3.85 (1H, m, CH₂CH(OH)CF₃), 4.34 (2H, t, *J* = 7.7 Hz, imidazole-CH₂CH₂), 7.04 (1H, s, imidazole 4-H), 7.06 (1H, s, imidazole 5-H); ¹⁹F NMR (376 MHz, CDCl₃) -80.44 (d, *J*_{H-F} = 5.8 Hz); IR (film) 3350 (br), 1545 (s), 1495 (s); MS (CI) 310 (M⁺, 100), 263 (20).



5-Trifluoroacetyl-3,4-dihydro-2H-pyran (52). 5-Trifluoroacetyl-3,4-dihydro-2H-pyran (**52**) was synthesised essentially by the method described by Hojo's group¹⁴¹. To stirred solution of 3,4-dihydro-2H-pyran (5.0 g, 59.4 mmol) and pyridine (1.6 ml, 19.8 mmol) in DCM (40 ml) was added TFAA (12.0 ml, 85.14 mmol) with caution. This produced a large exotherm which was controlled with cooling. Stirring was continued at ambient temperature for 16 h. Water (10 ml) was added to the reaction mixture producing a moderate

exotherm. The organic phase was washed with water (10 ml) and 0.6 M sodium hydrogen carbonate solution (10 ml). After being dried (MgSO_4), the solvent was evaporated to yield 10.4 g (97%) of 5-trifluoroacetyl-3,4-dihydro-2*H*-pyran (**52**) following distillation (Kugelrohr). Data: colourless liquid; bp_{20} 65–70°C (literature¹⁴¹ bp_{10} 64.6°C); ^1H NMR (400 MHz, CDCl_3) 1.96 (2H, br qu, $J = 6.0$ Hz, $\text{CH}_2\text{CH}_2\text{CH}_2$), 2.34 (2H, t, $J = 6.0$ Hz, $\text{CH}_2\text{CH}_2\text{-C=C}$), 4.21 (2H, t, $J = 6.0$ Hz, $\text{CH}_2\text{CH}_2\text{O}$), 7.83 (1H, s, OCH=CR_2); ^{13}C NMR (100 MHz, CDCl_3) 17.93 ($\text{CH}_2\text{CH}_2\text{CH}_2$), 20.53 ($\text{CH}_2\text{-C=C}$), 67.84 (CH_2O), 116.74 (q, $J_{\text{C-F}} = 292$ Hz, CF_3), 162.35 (q, $J_{\text{C-F}} = 35$ Hz, C=O); ^{19}F NMR (376 MHz, CDCl_3) -70.37(s); IR (film) 1685 (s), 1615 (s); MS (EI) 180.0395 (M^+ , 29) ($\text{C}_7\text{H}_7\text{F}_3\text{O}_2$ requires 180.0398), 111 (100), 83 (35), 55 (28), 27 (31).



α -(Trifluoromethyl)tetrahydropyran-3-methanol (55).

Method A:

5-Trifluoroacetyl-3,4-dihydro-2*H*-pyran (**52**) (0.50 g, 2.78 mmol) was dissolved in methanol (9 ml) and a slurry of 10% palladium on activated carbon (0.10 g) in methanol (1 ml) was added. The suspension was evacuated and charged with hydrogen ($\times 3$) before being stirred in a hydrogen atmosphere for 4 h. The flask was evacuated, air was admitted, the suspension was filtered through a pad of Celite[®] and the solvent was evaporated to yield 0.50 g (98%) of α -(trifluoromethyl)tetrahydropyran-3-methanol (**55**).

Method B:

5-Trifluoroacetyl-3,4-dihydro-2*H*-pyran (**52**) (0.50 g, 2.78 mmol) was dissolved in hexane (9 ml) and THF (0.5 ml) and a slurry of 10% palladium on activated carbon (0.10 g) in hexane (1 ml) was added. The suspension was evacuated and charged with hydrogen ($\times 3$) before being stirred in a hydrogen

atmosphere for 30 min. The flask was evacuated, air was admitted, the suspension was filtered through a pad of Celite® and the solvent was evaporated to yield 0.50 g (100%) of α -(trifluoromethyl)tetrahydropyran-3-methanol (**55**).

Method C:

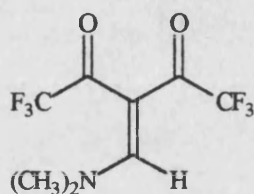
5-Trifluoroacetyl-3,4-dihydro-2*H*-pyran (**52**) (0.50 g, 2.78 mmol) was dissolved in methanol (9 ml) and potassium acetate (0.20 g) and a slurry of 10% palladium on activated carbon (0.10 g) in methanol (1 ml) were added. The suspension was evacuated and charged with hydrogen ($\times 3$) before being stirred in a hydrogen atmosphere for 2 h. The flask was evacuated, air was admitted, the suspension was filtered through a pad of Celite® and the solvent was evaporated. To the residue was added DCM (30 ml), and the resulting preprecipitate filtered. Removal of the solvent by evaporation yielded 0.39 g (76%) of α -(trifluoromethyl)tetrahydropyran-3-methanol (**55**).

Method D:

5-Trifluoroacetyl-3,4-dihydro-2*H*-pyran (**52**) (0.30 g, 1.67 mmol) was dissolved in methanol (9 ml) and a slurry of 10% palladium on activated carbon (0.08 g) in methanol (1 ml) was added. The temperature of the reaction mixture was reduced to -78°C and the suspension was evacuated and charged with hydrogen ($\times 3$) before being stirred in a hydrogen atmosphere. The temperature of the reaction mixture was maintained at -78°C for 3 h, after which t.l.c. indicated mostly starting material together with a small amount of a material with the same *R_f* value as that of the hydroxy compound (**55**). The temperature of the reaction mixture was allowed to rise in 10°C increments over a 3 h period, however, t.l.c. indicated little change until -10°C was reached. After 30 min at -10°C t.l.c. indicated that there was no starting material left. The flask was evacuated, air was admitted and the suspension was filtered through a pad of Celite®. The solvent was evaporated to yield 0.31 g (100%) of α -(trifluoromethyl)tetrahydropyran-3-methanol (**55**).

Data: colourless crystals; mp 35.0°C; ¹H NMR (270 MHz, CDCl₃) 1.52 (3H, m, pyran 4-H, OH), 1.77 (2H, m, pyran 5-H), 3.25 (2H, m, pyran 6-H), 3.76

(3H, m, pyran 2-H, 3-H), 6.21 (1H, m, pyran-CH(OH)CF₃); ¹⁹F NMR (376 MHz, (CD₃)₂SO) -74.87 (d, *J* = 8.1 Hz), -74.63 (d, *J* = 8.1 Hz); IR (film) 3380 (br), 1280 (s); MS (EI) 184.0709 (M⁺, 12) (C₇H₁₁F₃O₂ requires 184.0711), 166 (13), 57 (100); Anal. Calcd for C₇H₃F₃O₂: C, 45.65; H, 6.02. Found: C, 44.60; H, 5.90.

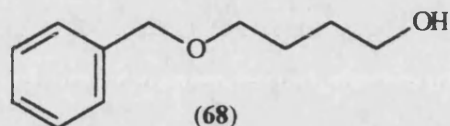


(62)

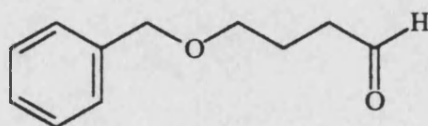
3-(Dimethylaminomethylene)-1,1,1,5,5,5-hexafluoropentan-2,4-dione (62).

Anhydrous DMF (0.73 g, 10.0 mmol) was dissolved in acetic anhydride (10 ml) and 1,1,1,5,5,5-hexafluoropentane-2,4-dione (1.41 ml, 10.0 mmol) was added slowly and the mixture was heated at 80°C for 18 h. Most of the solvent was removed by evaporation and the resulting residue was distilled (Kugelrohr) to yield 2.49 g (95%) of 3-(dimethylaminomethylene)-1,1,1,5,5,5-hexafluoropentan-2,4-dione (**62**). Data: yellow crystals; bp₃ 80°C; mp 36.5–37.5°C; ¹H NMR (400 MHz, (CD₃)₂SO, 20°C) 2.83 (3H, br s, NCH₃), 3.51 (3H, br s, NCH₃), 8.13 (1H, s, C=CH); ¹H NMR (400 MHz, (CD₃)₂SO, 100°C) 2.78 (3H, s, NCH₃), 3.54 (3H, s, NCH₃), 8.03 (1H, s, C=CH); ¹H NMR (400 MHz, (CD₃)₂SO, 150°C) 3.05 (6H, br s, NCH₃), 7.94 (1H, s, C=CH); ¹H NMR (400 MHz, CDCl₃, 21°C) 2.81 (3H, s, NCH₃), 3.45 (3H, s, NCH₃), 7.74 (1H, s, C=CH); ¹H NMR (400 MHz, CDCl₃, -50°C) 2.84 (3H, s, NCH₃), 3.55 (3H, s, NCH₃), 7.82 (1H, s, C=CH); ¹H NMR (400 MHz, *d*₈-THF, 20°C) 2.78 (3H, s, NCH₃), 3.47 (3H, s, NCH₃), 7.87 (1H, s, C=CH); ¹H NMR (400 MHz, *d*₈-THF, -90°C) 2.77 (3H, s, NCH₃), 3.58 (3H, s, NCH₃), 8.08 (1H, s, C=CH); ¹⁹F NMR (376 MHz, (CD₃)₂SO, 20°C) -72.09 (s); ¹⁹F NMR (376 MHz, (CD₃)₂SO, 100°C) -72.26 (s); ¹⁹F NMR (376 MHz, (CD₃)₂SO, 150°C) -72.31 (s); ¹⁹F NMR (376 MHz, CDCl₃, 21°C) -73.39 (s); ¹⁹F NMR (376 MHz, CDCl₃, -50°C) -72.94 (br s); ¹⁹F NMR (376 MHz, *d*₈-

THF, 20°C) -73.16 (s); ^{19}F NMR (376 MHz, d_8 -THF, -90°C) -72.6 (very br); ^{13}C NMR (100 MHz, CDCl_3) 43.17 (NCH_3), 49.04 (NCH_3), 101.45 ($((\text{CF}_3\text{CO})_2\text{C}=\text{C}(\text{H})\text{NMe}_2)$), 116.26 (q, $J_{\text{C-F}} = 292.4$ Hz, COCF_3), 159.41 ($((\text{CF}_3\text{CO})_2\text{C}=\text{C}(\text{H})\text{NMe}_2)$), 179.65 (q, $J_{\text{C-F}} = 36.7$ Hz, COCF_3); MS (EI) 263.0379 ($\text{M}^+ + \text{H}^+$) ($\text{C}_8\text{H}_7\text{F}_6\text{NO}_2$ requires 263.0381).

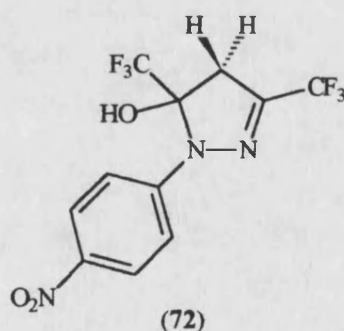


4-(Phenylmethoxy)butan-1-ol (68). 1,4-Butanediol (30.0 g, 333 mmol) was dissolved in DMF (200 ml) and sodium hydride (60% dispersion in oil, 6.66 g, 166 mmol) was added portionwise with caution. After 5 min, benzyl bromide (19.8 ml, 166 mmol) was added slowly, resulting in a moderate exotherm. The mixture was stirred at ambient temperature for 16 h followed by heating to 70°C for 1.5 h. After cooling, most of the solvent was removed by evaporation and to the residue was added DCM (20 ml) and water (30 ml). The aqueous phase was extracted with DCM (20 ml) and the combined organic extracts were washed with water (5 × 20 ml), 2 M aqueous HCl solution (20 ml), water (20 ml) and, finally, brine (20 ml). After being dried (MgSO_4), the solvent of the organic extracts was evaporated and the residue was distilled (Kugelrohr) to yield 22.5 g (75%) of 4-(phenylmethoxy)butan-1-ol (**68**). Data: colourless liquid; $\text{bp}_{0.1}$ 150°C; ^1H NMR (270 MHz, $(\text{CD}_3)_2\text{SO}$) 1.69 (4H, m, $\text{CH}_2\text{CH}_2\text{CH}_2\text{CH}_2$), 3.51 (2H, *ca.* t, $J = 6.0$ Hz, $\text{CH}_2\text{CH}_2\text{OH}$), 3.63 (2H, t, $J = 5.7$ Hz, $\text{BnOCH}_2\text{CH}_2$), 4.51 (2H, s, PhCH_2O), 7.33 (5H, m, Ph).



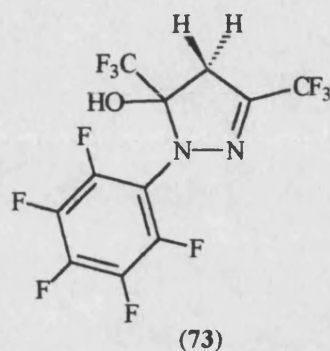
4-(Phenylmethoxy)butanal (69). A solution of oxalyl chloride (15.8 ml, 31.6 mmol) in anhydrous DCM (60 ml) under a nitrogen atmosphere was cooled to

-60°C, and a solution of DMSO (4.5 ml, 63.1 mmol) in DCM (20 ml) was added slowly. The reaction mixture was stirred for 2 min and a solution of 4-(phenylmethoxy)butan-1-ol (**68**) (5.0 g, 27.8 mmol) in DCM (20 ml) was added within 5 min. Triethylamine (20 ml, 143 mmol) was added and the reaction mixture was stirred for a further 5 min before being allowed to warm to ambient temperature. Water (200 ml) was added and the aqueous phase was extracted with DCM (3 × 50 ml). The combined organic phases were washed with 0.2 M aqueous HCl solution (20 ml), water (20 ml), 0.6 M sodium carbonate solution (20 ml), water (20 ml) and brine (20 ml). The organic phase was dried (MgSO₄) and the solvent was evaporated to yield 4.94 g (100%) of 4-(phenylmethoxy)butanal (**69**). Data: colourless oil; ¹H NMR (270 MHz, CDCl₃) 1.95 (2H, qu, *J* = 6.2 Hz, CH₂CH₂CH₂), 2.55 (2H, dt, *J* = 1.5, 7.0 Hz, CH₂CH₂CHO), 3.50 (2H, t, *J* = 6.0 Hz, BnOCH₂CH₂), 4.48 (2H, s, PhCH₂O), 7.32 (5H, m, Ph), 9.77 (1H, t, *J* = 1.5 Hz, CH₂CHO).

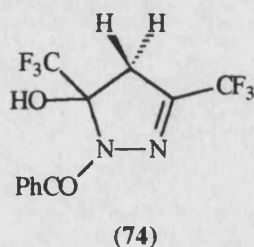


3,5-Bis(trifluoromethyl)-4,5-dihydro-5-hydroxy-1-(4-nitrophenyl)pyrazole (72). To a solution of 4-nitrophenylhydrazine (0.20 g, 1.30 mmol) in ethanol (50 ml) was added 1,1,1,5,5,5-hexafluoropentane-2,4-dione (0.30 g, 1.44 mmol). The mixture was boiled under reflux for 3 h and then was allowed to cool to ambient temperature. The solvent was evaporated to yield 0.45 g (99%) of 3,5-bis(trifluoromethyl)-4,5-dihydro-5-hydroxy-1-(4-nitrophenyl)-pyrazole (**72**). Data: yellow solid; mp 105-106°C (literature¹¹² mp 105-108°C claimed for pyrazole (**76**)); ¹H NMR (270 MHz, CDCl₃) 3.42 (1H, d septet, *J*_{H-H} = 19.6 Hz, *J*_{H-F} = 1.5 Hz, pyrazole 4-H), 3.74 (1H, br d, *J*_{H-H} = 19.6 Hz,

pyrazole 4-H), 5.75 (1H, br, OH), 7.60 (2H, d, $J = 9.4$ Hz, Ar 2,6-H₂), 8.12 (2H, d, $J = 9.4$ Hz, Ar 3,5-H₂); MS (EI) 343 (M^+ , 95), 274 (100), 228 (61); Anal. Calcd for C₁₁H₇F₆N₃O₃: C, 38.48; H, 2.06; N, 12.25. Found: C, 38.70; H, 2.03; N, 12.50.

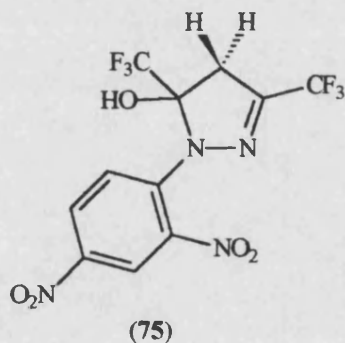


3,5-Bis(trifluoromethyl)-4,5-dihydro-5-hydroxy-1-(pentafluorophenyl)pyrazole (73). To a solution of pentafluorophenylhydrazine (0.20 g 1.00 mmol) in ethanol (50 ml) was added 1,1,1,5,5,5-hexafluoropentane-2,4-dione (0.30 g, 1.44 mmol). The mixture was boiled under reflux for 5 h and then was allowed to cool to ambient temperature. The solvent was evaporated to yield 0.38 g (98%) of 3,5-bis(trifluoromethyl)-4,5-dihydro-5-hydroxy-1-(pentafluorophenyl)pyrazole (73). Data: colourless prisms; mp 61-62°C (literature¹¹² mp 60-62°C claimed for pyrazole (77)); ¹H NMR (270 MHz, CDCl₃) 3.32 (1H, br d, $J = 18.9$ Hz, pyrazole 4-H), 3.59 (1H, dq, $J_{H-H} = 18.9$ Hz, $J_{H-F} = 1.5$ Hz, pyrazole 4-H), 6.13 (1H, br s, OH); MS (EI) 388.0099 (M^+ , 15) (C₁₁H₃F₁₁N₂O requires 388.0070), 319 (20), 139 (92), 69 (100).

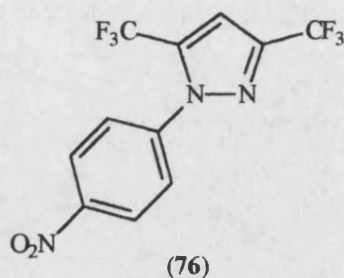


1-Benzoyl-3,5-bis(trifluoromethyl)-4,5-dihydro-5-hydroxypyrazole (74). To a solution of benzoic hydrazide (0.14 g, 1.00 mmol) in ethanol (50 ml) was

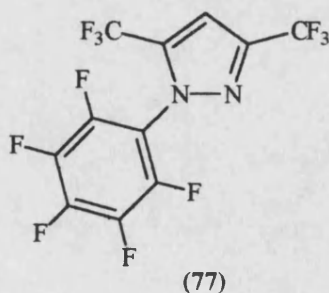
added 1,1,1,5,5,5-hexafluoropentane-2,4-dione (0.30 g, 1.44 mmol). The mixture was boiled under reflux for 5 h and then was allowed to cool to ambient temperature. The solvent was evaporated to yield 0.47 g (99%) of 1-benzoyl-3,5-bis(trifluoromethyl)-4,5-dihydro-5-hydroxypyrazole (**74**). Data: 82-84°C (literature¹¹² mp 84-85°C claimed for pyrazole (**78**)); ¹H NMR (270 MHz, CDCl₃) 3.38 (1H, d septet, $J_{\text{H-H}} = 19.5$ Hz, $J_{\text{H-F}} = 1.5$ Hz, pyrazole 4-H), 6.43 (1H, br s, OH), 7.47 (2H, *ca.* t, $J = 7.5$ Hz, Ar 3,5-H₂), 7.59 (1H, tt, $J = 7.5$ Hz, $J = 1.3$ Hz, Ar 4-H), 7.86 (2H, *ca.* d, $J = 7.5$ Hz, Ar 2,6-H₂); ¹⁹F NMR (84 MHz, CDCl₃) -81.40 (s), -68.18 (s); MS (EI) 326 (M^+ , 1), 105 (100); MS (FAB +ve ion) 327.0599 ($M^+ + H$) (C₁₂H₉F₆N₂O₂ requires 327.0568).



3,5-Bis(trifluoromethyl)-4,5-dihydro-1-(2,4-dinitrophenyl)-5-hydroxypyrazole (75**).** To a solution of 2,4-dinitrophenylhydrazine (0.30 g, 1.50 mmol) in ethanol (50 ml) was added 1,1,1,5,5,5-hexafluoropentane-2,4-dione (0.41 g, 1.97 mmol). The mixture was boiled under reflux for 5 h and then was allowed to cool to ambient temperature. The solvent was evaporated to yield 0.51 g (88%) of 3,5-bis(trifluoromethyl)-4,5-dihydro-1-(2,4-dinitrophenyl)-5-hydroxypyrazole (**75**). Data: orange-yellow solid; mp 81-83°C (literature¹¹² mp 82-83°C claimed for pyrazole (**79**)); ¹H NMR (400 MHz, CDCl₃) 3.06 (1H, d, $J = 14.6$ Hz, pyrazole 4-H), 3.18 (1H, d, $J = 14.6$ Hz, pyrazole 4-H), 5.10 (1H, br, OH), 8.04 (1H, d, $J = 9.5$ Hz, Ar 6-H), 8.40 (1H, dd, $J = 9.5$ Hz, $J = 2.4$ Hz, Ar 5-H), 9.14 (1H, d, $J = 2.4$ Hz, Ar 3-H); ¹⁹F NMR (376 MHz, (CD₃)₂SO) -78.93 (s), -65.60 (s); MS (EI) 343 (M^+ , 95), 274 (100), 228 (61); C₁₁H₇F₆N₃O₃ requires C 38.48, H 2.06, N 12.25; found C 38.70, H 2.03, N

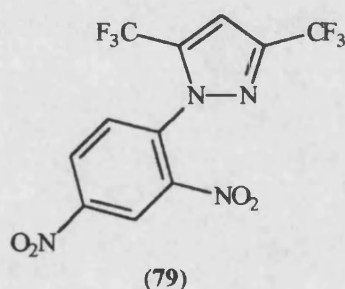


3,5-Bis(trifluoromethyl)-1-(4-nitrophenyl)pyrazole (76). A solution of 3,5-bis(trifluoromethyl)-4,5-dihydro-5-hydroxy-1-(4-nitrophenyl)pyrazole (72) (0.10 g, 0.29 mmol) in ethanol (10 ml) and concentrated HCl (0.5 ml) was stirred and heated under reflux for 72 h. The solvent was evaporated and the residue was dissolved in DCM (10 ml). Anhydrous MgSO₄ and sodium hydrogen carbonate were added and the suspension was filtered and the solvent was evaporated to give 0.09 g (96%) of 3,5-bis(trifluoromethyl)-1-(4-nitrophenyl)pyrazole (76). Data: yellow oil; ¹H NMR (400 MHz, CDCl₃) 7.18 (1H, s, pyrazole-H), 7.77 (2H, d, *J* = 8.9 Hz, Ar 2,6-H₂), 8.42 (2H, d, *J* = 8.9 Hz, Ar 3,5-H₂); ¹³C NMR (100 MHz, CDCl₃) 108.40 (CH, pyrazole 4-H), 118.74 (q, *J*_{C-F} = 270 Hz, CF₃), 120.04 (q, *J*_{C-F} = 270 Hz, CF₃), 124.84 (Ar 2,6-CH), 126.32 (Ar 3,5-CH), 134.50 (q, *J*_{C-F} = 40 Hz, C-CF₃), 142.73 (Ar 4-C), 144.04 (q, *J*_{C-F} = 40 Hz, C-CF₃), 148.36 (Ar 1-C); ¹⁹F NMR (376 MHz, CDCl₃) -63.18 (s, CF₃), -58.07 (s, CF₃); MS (EI) 325.0288 (M⁺, 100) (C₁₁H₅N₃F₆O₂ requires 325.0286), 279 (10).

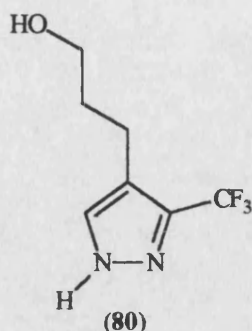


3,5-Bis(trifluoromethyl)-1-(pentafluorophenyl)pyrazole (77). 3,5-Bis(trifluoromethyl)-4,5-dihydro-5-hydroxy-1-(pentafluorophenyl)pyrazole (73)

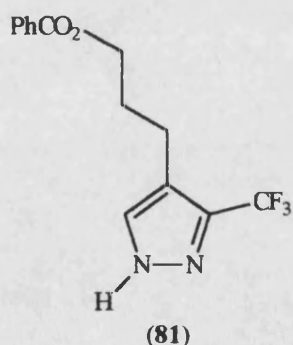
(0.85 g, 2.18 mmol) was dissolved in acetic anhydride (20 ml, 210 mmol) and acetic acid (15 ml, 260 mmol) and the solution heated under reflux for 16 h. Most of the acetic anhydride and acetic acid were removed by evaporation and the residue was dissolved in DCM (50 ml) and stirred with saturated sodium hydrogen carbonate solution (50 ml) for 1 h. The organic phase was separated and dried (MgSO₄) and the solvent was removed by evaporation to yield 0.23 g (62%) of 3,5-bis(trifluoromethyl)-1-(pentafluorophenyl)pyrazole (**77**). Data: yellow oil; ¹H NMR (400 MHz, CDCl₃) 7.17 (s); ¹⁹F NMR (376 MHz, CDCl₃) -159.84 (m, Ar 3,5-F₂), -147.30 (m, Ar 4-F), -144.45 (m, Ar 2,6-F₂), -63.49 (s, CF₃), -61.71 (s, CF₃); MS (EI) 369.9957 (M⁺, 100) (C₁₁H₂F₁₁N₂ requires 369.9964), 351 (35), 301 (50), 206 (45).



3,5-Bis(trifluoromethyl)-1-(2,4-dinitrophenyl)pyrazole (79). 3,5-Bis-(trifluoromethyl)-4,5-dihydro-1-(2,4-dinitrophenyl)-5-hydroxypyrazole (**75**) (0.13 g, 0.34 mmol) was dissolved in DCM (4 ml) and triethylamine (0.12 ml, 0.85 mmol), followed by the addition of methanesulphonyl chloride (0.04 g, 0.34 mmol). The solution was stirred for 7 d. DCM (30 ml) was added and the solution was washed with water (10 ml), 0.5 M H₂SO₄ (2 × 10 ml) and finally with water (2 × 10 ml). The organic phase was dried (MgSO₄) and the solvent evaporated to yield 0.01 g (10%) of 3,5-bis(trifluoromethyl)-1-(2,4-dinitrophenyl)pyrazole (**79**) after chromatography (petroleum ether bp 40-60°C : ethyl acetate ; 5 : 1). Data: bright yellow oil; ¹H NMR (400 MHz, CDCl₃) 6.70 (1H, s, pyrazole 4-H), 8.11 (1H, d, *J* = 9.3 Hz, Ar 6-H), 8.47 (1H, dd, *J* = 9.3, 2.4 Hz, Ar 5-H), 9.17 (1H, d, *J* = 2.4 Hz, Ar 6-H); ¹⁹F NMR (376 MHz, CDCl₃) -70.95 (s, CF₃), -67.39 (s, CF₃); MS (CI) 371 (M⁺ + H, 38), 279 (8).

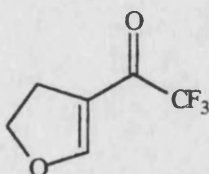


3-(3-Trifluoromethylpyrazol-4-yl)propanol (80). 5-Trifluoroacetyl-3-4-dihydro-2*H*-pyran (**52**) (1.00 g, 5.60 mmol) was dissolved in ethanol (10 ml) and hydrazine hydrate (0.81 ml, 16.6 mmol) in ethanol (3 ml) was added. The mixture was stirred and heated under reflux for 3 h. During this time the progress of the reaction was monitored by ^{19}F NMR. The solvent was evaporated and the residue was distilled (Kugelrohr) to yield 1.07 g (99%) of 3-(trifluoromethyl)pyrazole-4-propanol (**80**). Data: white solid; mp 84.0-85.0°C (literature¹⁵⁴ mp 85-87°C); bp_{0.4} 160°C; ^1H NMR (400 MHz, D_2O) 1.79 (2H, qu, $J = 7.0$ Hz, $\text{CH}_2\text{CH}_2\text{CH}_2$), 2.62 (2H, t, $J = 7.3$ Hz, RCH_2CH_2), 3.59 (2H, t, $J = 6.3$ Hz, $\text{CH}_2\text{CH}_2\text{OH}$); ^{19}F NMR (376 MHz, D_2O) -61.31 (s); MS (CI, iso-butane) 195.0745 ($\text{M}^+ + \text{H}$, 100) ($\text{C}_7\text{H}_{10}\text{F}_3\text{N}_2\text{O}$ requires 195.0745), 176 (22), 155 (8).



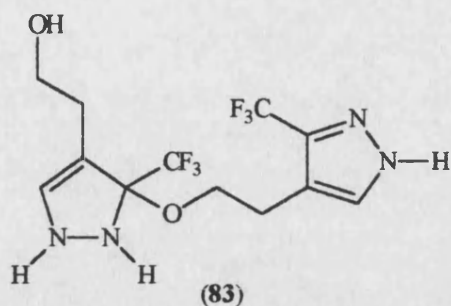
3-(3-Trifluoromethylpyrazol-4-yl)propyl benzoate (81). Benzoyl chloride (0.54 g, 3.90 mmol) was added dropwise to 3-(trifluoromethyl)pyrazole-4-propanol (**80**) (0.50 g, 2.60 mmol) and triethylamine (5.20 g, 51.5 mmol) in dichloromethane (20 ml) at 0°C and the mixture was allowed to warm to

ambient temperature during 16 h. The mixture was washed with saturated sodium hydrogen carbonate solution (10 ml), 2 M hydrochloric acid (5 × 10 ml) and brine (10 ml) and was dried (MgSO₄). Chromatography (hexane : ethyl acetate, 1 : 1) of the evaporation residue gave 0.62 g (81%) of 3-(3-trifluoromethylpyrazol-4-yl)propyl benzoate (**81**). Data: large white plates; mp 46.0-46.5°C; ¹H NMR (400 MHz, CDCl₃) 2.09 (2H, qu, *J* = 7 Hz, CH₂CH₂CH₂), 2.80 (2H, t, *J* = 7.6 Hz, pyrazole-CH₂), 4.38 (2H, t, *J* = 6.1 Hz, CH₂O), 7.44 (2H, br t, *J* = 8 Hz, Ar 3,5-H₂), 7.54 (1H, s, pyrazole 5-H), 7.56 (1H, br t, *J* = 8 Hz, Ar 4-H), 8.03 (2H, br d, *J* = 8 Hz, Ar 2,6-H₂); ¹⁹F NMR (376 MHz, CDCl₃) -61.30 (s); MS (CI) 299.1007 (*M*⁺ + H) (C₁₄H₁₄F₃N₂O₂ requires 299.1007). 176 (48), 105 (24).

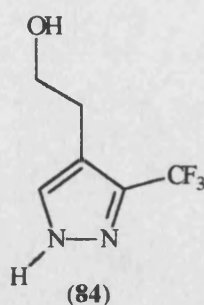


(82)

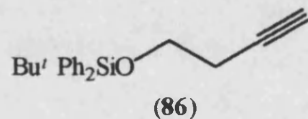
3-Trifluoroacetyl-4,5-dihydrofuran (82). 3-Trifluoroacetyl-4,5-dihydrofuran (**82**) was synthesised essentially by the method described by Hojo's group¹⁴¹. Trifluoroacetic anhydride (22.5 g, 107 mmol) was added dropwise with cooling to 2,3-dihydrofuran (5.00 g, 71.0 mmol) and pyridine (1.88 g, 24.0 mmol) in dichloromethane (40 ml) and the mixture was stirred for 18 h. Distillation gave 9.72 g (82%) of 3-trifluoroacetyl-4,5-dihydrofuran (**82**). Data: colourless liquid; bp₂₀ 80°C (literature¹⁴¹ bp_{10.5} 48.5°C); ¹H NMR (400 MHz, CDCl₃) 2.98 (2H, tq, *J*_{H-H} = 9.8 Hz, *J*_{H-F} = 0.6 Hz, 4-H₂), 4.68 (2H, t, *J*_{H-H} = 9.8 Hz, 5-H₂), 7.64 (1H, q, *J*_{H-F} = 1.5 Hz, 2-H); ¹⁹F NMR (376 MHz, CDCl₃) -73.88 (br s); ¹³C NMR (100, CDCl₃) 26.93 (4-C), 74.01 (5-C), 114.37 (3-C), 116.62 (q, *J*_{C-F} = 190 Hz, CF₃), 163.84 (q, *J*_{C-F} = 5.0 Hz, 2-C), 176.08 (q, *J*_{C-F} = 36.0 Hz, C=O); MS (EI) 166.0239 (*M*⁺, 45) (C₆H₅F₃O₂ requires 166.0242), 97 (100).



2-(3,4-Dihydro-3-trifluoromethyl-3-(2-(3-trifluoromethylpyrazol-4-yl)ethoxy)pyrazol-4-yl)ethanol (83). The furan (82) (1.00 g, 6.02 mmol) was boiled under reflux with hydrazine hydrate (0.30 g, 6.02 mmol) in ethanol (13 ml) for 3 h. Evaporation of the solvent gave 1.09 g (100%) of 2-(3,4-dihydro-3-trifluoromethyl-3-(2-(3-trifluoromethylpyrazol-4-yl)ethoxy)pyrazol-4-yl)ethanol (83). Data: white solid; mp 84-85°C; ^1H NMR (270 MHz, CD_3OD) 1.82 (1H, m) and 1.93 (1H, m) (dihydropyrazole- CH_2), 2.79 (2H, t, $J = 6.8$ Hz, pyrazole- CH_2), 3.31 (1H, br t, $J = 7$ Hz, dihydropyrazole 4-H), 3.71 (2H, t, $J = 6.8$ Hz, pyrazole- $\text{CH}_2\text{CH}_2\text{O}$), 3.73 (2H, m, dihydropyrazole- $\text{CH}_2\text{CH}_2\text{OH}$), 4.94 (3H, 2 \times NH + OH), 6.82 (1H, s, dihydropyrazole 5-H), 7.67 (1H, s, pyrazole 5-H); ^{19}F NMR (376 MHz, CD_3OD) -82.57 (s, dihydropyrazole- CF_3), -62.20 (s, pyrazole- CF_3); ^{13}C NMR (100 MHz, CD_3OD) 27.60 (CH_2), 28.36 (CH_2), 49.49 (dihydropyrazole 4-C), 60.92 (CH_2), 62.95 (CH_2), 92.93 (q, $J_{\text{H-F}} = 31.0$ Hz, dihydropyrazole 3-C), 117.52 (pyrazole 4-C), 123.70 (q, $J_{\text{C-F}} = 268$ Hz, CF_3), 125.68 (q, $J_{\text{C-F}} = 281$ Hz, CF_3), 131.36 (CH), 140.95 (q, $J_{\text{C-F}} = 37.0$ Hz, pyrazole 3-C), 146.30 (CH); MS (CI) 361.1099 ($\text{M}^+ + \text{H}$) ($\text{C}_{12}\text{H}_{15}\text{F}_6\text{N}_4\text{O}_2$ requires 361.1099); IR (Nujol) 3300 (s), 3180 (s), 1170 (s).

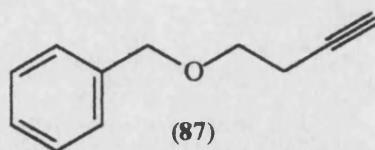


2-(3-Trifluoromethylpyrazol-4-yl)ethanol (84). 2-(3,4-dihydro-3-trifluoromethyl-3-(2-(3-trifluoromethylpyrazol-4-yl)ethoxy)pyrazol-4-yl)ethanol (**83**) (1.00 g, 2.80 mmol) was boiled under reflux with 9 M aqueous HCl solution (0.05 ml) in ethanol (12 ml) for 16 h. The solvent and reagent were evaporated to give 0.99 g (100%) of 2-(3-trifluoromethylpyrazol-4-yl)ethanol (**84**). Data: pale yellow solid; mp 90-91°C; ^1H NMR (270 MHz, $(\text{CD}_3)_2\text{SO}$) 2.65 (2H, br t, $J = 7.0$ Hz, pyrazole- CH_2), 3.54 (2H, t, $J = 7.0$ Hz, CH_2O), 4.9 (1H, br, OH), 7.78 (1H, br s, pyrazole 5-H); ^{19}F NMR (84 MHz, $(\text{CD}_3)_2\text{SO}$) -59.66 (br s); MS (EI) 180.0515 (M^+ , 30) ($\text{C}_6\text{H}_7\text{F}_3\text{N}_2\text{O}$ requires 180.0510), 159 (100).

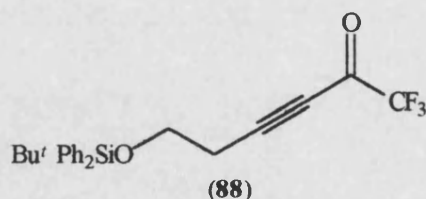


4-(1,1-Dimethylethyl)diphenylsilyloxybut-1-yne (86). A solution of 3-butyne-1-ol (9.81 g, 0.14 mmol) in anhydrous DMF (100 ml) was cooled to 0°C and imidazole (19.1 g, 0.28 mmol) was added portionwise followed by *tert*-butyldiphenylchlorosilane (35.8 ml, 0.14 mmol). The clear solution was allowed to warm to ambient temperature and after 45 min the temperature was lowered to 0°C and water (400 ml) was added slowly. The mixture was extracted with hexane (5×100 ml) and the combined organic extracts were washed with water (50 ml) and brine (2×50 ml). The organic phase was dried (MgSO_4) and the solvent evaporated to yield 43.2 g (100%) of 4-(1,1-dimethylethyl)diphenylsilyloxybut-1-yne (**86**). Data: colourless oil; ^1H NMR (270 MHz, CDCl_3) 1.06 (9H, s, *t*-Bu), 1.94 (1H, t, $J = 2.8$ Hz, $\text{CH}_2\text{C}\equiv\text{CH}$), 2.45 (2H, dt, $J = 7.1, 2.7$ Hz, $\text{CH}_2\text{CH}_2\text{C}\equiv\text{CH}$), 3.78 (2H, t, $J = 7.1$ Hz,

OCH₂CH₂), 7.40 (6H, m, 2 × Ar 3,4,5-H₃), 7.68 (4H, m, 2 × Ar 2,5-H₂).



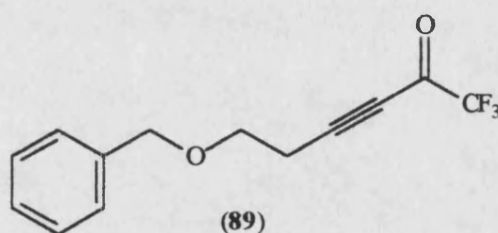
4-Phenylmethoxybut-1-yne (87). To a solution of 3-butynol (9.69 g, 138 mmol) in anhydrous DMF (65 ml) was added sodium hydride (60% dispersion in oil, 5.53 g, 138 mmol) portionwise. The mixture was stirred for 5 min before cooling to 0°C, and benzyl bromide (16.4 ml, 138 mmol) was added dropwise. The reaction mixture was allowed to rise to ambient temperature and stirred for 16 h. Most of the solvent was removed by evaporation. To the residue was added DCM (100 ml) and water (30 ml). The aqueous phase was extracted with DCM (50 ml) and the combined organic extracts were washed with water (5 × 20 ml), 2 M HCl solution (20 ml), water (20 ml) and finally brine (20 ml). The organic extracts were dried (MgSO₄) and the solvent was evaporated to yield 16.8 g (75%) of 4-phenylmethoxybut-1-yne (87) after chromatography (hexane : ethyl acetate ; 1 : 0 to 15 : 1). Data: colourless liquid; ¹H NMR (270 MHz, CDCl₃) 2.00 (1H, t, *J* = 2.8 Hz, CH₂C≡CH), 2.50 (2H, dt, *J* = 6.8, 2.6 Hz, CH₂CH₂C≡CH), 3.60 (2H, t, *J* = 7.0 Hz, OCH₂CH₂), 4.56 (2H, s, PhCH₂O), 7.34 (5H, m, Ph).



6-((1,1-Dimethylethyl)diphenylsilyloxy)-1,1,1-trifluorohex-3-yn-2-one

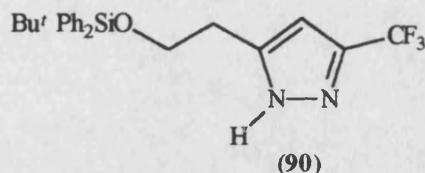
(88). *n*-Butyl lithium (2.5 M in hexanes; 13 ml, 32.4 mmol) was added to 4-((1,1-dimethylethyl)diphenylsilyloxy)but-1-yne (86) (10.0 g, 32.4 mmol) in THF (50 ml) at -78°C and the mixture was stirred at this temperature for 30 min. 2,2,2-Trifluoroethyl trifluoroacetate (7.00 g, 35.7 mmol) in THF (60 ml) was

added, followed immediately by boron trifluoride diethyl etherate (5.65 g, 40.0 mmol), and the mixture was stirred at -78°C for 90 min. Saturated aqueous ammonium chloride (18 ml) was added and the mixture was allowed to warm to ambient temperature. The solvent was evaporated and the residue, in diethyl ether (100 ml), was washed with water (20 ml) and with brine (2×20 ml) and was dried (MgSO_4). Evaporation of the solvent gave 12.4 g (95%) of 6-((1,1-dimethylethyl)diphenylsilyloxy)-1,1,1-trifluorohex-3-yn-2-one (**88**). Data: colourless liquid; ^1H NMR (270 MHz, CDCl_3) 1.06 (9H, s, *t*-Bu), 2.72 (2H, t, $J = 6.3$ Hz, $\text{CH}_2\text{C}\equiv\text{C}$), 3.85 (2H, t, $J = 6.3$ Hz, CH_2O), 7.35 (10H, $2 \times \text{Ph}$); ^{19}F NMR (376 MHz, CDCl_3) -78.63 (s); MS (CI) 405.1498 ($\text{M}^+ + \text{H}$) ($\text{C}_{22}\text{H}_{24}\text{F}_3\text{O}_2\text{Si}$ requires 405.1498).

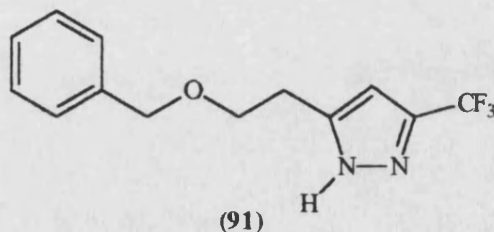


6-Phenylmethoxy-1,1,1-trifluorohex-3-yn-2-one (89). *n*-Butyl lithium (2.5 M in hexanes, 18 ml, 45.0 mmol) was added to 4-phenylmethoxybut-1-yne (**87**) (7.20 g, 45.0 mmol) in THF (100 ml) at -78°C and the mixture was stirred at this temperature for 30 min. 2,2,2-Trifluoroethyl trifluoroacetate (9.70 g, 50.0 mmol) in THF (70 ml) was added, followed immediately by boron trifluoride diethyl etherate (8.50 g, 60.0 mmol) and the mixture was stirred at -78°C for 90 min. Saturated aqueous ammonium chloride (30 ml) was added and the mixture was allowed to warm to ambient temperature. The solvent was evaporated and the residue, in dichloromethane (200 ml), was washed with water (50 ml) and with brine (2×50 ml) and was dried (MgSO_4). Evaporation of the solvent gave 11.1 g (97%) of 6-phenylmethoxy-1,1,1-trifluorohex-3-yn-2-one (**89**). Data: pale yellow oil; ^1H NMR (270 MHz, CDCl_3) 2.80 (2H, t, $J = 6.6$ Hz, $\text{CH}_2\text{C}\equiv\text{C}$), 3.69 (2H, t, $J = 6.6$ Hz, OCH_2CH_2), 4.58 (2H, s, PhCH_2O), 7.30-7.35 (5H, m, Ph); ^{19}F NMR (376 MHz, CDCl_3) -78.65 (s); MS (CI)

255.0633 ($M^+ - H$, 30) ($C_{13}H_{10}F_3O_2$ requires 255.0633), 197 (6).

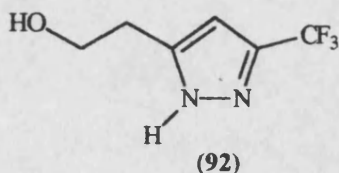


3-(2-((1,1-Dimethylethyl)diphenylsilyloxy)ethyl)-5-trifluoromethylpyrazole (90). 6-((1,1-Dimethylethyl)diphenylsilyloxy)-1,1,1-trifluorohex-3-yn-2-one (**88**) (0.38 g, 0.93 mmol) was boiled under reflux with hydrazine hydrate (0.07 g, 0.93 mmol) in ethanol (2.2 ml) for 90 min. The evaporation residue, in DCM (20 ml), was dried ($MgSO_4$) and the solvent was evaporated to give 0.39 g (99%) of 3-(2-((1,1-dimethylethyl)diphenylsilyloxy)ethyl)-5-trifluoromethylpyrazole (**90**). Data: colourless oil, 1H NMR (270 MHz, $CDCl_3$) 1.06 (9H, s, *t*-Bu), 2.88 (2H, t, $J = 5.7$ Hz, pyrazole- CH_2), 3.89 (2H, $J = 5.7$ Hz, CH_2O), 6.33 (1H, s, pyrazole 4-H), 7.3-7.7 (10H, m, $2 \times Ph$), ^{19}F NMR (376 MHz, $CDCl_3$) -62.31 (s); ^{13}C NMR (100 MHz, $CDCl_3$) 19.01 (CMe_3), 26.74 ($3 \times CH_3$), 28.44 (pyrazole- CH_2), 62.53 (CH_2O), 102.69 (pyrazole 4-C), 121.44 (q, $J_{C-F} = 268$ Hz, CF_3), 127.80 ($2 \times Ph$ 3,5- C_2), 129.89 ($2 \times Ph$ 4-C), 132.83 ($2 \times Ph$ 1-C), 134.81 (CH), 135.41 ($2 \times Ph$ 2,6- C_2), 142.87 (q, $J = 37.0$ Hz, pyrazole 5-C), 143.28 (pyrazole 3-C); MS (CI) 419.1767 ($M^+ + H$) ($C_{22}H_{26}F_3N_2OSi$ requires 419.1767).

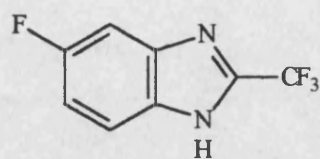


3-(2-Phenylmethoxyethyl)-5-trifluoromethylpyrazole (91). 6-Phenylmethoxy-1,1,1-trifluorohex-3-yn-2-one (**89**) (0.50 g, 1.95 mmol) was boiled under reflux with hydrazine hydrate (0.15 g, 1.95 mmol) in ethanol (4.6 ml) for 1 h. The evaporation residue, in DCM (50 ml), was dried ($MgSO_4$) and the

solvent was evaporated to give 0.48 g (91%) of 3-(2-phenylmethoxyethyl)-5-trifluoromethylpyrazole (**91**). Data: pale yellow oil: ^1H NMR (270 MHz, CDCl_3) 2.91 (2H, t, $J = 5.9$ Hz, pyrazole- CH_2), 3.68 (2H, t, $J = 5.9$ Hz, OCH_2CH_2), 4.51 (2H, s, PhCH_2O), 6.33 (1H, s, pyrazole 4-H), 7.2-7.4 (5H, m, Ph); ^{19}F NMR (376 MHz, CDCl_3) -62.35 (s); ^{13}C NMR (100 MHz, CDCl_3) 25.96 (pyrazole- CH_2), 68.31 (OCH_2), 73.21 (OCH_2), 102.33 (pyrazole 4-C), 121.46 (q, $J_{\text{C-F}} = 268$ Hz, CF_3), 127.75 (Ph 2,6- C_2), 127.91 (Ph 4-C), 128.48 (Ph 3,5- C_2), 137.44 (Ph 1-C), 142.66 (q, $J_{\text{C-F}} = 39.0$ Hz, pyrazole 5-C), 143.02 (pyrazole 3-C); MS (CI) 271.1058 ($\text{M}^+ + \text{H}$) ($\text{C}_{13}\text{H}_{14}\text{F}_3\text{N}_2\text{O}$ requires 271.1058).

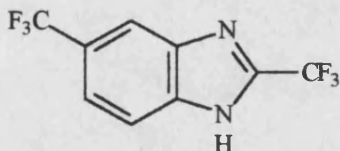


2-(5-Trifluoromethylpyrazol-3-yl)ethanol (92). To a solution of 3-(2-phenylmethoxyethyl)-5-trifluoromethylpyrazole (**91**) (0.32 g, 1.18 mmol) in methanol (4 ml) and perchloric acid (60% in water, 0.01 ml) was added a slurry of 10% palladium on activated carbon (0.1 g) in THF (1 ml). The suspension was evacuated and charged with hydrogen ($\times 3$) before being stirred in a hydrogen atmosphere for 70 min. The flask was evacuated, the suspension filtered through a pad of Celite[®] and the solvent evaporated to give a pale brown oil which was crystallised ($\text{CHCl}_3 / \text{CH}_3\text{CH}_2\text{OH}$) to yield 0.20 g (94%) of 2-(5-trifluoromethylpyrazol-3-yl)ethanol (**92**). Data: white solid; mp 85-86°C; (270 MHz, $(\text{CD}_3)_2\text{CO}$) 2.98 (2H, dt, $J = 0.5, 5.7$ Hz, pyrazole- CH_2), 4.12 (2H, t, $J = 5.7$ Hz, CH_2O), 6.40 (1H, br s, pyrazole 4-H); ^{19}F NMR (376 MHz, $(\text{CD}_3)_2\text{CO}$) -61.83 (s); MS (EI) 180.0541 (M^+ , 33) ($\text{C}_6\text{H}_7\text{F}_3\text{N}_2\text{O}$ requires 180.0510), 150 (100).



(94)

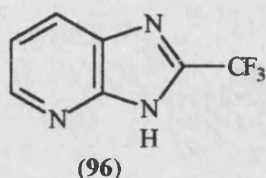
5-Fluoro-2-(trifluoromethyl)benzimidazole (94). 4-Fluorobenzene-1,2-diamine (1.00 g, 7.93 mmol) was dissolved in TFA (10 ml) and the solution was heated under reflux for 5 d. The excess TFA was removed by evaporation and the residue was subjected to heating at 200°C before sublimation at 200°C / 12 mmHg (Kugelrohr) to yield 1.56 g (95%) of 5-fluoro-2-(trifluoromethyl)-benzimidazole (94). Data: peach solid; mp 174-175°C (literature¹⁵⁷ 219-220°C); ¹H NMR (400 MHz, (CD₃)₂SO) 7.28 (1H, dt, *J* = 9.2, 2.1 Hz, 6-H), 7.56 (1H, br d, *J* = 8.9 Hz, 7-H), 7.79 (1H, m, 4-H), 14.2 (1H, br, NH); ¹³C NMR (100 MHz, (CD₃)₂SO) 112.74 - 112.98 (m, C-H), 118.82 (q, *J*_{C-F} = 271 Hz, CF₃), 141.20 (q, *J*_{C-F} = 41 Hz, CCF₃), 159.56 (d, *J*_{C-F} = 239 Hz, CF); ¹⁹F NMR (376 MHz, (CD₃)₂SO) -63.20 (s, CF₃), -116.79 (br m, 5-F); MS (EI) 204.0321 (*M*⁺, 100) (C₈H₄F₄N₂ requires 204.0311); Anal. Calcd for C₈H₄F₄N₂: C, 47.07; H, 1.98; N, 13.72. Found: C, 46.80; H, 1.93; N, 13.50.



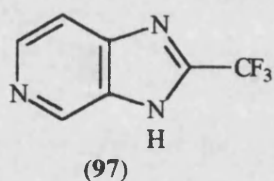
(95)

2,5-Bis(trifluoromethyl)benzimidazole (95). 3,4-Diaminobenzotrifluoride (1.00 g, 5.68 mmol) was dissolved in TFA (10 ml) and the solution was heated under reflux for 5 d 20 h. The excess TFA was removed by evaporation and the residue was subjected to heating at 200°C before sublimation at 150 °C / 10 mmHg (Kugelrohr) to yield 1.24 g (89%) of 2,5-bis(trifluoromethyl)benzimidazole (95). Data: white solid; mp 159-161°C (literature¹⁹² 198-199°C); ¹H NMR (270 MHz, (CD₃)₂SO) 7.72 (1H, dd, *J* = 8.8, 1.8 Hz, 6-H), 7.95 (1H, d, *J* = 8.4 Hz, 7-H), 8.16 (1H, br s, 4-H), 14.3 (1H, br, NH); ¹⁹F NMR (376 MHz, (CD₃)₂SO) -63.44 (s, 2-CF₃), -59.72 (br s,

5-CF₃); MS (EI) 254.0254 (M⁺, 100) (C₉H₄F₆N₂ requires 254.0279); Anal. Calcd for C₉H₄F₆N₂: C, 42.54; H, 1.59; N, 11.02. Found: C, 42.60; H, 1.55; N, 11.10.

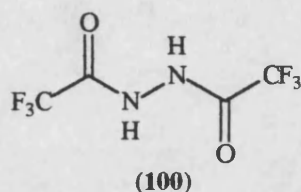


2-(Trifluoromethyl)imidazo[4,5-*b*]pyridine (96). 2,3-Diaminopyridine (1.00 g, 9.16 mmol) was dissolved in TFA (10 ml) and the resulting brown solution was heated under reflux for 2 d. The excess TFA was removed by evaporation and NMR of the remaining residue showed a mixture of intermediates. The residue was subjected to heating at 200°C before sublimation at 200 °C / 0.1 mmHg (Kugelrohr) to yield 1.67 g (98%) of 2-(trifluoromethyl)imidazo[4,5-*b*]pyridine (96). Data: yellow solid; mp 240-241°C; ¹H NMR (270 MHz, (CD₃)₂SO) 7.48 (1H, dd, *J* = 8.4, 4.8 Hz, 6-H), 8.29 (1H, br d, *J* = 8.1 Hz, 7-H), 8.59 (1H, dd, *J* = 4.8, 1.5 Hz, 5-H), 14.6 (1H, br, NH); ¹³C NMR (68 MHz, (CD₃)₂SO) 119.07 (q, *J*_{C-F} = 271 Hz, CF₃), 119.59 (br, 6,7-C₂), 142.73 (q, *J*_{C-F} ≈ 44 Hz, CCF₃), 145.76 (5-C); ¹⁹F NMR (376 MHz, (CD₃)₂SO) -63.65 (s); MS (EI) 187.0353 (M⁺, 100) (C₇H₄F₃N₃ requires 187.0357).

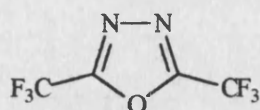


2-(Trifluoromethyl)imidazo[4,5-*c*]pyridine (97). 3,4-Diaminopyridine (1.00 g, 9.16 mmol) was dissolved in TFA (10 ml) and the resulting brown solution was heated under reflux for 3 d. The excess TFA was removed by evaporation and NMR of the remaining residue showed a mixture of intermediates. The residue was subjected to heating at 200°C before sublimation at 250 °C / 1 mmHg (Kugelrohr) to yield 1.71 g (98%) of 2-(trifluoromethyl)imidazo[4,5-*c*]pyridine (97). Data: white solid; mp 159-161°C (literature¹⁹³ 290-291°C); ¹H

NMR (270 MHz, $(\text{CD}_3)_2\text{SO}$) 7.98 (1H, d, $J = 6.6$ Hz, 7-H), 8.27 (1H, d, $J = 6.6$ Hz, 6-H), 9.25 (1H, s, 4-H), 14.2 (1H, br, NH); ^{13}C NMR (68 MHz, $(\text{CD}_3)_2\text{SO}$) 114.32 (7-C), 120.91 (q, $J_{\text{C-F}} = 270$ Hz, CF_3), 129.42 (m, CCF_3), 133.35 (6-C), 142.15 (4-C), 154.02 (br, C_q); ^{19}F NMR (376 MHz, $(\text{CD}_3)_2\text{SO}$) -63.60 (s); MS (EI) 187.0364 (M^+ , 100) ($\text{C}_7\text{H}_4\text{F}_3\text{N}_3$ requires 187.0357); Anal. Calcd for $\text{C}_7\text{H}_4\text{F}_3\text{N}_3$: C, 44.93; H, 2.15; N, 22.46. Found: C, 44.70; H, 2.12; N, 22.10.

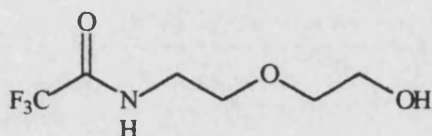


1,2-Bis(trifluoroacetyl)hydrazine (100). 1,2-Bis(trifluoroacetyl)hydrazine (**100**) was synthesised by a procedure based on that discribed by Reitz's group¹⁶⁰. A suspension of anhydrous potassium carbonate (10 g) and ethyl trifluoroacetate (9.95 g, 70.0 mmol) in ethanol (40 ml) was cooled to -10°C and treated dropwise over a 40 min period with hydrazine hydrate (1.70 ml, 35.0 mmol). The reaction mixture was allowed to warm to ambient temperature and stirring was continued for 16 h. After the mixture had been concentrated by evaporation, TFA (5 ml) was added, followed by the dropwise addition of TFAA (11.8 g, 56.0 mmol) over a 2 h period. The suspension was heated gently until it became a clear solution and reflux began. The solution was left for 16 h, after which colourless crystals were filtered off and placed over KOH in a desiccator for 16 h. Ether (200 ml) was added to the crystals and the resulting suspension was stirred for 20 min and the remaining solid was removed by filtration. The solvent of the filtrate was removed by evaporation to yield 7.37 g (94%) of 1,2-bis(trifluoroacetyl)hydrazine (**100**). Data: colourless crystals; mp $< 25^\circ\text{C}$ (literature¹⁶⁰ bp 65°C); ^{19}F NMR (84 MHz, CDCl_3) -73.75 (s); IR (film) 1680 (s), 1200 (s).



(101)

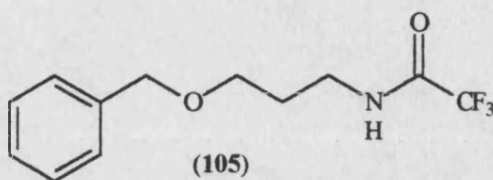
2,5-Bis(trifluoromethyl)-1,3,4-oxadiazole (101). 2,5-Bis(trifluoromethyl)-1,3,4-oxadiazole (101) was synthesised by a procedure based on that described by Reitz's group¹⁶⁰. 1,2-Bis(trifluoroacetyl)hydrazine (100) (6.0 g, 26.8 mmol) was thoroughly mixed with phosphorus pentoxide (15 g) and covered with additional phosphorous pentoxide (10 g). The mixture was slowly heated to 300°C under a static nitrogen atmosphere. The crude product was distilled off and trapped at -78°C and then was redistilled (Kugelrohr) from calcium hydride to yield 4.01 g (73%) of 2,5-bis(trifluoromethyl)-1,3,4-oxadiazole (101). Data: colourless liquid, bp 65°C (literature¹⁶⁰ bp 65°C); ¹⁹F NMR (84 MHz, CDCl₃) -65.34 (s).



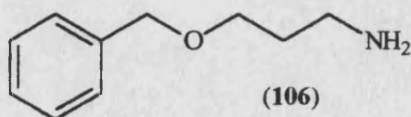
(104)

N-(2-(2-Hydroxyethoxy)ethyl)-2,2,2-trifluoroacetamide (104). N-(2-(2-Hydroxyethoxy)ethyl)-2,2,2-trifluoroacetamide (104) was synthesised by an attempted synthesis of 3,5-bis(trifluoromethyl)-4-(2-hydroxyethoxyethyl)-4*H*-1,2,4-triazole (103) using the method described by Reitz's group¹⁶⁰. A solution of 2,5-bis(trifluoromethyl)-1,3,4-oxadiazole (101) (4.01 g, 22.5 mmol) in methanol (25 ml) was cooled to 0°C and treated dropwise with 2-(2-aminoethoxy)ethanol (2.37 g, 22.5 mmol). The mixture was stirred at ambient temperature for 16 h. The solvent was evaporated and the crude material was distilled (Kugelrohr) to yield 4.32 g (96%) of N-(2-(2-hydroxyethoxy)ethyl)-2,2,2-trifluoroacetamide (104). Data: colourless liquid; bp₂₀ 195-200°C; ¹H NMR (270 MHz, CDCl₃) 3.35 (2H, t, *J* = 6.0 Hz, NCH₂CH₂O), 3.43 (2H, m, OCH₂CH₂N), 3.45 (2H, m, OCH₂CH₂OH), 3.51 (2H, m, CH₂CH₂OH), 4.59 (1H, br, NH); ¹³C NMR (68 MHz, CDCl₃) 39.50 (RCH₂N), 60.17 (RCH₂O),

67.85 (RCH₂O), 72.11 (RCH₂OH), 116.29 (q, $J_{\text{C-F}} = 288.6$ Hz, CF₃), 156.44 (q, $J_{\text{C-F}} = 35.2$ Hz, COCF₃); ¹⁹F NMR (84 MHz, CDCl₃) -74.01; IR (film) 3750 (br), 1715 (s), 1175 (s); MS (CI) 202.0691 (M⁺ + H, 100) (C₆H₁₀F₃NO₃ requires 202.0691), 140 (90).

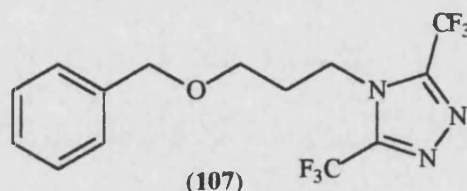


N-(3-(Phenylmethoxy)propyl)-2,2,2-trifluoroacetamide (105). To a stirred solution of trifluoroacetamide (0.78 g, 6.87 mmol) in THF (20 ml) was added potassium *tert*-butoxide (0.77 g, 6.87 mmol) portion-wise. Following dissolution, 3-(phenylmethoxy)propyl-4-methylbenzenesulphonate (**20**) (2.0 g, 6.24 mmol) and sodium iodide (*ca.* 50 mg) were added slowly. The solution was stirred at ambient temperature and reaction monitored by t.l.c.. After 4 h, the mixture was cooled with an ice bath to 0°C and ether (20 ml) and water (10 ml) were added. Following acidification to pH 1-2 the ether layer was washed with water (2 × 10 ml) and brine (10 ml), and dried (MgSO₄). Evaporation of the solvent gave 1.67 g (97%) of N-(3-(phenylmethoxy)-propyl)-2,2,2-trifluoroacetamide (**105**). Data: pale yellow oil ; ¹H NMR (400 MHz, CDCl₃) 1.87 (2H, m, CH₂CH₂CH₂), 3.50 (2H, m, CH₂CH₂NCO), 3.66 (2H, t, $J = 5.4$ Hz, BnO-CH₂CH₂), 4.45 (2H, s, PhCH₂O), 7.34 (5H, m, PhCH₂O); ¹⁹F NMR (84 MHz, CDCl₃) -76.71 (s); IR (film) 3650 (br), 1715 (s), 1170 (s).

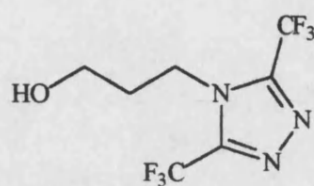


3-(Phenylmethoxy)propylamine (106). Sodium hydroxide (1.00 g, 50.0 mmol) was dissolved in methanol (40 ml) and added to N-(3-(phenylmethoxy)propyl)-2,2,2-trifluoroacetamide (**105**) (1.60 g, 5.80 mmol).

The mixture was stirred and heated under reflux for 4 h. The solvent was evaporated and the residue dissolved in ether (100 ml) and was washed with saturated sodium hydrogen carbonate solution. The organic layer was dried (MgSO_4), the solvent was evaporated and the residue was distilled (Kugelrohr) to yield 0.63 g (66%) of 3-(phenylmethoxy)propylamine (**106**). Data: colourless liquid; $\text{bp}_{0.6}$ 85-90°C (literature¹⁹⁴ $\text{bp}_{0.75}$ 93.5°C); ^1H NMR (270 MHz, CDCl_3) 1.43 (2H, br, NH_2), 1.75 (2H, qu, $J = 6.2$ Hz, $\text{CH}_2\text{CH}_2\text{CH}_2$), 2.82 (2H, t, $J = 6.8$ Hz, $\text{CH}_2\text{CH}_2\text{NH}_2$), 3.55 (2H, t, $J = 6.2$ Hz, $\text{BnOCH}_2\text{CH}_2$), 4.51 (2H, s, PhCH_2O), 7.33 (5H, m, PhCH_2O).

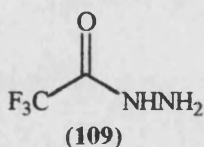


3,5-Bis(trifluoromethyl)-4-[3-(phenylmethoxy)propyl]-4H-1,2,4-triazole (107). 3,5-Bis(trifluoromethyl)-4-[3-(phenylmethoxy)propyl]-4H-1,2,4-triazole (**107**) was synthesised by a procedure based on that described by Reitz's group⁶⁹. A solution of 3-(phenylmethoxy)propylamine (**106**) (0.30 g, 1.80 mmol) in methanol (0.6 ml) was cooled to 0°C and treated dropwise with 2,5-bis(trifluoromethyl)-1,3,4-oxadiazole (**101**) (0.37 g, 1.80 mmol). The solution was boiled under reflux for 9 d. After cooling, the solvent was evaporated to yield 0.27 g (42%) of 3,5-bis(trifluoromethyl)-4-[3-(phenylmethoxy)propyl]-4H-1,2,4-triazole (**107**) following distillation (Kugelrohr). Data: colourless liquid; $\text{bp}_{0.6}$ 150-155°C; ^1H NMR (400 MHz, CDCl_3) 2.12 (2H, m, $\text{CH}_2\text{CH}_2\text{CH}_2$), 3.57 (2H, t, $J = 5.5$ Hz, $\text{BnOCH}_2\text{CH}_2$), 4.38 (2H, t, $J = 8.2$ Hz, $\text{R}_2\text{NCH}_2\text{CH}_2$), 4.51 (2H, s, PhCH_2O), 7.30 (5H, m, PhCH_2O); ^{19}F NMR (376 MHz, CDCl_3) -62.80 (s); MS (CI, iso-butane) 354.1041 ($\text{M}^+ + \text{H}$, 100) ($\text{C}_{14}\text{H}_{14}\text{F}_6\text{N}_3\text{O}$ requires 354.1041), 91 (26).



(108)

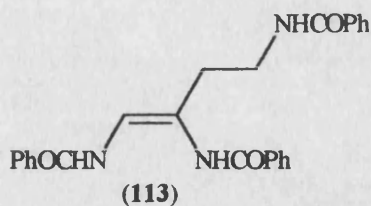
3,5-Bis(trifluoromethyl)-4-(3-hydroxypropyl)-4H-1,2,4-triazole (108). To a solution of 3,5-bis(trifluoromethyl)-4-[3-(phenylmethoxy)propyl]-4H-1,2,4-triazole (**107**) (0.20 g, 0.57 mmol) in ethanol (2 ml) was added a slurry of 10% palladium on activated carbon (0.03 g) and ethanol (0.5 ml). The suspension was evacuated and charged with hydrogen ($\times 3$) before being stirred in a hydrogen atmosphere. After 24 h perchloric acid (60% in water, 0.01 ml) was added and the mixture was stirred for a further 5 h in the presence of hydrogen. The flask was evacuated, and the suspension was filtered through a pad of Celite[®], which was thoroughly washed with ethanol (15 ml). NaHCO₃ (1 g) was added to the filtrate and the suspension was stirred for 1 h, filtered and the solvent evaporated to yield 0.14 g (94%) of 3,5-bis(trifluoromethyl)-4-(3-hydroxypropyl)-4H-1,2,4-triazole (**108**). Data: white crystals; mp $<25^{\circ}\text{C}$; ¹H NMR (400 MHz, D₂O) 2.14 (2H, m, CH₂CH₂CH₂), 3.74 (2H, t, $J = 7.9$ Hz, CH₂CH₂OH), 4.48 (2H, t, $J = 5.8$ Hz, R₂NCH₂CH₂); ¹⁹F NMR (376 MHz, D₂O) -63.49 (s); MS (EI) 264 (M⁺ + H, 1); MS (CI, iso-butane) 264.0720 (M⁺ + H, 100) (C₇H₈F₆N₃O requires 264.0720), 206 (5).



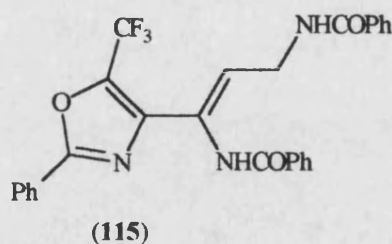
(109)

Trifluoroacetylhydrazine (109). Anhydrous hydrazine (3.09 ml, 98.5 mmol) was added dropwise to a solution of ethyl trifluoroacetate (10.0 g, 70.4 mmol) in ethanol (80 ml) at -10°C over a 45 min period. The reaction mixture was allowed to warm to ambient temperature and stirred for 16 h. The solvent and excess reagent were removed by evaporation to yield 9.02 g (100%) of trifluoroacetylhydrazine (**109**). Data: cream solid; mp $115\text{--}116^{\circ}\text{C}$ (literature¹⁹⁵

110-113°C).

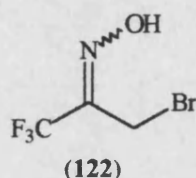


Z-1,2,4-Tris(benzamido)but-1-ene (113). Z-1,2,4-Tris(benzamido)but-1-ene (113) was synthesised by Bamberger fragmentation as generally described by Windaus's group¹⁶⁶. To a solution of imidazole-4-ethanamine hydrochloride (1.00 g, 5.40 mmol) in water (20 ml) at 0°C was added sodium hydroxide (1.08 g, 27.0 mmol) and benzyl chloride (1.94 ml, 16.7 mmol) in alternating portions, followed by water (15 ml). The temperature of the reaction mixture was maintained at 0°C and stirred for 3 h. After standing for 16 h, the suspension was filtered and the solid was washed with cold water to yield 6.52 g (73%) of Z-1,2,4-tris(benzamido)but-1-ene (113). Data: white solid; mp 189°C (literature¹⁶⁶ mp 191°C); ¹H NMR (270 MHz, (CD₃)₂SO) 2.70 (2H, t, *J* = 6.6 Hz, C=C-CH₂), 3.42 (2H, m, CH₂N), 6.60 (1H, d, *J* = 9.2 Hz, C=CH), 7.4 - 8.0 (15H, m, 3 × NHCOPh), 8.47 (1H, t, *J* = 5.4 Hz, CH₂NHCOPh), 9.47 (1H, s, C=C(CH₂CH₂NHCOPh)NHCOPh), 9.87 (1H, d, *J* = 9.5 Hz, PhCONHC=CH=C)

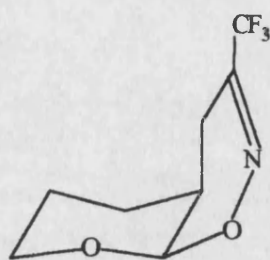


Z-4-(1,3-Bis(benzamido)prop-1-enyl)-2-phenyl-5-trifluoromethyloxazole (115). Z-1,2,4-Tris(benzamido)but-1-ene (113) (0.39 g, 0.91 mmol) was boiled under reflux with trifluoroacetic anhydride (4 ml) for 16 h. The excess reagent was evaporated and the residue was boiled under reflux in methanol (5 ml) for 1 h. The solid was collected by filtration from the cooled mixture to give 0.08

g (18%) of *Z*-4-(1,3-bis(benzamido)prop-1-enyl)-2-phenyl-5-trifluoromethyl-oxazole (**115**). Data: white solid; mp 216-217°C; ^1H NMR (400 MHz, $(\text{CD}_3)_2\text{SO}$) 4.19 (2H, br t, $J = 5.0$ Hz, CH_2), 6.29 (1H, br t, $J = 5.0$ Hz, $\text{C}=\text{CH}$), 7.58-7.68 (9H, m, $3 \times \text{Ar}$ 3,4,5- H_3), 7.99 (2H, d, $J = 6.7$ Hz, 2,6- H_2 of oxazole-2-Ph), 8.15 (4H, m, $2 \times \text{benzamide}$ 2,6- H_4), 9.08 (1H, br t, NHCH_2), 10.50 (1H, s, NH); ^{13}C NMR (100 MHz, $(\text{CD}_3)_2\text{SO}$) 36.59, 119.07 (q, $J_{\text{C-F}} = 268$ Hz, CF_3), 124.87, 126.00, 126.48, 126.53, 129.90, 127.17, 127.94, 128.11, 128.98, 130.96, 131.38, 131.73, 132.53 (q, $J_{\text{C-F}} = 44$ Hz, C- CF_3), 133.43, 133.83, 140.54, 160.38, 164.96, 166.62; ^{19}F NMR (376 MHz, $(\text{CD}_3)_2\text{SO}$) -58.89 (s); MS (CI) 492.1535 ($\text{M}^+ + \text{H}$, 55) ($\text{C}_{27}\text{H}_{21}\text{F}_3\text{N}_3\text{O}_3$ requires 492.1535).



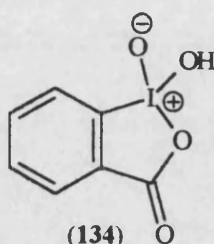
1-Bromo-3,3,3-trifluoropropan-2-one oxime (122). 1-Bromo-3,3,3-trifluoropropan-2-one oxime (**122**) was synthesised essentially by the method described by Reißig's group¹⁷⁶. To a solution of 1-bromo-3,3,3-trifluoropropanone (10.0 g, 52.4 mmol) in acid-free chloroform (50 ml) was added hydroxylamine hydrochloride (5.46 g, 78.6 mmol) in water (10 ml). The mixture was boiled under reflux for 24 h. After cooling, the aqueous layer was extracted with chloroform (3×20 ml) and the combined organic extracts were dried (MgSO_4). The solvent was removed and the crude material was purified by distillation (Kugelrohr) to yield 6.45 g (60%) of 1-bromo-3,3,3-trifluoropropan-2-one oxime (**122**) as a 1 : 1 mixture of *E* and *Z* geometrical isomers. Data: colourless liquid; bp_{20} 80°C (literature¹⁷⁶ bp_{85} 80-90°C); ^1H NMR (400 MHz, $(\text{CD}_3)_2\text{SO}$) 4.33 (1H, s, CH_2), 4.42 (1H, s, CH_2), 10.1 (1H, br, OH); ^{19}F NMR (376 MHz, $(\text{CD}_3)_2\text{SO}$) -66.52 (s), -65.37 (s).



(124)

4,4a,5,6,7,8a-Hexahydro-3-(trifluoromethyl)pyrano[4,5-*e*]-1,2-oxazine

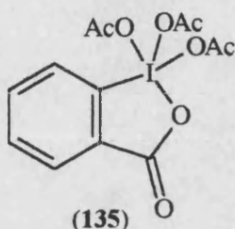
(124). 1-Bromo-3,3,3-trifluoropropan-2-one oxime (122) (0.57 g, 2.75 mmol) was dissolved in anhydrous methyl *tert*-butyl ether (110 ml) and sodium carbonate (1.75 g, 16.5 mmol) was added, followed immediately by 3,4-dihydro-2*H*-pyran (5.02 g, 55.0 mmol). The suspension was stirred in a nitrogen atmosphere in the dark for 5 d. The suspension was filtered through a Celite® pad and the solvent of the filtrate was evaporated to give a yellow oil which was distilled (Kugelrohr) to yield 0.50 g (87%) of 4,4a,5,6,7,8a-hexahydro-3-(trifluoromethyl)pyrano[4,5-*e*]-1,2-oxazine (124). Data: colourless liquid; bp₃ 125°C (literature¹⁷⁶ bp₅ 75°C); ¹H NMR (270 MHz, CDCl₃) 1.5-1.8 (4H, m, 5-H, 6-H), 2.21 (1H, m, 4a-H), 2.30 (1H, dd, *J* = 18.7, 4.4 Hz, 4-H_{eq}), 2.52 (1H, dd, *J* = 18.9, 6.8 Hz, 4-H_{ax}), 3.75 (1H, ddd, *J* = 1.3, 7.2, 11.5 Hz, 7-H_{ax}), 3.95-4.05 (1H, m, 7-H_{eq}), 5.22 (1H, d, *J* = 2.7 Hz, 8a-H); ¹⁹F NMR (84 MHz, CDCl₃) -71.05 (s).



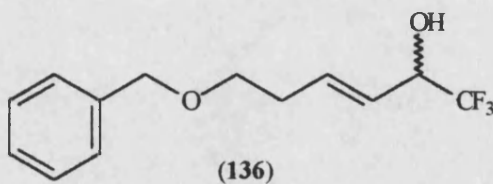
(134)

2-Iodoxybenzoic Acid (134). 2-Iodoxybenzoic acid (134) was synthesised by the method described by Dess and Martin¹⁸². To a mixture of 2-iodosobenzoic acid (20.0 g, 73.5 mmol) and 0.73 M sulphuric acid solution (157 ml) was added potassium bromate (16.2 g, 97.3 mmol) over a 1 h period, during which the temperature was kept below 50°C. The mixture was warmed to 65°C and

stirred for 4 h. The orange solution and white suspension of the reaction mixture were cooled to 0°C and filtered. The solid was washed with cold water (700 ml) and cold ethanol (30 ml) to yield 21.75 g (88%) of 2-iodoxybenzoic acid (**134**). Data: white solid.

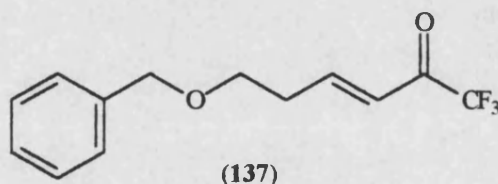


3,3,3-Triacetoxy-3-iodaisobenzofuran-1-one (135). 3,3,3-Triacetoxy-3-iodaisobenzofuran-1-one (**135**) was synthesised by the method described by Dess and Martin¹⁸². A stirred slurry of 2-iodoxybenzoic acid (**134**) (19.15 g, 64.7 mmol) in acetic anhydride (56.9 ml, 603 mmol) and acetic acid (54 ml) was heated to 100°C for 40 min. After cooling to ambient temperature, most of the solvent was evaporated at 29°C / 1 mmHg (The Dess-Martin reagent has been reported to explode upon heating under confinement¹⁸³). The white slurry was cooled and filtered in a nitrogen atmosphere and the solid was washed with cold ether (150 ml) to yield 17.48 g (61%) of 3,3,3-triacetoxy-3-iodaisobenzofuran-1-one (**135**). Data: white solid; mp 121-122°C (literature¹⁸² 124-126°C).



E-1,1,1-Trifluoro-6-(phenylmethoxy)hex-3-en-2-ol (136). A suspension of lithium aluminium hydride (2.50 g, 62.0 mmol) was prepared by the introduction of the solid in small portions to anhydrous THF (70 ml). The suspension was cooled to 0°C and 6-phenylmethoxy-1,1,1-trifluorohex-3-yn-2-one (**89**) (10.0 g, 39.0 mmol) was added dropwise as a solution in THF (20

ml). After stirring for 30 min, the temperature of the reaction mixture was allowed to rise to ambient temperature before gentle boiling under reflux for 15 h. The mixture was cooled to 0°C and water (3.27 ml), 5M sodium hydroxide solution (3.27 ml) and water (9.81 ml) were added in succession with vigorous stirring. The suspension was allowed to warm to ambient temperature and stirred for 30 min. The precipitate was removed by filtration and the filtrate was extracted with ether (5 × 50 ml). The combined organic extracts were washed with saturated ammonium chloride solution (50 ml), water (50 ml) and brine (2 × 50 ml). The solvent was evaporated and DCM (150 ml) was added. The solution was dried (MgSO₄) and the solvent was evaporated to yield 8.13 g (80%) of *E*-1,1,1-trifluoro-6-(phenylmethoxy)hex-3-en-2-ol (**136**). Data: yellow liquid; ¹H NMR (270MHz, CDCl₃) 2.41 (2H, br q, *J* = 6.4 Hz, CH₂CH₂CH=CH), 2.98 (1H, br s, OH), 3.55 (2H, t, *J* = 6.4 Hz, BnOCH₂CH₂), 5.52 (1H, m, CH=CHCH(OH)CF₃), 4.51 (2H, s, PhCH₂O), 5.59 (1H, dd, *J* = 15.6, 6.8 Hz *trans*, CH=CHCH(OH)CF₃), 5.98 (1H, dt, *J* = 15.6, 6.8 Hz *trans*, CH₂CH=CHCH(OH)CF₃), 7.33 (5H, m, Ph); ¹⁹F NMR (376 MHz, CDCl₃) -79.79 (d, *J*_{H-F} = 6.9 Hz); MS (EI) 260.0990 (M⁺, 50) (C₁₃H₁₅F₃O₂ requires 260.1024), 91 (100).



***E*-1,1,1-Trifluoro-6-(phenylmethoxy)hexan-3-en-2-one (137).** *E*-1,1,1-Trifluoro-6-(phenylmethoxy)hex-3-en-2-ol (**136**) (2.00 g, 7.68 mmol) in anhydrous DCM (10 ml) was added dropwise to a stirred solution of 3,3,3-triacetoxy-3-iodaisobenzofuran-1-one (**135**) (12.5 g, 28.4 mmol) in DCM (150 ml) over a period of 10 min. The reaction mixture was stirred at ambient temperature under a nitrogen atmosphere for 2.5 h. Ether (110 ml) and 1.3 M sodium hydroxide solution (220 ml) were added and the mixture stirred for 45 min. The layers were separated and the aqueous phase was extracted with

ether (3 × 50 ml). The combined organic extracts were washed with saturated ammonium chloride solution (100 ml), water (100 ml) and brine (100 ml). The solvent was evaporated and the residue was dissolved in DCM (100 ml). The solution was dried (MgSO₄) and the solvent was evaporated to yield 1.47 g (74%) of *E*-1,1,1-trifluoro-6-(phenylmethoxy)hex-3-en-2-one (**137**). Data: yellow liquid; ¹H NMR (400MHz, CDCl₃) 2.63 (2H, dq, *J* = 6.1, 1.5 Hz, CH₂CH₂CH=CH), 3.64 (2H, t, *J* = 6.1 Hz, BnOCH₂CH₂), 4.52 (2H, s, PhCH₂O), 6.49 (1H, d, *J* = 15.9 Hz *trans*, CH=CHCOCF₃), 7.33 (6H, m, PhCH₂OCH₂CH₂CH₂CH=CHCOCF₃); ¹⁹F NMR (376 MHz, CDCl₃) -77.99 (s); IR (film) 1733 (s), 1632 (s); MS (CI) 259.0946 (*M*⁺ + H, 29) (C₁₃H₁₄F₃O₂ requires 259.0946), 91 (100).

REFERENCES

1. Huxley, T. H. *Proc. R. Soc.* **1885**, 277.
2. Dennis, S. C.; Grevers, W.; Opie, L. H. *J. Mol. Cell. Cardiol.* **1991**, 23, 1077-1086.
3. Navon, G.; Werrmann, J. G.; Maron, R.; Cohen, S. M. *Magn. Reson. Med.* **1994**, 32, 556-564.
4. Roos, A.; Boron, W. F. *Physiological Reviews* **1981**, 61, 296-434.
5. Gadian, D. G. *Therapie* **1987**, 42, 463-465.
6. Pirttilä, T-R. M.; Kauppinen, R. A. *NeuroReport* **1993**, 5, 213-216.
7. Bremner, J. C. M.; Counsell, C. J. R.; Edwards, H. S.; Stratford, I. J.; Adams, G. E.; Nethersell, A. B. E.; Bedford, P. *Int. J. Radiat. Biol.* in press.
8. *The Metabolism of Tumors*, Warburg, O.; Arnold Constable, 1930.
9. Frenzel, T.; Koßler, S.; Bauer, H.; Niedballa, U.; Weinmann, H. J. *Investigative Radiobiology* **1994**, 29, S220-S222.
10. Rotin, D.; Steele-Norwood, D.; Grinstein, S.; Tannock, I. *Cancer Res.* **1989**, 49, 205-211.
11. Gerweek, L. E.; Rhee, J. G.; Koutcher, J. A.; Song, C. W.; Urano, M. *Radiat. Res.* **1991**, 126, 206-209.
12. Stubbs, M.; Rodrigues, L.; Howe, F. A.; Wang, J.; Jeong, K-S.; Veech, R. L.; Griffiths, J. R. *Cancer Res.* **1994**, 54, 4011-4016.
13. Vaupel, P.; Kallinowski, F.; Okunieff, P. *Cancer Res.* **1989**, 49, 6449-6465.
14. Deutsch, C.; Taylor, J. S.; Wilson, D. F. *Proc. Natl. Acad. Sci. USA* **1982**, 79, 7944-7948.
15. Martin, G. R.; Jain, R. K. *Cancer Res.* **1994**, 54, 5670-5674.
16. Gadian, D. G. *Eur. J. Cancer* **1991**, 27, 528-530.
17. Steen, R. G. *Cancer Res.* **1989**, 49, 4075-4085.

18. Maxwell, R. J.; Workman, P.; Griffiths, J. R. *Int. J. Radiation Oncology Biol Phys.* **1989**, 16, 925-929.
19. Franko, A. J.; Raleigh, J. A.; Sutherland, R. G.; Soderlind, K. J. *Biochemical Pharmacology* **1989**, 38, 665-670.
20. Jähde, E.; Glüsenkamp, K-H.; Klünder, I.; Hülser, D. F.; Tietze, L-F.; Rajewsky, M. F. *Cancer Res.* **1989**, 49, 2965-2972.
21. Chen, M.; Stolk, J. A.; Olsen, J. I.; Schweizer, M. P. *Magn. Reson. Med.* **1994**, 32, 401-404.
22. Lyng, H.; Olsen, D. R.; Southon, T. E.; Rofstad, E. K. *Br. J. Cancer* **1993**, 68, 1061-1070.
23. Boyer, M. J.; Barnard, M.; Hedley, D. W.; Tannock, I. F. *Br. J. Cancer* **1993**, 68, 890-897.
24. Tannock, I. F.; Rotin, D. *Cancer Res.* **1989**, 49, 4373-4384.
25. Song, C. W. *Cancer Res.* **1984**, 44, 4721s-4730s.
26. Bhujwalla, Z. M.; Shungu, D. C.; Chathan, J. C.; Wehrle, J. P.; Glickson, J. D. *Magn. Reson. Med.* **1994**, 32, 303-309.
27. Volk, T.; Jähne, E.; Fortmeyer, H. P.; Glüsenkamp, K-H.; Rajewsky, M. F. *Br. J. Cancer* **1993**, 68, 492-500.
28. Song, C. W.; Lyons, J. C.; Griffin, R. J.; Makepeace, C. M.; Cragoe, E. *J. Cancer Res.* **1993**, 53, 1599-1601.
29. Kremer, A. B.; Mikita, T.; Beardsley, P. G. *Biochemistry* **1987**, 26, 391-397.
30. Sowers, L. C.; Eritja, R.; Kaplan, B.; Goodman, M. F.; Fazakerly, G. V. *J. Biol. Chem.* **1988**, 263, 14794-14801.
31. Roepe, P. D.; Wei, L-Y.; Cruz, J.; Carlson, D. *Biochemistry* **1993**, 32, 11042-11056.
32. Luz, J. G.; Wei, L-Y.; Basu, S.; Roepe, P. D. *Biochemistry* **1994**, 33, 7239-7249.
33. Sanford, S.; Deborshi, R.; Schindler, M. *Proc. Natl. Acad. Sci. USA* **1994**, 91, 1128-1132.

34. Gibson, S. L.; Ceckler, T. L.; Bryant, R. G.; Hilf, R. *Cancer Biochem. Biophys.* **1989**, 10, 319-328.
35. Madden, A.; Leach, M. O.; Sharp, J. C.; Collins, D. J.; Easton, D. *NMR Biomed.* **1991**, 4, 1-11.
36. Li, S-J.; Wehrle, J. P.; Rajan, S. S.; Steen, R. G.; Glickson, J. D.; Hilton, J. *Cancer Res.* **1988**, 48, 4736-4742.
37. Li, S-J.; Jin, G-Y.; Moulder, J. E. *Cancer Commun.* **1991**, 3, 133-139.
38. Steen, R. G.; Graham, M. M. *NMR Biomed.* **1991**, 4, 117-124.
39. Radda, G. K. *Science* **1986**, 233, 640-645.
40. Madshus, I. H. *Biochem. J.* **1988**, 250, 1-8.
41. Ramasamy, R.; Lazar, I.; Brucher, E.; Sherry, A. D.; Malloy, C. R. *FEBS Lett.* **1991**, 280, 121-124.
42. Iles, R. *Bioscience Reports* **1981**, 1, 687-699.
43. Kashiwagura, T.; Deutsch, C. J.; Taylor, J.; Erecinska, M.; Wilson, D. F. *J. Biol. Chem.* **1984**, 259, 237-243.
44. Taylor, D. J.; Coppack, S. W.; Cadoux-Hudson, T. A. D.; Kemp, G. J.; Radda, G. K.; Frayn, K. N.; Ng, L. L. *Clin. Sci.* **1991**, 81, 123-128.
45. Schunldiner, S.; Rozengurt, E. *Proc. Natl. Acad. Sci. USA* **1982**, 79, 7778-7782.
46. Moolenaar, W. H.; Tsien, R. Y.; van der Saag, P. T.; de Laat, S. W. *Nature* **1983**, 304, 645-648.
47. Hesketh, T. R.; Moore, J. P.; Morris, D. H.; Taylor, M. V.; Rogers, J.; Smith, G. A.; Metcalfe, J. C. *Nature* **1985**, 313, 481-485.
48. Moolenaar, W. H.; Teroolen, L. G. J.; de Laat, S. W. *Nature* **1984**, 312, 371-373.
49. Johnson, C. H.; Epel, D. *J. Cell Biol.* **1981**, 89, 284-291.
50. Christen, R.; Schackmann, R. W.; Sphapiro, B. M. *J. Biol. Chem.* **1982**, 257, 14881-14890.
51. Gross, J. D.; Bradbury, J.; Kay, R. R.; Peacey, M. J. *Nature* **1983**, 303, 244-245.

52. Civan, M. M.; Lin, L.; Peterson-Yantorno, K.; Taylor, J.; Deutsch, C. *Am. J. Physiol.* **1984**, C506-C510.
53. Futsaether, C. M.; Kjeldstad, B.; Johnsson, A. *Can. J. Microbiol.* **1993**, 39, 180-186.
54. Thomas, R. C. *J. Physiol.* **1984**, 354, 3P-22P.
55. *Fluid and electrolytes: Physiology and Pathophysiology*, Cogan, M. G; Appleton and Lange, 1991.
56. Frelin, C.; Vigne, P.; Landoux, A.; Lazdunski, M. *Eur. J. Biochem.* **1988**, 174, 3-14.
57. Aronson, P. S. *Am. J. Physiol.* **1983**, 245, F647-F659.
58. Franchi, A. F.; Cragoe, E.; Pouyssegur, J. *J. Biol. Chem.* **1986**, 261, 14614-14620.
59. Ganz, M. B.; Boyarsky, G.; Sterzel, R. B.; Boron, W. F. *Nature* **1989**, 337, 648-651.
60. Magnaldo, I.; L'Allemain, G.; Chambard, J. C.; Moenner, M.; Barritault, D.; Pouyssegur, J. *J. Biol. Chem.* **1987**, 261, 16916-16922.
61. Boyer, M. J.; Tannock, I. F. *Cancer Res.* **1992**, 52, 4441-4447.
62. Reuss, L.; Petersen, K. U. *J. Gen. Physiol.* **1985**, 85, 409-429.
63. Olsnes, S.; Tonnessen, T. I.; Sandvig, K. *J. Cell Biol.* **1986**, 101, 967-971.
64. Reuss, L. *J. Gen. Physiol.* **1987**, 90, 173-196.
65. Grassl, S. M.; Aronson, P. S. *J. Biol. Chem.* **1986**, 262, 8778-8783.
66. Jentsch, T. J.; Stahlknecht, T. R.; Hollwede, H.; Fischer, D. G.; Keller, S. K.; Wiederholt, M. *J. Biol. Chem.* **1985**, 260, 795-801.
67. Gluck, S.; Kelly, S.; Al-awqati, Q. *J. Biol. Chem.* **1982**, 257, 9230-9233.
68. Gluck, S.; Cannon, C.; Al-Awgahi, Q. *Proc. Natl. Acad. Sci. USA* **1982**, 79, 4311-4327.
69. Reenstra, W. W.; Warnock, D. G.; Yee, V. J.; Forte, J. G. *J. Biol. Chem.* **1981**, 256, 11663-11666.
70. Thomas, R. C.; Meech, R. W. *Nature* **1982**, 299, 826-828.
71. Michaelis, L.; Davidoff, W. *Biochem. Z* **1912**, 46, 131-150.

72. Hagberg, H.; Larsson, S.; Haljamäe, H. *Acta. Physiol. Scand.* **1983**, 118, 149-153.
73. Vigne, P.; Frelin, C.; Lzdunski, M. *FEBS Lett.* **1984**, 172, 275-278.
74. Rogers, J.; Hesketh, T. R.; Smith, G. A.; Metcalfe, J. C. *J. Biol. Chem.* **1983**, 258, 5994-5997.
75. Karuri, A. R.; Dobrowsky, E.; Tannock, I. F. *Br. J. Cancer* **1993**, 68, 1080-1087.
76. Taylor, J. S.; Deutsch, C. *Biophys. J.* **1983**, 43, 261-267.
77. Grigg, R.; Amilaprasadh Norbert, W. D. J. *J. Chem. Soc., Chem. Commun.* **1992**, 1298-1300.
78. Grigg, R.; Amilaprasadh Norbert, W. D. J. *J. Chem. Soc., Chem. Commun.* **1992**, 1300-1302.
79. Grigg, R.; Holmes, J. M.; Jones, S. K.; Amilaprasadh Norbert, W. D. J. *J. Chem. Soc., Chem. Commun.* **1994**, 185-187.
80. La Manna, J. C.; McCracken, K. A. *Analytical Biochemistry* **1984**, 142, 117-125.
81. Thomas, R. C. *J. Physiol.* **1974**, 238, 159-180.
82. Balakirev, M. Y.; Khramtsov, V. V.; Berezina, T. A.; Martin, V. V.; Volodarsky, L. B. *Synthesis* **1992**, 1223-1225.
83. Moon, R. B.; Richards, J. H. *J. Biol. Chem.* **1973**, 248, 7276-7278.
84. Rabenstein, D. L.; Isab, A. A. *Analytical Biochemistry* **1982**, 121, 423-432.
85. Legerton, T. L.; Kanamori, K.; Weiss, R. L.; Roberts, J. D. *Biochemistry* **1983**, 22, 899-903.
86. Smith, G. A.; Hesketh, R. T.; Metcalfe, J. C.; Feeney, J.; Morris, P. G. *Proc. Natl. Acad. Sci. USA* **1983**, 80, 7178-7182.
87. Akerman, J. J. H.; Lowry, M.; Radda, G. K.; Ross, B. D.; Wong, G. G. *J. Physiol.* **1981**, 319, 65-79.
88. Oberhaensli, R. D.; Bore, P. J.; Rampling, R. P.; Hilton-Jones, D.; Hands, L. J.; Radda, G. K. *Lancet* **1986**, 8-11.

89. Nuccitelli, R.; Webb, D. J.; Langier, S. T.; Matson, G. B. *Proc. Natl. Acad. Sci. USA* **1981**, 78, 4421-4425.
90. Mehta, V. D.; Kulkarni, P. V.; Mason, R. P.; Antich, P. P. *BioMed. Chem. Lett.* **1993**, 3, 187-192.
91. Daly, P. F.; Cohen, J. S. *Cancer Res.* **1989**, 49, 770-779.
92. Roberts, J. K. M.; Wade-Jardetzky, N.; Jardetzky, O. *Biochemistry* **1981**, 20, 5389-5394.
93. Mahmood, U.; Alfieri, A. A.; Thaler, H.; Cowburn, D.; Koutcher, J. A. *Cancer Res.* **1994**, 54, 4885-4891.
94. Bernadou, J.; Martino, R.; Malet, M. C.; Lopez, A.; Armand, J. P. *TIPS* **1985**, 103-105.
95. Brown, F. F.; Campbell, I. D.; Kuchel, P. W.; Rabenstein, D. L. *FEBS Lett.* **1977**, 82, 12-16.
96. Brown, F. F.; Campbell, I. D. *FEBS Lett.* **1976**, 65, 322-326.
97. Gil, M. S.; Cruz, F.; Cerdán, S.; Ballesteros, P. *BioMed. Chem. Lett.* **1992**, 2, 1717-1722.
98. Martino, R.; Malet-Martino, M. C.; Vialaneix, C.; Lopez, A.; Bon, M. *Drug Metab. Dispos.* **1987**, 15, 897-904.
99. Komoroski, R. A.; Newton, J. E. O.; Cardwell, D.; Sprigg, J.; Pearce, J.; Karson, C. N. *Mag. Reson. Med.* **1994**, 31, 204-211.
100. Pederson, N. V.; Zanghi, J. A.; Miller, W. M.; Knop, R. H. *Mag. Reson. Med.* **1994**, 31, 224-228.
101. Metzler, W. J.; Lu, P. *J. Mol. Biol.* **1989**, 205, 149-164.
102. Gmeiner, W. H.; Pon, R. T.; Lown, J. W. *J. Org. Chem.* **1991**, 56, 3602-3608.
103. Hardin, C. C.; Gollnick, P.; Horowitz, J. *Biochemistry* **1988**, 27, 487-495.
104. Levy, L. A.; Murphy, E.; Raju, B.; London, R. E. *Biochemistry* **1988**, 27, 4041-4048.
105. Taylor, J. S.; Deutsch, C.; McDonald, G. G.; Wilson, D. F. *Analytical Biochemistry* **1981**, 114, 415-418.

106. Taylor, J. S.; Deutsch, C. *Biophys. J.* **1988**, 53, 227-233.
107. Deutsch, C.; Taylor, J. S. *Biophys. J.* **1989**, 55, 799-804.
108. Mehta, V. D.; Kulkarni, P. V.; Mason, R. P.; Constantinescu, A.; Aravind, S.; Goomer, N.; Antich, P. P. *FEBS Lett.* **1994**, 349, 234-238.
109. Plenio, H.; Burth, D. *J. Chem. Soc., Chem. Commun.* **1994**, 2297-2298.
110. Elguero, J.; Yranzo, G. I.; Laynez, J.; Jiménez, P.; Menéndez, M.; Catalán, J.; de Paz, J. L. G.; Anvia, F.; Traft, R. W. *J. Org. Chem.* **1991**, 56, 3942-3947.
111. Ernst, Z. L.; Menashi, J. *Trans. Faraday Soc.* **1963**, 59, 230-234.
112. Claire, P. P. K.; Coe, P. L.; Jones, C. J.; McCleverty, J. A. *J. Fluorine Chem.* **1991**, 51, 283-289.
113. Renn, O.; Venanzi, L. M.; Marteletti, A.; Gramlich, V. *Helv. Chim. Acta* **1995**, 78, 993-1000.
114. Atherton, J. H.; Fields, R. *J. Chem. Soc. (C)* **1968**, 1507-1513.
115. Hargittai, I.; Brunvoll, J.; Foces-Foces, C.; Llamas-Saiz, A. L.; Elguero, J. *J. Mol. Struct.* **1993**, 291, 211-217.
116. Bassetti, M.; Cerichelli, G.; Floris, B. *Tetrahedron* **1988**, 44, 2997-3004.
117. Elguero, J.; Yranzo, G. I. *J. Chem. Research (S)* **1990**, 120-121.
118. Katritzky, A. R.; Lue, P.; Akutagawa, K. *Tetrahedron* **1989**, 45, 4253-4262.
119. Iwata, S.; Qian, C-P.; Tanaka, K. *Chem. Lett.* **1992**, 357-360.
120. Katritzky, A. R.; Rewcastle, G. W.; Fan, W-Q. *J. Org. Chem.* **1988**, 53, 5685-5689.
121. Wright, R. S.; Coville, N. J. *South African Journal of Chemistry* **1989**, 42, 89-95.
122. Unpublished results, Threadgill, M. D.; Heer, A. K.
123. Hojo, M.; Masuda, R.; Kokuryo, Y.; Shioda, H.; Matsuo, S. *Chem. Lett.* **1976**, 499-502.
124. Bégué, J-P.; Bonnet-Delpon, D.; Mesureur, D.; Née, G.; Wu, S-W. *J. Org. Chem.* **1992**, 57, 3807-3814.
125. Hrubiec, R. T.; Smith, M. B. *J. Org. Chem.* **1984**, 49, 431-435.

126. Prugh, J. D.; Hartman, G. D.; Mallorga, P. J.; McKeever, B. M.; Michelson, S. R.; Murcko, M. A.; Schwam, H.; Smith, R. L.; Sondey, J. M.; Springer, J. P.; Sugrue, M. F. *J. Med. Chem.* **1991**, 34, 1805-1818.
127. Corey, E. J.; Gray, J.-L.; Ulrich, P. *Tetrahedron Lett.* **1976**, 17, 809-812.
128. Fletcher, H. G. *Methods Carbohydrate Chem.* **1963**, II, 166-169.
129. Kozikowski, A. P.; Stein, P. D. *J. Org. Chem.* **1984**, 49, 2301-2314.
130. Henne, A. L.; Newman, M. S.; Quill, L. L.; Staniforth, R. A. *J. Am. Chem. Soc.* **1947**, 69, 1819-1820.
131. Archer, S.; Perianayagam, C. *J. Med. Chem.* **1979**, 22, 306-309.
132. Bégué, J.-P.; Bonnet-Delpon, D. *Tetrahedron* **1991**, 47, 3207-3258.
133. Boivin, J.; El Kaim, L.; Zard, S. Z. *Tetrahedron* **1992**, 33, 1285-1288.
134. Boivin, J.; El Kaim, L.; Zard, S. Z. *Tetrahedron* **1995**, 51, 2573-2584.
135. Boivin, J.; El Kaim, L.; Zard, S. Z. *Tetrahedron* **1995**, 51, 2585-2592.
136. Villuendas, I.; Parrilla, A.; Guerrero, A. *Tetrahedron* **1994**, 50, 12673-12684.
137. Aubert, C.; Bégué, J.-P.; Charpentier-Morize, M.; Nee, G.; Langlois, B. *J. Fluorine Chem.* **1989**, 44, 377-394.
138. Felix, C.; Laurent, A.; Mison, P. *J. Fluorine Chem.* **1995**, 70, 71-82.
139. Danheiser, R. L.; Miller, R. F.; Brisbois, R. G.; Park, S. Z. *J. Org. Chem.* **1990**, 55, 1959-1964.
140. Hojo, M.; Masuda, R. *Synthesis* **1990**, 347-350.
141. Hojo, M.; Masuda, R.; Sakaguchi, S.; Takagawa, M. *Synthesis* **1986**, 1016-1017.
142. Augustine, R. L. *J. Org. Chem.* **1958**, 23, 1853-1856.
143. McMurry, J. E. *Acc. Chem. Res.* **1974**, 7, 281-286.
144. Blaszcak, L. C.; McMurry, J. E. *J. Org. Chem.* **1974**, 39, 258-259.
145. House, H. O.; Umen, M. J. *J. Am. Chem. Soc.* **1972**, 94, 5495-5497.
146. Lipshutz, B. H.; Ung, C. S.; Sengupta, S. *Synlett* **1989**, 64-66.
147. Hannock, M.; Bailer, G.; Hackenberg, J.; Subramanian, L. R. *Synthesis* **1991**, 1205-1208.
148. Zhu, S.-Z. *Synthesis* **1994**, 261-263.

149. *Spectroscopic Methods in Organic Chemistry*, Williams, D. H.; Fleming, I.; McGraw-Hill, 1989.
150. Mancuso, A. J.; Swern, D. *Synthesis* **1981**, 165-185.
151. Lyga, J. W.; Patera, R. M. *J. Heterocyclic Chem.* **1990**, 27, 919-921.
152. Singh, S. P.; Kumar, D.; Threadgill, M. D. *Indian J. Chem.* **1992**, 31B, 233-235.
153. Tensmyer, L. G.; Ainsworth, C. *J. Org. Chem.* **1976**, 31, 1878-1881.
154. Tang, X-Q.; Hu, C-M. *J. Chem. Soc. Perkin Trans. I* **1995**, 1039-1043.
155. Delome, D.; Girard, Y.; Rokech, J. *J. Org. Chem.* **1986**, 54, 3635-3637.
156. Johnson, W. S.; Wiedhaup, K.; Brady, S. F.; Olson, G. L. *J. Am. Chem. Soc.* **1974**, 96, 3979-3982.
157. Smith, W. T.; Steinle, E. C. *J. Am. Chem. Soc.* **1953**, 75, 1292-1294.
158. Elguero, J.; Fruchier, A.; Jagerovic, N.; Werner, A. *Organic Preparations and Procedures Int.* **1994**, 26, 35-74.
159. Doherty, G. O. P. *U.S. Patent 3,681,369* **1972**.
160. Reitz, D. B.; Finkes, M. J. *J. Heterocyclic Chem.* **1989**, 26, 225-230.
161. Vasiliev, N. V.; Lyashenko, Y. E.; Patalakha, A. E.; Sokolski, G. A. *J. Fluorine Chem.* **1993**, 65, 227-231.
162. Sitzmann, M. E. *J. Fluorine Chem.* **1995**, 70, 31-38.
163. Pesson, M.; Dupin, S.; Antoine, M. *Bull. Soc. Chim. France* **1962**, 1364-1366.
164. Atkinson, M. R.; Polya, J. B. *J. Chem. Soc.* **1952**, 3418.
165. Kimoto, H.; Kirk, K. L.; Cohen, L. A. *J. Org. Chem.* **1978**, 43, 3403-3405.
166. Windaus, A.; Vogt, W. *Chem. Ber.* **1907**, 40, 3691-3695.
167. Ogoshi, H.; Homma, M.; Yokota, K.; Toi, H.; Aoyama, Y. *Tetrahedron Lett.* **1983**, 24, 929-931.
168. Nishida, M.; Kimoto, H.; Fujii, S.; Hayakawa, Y.; Cohen, L. A. *Bull. Chem. Soc. Jpn.* **1991**, 64, 2255-2259.
169. Tian, W-S.; Luo, Y-R.; Chen, Y-Q.; Yu, A-J. *J. Chem. Soc., Chem. Commun.* **1993**, 101-102.

170. Ono, N.; Kawamura, H.; Maruyama, K. *Bull. Chem. Soc. Jpn.* **1989**, 62, 3386-3388.
171. Kaesler, R. W.; LeGoff, E. *J. Org. Chem.* **1982**, 47, 4779-4780.
172. Hoffmann, M. G.; Wenkert, F. *Tetrahedron* **1993**, 49, 1057-1062.
173. Leroy, J. *J. Fluorine Chem.* **1991**, 53, 61-70.
174. Yoshida, M.; Yoshida, T.; Kobayashi, M.; Kamigata, N. *J. Chem. Soc. Perkin Trans.* **1989**, 909-914.
175. Leroy, J.; Cantacuzene, D.; Wakselman, C. *Synthesis* **1982**, 313-315.
176. Zimmer, R.; Reißig, H-U. *J. Org. Chem.* **1992**, 57, 339-347.
177. Hippeli, C.; Zimmer, R.; Reißig, H-U. *Liebigs Ann. Chem.* **1990**, 469-474.
178. Baraldi, P. G.; Barco, A.; Benetti, S.; Manfredini, S.; Simoni, D. *Synthesis* **1987**, 276-278.
179. Nitta, M.; Kobayashi, T. *J. Chem. Soc. Perkin Trans.* **1985**, 1401-1406.
180. Corey, E. J.; Gross, A. W. *Tetrahedron Lett.* **1984**, 25, 495-498.
181. Kitazume, T.; Ishikawa, N. *Chem. Lett.* **1984**, 1815-1818.
182. Dess, D. B.; Martin, J. C. *J. Org. Chem.* **1983**, 48, 4155-4156.
183. Linderman, R. J.; Jamois, E. A.; Tennyson, S. D. *J. Org. Chem.* **1994**, 59, 957-962.
184. Linderman, R. J.; Lonikar, M. S. *J. Org. Chem.* **1988**, 53, 6013-6022.
185. Janssen, J. W. A. M.; Kruse, C. G.; Koeners, H. J.; Habraken, C. L. *J. Heterocyclic Chem.* **1973**, 10, 1055-1058.
186. *CRC Handbook of Chemistry and Physics*, Weast, R. C., CRC Press Inc., Cleavland, 1978, pD148.
187. *British Pharmacopoeia* 1988, Volume II, A70, Appendix 1E.
188. Butler, C. L.; Renfrew, A. G.; Clapp, M. *J. Am. Chem. Soc.* **1938**, 60, 1472-1473.
189. Umio, S.; Hitomi, M.; Nojima, H.; Kumadaki, N.; Ueda, I.; Kanaya, T.; Deguchi, Y. *J. Med. Chem.* **1972**, 15, 891-894.
190. Bonnet-Deplon, D.; Cambillau, C.; Charpentier-Morize, M.; Jacquot, R.; Mesureur, D.; Ourevitch, M. *J. Org. Chem.* **1988**, 53, 754-759.

191. Sukenik, C. N.; Bergman, R. G. *J. Am. Chem. Soc.* **1976**, 98, 6613-6623.
192. Mandel, L. R.; Porter, C. C.; Kuehl, F. A. *J. Med. Chem.* **1970**, 13, 1043-1047.
193. *Patent Brit. 1, 114, 199 (Cl.C 07d)* **1968**.
194. Utermohlen, W. P. *J. Am. Chem. Soc.* **1945**, 67, 1505-1506.
195. Handes, G. A. *Justus Liebigs Ann. Chem.* **1961**, 644, 145.

APPENDIX

pH	Chemical Shift (ppm)		
	Series 1	Series 2	Series 3
5.31	-61.8479	-61.8448	-61.8479
6.01	-61.7987	-61.7987	-61.7987
6.48	-61.7034	-61.7127	-61.7096
6.95	-61.5498	-61.5590	-61.5590
7.18	-61.3808	-61.3962	-61.3870
7.42	-61.2118	-61.2118	-61.2026
7.78	-60.9107	-60.9107	-60.9107
7.91	-60.8032	-60.8032	-60.8032
8.41	-60.5543	-60.5574	-60.5604
9.12	-60.4283	-60.4283	-60.4314
9.87	-60.3976	-60.3976	-60.3945
10.29	-60.3822	-60.3822	-60.3792

Table 8. Data for 3,5-bis(trifluoromethyl)pyrazole (**2**).

pH	Chemical Shift (ppm)		
	Series 1	Series 2	Series 3
8.37	-61.2702	-61.2702	-61.2733
9.10	-61.2733	-61.2733	-61.2733
10.05	-61.2549	-61.2579	-61.2579
10.78	-61.1565	-61.1565	-61.1596
11.24	-60.9630	-60.9660	-60.9660
11.92	-60.3239	-60.3362	-60.3454
12.32	-59.7739	-59.7800	-59.7862
12.79	-59.3468	-59.3468	-59.3529
13.06	-59.1778	-59.1747	-59.1809
13.43	-59.0610	-59.0580	-59.0610

Table 9. Data for 3-(trifluoromethyl)pyrazole-4-propanol (**79**).

pH	Chemical Shift (ppm)		
	Series 1	Series 2	Series 3
8.56	-61.1135	-61.1135	-61.1135
9.54	-61.1166	-61.1166	-61.1135
10.11	-61.1043	-61.1074	-61.1043
10.64	-61.0060	-61.0060	-61.0090
10.91	-60.9199	-60.9199	-60.9199
11.56	-60.4498	-60.4468	-60.4529
12.17	-59.7493	-59.7616	-59.7647
12.77	-59.2085	-59.2147	-59.2116
13.02	-59.1041	-59.1010	-59.1010
13.26	-59.0242	-59.0242	-59.0211

Table 10. Data for 2-(3-trifluoromethylpyrazol-4-yl)ethanol (**83**).

pH	Chemical Shift (ppm)		
	Series 1	Series 2	Series 3
7.95	-62.4992	-62.4962	-62.4962
8.78	-62.5023	-62.4992	-62.4992
9.59	-62.4747	-62.4777	-62.4747
10.04	-62.4839	-62.4777	-62.4747
10.55	-62.3886	-62.3856	-62.3856
11.03	-62.1582	-62.1582	-62.1582
11.50	-61.6666	-61.6696	-61.6666
12.02	-60.9660	-60.9660	-60.9691
12.76	-60.3638	-60.3638	-60.3669
13.05	-60.2716	-60.2716	-60.2716
13.35	-60.1733	-60.1733	-60.1702

Table 11. Data for 2-(5-trifluoromethylpyrazol-3-yl)ethanol (**91**).

pH	Chemical Shift (ppm)		
	Series 1	Series 2	Series 3
5.45	-59.9676	-59.9676	-59.9676
6.04	-59.9461	-59.9430	-59.9430
6.96	-59.9830	-59.9830	-59.9860
7.92	-59.9246	-59.9246	-59.9246
9.07	-59.3807	-59.3838	-59.3869
9.49	-58.9536	-58.9506	-58.9567
10.24	-58.1609	-58.1671	-58.1609
10.72	-57.9766	-57.9735	-57.9735
11.08	-57.9366	-57.9366	-57.9397
11.54	-57.9213	-57.9213	-57.9213
12.26	-57.9151	-57.9120	-57.9090
13.12	-57.9274	-57.9243	-57.9274

Table 12. Data for 3-(pyridin-4-yl)-5-(trifluoromethyl)pyrazole.

pH	Chemical Shift (ppm)		
	Series 1	Series 2	Series 3
0.90	-65.1755	-65.1785	-65.1755
1.91	-65.1123	-65.1095	-65.1123
3.17	-64.9604	-64.9604	-64.9604
4.10	-64.9512	-64.9512	-64.9481
5.38	-64.8928	-64.8928	-64.8897
6.48	-64.7453	-64.7453	-64.7392
7.11	-64.5860	-64.5886	-64.5917
7.71	-64.4811	-64.4811	-64.4780
8.28	-64.3950	-64.3981	-64.3981
9.59	-64.3889	-64.3858	-64.3858
12.00	-64.4042	-64.3981	-64.4012

Table 13. Data for 2-(trifluoromethyl)imidazo[4,5-*b*]pyridine (**95**).

pH	Chemical Shift (ppm)		
	Series 1	Series 2	Series 3
2.12	-65.2960	-65.2707	-65.2738
3.22	-65.2277	-65.2277	-65.2246
4.25	-65.1570	-65.1570	-65.1540
5.37	-65.1202	-65.1171	-65.1202
6.54	-65.0894	-65.0864	-65.0894
7.01	-65.1447	-65.1447	-65.1447
7.55	-65.0925	-65.0925	-65.0925
8.58	-64.7177	-64.7177	-64.7177
9.77	-64.3260	-64.3260	-64.3229
10.25	-64.2922	-64.2953	-64.2953
11.48	-64.2721	-64.2691	-64.2691
12.02	-64.2783	-64.2783	-64.2752

Table 14. Data for 2-(trifluoromethyl)imidazo[4,5-*c*]pyridine (**96**).

pH	Chemical Shift (ppm)		
	Series 1	Series 2	Series 3
0.48	-63.9065	-63.9065	-63.9065
1.06	-63.8880	-63.8850	-63.8880
1.54	-63.8481	-63.8481	-63.8481
1.93	-63.7744	-63.7744	-63.7774
2.52	-63.6054	-63.6084	-63.6115
3.02	-63.0677	-63.0615	-63.0646
3.55	-62.9724	-62.9693	-62.9693
4.23	-62.9263	-62.9263	-62.9233
4.95	-62.9110	-62.9110	-62.9110
5.39	-62.9048	-62.9048	-62.9048
6.06	-62.9048	-62.9048	-62.9048
6.52	-62.9048	-62.9048	-62.9110

Table 15. Data for 3-(trifluoromethyl)pyridine.

pH	Chemical Shift (ppm)
0.02	-63.5593
0.75	-63.5746
1.37	-63.5746
1.89	-63.5869
2.52	-63.5839
2.96	-63.5931
5.50	-63.6463
9.50	-63.6463

Table 16. Data for 3,5-bis(trifluoromethyl)-4-(3-hydroxypropyl)-4*H*-1,2,4-triazole (**107**).